Department of Geosciences
University of Fribourg (Switzerland)

PROCESS ORIENTED REPRESENTATION OF PERMAFROST SOIL THERMAL DYNAMICS IN EARTH SYSTEM MODELS

THESIS

presented to the Faculty of Science of the University of Fribourg (Switzerland)
in consideration for the award of the academic grade of *Doctor rerum naturalium*

by

Sait Altug Ekici

from

Iskenderun, Turkey

Accepted by the Faculty of Science of the University of Fribourg (Switzerland) upon the recommendation of Prof. Christian Hauck, Dr. Christian Beer, and Dr. Victor Brovkin.

Fribourg, 14.01.2015

Thesis supervisor

Dean

10.9.15

Prof. Christian Hauck

Prof. Fritz Müller

ABSTRACT

The Arctic cryosphere is changing at an alarming rate and observed to be more sensitive to climate change than the other regions on Earth. Due to its unique location and complex interactions with the rest of the planet, Arctic permafrost is analogous to a miner's canary - an early indicator of global change. However, current permafrost modeling approaches are largely unconstrained due to insufficient model evaluations, and lacking permafrost-specific processes. This thesis introduces a carefully designed permafrost model that is able to reproduce several observed datasets, allowing the identification of several key processes, and therefore facilitating the projections of the permafrost response to future climate change. This is completed through a series of iterative steps.

This begins with the systematic development of the JSBACH permafrost model as well as its evaluations with observed datasets reflecting that permafrost soil thermal dynamics can be successfully parameterized within an Earth System Model. Comprising freeze-thaw dynamics, multi-layer snow physics, vegetation insulation, and coupled soil thermal and hydrological schemes, this model compares well to site and global observations within an acceptable level of uncertainty.

Compared to other models with varying complexity, JSBACH now captures the soil thermal dynamics in various cold region landscape types quite well. This highlights the importance of incorporating cold region specific processes to capture the soil physical state of Arctic regions within global models. Further improvements to the model formulation revealed the sensitivity of soil thermal regime to model process representations. Results signify the importance of surface insulation and model internal soil physics as well as technical model design with regards to soil layering. This process analyses show the level of detail required for such experiments in global models.

Consequently, these model improvements allow the potential response of permafrost to future climate change to be projected and constrained. Model predictions estimate up to 80% loss of permafrost area compared to present-day conditions. These future projections of the permafrost thermal state show the noteworthy consequences of expected climate change to this region.

Overall, this study shows a comprehensive analysis of incorporating permafrost processes in global models and signifies the importance of several environmental factors on estimating the soil thermal dynamics of the permafrost systems. The modeling approach presented here fills the current gap in modeling permafrost physical states within global models, and provides a scientifically evaluated tool for a better understanding of the complex interactions in the Arctic and the Earth system. This approach could also be used to develop a complete biogeochemical representation, applicable to studying the several complex feedback mechanisms of the Earth system. Using such a model to assess present-day and future changes to the Arctic region provides numerous insights applicable to framing successful mitigation strategies for the future.

ZUSAMMENFASSUNG

Die arktische Kryosphäre verändert sich mit alarmierender Geschwindigkeit und reagiert Beobachtungen zufolge sensibler als die anderen Regionen der Erde auf den Klimawandel. Aufgrund seiner einzigartigen Lage und komplexer Interaktionen mit dem Rest des Planeten ist der arktische Permafrost, vergleichbar dem Kanarienvogel eines Bergmanns, ein frühzeitiger Indikator für den globalen Wandel. Trotzdem sind aktuelle Permafrost-Modellansätze aufgrund von ungenügenden Modellevaluierungen zu großen Teilen unbestimmt und ihnen fehlen permafrostspezifische Prozesse. Diese Doktorarbeit stellt ein sorgsam konzipiertes Permafrostmodell vor, das in der Lage ist, verschiedene Beobachtungsdatensätze zu reproduzieren. Dies erlaubt es, diverse Schlüsselprozesse zu identifizieren, und ermöglicht deshalb Projektionen der Reaktionen des Permafrosts auf den zukünftigen Klimawandel. Dies wird durch eine Reihe iterativer Schritte bewerkstelligt.

Am Beginn steht die systematische Entwicklung des JSBACH Permafrostmodells und seiner Evaluierung mit Hilfe von Beobachtungsdaten. Diese Evaluierung legt nahe, daß die thermische Dynamik von Permafrostböden im Rahmen eines Erdsystemmodells erfolgreich parametrisiert werden kann. Dieses Modell beinhaltet Gefrier-Auftau-Dynamiken, Mehrschichten-Schneephysik, thermische Isolation durch Vegetation sowie gekoppelte bodenthermische und -hydrologische Aspekte. Der Vergleich mit lokalen und globalen Beobachtungsdaten ergibt gute Übereinstimmungen bei einem akzeptablen Maß an Unsicherheit.

Verglichen mit anderen Modellen variierender Komplexität stellt JSBACH jetzt die thermische Dynamik von Böden in diversen Landschaftstypen kalter Regionen ziemlich gut dar. Das verdeutlicht, wie wichtig es ist, Prozesse, die für kalte Regionen spezifisch sind, zu berücksichtigen, um den bodenphysikalischen Zustand arktischer Gebiete innerhalb globaler Modelle korrekt darzustellen. Weitere Verbesserungen im Modellaufbau offenbaren die Sensitivität des thermischen Systems Boden in Bezug auf die Formulierung der Prozesse im Modell.

Die Ergebnisse heben die Wichtigkeit der Oberflächenisolierung und der modellinternen Darstellung der Bodenphysik sowie des technischen Modelldesigns bezüglich der Aufteilung des Bodens in Schichten hervor. Diese Prozessanalysen zeigen die Detailgenauigkeit, die für solche Experimente in globalen Modellen nötig ist.

Infolgedessen erlauben es diese Modellverbesserungen, die potentielle Reaktion des Permafrosts auf den zukünftigen Klimawandel abzubilden und einzugrenzen. Die Schätzung des Modells beläuft sich auf einen Verlust von bis zu 80% der Permafrostfläche im Vergleich zu heutigen Bedingungen. Diese Zukunftsprojektionen des thermischen Zustands des Permafrosts zeigen die beachtlichen Konsequenzen des erwarteten Klimawandels für diese Region.

In der Gesamtheit betrachtet, zeigt diese Studie eine umfassende Analyse der Berücksichtigung von Permafrostprozessen in globalen Modellen und stellt die Wichtigkeit verschiedener Umweltfaktoren für die Abschätzung der thermischen Dynamik des Bodens von Permafrostsystemen heraus. Der hier präsentierte Modellansatz füllt die derzeitige Lücke im Bereich der Modellierung des physikalischen Zustands von Permafrost in globalen Modellen und stellt ein wissenschaftlich evaluiertes Werkzeug für ein besseres Verständnis der komplexen Wechselwirkungen in der Arktis und dem Erdsystem bereit. Dieser Ansatz könnte auch verwendet werden, um eine vollständige biogeochemische Repräsentation zu entwickeln, die angewendet werden kann, um diverse komplexe Rückkopplungsmechanismen des Erdsystems zu untersuchen. Solch ein Modell anzuwenden, um die heutigen und zukünftigen Veränderungen in der Arktis abzuschätzen, liefert zahlreiche Erkenntnisse, die bei der Gestaltung erfolgreicher Strategien zur Schadensminderung für die Zukunft angewendet werden können.

RIASSUNTO

La criosfera artica sta cambiando ad un ritmo allarmante, tale da indicare come sia molto piu' sensibile ai cambiamenti climatici rispetto ad altre aree sulla Terra. A causa della sua ubicazione alquanto unica e alle complesse interazioni con il resto del pianeta, il permafrost artico e' analogo ai canarini usati nelle miniere di carbone – un indicatore precoce dei cambiamenti climatici. Cio' nonostante, gli attuali approcci modellistici per simulare le dinamiche del permafrost non sono robusti a causa di un'insufficiente valutazione dei modelli e mancanza di specifici processi legati a tali dinamiche. Il presente lavoro introduce un modello di permafrost attentamente sviluppato in grado di riprodurre diversi datasets di osservazioni, permettendo l'identificazione di diversi processi-chiave e facilitando le proiezioni della risposta del permafrost ai cambiamenti climatici. Il lavoro e' strutturato attraverso una serie di steps iterativi.

Initialmente si e' proceduto allo sviluppo sistematico del modello di permafrost all'interno di JSBACH, cosi' come la sua valutazione con osservazioni. Questo step ha permesso di evidenziare come le dinamiche termiche all'interno del permafrost possono essere parametrizzate con successo all'interno di un Earth System Model. Includendo dinamiche termo-fisiche come gelo e disgelo, fisica della neve in diversi strati, isolamento termico da parte della vegetazione e accoppiamento di processi termici ed idrologici nel suolo, il modello e' in grado di riprodurre osservazioni a scala di sito e globale con un livello accettabile di incertezza.

Se confrontato con altri modelli di diversa complessita', JSBACH ora simula abbastanza bene processi termici nel suolo in diverse regioni fredde. Questo sottolinea l'importanza di incorporare processi specifici delle regioni fredde per rappresentare lo stato fisico del suolo nelle regioni Artiche in modelli globali. I miglioramenti apportati al modello hanno indicato come la riproduzione del regime termico del suolo sia sensibile alla rappresentazione dei processi coinvolti. I risultati indicano come siano importanti l'insolazione superficiale e i processi fisici specifici del suolo cosi' come aspetti tecnici legati alla discretizzazione verticale del suolo. Queste analisi danno un'indicazione del livello di dettaglio neccessario per condurre tali esperimenti con modelli globali.

I miglioramenti apportati al modello hanno di conseguenza permesso una piu' robusta stima della potenziale risposta del permafrost ai cambiamenti climatici futuri. Le predizioni del modello indicano una perdita di area interessata da permafrost stimata fino all'80% rispetto allo stato attuale. Tali proiezioni future dello stato termico del permafrost evidenziano le significative consequenze dei cambiamenti climatici futuri in queste regioni.

In generale, questo studio mostra un'analisi comprensiva del lavoro di incorporazione di processi relativi al permafrost nei modelli globali e denota l' importanza di diversi fattori ambientali nella stima delle dinamiche termiche nel permafrost. L'approccio modellistico qui presentato, colma le attuali lacune nella simulazione dello stato fisico del permafrost in modelli globali, e fornisce uno strumento scientificamente validato a supporto di una migliore comprensione delle complesse interazioni nelle zone artiche e nel sistema terrestre. Tale approccio potrebbe anche essere usato per sviluppare una completa rappresentazione biogeochimica, a supporto di studi rivolti all'analisi dei complessi meccanismi di feedback all'interno del sistema terrestre. L' utilizzo di un tale modello, in grado di valutare i cambiamenti odierni e futuri nelle regioni artiche, fornisce numerose informazioni a supporto di strategie di mitigazione di successo, applicabili a scenari futuri.

CONTENTS

Bibliography

Acknowledgements

Curriculum Vitae

CHAPTER 1

INTRODUCTION

A complex and interconnected Earth System, where something happening at one location affects processes at the opposite side of the globe should no longer be a surprise (Mackenzie and Mackenzie, 1998). Yet, novel discoveries of how this connection is maintained still fascinate and complicate present-day scientific pursuits. Not long ago, little was known about: the deep water circulation connecting the world oceans (Broecker, 1997), the plastics dumped in northern Europe ending up in the Pacific Ocean Gyre (Robards et al., 1997), China's dust affecting weather patterns in Canada (McKendry et al., 2001), or the sand swept from the Sahara Desert fertilizing the Amazon Forest (Swap et al., 1992). Like a jigsaw puzzle, each interconnected piece matters and affects each other in the Earth System.

Specific to the high latitudes, recent discoveries highlight how strongly these areas are connected to the rest of the Earth System. The amount of ice accumulated upon Greenland and Antarctica is tightly related to global sea levels (Lambeck et al., 2002); the sunlight reflected from this ice and snow regulates our planet's temperature (Curry et al., 1995); and frozen soils store more carbon than vegetation and atmosphere combined (Tarnocai et al., 2009). Regardless of how far away they seem, a more clear understanding of how processes at high-latitudes relate to the global Earth System is presently critical.

1.1   Background

There have been abrupt environmental changes in the high latitudes (Duarte et al., 2012; AMAP, 2012; ACIA, 2005; Serreze et al., 2000). Retreating ice sheets of Greenland (Rignot and Kanagaratnam, 2006), shrinking Arctic sea ice (Stroeve et al., 2007), increased forest fires in Canada and Russia (Goetz et al., 2007), amplified atmospheric warming in Siberia and Alaska (McGuire et al., 2006; Serreze and Barry, 2011), soil warming in Russia (Romanovsky et al., 2010a), Alaska, and Canada (Smith et al., 2010) are a few examples of the recent environmental transformations in these regions. Such strong shifts have broad implications for the rest of the world (Jeffries et al., 2013; AMAP, 2012). Most importantly, the current change in these regions is attracting governments and businesses for new lands to exploit, and possibly leading to even further changes in the area. With the lower sea ice cover, there is lower risk of drilling for oil in

the Arctic Ocean, which can sustain more industrial developments in the Arctic Coast. Similarly, with all the valuable resources under the Arctic Ocean, governments are claiming new territories and starting military actions for their claims. On the other hand, thawing permafrost affects the local population, who depend on the existence of frozen ground. The collapsing ground and coastal erosions are damaging their infrastructure and putting them under pressure for finding new territories for settlement as well as herding animals and hunting for food. The social and economical aspects of a changing Arctic are quite diverse and needs better planning for the sake of future global economy. That's why better understanding of the natural system in the polar regions is required and many scientific projects are supported studying the high latitudes.

Apart from the Arctic Ocean and the Antarctic continent, terrestrial systems of the northern high latitudes constitute a very important part of the cryosphere, especially the permafrost underlying these lands (Overland et al., 2013). Permafrost is soil, rock or sediments that stays below 0 °C for at least two consecutive years (Van Everdingen, 1998). The current estimate is that around 21 million km^2 of Earth surface is underlain by permafrost (Gruber, 2012). That includes roughly 24% of the northern hemisphere lands (Zhang et al., 2008). Over 4 million people live on permafrost-covered lands in the Arctic (Romanovsky et al., 2010b), and these regions hold important amounts of natural resources (Goins et al., 2012). By keeping organic carbon inactively stored in the soil (Tarnocai et al., 2009; Ping et al., 2008), permafrost has been an important part of the global carbon cycle (Ciais et al., 2011), thus the climate. With more carbon stored within the permafrost, atmospheric greenhouse effect is reduced (Schuur et al., 2008). Meanwhile, annual melting of permafrost ice regulates the runoff patterns in major rivers (McGuire et al., 2006). Additionally, landscape and the infrastructure above the permafrost depends on its stability (Larsen et al., 2008). Simple changes in these environments have notable implications due to many feedback mechanisms connecting permafrost areas to the rest of the climate system (AMAP, 2012). As described in Chapin et al. (2005), decrease in snow season length relates to shrub growth and change in the summer surface albedo, which in turn warms the surface. There are other feedback mechanisms related to ice albedo effects, water vapor greenhouse

effect (McGuire et al., 2006, 2009), and increasing greenhouse effect from released permafrost carbon (Schuur 2008; Heimann and Reichstein, 2008). The role of permafrost in the global climate system is discussed by many research initiatives and its future state stays as an important questions for social, economic, and natural cycles.

1.2   Permafrost: evolution, types, and processes

As its definition is solely based on temperature, permafrost is common in the universe. Among the many other planetary bodies, our Earth belongs to the cold ones with cryogenically stable discontinuous permafrost that experiences seasonal thawing (Yershov, 1998). Due to strong internal heating and developing continents, the evolution of permafrost on Earth started in the second half of its life (2-2.5 billion years ago). Although the permafrost evolution experienced several periods of degradation in many parts, most common areas of permafrost occurrence were in North America, Europe, Asia, Antarctica, and Greenland. Within this irregular timeline of frozen ground, the most recent cooling of the Earth's ground started in the Pliocene and Pleistocene (Yershov, 1998; Burn, 1994). Rozenbaum and Shpolyanskaya (1998) explains the permafrost formation history in different parts of the globe. Current evidence shows traces of permafrost from the Early Pleistocene (700 thousand years ago) and late Pliocene (1.8 million years ago) at Kolyma river basin and North America.

Within the permafrost regions, the ground can be fully or partly covered with frozen soil. The international permafrost association (IPA) has categorized four permafrost classes depending on this coverage fraction. Continuous permafrost is found in areas with high permafrost occurrence (90%-100% of the ground), mostly at the northernmost parts of Asia, Europe and North America. However, areas with less permafrost coverage (50%-90% of the ground) are considered as discontinuous permafrost, which can occur in more southern parts than continuous permafrost areas in the northern hemisphere. When the ground is more heterogeneous and only less than half of it is underlain by permafrost (10%-50% of the ground), it is classified as sporadic permafrost and it usually constitutes the border of permafrost extent. Finally, the regions with very rare occurrence of permafrost (<10% of the ground) are classified as isolated patches and they are mostly found on southern edges of northern hemisphere

permafrost areas and on top of mountains. There is also subsea permafrost found under the Arctic Ocean at the continental shelf, but this is not discussed in this thesis.

Specific processes are found in these permafrost regions. Study of permafrost requires understanding of the harsh environmental conditions and the unusual distribution of water. The soil thermal regime is mainly controlled by phase change of the soil water and the coupling of atmosphere and land through the insulating snow and vegetation covers. The distribution of soil water in and above the soil creates unique landscape types such as polygonal structures, elevated/degraded circles, pingos, palsas, thermokarst lakes etc. On the other hand, snow and/or vegetation distribution can control the permafrost occurrence and its thickness. Inside the soil, years of freezing and thawing of soil water allows a mixing process solely controlled by soil churning and is called cryoturbation. On the other hand, several other microprocesses play important roles in different landscapes, like the snowmelt water infiltration into soil, talik formations from thawed segments of frozen soils, and anaerobic conditions due to high saturation in soil layers etc.

1.3   Field observations and international projects

In the northern permafrost areas there have been several field sites at Alaska, Siberia, Norway, and Canadian Arctic. The observational methods usually include measuring soil temperatures and estimating active layer thicknesses (ALT) either by probes, or drilling. There are also observations of soil ice content, vegetation characteristics, snow distributions and several other ecosystem properties like growing season, carbon fluxes, and animal impacts. Although there are many other field sites all around the Arctic, most of them are only active during the field seasons of researchers and some of them are measuring just the ecosystem related variables and no continuous data of soil thermal state is available.

In the recent decades, most of these sites are combined under Global Terrestrial Network for Permafrost (GTN-P), which is developed by the International Permafrost Association (IPA). From these efforts, Circumpolar Active Layer Monitoring (CALM) and international Borehole Dataset are created and these are very important in studying the current and previous states of

permafrost. Like the GTN-P, there have been many international projects aiming to address better monitoring of the permafrost and understanding its deeper connections with the rest of the Earth system. Among these are the Nordic INTERACT, NORPERM, DEFROST projects, European international PAGE21 and GREENCYCLESII projects, Swiss mountain permafrost project TEMPS, Canadian ADAPT project, European Space Agency's ESA-DUE project, German-Russian cooperated Carbo-Perm project.

Results of the last international polar year (2007-2008) have shown increase in soil temperatures almost everywhere in the Arctic circumpolar zone (Romanovsky et al., 2010b). Warming trends in Siberian permafrost are described in Romanovsky et al. (2010a). Similarly, Smith et al. (2010) showed the changes in Canadian Arctic, while Christiansen et al. (2010) documented the warming situation in Nordic areas. Many other observational evidence indicate that permafrost soils are warming, but diverse local conditions affect the warming trends and create different types of changes in separate geographical regions. This makes it harder to estimate an accurate circumpolar trend that is representative of all the permafrost regions in the north. Even though the observation networks have improved in the recent decades, the CALM network has less than 250 points (Shiklomanov et al., 2008), which are not equally distributed around the northern circumpolar zone. Same goes for the borehole locations (Romanovsky et al., 2010b), unequally distributed with a small number of sites. Harsh physical conditions and sparse settlements in these areas make it harder to increase the ground observation networks. That's why the quality of maps created by the ground-collected data is inadequate to paint the actual picture, whereas the satellite maps cannot provide the desired detail in spatial and vertical domains.

1.4   Modeling of the permafrost

When application is restricted or limited, theoretical applications support the advance of our understanding. There is no reason to limit scientific pursuits due to environmental or technical limitations. The fundamental laws governing the natural systems are well maintained and can be applied to anywhere on Earth by a numerical model. When the conditions limit the accessibility to sites or restrict the continuous measurements of the system, models come to help by simulating

the soil thermal and hydrological regimes with built-in physical equations. Especially in cold regions and permafrost areas, models are extremely useful for undertaking the scientific advancement of our understanding. The first models that were applied to the permafrost areas are from the 1970s where simple linear relationships of air and ground temperatures were elaborated and used to investigate the active layer thickness (upper part of frozen soil that thaws each summer). Most famous of all these approaches are models based on the Stefan's solution (1891), where a linear relationship between active layer thickness and the ground temperatures is formulized. Similar methods are presented and widely accepted by the scientific community (e.g. Lunardini, 1981). Among these, Kudryavtsev's formula (Kudryavtsev et al., 1974) is notably popular. These kind of empirical approaches are used in models with no explicit soil physics (Anisimov et al., 1997; Stendel and Christensen, 2002; Beer et al., 2007).

However, modeling approaches evolved since then (Riseborough et al., 2008). Soil physics with explicit heat transfer formulations are included and successfully applied in models (Oelke et al., 2003; Mölders et al., 2003; Khvorostyanov et al., 2008). Further improvements supported the implementation of explicit soil representation and cold region physics into global models. This approach allowed a coupling of the rest of the climate system with permafrost for a more accurate estimation of the climate feedbacks between different parts of the system. Frozen soil physics used in global Earth System Models were documented in several studies such as Takata and Kimoto (2000), Poutou et al. (2004), Lawrence and Slater (2005), Saito et al. (2007), Nicolsky et al. (2007), Schaefer et al. (2009), Dankers et al. (2011), Koven et al. (2011), and Gouttevin et al. (2012). These studies are the early efforts of incorporating permafrost related processes within Earth System models. As they focus on implementing explicit soil thermal and hydrological processes, their approaches on modeling complementary processes like the effects of snow insulation, vegetation and organic matter on soil temperature are quite diverse. Also the future projections of the permafrost state is studied with these models but the results show a big range of estimates (Koven et al., 2013; Slater et al., 2013) with broad circumpolar trends without spatial analysis of different regions in the high latitudes.

1.5 JSBACH model

In this work, a modeling approach for the northern high latitude permafrost physical conditions is documented. The choice of model for the experiments in the next chapters is the JSBACH model, which is part of the Max Planck Insistute's Earth System model (MPI-ESM). MPI-ESM includes atmosphere, ocean, sea ice, and land components. It is one of the major models benchmarked in the world today and it has been used in the recent IPCC reports. The land component used to be just a part of vegetation functions mostly done as it was in BETHY model (Knorr, 2000) and a simple soil representation following the scheme in ECHAM5 (Roeckner et al., 2003). It has been improved to make it a more interactive land model with multi layer soil representation together with soil hydrology and soil carbon cycles that feedbacks to the atmosphere. The new model is renamed as JSBACH.

1.6 Motivation

Even though there are currently numerous efforts to model the permafrost systems to date, there is still a huge diversity in model outputs (Koven et al., 2013). Validation against observed data is a required task of any modeling approach; however, due to limited datasets in the Arctic region, the validation process has been neglected or limited to a few site observations. This led to a broad range of model representations from different research groups. Due to the complex dynamics of permafrost related processes, there are many ways to deal with physical processes resulting in different suites of complexities in models. Therefore there is a need to assess and compare different formulations of process representations in a single model as well as comparing different types of models in order to find the required complexity for a desired accuracy. Different representations of the same process have to be compared in order to find a compromise for both accuracy and computational feasibility. Issues in current modeling approaches include:

- *Validation of model performance with multi-source observational datasets in order to understand the limitations of model formulations*
- *Comparison of current modeling approaches of permafrost processes to understand the required complexity for global models*

- *Finding the level of detail needed to represent permafrost related processes within a global model*
- *Identifying spatial patterns of changes in permafrost states in response to climate change*

A physically advanced model capable of representing high latitude soil processes is a focal point to study more complex processes such as methane balance, thermokarst, and cryoturbation in the long run. The permafrost within the climate system must be constrained by a carefully designed model and the soil processes must be investigated through detailed analyses and evaluations with as many data sources as possible. Only then, the role of permafrost in the global climate system can be studied and the future projections can be used to investigate the potential changes.

This thesis aims to answer the following questions:

1. *Can permafrost processes be included within an Earth System model that compare well to site- and global-scale datasets?*
2. *What is the required level of complexity in global models to estimate permafrost thermal dynamics?*
3. *What should be the level of detail needed in computationally efficient and physically precise process representation for permafrost soil physics?*
4. *What will be the thermal state of Arctic permafrost during the 21st century?*
5. *How will climate change affect permafrost states in different regions of the Arctic?*

1.7   Outline

In this thesis, the above-mentioned questions will be addressed from a global modeling perspective. Chapter 2 will illustrate the JSBACH model development specific to permafrost processes, and evaluations of the model performance at multi-scale datasets, particularly for the northern high latitude environments. After the JSBACH model is improved, Chapter 3 will compare it to the current modeling approaches within a broader multi-model intercomparison study, which investigates the complexity necessary for models to capture the physical conditions of cold region soils. Following on that, Chapter 4 will go deeper into analyzing the details of JSBACH model formulation by extending the process

representation of the improved model in representing site-level thermal dynamics. From that on, Chapter 5 will focus on the global context and display the application of the validated JSBACH model to project the future state of permafrost and cold region conditions within the climate change context during the 21st century. In conclusion, Chapter 6 will summarize all the new information included in the individual chapters, ending with several conclusive statements and future outlooks.

The thesis consists of 4 main chapters, all written individually and some in the form of journal articles. Each contains its own introduction, methods, results, discussions, and conclusions and can be read individually. Chapter 2 has been published in the journal *Geoscientific Model Development* and Chapter 3 has been published in the journal *The Cryosphere*. Chapters 4 and 5 are written solely for this thesis and they are not published in any journal yet.

CHAPTER 2

MODEL DEVELOPMENT AND EVALUATION

2.1 Introduction and Summary

This chapter includes the article "Simulating high latitude permafrost regions by the JSBACH terrestrial ecosystem model"[1] that has been published in the journal *Geoscientific Model Development*. This article is prepared as a main part of this thesis and describes the model development for permafrost soils together with evaluations of model performance with observed datasets. The work leading to this article has primarily been performed by the main author of this thesis, within the EU project "Greencycles II". The article itself is appended in the next section, such that it contains its own sub-sections with abstract and references.

The aim of the work presented in this paper is to prepare the JSBACH model for the permafrost and cold region specific experiments. By adding freezing of soil water, coupling heat and water transfer within the soil via heat transfer parameters and latent heat of phase change, and including surface insulation processes from snow and moss cover, the JSBACH model is extended to represent the soil thermal state and evolution within the permafrost areas.

The evaluation procedure with the site and global datasets have revealed that the new model version is applicable to cold region soils and represents the permafrost conditions close to observations. Further improvements are required to overcome the overestimated active layer thickness and underestimated subsoil temperatures.

---

1 Ekici, A., Beer, C., Hagemann, S., Boike, J., Langer, M., and Hauck, C.: Simulating high-latitude permafrost regions by the JSBACH terrestrial ecosystem model, Geosci. Model Dev., 7, 631-647, doi:10.5194/gmd-7-631-2014, 2014.

Geoscientific
Model Development

Open Access

Simulating high-latitude permafrost regions by the JSBACH terrestrial ecosystem model

A. Ekici[1,2], C. Beer[1,3], S. Hagemann[4], J. Boike[5], M. Langer[5], and C. Hauck[2]

[1]Department of Biogeochemical Integration, Max Planck Institute for Biogeochemistry, Jena, Germany
[2]Department of Geosciences, University of Fribourg, Fribourg, Switzerland
[3]Department of Applied Environmental Science (ITM) and Bolin Centre for Climate Research, Stockholm University, Stockholm, Sweden
[4]Department of Land in the Earth System, Max Planck Institute for Meteorology, Hamburg, Germany
[5]Alfred Wegener Institute for Polar and Marine Research, Potsdam, Germany

Correspondence to: A. Ekici (aekici@bgc-jena.mpg.de)

Abstract. The current version of JSBACH incorporates phenomena specific to high latitudes: freeze/thaw processes, coupling thermal and hydrological processes in a layered soil scheme, defining a multilayer snow representation and an insulating moss cover. Evaluations using comprehensive Arctic data sets show comparable results at the site, basin, continental and circumarctic scales. Such comparisons highlight the need to include processes relevant to high-latitude systems in order to capture the dynamics, and therefore realistically predict the evolution of this climatically critical biome.

1 Introduction

The effects of global climate change are felt stronger in the northern high latitudes than elsewhere in the world (ACIA, 2005). During recent decades, polar regions have experienced an increase from around $+0.5$ to $+1\,°C$ in surface atmospheric temperatures, while the global mean has risen by only from $+0.2$ to $+0.3\,°C$ (Serreze et al., 2000). Furthermore, soil temperature in the Arctic is also undergoing warming, which is observed from borehole and active-layer measurements. After the International Polar Year (2007–2008), these measurements were summarized to show that permafrost is warming and active-layer thickness is increasing in the Nordic regions, Russia, and North America (Christiansen et al., 2010; Romanovsky et al., 2010a; Smith et al., 2010).

Based on a simple relationship between air temperature and the permafrost probability, Gruber (2012) estimated that around 22 % (± 3 %) of the Northern Hemisphere land is underlain by permafrost. During the past glacial/interglacial cycles vast amounts of organic matter have been accumulated in these soils (Zimov et al., 2006). With the abundant resources in interglacial periods, life has flourished and left huge amounts of organic matter behind; while the glacial periods created unfavorable conditions for decomposition and kept the remnants locked away in the frozen soil (DeConto et al., 2012; Schirrmeister et al., 2013). Supporting that, recent findings on the amount of soil carbon in northern circumpolar permafrost soils are larger than the previous estimates (Hugelius et al., 2010; Ping et al., 2008; Tarnocai et al., 2009; Zimov et al., 2006). According to Tarnocai et al. (2009), there are 1672 Pg of carbon stocked in the northern permafrost soils. With the current trend of increasing air temperature, this carbon rich soil is susceptible to thawing and being released to the atmosphere in the form of greenhouse gases and thus contributing to even further warming of the atmosphere (Heimann and Reichstein, 2008; Schuur et al., 2008; ACIA, 2005). Therefore, it is important to understand the underlying processes and to quantify future interactions of permafrost regions within a changing climate (Beer, 2008).

The recognition of this importance has spurred recent advances of dynamic global vegetation models and Earth system models by representing processes that are specific to

high-latitude regions. With the understanding of feedback mechanisms and recent estimates of vast amounts of soil carbon, progress has been made to address uncertainties in Arctic simulations. At present, most of the global models include common processes related to permafrost regions, e.g., latent heat release/consumption from the phase change of soil water (Riseborough et al., 2008), organic matter decomposition at freezing conditions, methanogenesis and methane-related processes. Li et al. (2010) have shown a comprehensive review of different freezing schemes in sophisticated models. However, within the global models either an extra term of latent heat is added (e.g., Mölders et al., 2003; Takata and Kimoto, 2000) or the method of "apparent heat capacity" is incorporated into temperature calculations (e.g., Beer et al., 2007; Hinzman et al., 1998; Nicolsky et al., 2007; Oelke, 2003; Poutou et al., 2004; Schaefer et al., 2009). In either way, the models showed a significant improvement in simulating soil temperature or active-layer thickness (e.g., Dankers et al., 2011; Gouttevin et al., 2012a; Lawrence et al., 2012; Zhang et al., 2008).

Besides the freeze/thaw events, the coupling of snow and soil thermal constitutes the basis for the soil thermal profile during winter (Dutra et al., 2010; Slater et al., 2001; Stieglitz et al., 2003). Due to strong insulating properties of snow, the winter soil temperature is kept warmer than the much colder atmospheric temperature. Furthermore, the timing of snowmelt influences the duration of the growing season and the active-layer thickness, which is also related to the amount of infiltrating snowmelt water into the soil. Goodrich (1982), Kelley et al. (1968) and Groffman et al. (2006) found that snow cover strongly influences the ground thermal regime. Using the ORCHIDEE (Organising Carbon and Hydrology In Dynamic Ecosystems) model, Gouttevin et al. (2012b) showed that the snow cover and the disappearance of snow are important factors for the plant and soil metabolic activity and biogeochemical feedbacks between the soil and the atmosphere. However, in most cases snow is represented rather simply in the models. Due to the high complexity of snow types and snow processes, a simple parameterization yielding a realistic heat insulation effect was used (e.g., Beer et al., 2007; Koren et al., 1999; Verseghy, 1991). While more advanced snow schemes were developed in some modeling studies (Boone and Etchevers, 2001; Loth and Graf, 1998), it is not always practical for global modeling exercises to include such a complex approach due to its computational requirements.

Impacts of changing permafrost conditions on the climate system and vegetation activity have also been investigated. It is shown by Poutou et al. (2004) that including soil freezing in their model leads to dryer summers and warmer winters in different regions. Beer et al. (2007) have found out that with the permafrost-specific processes the high-latitude vegetation carbon stocks are better represented in a dynamic global vegetation model. In other modeling studies, future implications of possible permafrost carbon release are investigated

and their effects on global climate are shown under different warming scenarios (Burke et al., 2012; Hayes et al., 2011; Koven et al., 2011; Schaefer et al., 2011; Schneider von Deimling et al., 2011; Zhuang et al., 2006). A good review of permafrost carbon cycle models is documented in McGuire et al. (2009).

Although progress has been undertaken on representing permafrost processes in land surface models, there is still a considerable uncertainty regarding the magnitude of the effects of permafrost feedbacks on climate. A consensus is not yet close to being reached regarding the timing of permafrost response to climate change and consequences of permafrost feedback mechanisms on the climate system. An intercomparison study of different land surface schemes especially with respect to cold regions' climate and hydrology revealed large differences between the models, even in case of a similar implementation of frozen ground physics (Luo et al., 2003). Due to missing processes and related deficiencies of their land surface schemes, climate models often show substantial biases in hydrological variables over high northern latitudes (Luo et al., 2003; Swenson et al., 2012). Thus, the representation of the complex dynamics of permafrost-related processes within global models is a challenging yet essential task (Hagemann et al., 2013). To contribute to this progress, we have advanced the land surface model JSBACH (Jena Scheme for Biosphere–Atmosphere Coupling in Hamburg) and we show the reliability of the new model version in multiscale evaluations.

2 Methods

2.1 Model description and improvements

JSBACH is the land surface component of the Max Planck Institute Earth System Model (MPI-ESM) that comprises ECHAM6 for the atmosphere (Stevens et al., 2012) and MPI-OM (Max Planck Institute Ocean Model) for the ocean (Jungclaus et al., 2012). It is designed to serve as a land surface boundary for the atmosphere in the coupled simulations; but it can also be used offline given that it is a comprehensive terrestrial ecosystem model with a process-based approach for representing key ecosystem functions. JSBACH simulates photosynthesis, phenology and land physics with hydrological and biogeochemical cycles (Raddatz et al., 2007; Brovkin et al., 2009). The photosynthesis scheme follows Farquhar et al. (1980) and Collatz et al. (1992). The BETHY (Biosphere Energy-Transfer Hydrology) model (Knorr, 2000) covers most of the fast canopy processes. The current version employs a relatively simple carbon cycle model (Raddatz et al., 2007). Vegetation carbon is classified as "green", "wood" or "reserve" carbon and these are transported into soil carbon pools via litter fluxes. The soil organic matter is stored in "fast" or "slow" soil carbon pools with different decomposition rates. All carbon pools have a constant
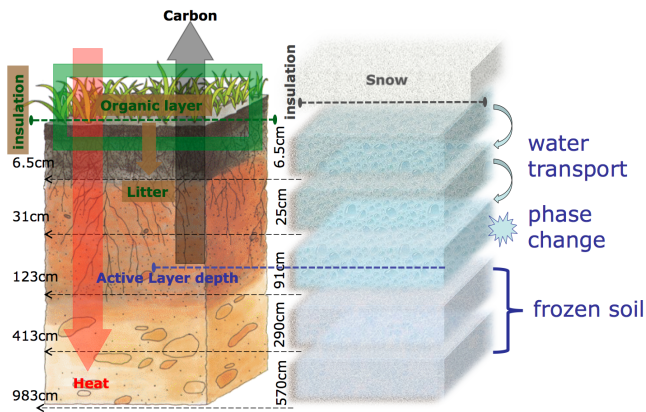
Fig. 1. Vertical soil model structure of the new JSBACH version. The numbers left of the soil column show the depths of the bottom of each layer while the numbers right of the soil column show layer thicknesses. Here snow and organic layers are simply shown to represent a multilayered snow scheme and constant moss layer described in the text.

turnover time, which is only modified by temperature and moisture in the case of soil carbon pools.

The current version of the model can be run with 30 min temporal resolution and global simulations are usually performed at 0.5° spatial resolution; however, the 1-D point model can also be run for a single location. The grid cells are usually divided into tiles of homogeneous vegetation cover. In the version discussed here, we prescribed the vegetation cover and kept it constant over time (cf. Sects. 2.2 and 2.3).

The soil is discretized into five layers with increasing thicknesses (Fig. 1). Heat conduction through the vertical soil layers is assumed to be the dominant method of heat transfer; therefore convective and radiative heat transfer processes are neglected. Surface temperature is calculated by considering incoming radiation and surface albedo, then it is used as the upper boundary forcing for the soil temperature calculations. During the snow period, the uppermost snow layer is forced by surface temperature and the bottom snow-layer temperature is used to force the soil column. In the simulations mentioned here, a constant moss layer is present over the soil. Hence the upper boundary condition for the soil temperature calculations is the moss-layer temperature, while a zero heat flux is assumed for the bottom boundary condition at 10 m depth. The one-dimensional heat transfer equation (Eq. 1) is solved for each layer. For each time step, and each soil layer, the numerical solution to heat conduction (first term on the right side of Eq. 1) gives the soil-layer temperature and then as a second step, this temperature is updated with respect to the heat used for (or gained from) phase change of soil water (second term on the right side of Eq. 1) in that layer. This routine continues from the top to the bottom to calculate all the soil-layer temperatures.

$$c \frac{\partial T}{\partial t} = \frac{\partial}{\partial z}\left(\lambda \frac{\partial T}{\partial z}\right) + L_f \rho_i \frac{\partial \theta_i}{\partial t}, \qquad (1)$$

with T: soil-layer temperature (K), c: volumetric heat capacity of the soil layer ($J\,m^{-3}\,K^{-1}$), λ: heat conductivity of the soil layer ($W\,K^{-1}\,m^{-1}$), L_f: Latent heat of fusion ($J\,kg^{-1}$), ρ_i: density of ice ($kg\,m^{-3}$), θ_i: volumetric soil ice content (m^3, m^{-3}), t: time (s), and z: soil-layer depth (m).

JSBACH mainly uses the physics package of ECHAM5 (Roeckner et al., 2003). This comprises the separation of rainfall and snowmelt into surface runoff and infiltration and the calculation of lateral drainage following the Arno scheme (Dümenil and Todini 1992). A new soil hydrology scheme (Hagemann and Stacke, 2014) has been implemented into JSBACH that uses the same five-layer structure (see Fig. 1) as the thermal module and calculates soil water transport by using the one-dimensional Richards equation (Richards, 1931) shown in Eq. (2). Here, the local change rate of moisture $\partial \theta_w / \partial t$ is related to vertical diffusion (first term on the right side of Eq. 2) and percolation by gravitational drainage of water (second term). Both processes are considered separately. Percolation is calculated following the Van Genuchten (1980) method and the diffusion is calculated using the Richtmyer and Morton (1967) diffusion scheme. For the latter, the soil water diffusivity D of each layer is parameterized following Clapp and Hornberger (1978).

The soil water content may be greater than 0 for each layer above the bedrock. There is no water available for the land surface scheme below the bedrock. Consequently, horizontal drainage (ECHAM4 formulation following Dümenil and Todini, 1992) may occur only from those layers above the bedrock. The formulation has been slightly modified as now drainage may only occur if the soil moisture is above the wilting point. Note that the previously used bucket model soil moisture now corresponds to the root zone soil moisture. The associated rooting depth determines the depth from where transpiration may occur. Bare soil evaporation is occurring only from the uppermost layer.

In the hydrology module, first the input/output terms (precipitation, snowmelt, evapotranspiration) are accumulated and infiltrated into (removed from) the soil. Then, the phase change routine updates the water and ice contents of each layer before the vertical water movement is executed. Each layer's field capacity is updated with the corresponding layer's ice content that is created or melted in the same time step. This allows for a more realistic water transport within the frozen layers. Finally the vertical water movement is performed as described above and the soil water content at each layer is updated.

$$\frac{\partial \theta_w}{\partial t} = \frac{\partial}{\partial z}\left(D \frac{\partial \theta_w}{\partial z}\right) + \frac{\partial K}{\partial z} + S, \qquad (2)$$

with θ_w: volumetric soil water content ($m^3\,m^{-3}$), D: soil water diffusivity ($m^2\,s^{-1}$), K: soil hydraulic conductivity ($m\,s^{-1}$), and S: source and sink terms (s^{-1}).

As shown in Eq. (3), a supercooled water formulation is also incorporated to allow liquid water to coexist with ice under freezing temperatures. This approach follows the Niu and Yang (2006) formulation.

$$\theta_{w\,max} = \theta_{sat} \left\{ \frac{L_f (T - T_{frz})}{g\,T\,\psi_{sat}} \right\}^{-1/b}, \tag{3}$$

with $\theta_{w\,max}$: maximum supercooled water content (m), θ_{sat}: soil porosity ($m^3\,m^{-3}$), T_{frz}: freezing temperature of water (K), g: gravitational acceleration ($m\,s^{-2}$), ψ_{sat}: saturated soil matric potential (m), and b: Clapp and Hornberger exponent (–).

Soil heat transfer is coupled with the hydrological scheme through latent heat from phase change and two parameters: the volumetric heat capacity (c) and the soil heat conductivity (λ) in Eq. (1). We have parameterized the heat capacity using the de Vries (1963) formulation (Eq. 4) and the heat conductivity following Johansen's (1975)method (Eq. 5). Equations (6–9) describe the terms in Eq. (5). With these formulations, the amounts of water and ice influence the soil thermal properties. In concert with the latent heat of fusion effect on temperature (second term on the right side of Eq. 1), a coupling of the hydrology and soil thermal dynamics is achieved. For Eq. (8), bulk density needs to be inserted with the given unit below.

$$c = (1 - \theta_{sat})\,\rho_s c_s + \rho_w c_w \theta_w + \rho_i c_i \theta_i \tag{4}$$

with ρ_s, ρ_w, and ρ_i: density of soil solids, water and ice, respectively ($kg\,m^{-3}$); c_s, c_w, and c_i: specific heat capacities of soil solids, water and ice, respectively ($J\,kg^{-1}\,K^{-1}$).

$$\lambda = K_e \lambda_{sat} + (1 - K_e)\lambda_{dry}, \tag{5}$$

$$K_e = \begin{pmatrix} \log(\text{Sat}) + 1 \ge 0 & T \ge T_{frz} \\ \text{Sat} & T < T_{frz} \end{pmatrix}, \tag{6}$$

$$\lambda_{sat} = \lambda_s^{1-\theta_{sat}} \lambda_w^{\theta_w} \lambda_i^{\theta_{sat}-\theta_w}, \tag{7}$$

$$\lambda_{dry} = \frac{0.135\rho_{bulk} + 64.7}{2700 - 0.947\rho_{bulk}}, \tag{8}$$

$$\rho_{bulk} = 2700\,(1 - \theta_{sat}), \tag{9}$$

with K_e: Kersten number (–), λ_{sat}: heat conductivity of the saturated soil ($W\,K^{-1}\,m^{-1}$), λ_{dry}: heat conductivity of the dry soil ($W\,K^{-1}\,m^{-1}$), Sat: saturation (($\theta_w + \theta_i)/z/\theta_{sat}$), λ_s, λ_w, and λ_i: heat conductivities of soil solids, water and ice, respectively ($W\,K^{-1}\,m^{-1}$), and ρ_{bulk}: soil bulk density ($kg\,m^{-3}$).

Snow is treated as external layers above the soil column. With increasing snow depth in winter, new layers are added up to maximum of five snow layers. The top four layers are always 5 cm in thickness, while the bottom layer is unlimited in size. A 5 cm snow layer is always kept in contact with the atmosphere in order to maintain the numerical stability due to rapid changes in air temperature. The uncertainty of representing 5 cm snow layers is assumed to be negligible when compared to having a nonlayered snow scheme. The snow properties are kept constant for simplicity. A snow density of $250\,kg\,m^{-3}$ is used for the snow depth calculations and the snow heat conductivity is fixed at $0.31\,W\,K^{-1}\,m^{-1}$ with a snow heat capacity of $522\,500\,J\,m^{-3}\,K^{-1}$. This simple approach is chosen to ensure the heat insulation for the soil rather than providing a complex snow model. For this reason, the snow layers are hydrologically inactive, meaning there is no water held within each snow layer, thus neither the transfer of meltwater within the snowpack nor refreezing effects are considered. Water infiltration from snowmelt into the soil is treated separately in the hydrology module.

In addition to the snow layers, the importance of moss cover in the Arctic is mentioned in several studies (Beringer et al., 2001; Rinke et al., 2008). The moss cover above soil affects the soil heat transfer through thermal and hydrological insulation depending on the thickness and wetness of the moss. Also in reality, the moss distribution shows great spatial differences. This geographic dependence of moss cover brings additional heterogeneity to the soil thermal dynamics in the Arctic. To have the first step to represent such complexity, a constant uniform moss cover without the hydrological effects is assumed for the entire domain. This moss layer has similar functions as the snow layers, i.e., not having dynamic hydrology but rather providing constant heat insulation for the underlying soil layers. For the simulations presented in this paper, a 10 cm thick moss layer is chosen for all the seasons. The heat parameters for the moss layer follow Beringer et al. (2001), with heat conductivity of $0.25\,W\,K^{-1}\,m^{-1}$ and volumetric heat capacity of $2\,500\,000\,J\,m^{-3}\,K^{-1}$.

2.2 Global forcing data

For the period 1901–1978, daily forcing data with 0.5° spatial resolution from the EU project WATCH (Water and Global Change) has been used (Weedon et al., 2010, 2011). This data is based on ERA-40 (ECMWF 40 year Re-Analysis) reanalysis results that were bias-corrected by using several observation-based data sets, such as climate grids from the Climate Research Unit, University of East Anglia (CRU). For the 1979–2010 period, ECMWF (European Centre for Medium-Range Weather Forecasts) ERA-Interim reanalysis data (Dee et al., 2011) has been used. This data set was downloaded at 0.5° spatial resolution and bias-corrected against the WATCH-forcing data following Piani et al. (2010). A more detailed description of the climate forcing data set can be found in Beer et al. (2014). With this approach, a consistent time series of climate data for the period 1901–2010 is ensured.

Table 1. JSBACH model parameters used in the site simulations.

	NUUK	SAMOYLOV
Veg. cover type	Tundra	Tundra
Porosity (θ_{sat})	46 %	42 %
Field capacity	36 %	36 %
Soil depth before bedrock	36 (cm)	800 (cm)
Soil mineral heat capacity (c_s)	2 213 667 (Jm^{-3} K^{-1})	2 187 782 (Jm^{-3} K^{-1})
Soil mineral heat conductivity (λ_s)	6.84 (Wm^{-1} K^{-1})	7.43 (Wm^{-1} K^{-1})
Saturated hydraulic conductivity	2.42×10^{-6} (m s^{-1})	8.009×10^{-6} (m s^{-1})
Saturated moisture potential (ψ_{sat})	0.00519 (m)	0.00385 (m)
Clap and Hornberger exponent (b)	5.389 (–)	4.885 (–)

The sand, silt and clay fractions from the Harmonized World Soil Database v.1.1 (FAO et al., 2009) were the basis for deriving the soil thermal properties. Up to four tiles per 0.5° grid cell area are distinguished for vegetation-related model parameters (Raddatz et al., 2007). The coverage of these tiles has been estimated by combining the GLC2000 land cover map (GLC2000 database, 2003), the MODIS (Moderate Resolution Imaging Spectroradiometer) Vegetation Continuous Fields product (Hansen et al., 2003) and the WWF (World Wildlife Fund) biome map (Olson et al., 2001).

JSBACH was forced by global atmospheric carbon dioxide concentrations following the CMIP5 (Coupled Model Intercomparison Project Phase 5) protocol (Meinshausen et al., 2011).

2.3 Simulation setup

Site-level simulations were performed running the model at a single point, forced by meteorological site observations (see below section). Soil parameters were extracted from the above-mentioned global land surface data and given in Table 1. Using the observed meteorological data, an average seasonal cycle was prepared and repeated for 30 years to force a spin-up simulation for bringing the soil thermal and hydrological profiles to equilibrium. Then, the transient simulation for the site was conducted using multiple years of observed climate and the results were used for comparison with the soil temperature observations. The time period used for the site simulations is from August 2008 to December 2009 for Nuuk, and from July 2003 to October 2005 for Samoylov.

For the circumpolar simulations, the model was run using the previously described global daily forcing data for the grids above 50° north. First, the model's physical state was brought into equilibrium with a 30-year run repeating an average seasonal cycle of climate variables from the period 1901–1930. Then, a climate-transient run with constant atmospheric CO$_2$ concentration at the 1901 value was executed for the same period. These 30-year model results were further used to force a 1000-year carbon balance model run in order to prepare equilibrated carbon pools. Finally, these carbon pools are used as the initial condition to start a fully transient run from 1901 to 2010.

2.4 Validation data sets

2.4.1 Nuuk-site observations

The Nuuk observational site is on the southwestern coast of Greenland, 250 km south of the polar circle at around 64° north and 51° west. It is situated in the Kobbefjord at an altitude of 500 m a.s.l. (above sea level) close to the city of Nuuk. Ambient climate is arctic/polar with mean annual temperature of $-1.5\,°C$ in 2008 and $-1.3\,°C$ in 2009 (Jensen and Rasch, 2009, 2010). Vegetation type consists of *Empetrum nigrum* with *Betula nana* and *Ledum groenlandicum* with a vegetation height of 3–5 cm. The study site's soil lacks mineral soil horizons due to cryoturbation and lack of podsol development due to its dry location. Soil type is categorized as mostly sandy soil with 10 % organic matter in the top 10 cm, no ice lenses in the profile and no permafrost. No soil ice or permafrost formations have been observed within the drainage basin. Snow cover is measured at the Climate Basic station 1.65 km from the soil station but at the same altitude. At the time of the annual Nuuk basic snow survey in mid-April, the snow depth at the soil station is much alike the snow depth at the Climate Basic station: ± 0.1 m when the snow depth is high (near 1 m) and much alike if it is much lower. Strong winds (> 20 m s^{-1}) have a strong influence on the redistribution of newly fallen snow especially in the beginning of the snow season, so the formation of a permanent snow cover at the soil station can be delayed by as much as one week; while the end of the snow cover season is more or less alike the date at the Climate Basic station. In some winters there is some depth hoar formation in the snowpack (B. U. Hansen, personal communication, 2013).

The meteorological (half-hourly incoming radiation, air temperature, precipitation, wind speed) and soil observations (hourly soil temperature) were downloaded from the Greenland Ecosystem Monitoring database web server (ZackenbergGIS). For the meteorological variables, the time period used was July 2008 to December 2010, while the

soil temperature was available from August 2008 to December 2009. The downloaded ASCII (American Standard Code for Information Interchange) files have been combined in a netCDF (network Common Data Form) format file; minor-gap filling was needed to create a continuous climate forcing to force the Nuuk site-level simulations.

2.4.2 Samoylov-site observations

The Samoylov field site is located in northern Siberia (72.4° N, 126.5° E) at the Lena River delta. The site represents a typical lowland tundra landscape and is characterized by continuous and ice-rich permafrost, which reaches depths of about 200 m (Grigoriev et al., 1996). The local climate is Arctic–continental with a mean annual air temperature of about -13 °C. The annual temperature range spans from about -45 °C in winter to 20 °C in summer (Boike et al., 2013). The total annual precipitation is about 200 mm, of which about 25 % contributes to snowfall (Boike et al., 2008; Langer et al., 2011). The snow cover is strongly characterized by wind drift and is usually very shallow with maximum depths of about 0.5 m (Boike et al., 2013). The land surface at the field site is dominated by polygonal tundra mainly vegetated by mosses and sedges (Kutzbach et al., 2004). The tundra soil consists of water-/ice-saturated sandy peat with the water table usually close to the surface (Langer et al., 2011). The volumetric mineral content is reported to range between 20 and 40 % while the volumetric organic content is on the order of 5–10 % (Kutzbach et al., 2004; Langer et al., 2011). The peat soil complex reaches depths of 10–15 m and is underlain by sandy-to-silty river deposits reaching depths of at least 1 km.

Hourly values of air temperature, precipitation (not in winter), wind speed and incoming longwave radiation is provided by the site measurements. Winter precipitation and incoming shortwave radiation are complemented by WATCH reanalysis data. Altogether a continuous model forcing data set is created. Minor gap filling was needed to fill in the missing data. The time period for the prepared data set is from July 2003 to October 2005.

2.4.3 Circumarctic data sets

The International Permafrost Association's (IPA) permafrost map (Brown et al., 2002) was used for comparing the simulated permafrost extent with the observations. Although the IPA map has distinct permafrost classes, only the outer border of the discontinuous and sporadic zones was considered when comparing with the model's permafrost extent, which is calculated using the simulated soil temperatures from the circumarctic model simulation. Following the permafrost definition of IPA (soils under freezing temperatures for at least 2 consecutive years), the permafrost state of each grid box is determined. The permafrost condition for each grid box was calculated with regards to the soil

temperature only. For all of the five soil layers the temperatures are checked if any of the layers are staying below 0° for at least 2 years. For comparing with the IPA map, the 1980–1990 average values of the model's permafrost state were used.

The Circumpolar Active Layer Monitoring network's (CALM) data set (Brown et al., 2000) was used for evaluating the simulated active-layer thickness. The CALM network maintains active layer thickness measurements at more than 200 sites since the 1990s. We have chosen the CALM sites within the continuous permafrost zone in our simulation domain and compared them with the corresponding $0.5° \times 0.5°$ grid box of the results from the simulation conducted using global climate and soil texture data as forcing. Using a linear piecewise interpolation the simulated soil temperatures in five soil layers are interpolated into 200 evenly spaced nodes and the depth of 0° is calculated afterwards to represent the thawing depth at each time step. Then the maximum thawing depth during the summer season is taken to be the active-layer depth for comparison. If there were more than one CALM site within one model grid box, the most appropriate one is chosen for the comparison. Averaging several CALM sites within one grid box is avoided since the average value could represent a nonrealistic condition due to surface heterogeneity. We tried to select the site that is most comparable with the model assumptions (e.g., upland soils) and the soil conditions represented by the global soil map. Since not all the sites had recorded measurements during the 1990–2010 period, we have averaged the existing years of data and compared it with the averages of corresponding years from the model output.

Numerous borehole observations from circumarctic stations were gathered during the International Polar Year (IPY 2007/2008). They include deep and shallow borehole temperature observations representing the state of the permafrost (Romanovsky et al., 2010b). These borehole measurements are available through Global Terrestrial Network for Permafrost (GTN-P). Observations from these borehole measurements were compared with the simulated temperatures. As in the CALM comparison, the corresponding grid box values of the JSBACH simulation results were used for comparison. Since there were more boreholes in most of the grid boxes and surface heterogeneity has less effect on deep soil temperatures (7–10 m depth), we have performed a grid averaging to compare with the model outputs. The time period chosen for the comparison follows the IPY period: averaging years 2007 and 2008 outputs.

2.4.4 Continental-scale maps

The Russian permafrost temperature map (Land Resources of Russia CD-ROM, 2002) was prepared by the Russian Academy of Sciences and The International Institute for Applied Systems Analysis (IIASA). This map is an upscaled product of several meteorological and soil station data that
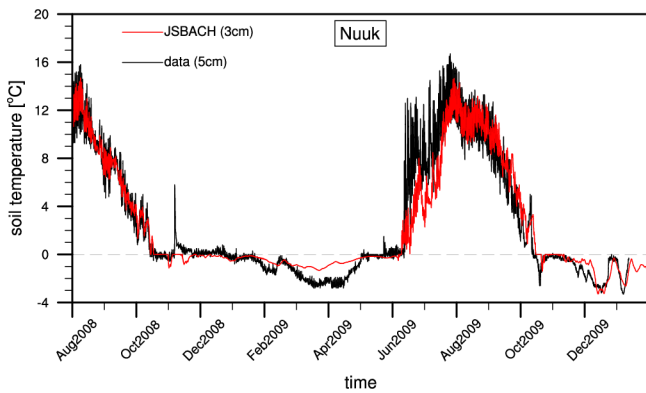
Fig. 2. Observed and simulated upper-layer soil temperature at the Nuuk site. Observed soil temperature at 5 cm is plotted with the black line and the red line shows the JSBACH-simulated soil temperature in the first layer (ca. 3 cm).
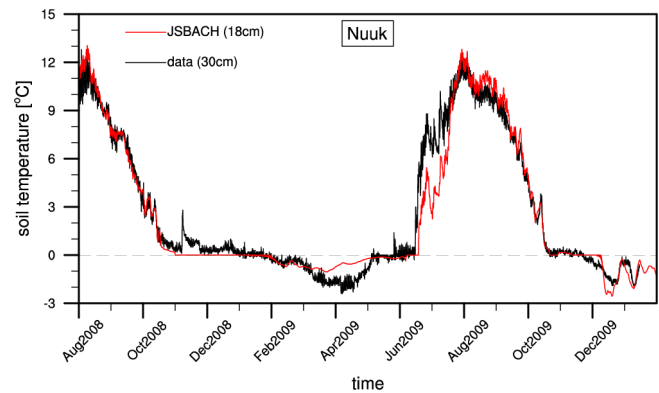

Fig. 3. Observed and simulated soil temperature at the Nuuk site. Observed soil temperature at 30 cm is plotted with the black line and the red line shows the JSBACH-simulated soil temperature in the second layer (ca. 18 cm).

are gathered during the expeditions in the second half of the 20th century. The data is digitally available (Land Resources of Russia CD-ROM, 2002) and downloadable from the web server of the IIASA (Land Resources of Russia). In the map, permafrost temperature is distinguished as 9 temperature classes and the temperature ranges (range of 1 or 2 °C) show a scale from 0 to −17 °C. To prepare a map comparable with JSBACH simulation results, the mean of the observed temperature classes were used to plot the observational map in this paper. Since there was no detailed information about the depths of these observations, values are assumed to be representative of those at depth of no seasonal temperature change. Following the observational time period, mean JSBACH subsoil temperature (last soil layer, ca. 7 m) of the 1960–1990 period was used for comparison.

The 0.5° active-layer thickness map (Beer et al., 2013) from Yakutia is an upscaled digitized version of the map of landscapes and permafrost conditions in Yakutia (Fedorov et al., 1989, 1991). Covering most of eastern Siberia, this map is very useful to understand the permafrost conditions at a 1 : 2 500 000 spatial scale during the period 1960–1987. Maps of mean and standard deviation of active-layer thickness were prepared at 0.5° spatial resolution based on 0.001° raster images. Active-layer thickness values range from 0.4 m at the northern continuous permafrost zone to 2.5 m at the southern borders of permafrost where isolated patches dominate the landscape.

For comparison with the active-layer thickness map, soil temperatures simulated at a 0.5° spatial scale during the period 1960–1990 were used to derive the model's active-layer thickness, and then the mean of all these years is used to prepare the comparison map.

2.4.5 Arctic river runoff data

There are several big rivers flowing into the Arctic Ocean from Russia, Canada and Alaska; and they are all affected by the conditions of permafrost underlying their respective basins. By comparing the temporal dynamics of runoff values at the river mouths, the model performance in representing the interactions between permafrost processes and the hydrological scheme can be assessed all around the basin areas. For testing model hydrological processes, runoff data from the Lena and Yenisey rivers were compared to simulation results. The runoff observations at the river mouth stations were gathered from the R-ArcticNET database (Lammers et al., 2001). The simulated runoff values in all the grid boxes within river basins were accumulated. For the evaluation of the seasonal cycle, simulation results were shifted by 2 months accounting for the time lag between the further grid cells and the river mouth station, for the reason that JSBACH does not include a river routing scheme.

3 Results and discussions

3.1 Site-level validation

By forcing JSBACH with the meteorological data from the Nuuk synoptic station, a site-level simulation was performed. JSBACH successfully captured the topsoil temperature dynamics during the simulation period (Figs. 2 and 3). Following the observations, summer 2008 topsoil temperatures gradually cool down to 0 °C. Simulated temperatures fluctuate around 0 °C from October to February, in agreement with the observed data. After June, when the simulated temperatures are above zero, it takes until mid-July to capture the observations again during the summer of 2009.
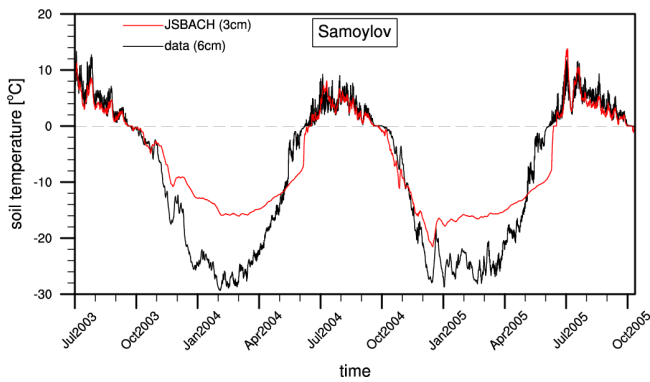
Fig. 4. Observed and simulated upper-layer soil temperature at the Samoylov site. Observed soil temperature at 6 cm is plotted with the black line and the red line shows the JSBACH-simulated soil temperature in the first layer (ca. 3 cm).
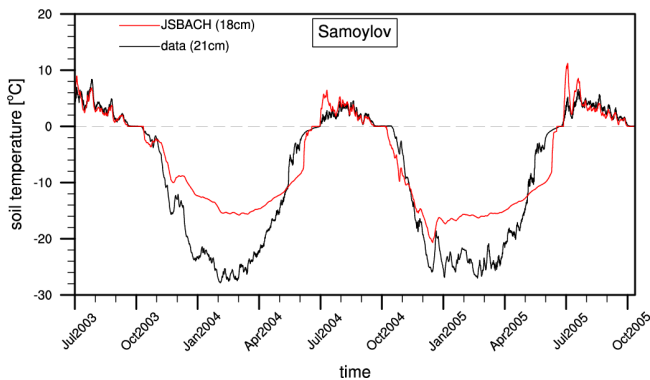

Fig. 5. Observed and simulated soil temperature at the Samoylov site. Observed soil temperature at 21 cm is plotted with the black line and the red line shows the JSBACH-simulated soil temperature in the second layer (ca. 18 cm).

The second site's simulation is performed at the Samoylov site, where the conditions are representative of wet tundra permafrost. Except for the overestimations during early summer, JSBACH results successfully captured the summer temperature dynamics at different soil depths (Figs. 4 and 5). During autumn, simulated temperatures are falling down with a similar slope to the observations, while the warming up period (May–June) displays an underestimation compared to the observed values. However, winter temperatures are not simulated as cold as the observed values. The minimum value of the JSBACH winter temperatures are 10–15 °C warmer than the observations (Figs. 4–6). As in the Nuuk comparison, the zero curtain is also seen at Samoylov. The timing of the freezing is also well represented by the model. Both observed and simulated temperatures are stagnating at around 0 °C during the freezing period of September–October (Fig. 5). Figure 6 shows the temperatures at a year-long frozen depth, where the model comparison to the observed values show similar dynamics.
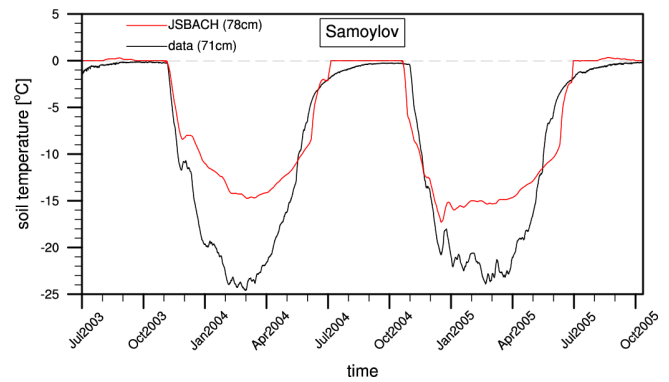

Fig. 6. Observed and simulated soil temperature at the Samoylov site. Observed soil temperature at 71 cm is plotted with the black line and the red line shows the JSBACH-simulated soil temperature in the third layer (ca. 78 cm).

A more detailed analysis of these comparisons requires mentioning the effects of freeze/thaw cycles. The latent heat released (consumed) when the soil water freezes (melts) is responsible for delaying the cold (heat) penetration into the soil. The site simulation results show that the topsoil temperatures are wavering around 0 °C during the phase change event. This so-called zero-curtain effect is also visible in the observational data (Figs. 2–5). This match indicated that the phase change is accurately represented by the model.

It is seen from both site-level comparisons that winter soil temperatures do not drop as low as might be expected due to atmospheric conditions alone. Even when the air temperature is minimal in high winter (ca. −20 °C for Nuuk and −40 °C for Samoylov, not shown), soil keeps a rather warm temperature profile (ca. −3 °C for Nuuk and −25 °C for Samoylov) as long as snow exists on top.

However, in reality, snow has rather complicated characteristics. Within the snowpack, metamorphism processes create various types of snow with different thermal properties (Loth and Graf, 1993). When there is new snowfall, fresh snow presses down to squeeze the air out of deeper snow layers, thus increasing the snow density. With higher density, the snow insulation effect decreases due to increased snow heat conductivity. However, depending on site-specific conditions, springtime snow insulation can be altered due to the effects of depth hoar formation, wind drift or snowmelt water. Snow properties can also be modified by rainwater percolation into the snowpack. Also, snowmelt water infiltration into the soil can change the temperature profile of the soil. Additionally snow albedo changes with these processes. Boike et al. (2013) explained the strong wind conditions at Samoylov, where the maximum snow depth does not exceed 0.5 m. However this is not the case in JSBACH simulations, so there is an overestimation in simulated snow depths (Fig. 7). Such effects are still not represented in the current version of JSBACH and they can explain the mismatch in
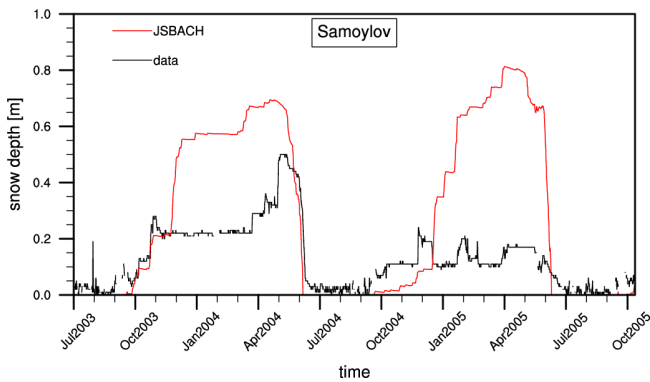
Fig. 7. Observed and simulated snow depth at the Samoylov site.

simulated versus observed springtime soil temperature in the Samoylov site-level simulations (Figs. 4 and 5). Without dynamically changing snow properties and lack of these snow-specific processes, our model cannot correctly represent the lower spring insulation and keeps a colder soil temperature profile. Similar effects were also shown by Westermann et al. (2013). Zhang et al. (2005) and Langer et al. (2013) pointed out the importance of correct parameterization of the snow thermal properties in permafrost simulations. Further progress in resolving these issues will be shown in the next model version.

3.2 Circumarctic validation

To evaluate the model's reliability at circumarctic scale, we compared the IPA permafrost map (Brown et al., 2002) with the simulated permafrost extent. Depending on the permafrost coverage, the IPA map classifies the permafrost zones as continuous, discontinuous, sporadic permafrost and isolated patches. However, within a global model, we do not represent such classification inside a grid cell, but rather classify permafrost or non-permafrost conditions. Having this in mind, it is seen in Fig. 8 that in general the simulated permafrost extent is in good agreement with the IPA map. It covers all the continuous and discontinuous zones and extends further to include some parts of the sporadic permafrost zone and isolated patches. By definition, sporadic permafrost has 10–50 % of permafrost coverage and isolated patches have less than 10 %. Simulating permafrost in some of these regions is assumed to be realistic when the binary criterion permafrost/no permafrost is used in the model.

Another criterion for assessing the validity of our simulation results is to evaluate active-layer thickness. By definition, active-layer thickness is the maximum thawing depth in permafrost areas during any given year. It can be considered a good measure of climate state since it is affected by summer temperature, precipitation, timing of snowmelt and history of soil temperature combined. For this reason, we have compared the current state (1990–2010) of the simulated active-layer thickness with the CALM network data.
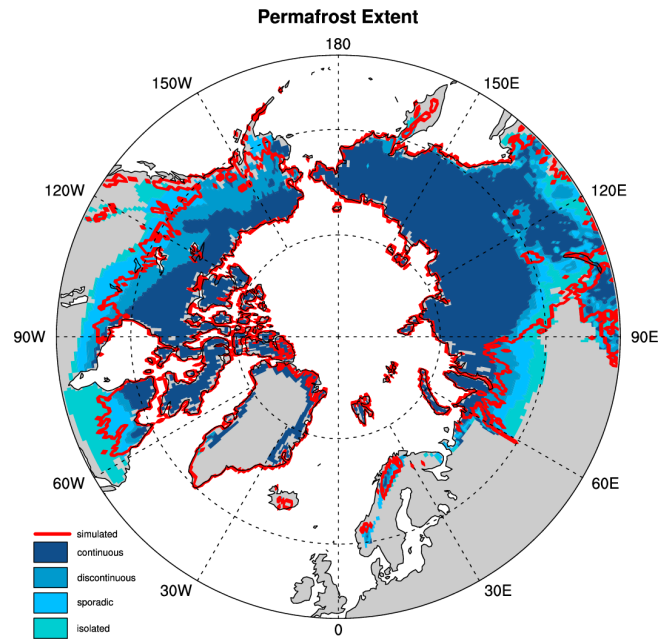

Fig. 8. Northern Hemisphere permafrost extent according to the International Permafrost Association's permafrost map (Brown et al., 2002). Different permafrost classes are plotted in different colors and the red line shows the border of the permafrost extent calculated from the JSBACH simulation (1980–1990 average values).
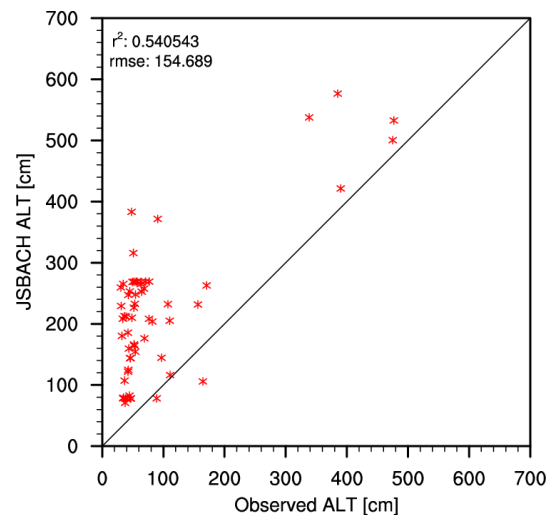

Fig. 9. Scatter plot of the observed ALT from the CALM network (Brown et al., 2000) versus the JSBACH results. See text for further info.

JSBACH matched the active-layer thickness of some of the sites better than the others but in general there is an overestimation in simulated active-layer thickness (Fig. 9).

Reasons for this mismatch are mostly explained by scale issues and site-specific conditions together with the model's vertical resolution. First, the model output from a $0.5° \times 0.5°$ grid box cannot be taken as equally comparable to the site's

observations given that the grid-box average is not fully representative for the heterogeneous surface conditions in this area. Even though some of the CALM observations were averaged over 1 km ×1 km areas, the landscape variability still brings up a big uncertainty when compared to a model grid-box average. It is important to note that for this comparison, the model was driven by global climate and soil properties data sets (Sect. 2.2) and not by specific characteristics at CALM stations. Hence, part of the scatter in Fig. 9 can be explained by the wrong representation of soil properties or local climate conditions. Therefore, the overestimation of site-level active-layer thickness should be interpreted in concert with the comparisons of spatial details of active-layer thickness (ALT) and permafrost temperature (see next section). All things considered, site-level model estimates are fairly comparable to observations (r^2: 0.54, Fig. 9). Similar results are observed in some other modeling studies. Dankers et al. (2011) have shown a deeper simulated ALT using the JULES (Joint UK Land Environment Simulator) model. Lawrence et al. (2012) have shown that the coupled and uncoupled CLM (Community Land Model) model runs are resulting in deeper ALT in general; although the offline run from the CLM4 model version showed a more distributed result with positive and negative differences. Additionally, it is explained by Gouttevin et al. (2012a) that the freezing scheme brought a better match with the CALM observations but still with a positive bias.

Complementary to CALM comparisons, borehole temperature records from GTN-P were used to evaluate simulated subsoil temperatures (last model layer, ca. 7 m). In general, the model can explain about 48 % of observed subsoil temperature variation with a tendency to a cold bias at some sites (Fig. 10). This cold bias can partly be related to the model assumption of zero heat flux at the bottom of the soil. Previously shown by Lawrence and Slater (2005), the CLM3 model (with 3.43 m soil depth and vanishing heat flux at the bottom) simulated strong permafrost degradation by 2100. Delisle (2007) responds to that by showing the importance of including bottom energy flux of the permafrost layer in the model. Delisle (2007) also suggests the necessity of representing soil heat transfer by moving groundwater while Burn and Nelson (2006) explain the CLM3 overestimation of permafrost loss by using wrong surface temperatures and lack of near-surface ground ice in their model. In a newer model version (CLM4), Lawrence et al. (2012) explain the cold bias in deep soil temperatures with the dry active layers in their model, which again brings up the importance of hydrology–heat transfer interactions. Also a deeper soil column representing up to 50 m is suggested to improve the permafrost temperature results by around 10 m for future model versions; although the effects of having this deep soil column is not clear yet. Alexeev et al. (2007) suggests using at least a 30 m soil depth to capture the seasonal temperature variability. So it seems there are a few possible reasons for the cold bias in the JSBACH deep soil temperatures (Fig. 10).
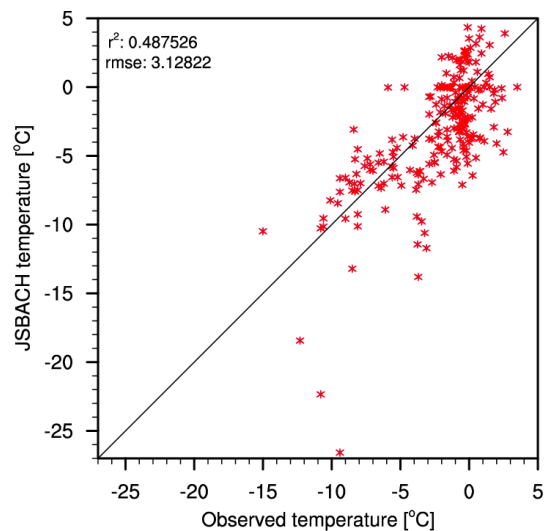

Fig. 10. Scatter plot of observed soil temperature from the GTN-P borehole temperature data set (Romanovsky et al., 2010b) versus simulated subsoil temperature (deepest soil layer, ca. 7 m). See text for further info.

Nonetheless, the borehole temperature comparison illustrates the current status of our model in representing permafrost temperatures and shows the need for future model developments for improvement.

Model results showing deeper active layers seem to disagree with colder soil temperatures at first. However, the active-layer thickness is more related to topsoil temperature, whereas borehole comparisons were used to evaluate deeper layers. The topsoil is strongly coupled to atmospheric conditions and hydrological changes. However, deep soil temperature is less influenced by variable surface conditions, but show a decadal trend that is strongly affected by long-term atmospheric changes, snow depth and vegetation cover dynamics and the boundary conditions at the bottom of the soil column. As described in Dankers et al. (2011), active-layer comparisons are mostly affected by phase change events in the upper layers, but the colder soil temperature in the deeper layers is not strongly related to these phase change effects. Similar cold biases in deep soil temperature are also documented in other modeling studies (Gouttevin et al., 2012a; Lawrence et al., 2012).

3.3 Continental-scale validation

Spatial details of modeled permafrost temperature were compared to the Russian permafrost temperature map (Land Resources of Russia CD-ROM, 2002). The simulated latitudinal temperature gradient acts in accordance with the observation-based map albeit with regional underestimation of the model output (Fig. 11). Figure 12 shows the spatial pattern of this cold bias. In general, permafrost temperature differs from −2 to −5 °C, except in northern Yakutia where the
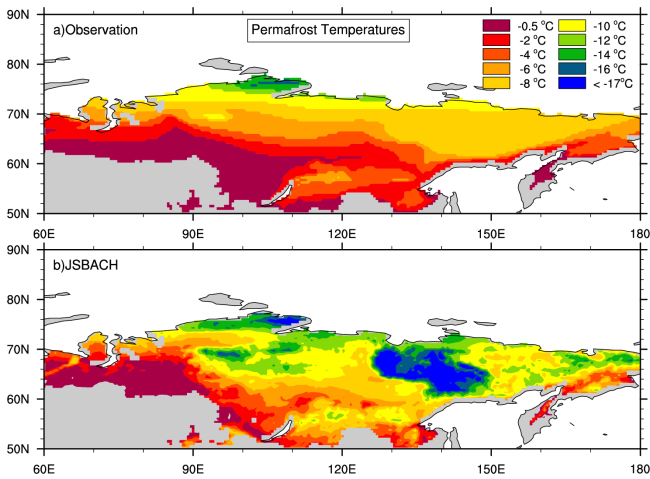
Fig. 11. Comparison of Russian permafrost temperature. Observed (map **a**; see text for more details) (Land Resources of Russia CD-ROM, 2002) and simulated (map **b**) Russian permafrost temperature during the period 1960–1990. The average values in different temperature classes are plotted with the same color in both maps.
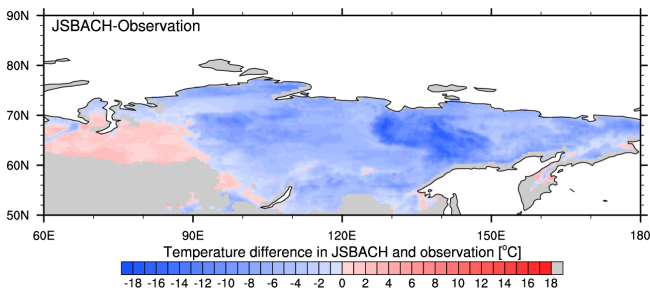

Fig. 12. Difference of simulated and observed permafrost temperatures (map **b−a** from Fig. 11).

Fig. 13. Observed (map **a**; see text for more details) (Beer et al., 2013) and simulated active-layer thickness (map **b**) in the Yakutsk area.

difference can be as great as −16 °C. A cold bias in subsoil temperature was also seen in the borehole temperature comparison, supporting the fact that it is not a regional issue but rather a global deficiency of the model or the global climate forcing data set. As discussed above, one potential reason for the colder soil temperature is the bottom boundary zero heat flux assumption. This assumption is widely used in the global modeling community (Dankers et al., 2011; Lawrence et al., 2008), but evidently the soil column depth also plays an important role (Alexeev et al., 2007).

It is also important to mention the higher spatial heterogeneity of JSBACH soil temperature when compared to the observation-based map. Since the observations were gathered very sparsely (due to harsh climate conditions and remote locations in Siberia) and widely interpolated to create such a large regional product, many features from landscape heterogeneity were lost in making the Russian permafrost temperature map. On the contrary, the model simulates each grid box individually by using meteorological forcing and surface conditions specific to each grid box. This explains
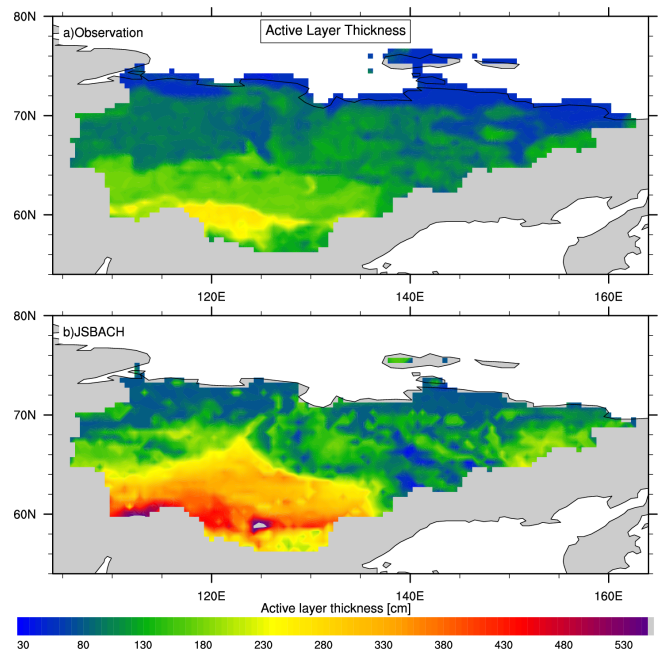
the longitudinal changes in the model output (Fig. 11). Also, representing a different snow depth as well as not matching the distribution of moss cover affect the amount of heat insulation for the soil and alter the whole soil temperature profile.

Another regional evaluation performed was the comparison of observed and simulated active-layer thickness maps. Figure 13 shows the comparison of the active-layer thickness map of Yakutia (Beer et al., 2013) and the spatial distribution of active-layer thickness estimated by JSBACH. As in the permafrost temperature comparison (Fig. 11), a similar latitudinal gradient is observed in both maps. Although the observation-based map shows smaller values in the northern coastal regions, the transition of values from 50 cm at the coast to 250 cm further inland is comparable to the JSBACH map. The mismatches at the coast can be due to the thick ice overburden in those areas, which are not represented by JSBACH. The differences between the observed and simulated results (Fig. 14) show a more diverse spatial pattern than the map of temperature differences (Fig. 12). This is due to the complex nature of confounding factors of active-layer thickness i.e., soil temperature, snow-moss cover and soil moisture. In general there is an overestimation in simulated active-layer thicknesses. As seen from the CALM comparison (Fig. 9), JSBACH simulates deeper active-layer depths. However, regional differences are apparent in this comparison. Unlike the CALM comparison where all the sites were overestimated, the blue regions in the difference map (Fig. 14) show the underestimated active-layer depths from model results. These mismatches can be attributed to
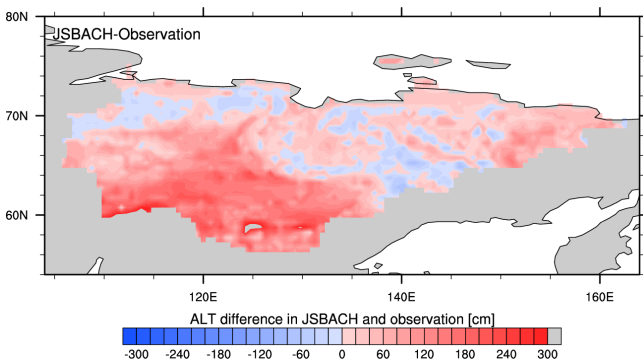
Fig. 14. Difference of simulated and observed active-layer thickness-ALT (map b−a from Fig. 13).

Fig. 15. Simulated and observed annual Lena River runoff. Red line represents the JSBACH model version with the permafrost representation. The black line shows the observed values from the R-ArcticNet database (Lammers et al., 2001).

Fig. 16. Simulated and observed monthly mean Lena River runoff. Line colors are the same as annual runoff plot (red: model values; black: observed values). Since the model does not use a river routing scheme, the model results are shifted 2 months to match the actual peak time in spring.

not representing vegetation and snow cover properly. Finally, the southern borders of the comparison map (Fig. 14) illustrate a strong positive bias (ca. +250 cm). As explained in Beer et al. (2013), isolated permafrost patches are dominant in these areas. However, the comparison is not very useful for these areas since the 0.5° values in the observation-based map represent an average of values in permafrost islands while the model is simulating a mean soil temperature profile for the 0.5° grid cell from which active-layer thickness is estimated. Therefore, model results of ALT are expected to be higher in these areas.

3.4　River runoff validation

To evaluate the hydrological processes, Arctic river runoff dynamics were compared to the model results. The Lena River was chosen since it has one of the basin areas least influenced by anthropogenic activities and represents a more natural pattern that is easily comparable to the model results. The current model version can simulate the annual changes (Fig. 15) and the monthly dynamics (Fig. 16) of the Lena River runoff close to the observations. Permafrost conditions allow the soil to block water infiltration during the snowmelt period leading to a dramatic runoff peak in spring. JSBACH successfully captured these effects. Similar results have been observed in other studies (Beer et al., 2007; Gouttevin et al., 2012a).

In addition, the Yenisey River was chosen as a secondary basin since it has one of the biggest basins among the Arctic rivers. In general, this comparison is similar to the Lena Basin comparison. JSBACH underestimated the annual runoff values (Fig. 17) but matched the monthly dynamics (Fig. 18). The only issue here is the low values of the annual runoff. Simulating the Yenisey Basin has a higher uncertainty, since more landscape types are involved. Nevertheless, JSBACH captured the temporal dynamics of the Yenisey River runoff values, thus supporting the validity of the permafrost–hydrology interactions within the model. Interestingly, the model fails to reproduce the runoff increase
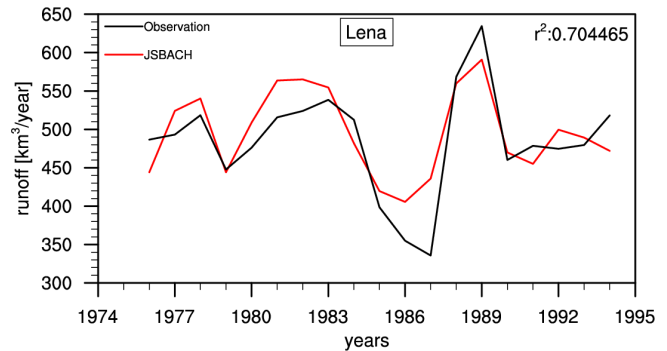
since 1983. This could be partly due to a global dimming effect on stomatal conductance, which influences transpiration (Gedney et al., 2006). However, other effects, such as snowmelt dynamics have an impact as well.

4　Conclusions

In this paper, we have presented an advanced version of the process-oriented ecosystem model JSBACH that simulates cold regions through enhanced representation of snow and soil physics. By including the phase-change process, coupled thermal and hydrological processes and heat insulation from snow and moss cover, the current model version is a capable tool for simulating the physical state of high-latitude terrestrial environments. A multiscale evaluation was conducted and the results demonstrate the strength and weaknesses of the model. Site-level comparisons at both permafrost and non-permafrost sites indicate the importance of freezing and thawing together with snow insulation for

Fig. 17. Simulated and observed annual Yenisey River runoff. Red line represents the JSBACH model version with the permafrost representation. The black line shows the observed values from the R-ArcticNet database (Lammers et al., 2001).
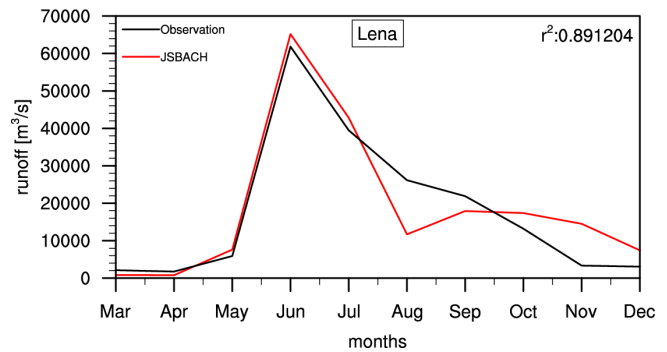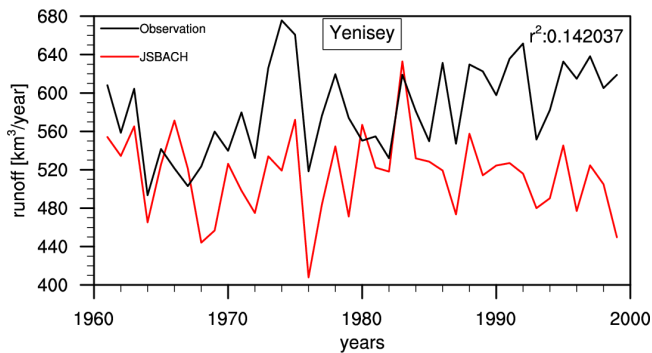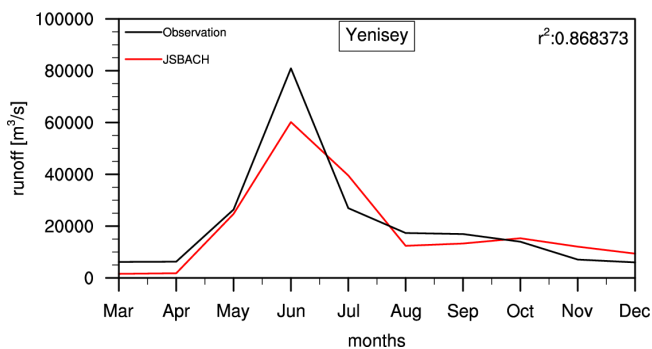

Fig. 18. Simulated and observed monthly mean Yenisey River runoff. Line colors are as in Fig. 17. As for the simulated Lena River runoff in Fig. 16, the model results are shifted 2 months to match the actual peak time in spring due to the lack of river routing scheme in the model.

representing soil temperature dynamics. On the larger scale, permafrost extent is successfully reproduced. Comparisons with circumarctic observational data sets revealed that the model simulates deeper active-layer thicknesses accompanied with colder subsoil temperatures. These issues are explained by the differences in snow cover and moss-layer distributions that are not captured by the model, shallow depth of the soil column and the vanishing heat flux assumption at the bottom. Additionally, regional comparisons drew attention to the heterogeneous vegetation cover and the influence of topographic effects. In conclusion, this modeling study highlights the importance of the effects of latent heat and insulation from snow/moss cover in simulating the permafrost state in high-latitude regions.

References

ACIA: Arctic Climate Impact Assessment, Cambridge University Press, New York, USA, 1042 pp., 2005.

Alexeev, V. A., Nicolsky, D. J., Romanovsky, V. E., and Lawrence, D. M.: An evaluation of deep soil configurations in the CLM3 for improved representation of permafrost, Geophys. Res. Lett., 34, L09502, doi:10.1029/2007GL029536, 2007.

Beer, C.: The Arctic carbon count, Nat. Geosci., 1, 569–570, doi:10.1038/ngeo292, 2008.

Beer, C., Lucht, W., Gerten, D., Thonicke, K., and Schmullius, C.: Effects of soil freezing and thawing on vegetation carbon density in Siberia: A modeling analysis with the Lund-Potsdam-Jena Dynamic Global Vegetation Model (LPJ-DGVM), Global Biogeochem. Cy., 21, GB1012, doi:10.1029/2006GB002760, 2007.

Beer, C., Fedorov, A. N., and Torgovkin, Y.: Permafrost temperature and active-layer thickness of Yakutia with 0.5-degree spatial resolution for model evaluation, Earth Syst. Sci. Data, 5, 305–310, doi:10.5194/essd-5-305-2013, 2013.

Beer, C., Weber, U., Tomelleri, E., Carvalhais, N., Mahecha, M., and Reichstein, M.: Harmonized European long-term climate data for assessing the effect of changing temporal variability on landatmosphere CO_2 fluxes, J. Climate, doi:10.1175/JCLI-D-13-00543.1, in press, 2014.

Beringer, J., Lynch, A. H., Chapin III, F. S., Mack, M., and Bonan, G. B.: The representation of Arctic Soils in the Land Surface Model: The Importance of Mosses, J. Climate, 14, 3324–3335, 2001.

Boike, J., Wille, C., and Abnizova, A.: Climatology and summer energy and water balance of polygonal tundra in the Lena River Delta, Siberia, J. Geophys. Res., 113, G03025, doi:10.1029/2007JG000540, 2008.

Boike, J., Kattenstroth, B., Abramova, K., Bornemann, N., Chetverova, A., Fedorova, I., Fröb, K., Grigoriev, M., Grüber, M., Kutzbach, L., Langer, M., Minke, M., Muster, S., Piel, K., Pfeiffer, E.-M., Stoof, G., Westermann, S., Wischnewski, K., Wille, C., and Hubberten, H.-W.: Baseline characteristics of climate, permafrost and land cover from a new permafrost observatory in the Lena River Delta, Siberia (1998–2011), Biogeosciences, 10, 2105–2128, doi:10.5194/bg-10-2105-2013, 2013.

Boone, A. and Etchevers, P.: An Intercomparison of Three Snow Schemes of Varying Complexity Coupled to the Same Land Surface Model: Local-Scale Evaluation at an Alpine Site, J. Hydrometeorol., 2, 374–394, 2001.

Brovkin, V., Raddatz, T., Reick, C. H., Claussen, M., and Gayler, V.: Global biogeophysical interactions between forest and climate, Geophys. Res. Lett., 36, L07405, doi:10.1029/2009GL037543, 2009.

Brown, J., Hinkel, K. M., and Nelson, F. E.: The circumpolar active layer monitoring (CALM) program: research designs and initial results, Polar Geography, 3, 165–258, 2000.

Brown, J., Ferrians Jr., O. J., Heginbottom, J. A., and Melnikov, E. S.: Circum-Arctic map of permafrost and ground-ice conditions (Version 2), National Snow and Ice Data Center, Boulder, CO, USA, available at: http://nsidc.org/data/ggd318.html (last access: 10 September 2012), 2002.

Burke, E. J., Hartley, I. P., and Jones, C. D.: Uncertainties in the global temperature change caused by carbon release from permafrost thawing, The Cryosphere, 6, 1063–1076, doi:10.5194/tc-6-1063-2012, 2012.

Burn, C. R. and Nelson, F. E.: Comment on "A projection of severe near-surface permafrost degradation during the 21st century" by Lawrence, D. M. and Slater, A. G., Geophys. Res. Lett., 33, L21503, doi:10.1029/2006GL027077, 2006.

Christiansen, H. H., Etzelmüller, B., Isaksen, K., Juliussen, H., Farbrot, H., Humlum, O., Johansson, M., Ingeman-Nielsen, T., Kristensen, L., Hjort, J., Holmlund, P., Sannel, A. B. K., Sigsgaard, C., Åkerman, H. J., Foged, N., Blikra, L. H., Pernosky, M. A., and Ødegård, R. S.: The thermal state of permafrost in the nordic area during the international polar year 2007–2009, Permafrost Periglac. Process., 21, 156–181, 2010.

Clapp, R. B. and Hornberger, G. M.: Empirical equations for some soil hydraulic properties, Water Resour. Res., 14, 601–604, 1978.

Collatz, G., Ribas-Carbo, M., and Berry, J.: Coupled photosynthesis-stomatal conductance model for leave of C4 plants, Aust. J. Plant Physiol., 19, 519–538, 1992.

Dankers, R., Burke, E. J., and Price, J.: Simulation of permafrost and seasonal thaw depth in the JULES land surface scheme, The Cryosphere, 5, 773–790, doi:10.5194/tc-5-773-2011, 2011.

DeConto, R. M., Galeotti, S., Pagani, M., Tracy, D., Schaefer, K., Zhang, T., Pollard, D., and Beerling, D. J.: Past extreme warming events linked to massive carbon release from thawing permafrost, Nature, 484, 87–91, 2012.

Dee, D. P., Uppala, S. M., Simmons, A. J., Berrisford, P., Poli, P., Kobayashi, S., Andrae, U., Balmaseda, M. A., Balsamo, G., Bauer, P., Bechtold, P., Beljaars, A. C. M., van de Berg, L., Bidlot, J., Bormann, N., Delsol, C., Dragani, R., Fuentes, M., Geer, A. J., Haimberger, L., Healy, S. B., Hersbach, H., Holm, E. V., Isaksen, L., Kalberg, P., Kohler, M., Matricardi, M., McNally, A. P., Monge-Sanz, B. M., Morcrette, J. J., Park, B. K., Peubey, C., de Rosnay, P., Tavolato, C., Thepaut, J. N., and Vitart F.: The ERA-Interim reanalysis: Configuration and performance of the data assimilation system, Q. J. Roy. Meteorol. Soc., 137, 553–597, 2011.

Delisle, G.: Near-surface permafrost degradation: How severe during the 21st century?, Geophys. Res. Lett., 34, L09503, doi:10.1029/2007GL029323, 2007.

De Vries, D. A.: Thermal properties of soils, Physics of Plant Environment, edited by: van Wijk, W. R., North Holland, Amsterdam, 1963.

Dümenil, L. and Todini, E.: A rainfall-runoff scheme for use in the Hamburg climate model, in: Advances in theoretical hydrology – a tribute to James Dooge, edited by: Kane, J. P., 129–157, 1992.

Dutra, E., Balsamo, G., Viterbo, P., Miranda, P. M. A., Beljaars, A., Schär, C., and Elder, K.: An Improved Snow Scheme for the ECMWF Land Surface Model: Description and Offline Validation, J. Hydrometeorol., 11, 899–916, 2010.

FAO, IIASA, ISRIC, ISS-CAS, and JRC: Harmonized World Soil Database (version 1.1) FAO, Rome, Italy and IIASA, Laxenburg, Austria, 2009.

Farquhar, G., Caemmerer, S., and Berry, J.: A biochemical-model of photosynthetic CO_2 assimilation in leaves of C3 Species, Planta, 149, 78–90, 1980.

Fedorov, A. N., Botulu, T. A., and Varlamov, S. P.: Permafrost Landscape of Yakutia Novosibirsk: GUGK, 170, 1989 (in Russian).

Fedorov, A. N., Botulu, T. A., Varlamov, S. P., and Melnikov, P. I.: Permafrost Landscape Map of Yakutia ASSR, Scale 1:2500000, Moscow: GUGK, 1991.

Gedney, N., Cox, P. M., Betts, R. A., Boucher, O., Huntingford, C., and Stott, P. A.: Detection of a direct carbon dioxide effect in continental river runoff records, Nature, 439, 835–838, 2006.

GLC2000 database: Global Land Cover 2000 database, European Commission, Joint Research Centre, available at: http://bioval.jrc.ec.europa.eu/products/glc2000/glc2000.php (last access: 5 May 2012), 2003.

Goodrich, L.: The influence of snow cover on the ground thermal regime, Can. Geotech. J., 19, 421–432, 1982.

Gouttevin, I., Krinner, G., Ciais, P., Polcher, J., and Legout, C.: Multi-scale validation of a new soil freezing scheme for a land-surface model with physically-based hydrology, The Cryosphere, 6, 407–430, doi:10.5194/tc-6-407-2012, 2012a.

Gouttevin, I., Menegoz, M., Dominé, F., Krinner, G., Koven, C., Ciais, P., Tarnocai, C., and Boike, J.: How the insulating properties of snow affect soil carbon distribution in the continental pan-Arctic area, J. Geophys. Res., 117, G02020, doi:10.1029/2011JG001916, 2012b.

Grigoriev, M., Imaev, V., Imaeva, L., Kozmin, B., Kunitzkiy, V., Lationov, A., Mikulenko, K. I., Skrjabin, R. M., and Timirsin, K. V.: Geology, seismicity and cryogenic processes in the arctic areas of Western Yakutia, Yakutsk: Yakut Scientific Centre SD RAS, 84, 1996.

Groffman, P. M., Hardy, J. P., Driscoll, C. T., and Fahey, T. J.: Snow depth, soil freezing, and fluxes of carbon dioxide, nitrous oxide and methane in a northern hardwood forest, Glob. Change Biol., 12, 1748–1760, doi:10.1111/j.1365-2486.2006.01194.x, 2006.

Gruber, S.: Derivation and analysis of a high-resolution estimate of global permafrost zonation, The Cryosphere, 6, 221–233, doi:10.5194/tc-6-221-2012, 2012.

Hagemann, S. and Stacke, T.: Impact of soil hydrology scheme on simulated soil moisture memory, Clim. Dynam., submitted, 2014.

Hagemann, S., Blome, T., Saeed, F., and Stacke, T.: Perspectives in modelling climate-hydrology interactions, Surveys in Geophysics, ISSI special issue on Hydrological Cycle, doi:10.1007/s10712-013-9245-z, online first, 2013.

Hansen, M., DeFries, R., Townshend, J., Carroll, M., Dimiceli, C., and Sohlberg, R.: Vegetation Continuous Fields MOD44B, 2001 Percent Tree Cover, Collection 3 University of Maryland, College Park, Maryland, 2003.

Hayes, D. J., McGuire, A. D., Kicklighter, D. W., Gurney, K. R., Burnside, T. J. and Melillo, J. M.: Is the northern high-latitude

land-based CO_2 sink weakening?, Global Biogeochem. Cy., 25, 1–14, 2011.

Heimann, M. and Reichstein, M.: Terrestrial ecosystem carbon dynamics and climate feedbacks, Nature, 451, 289–292, 2008.

Hinzman, L. D., Goering, D. J., and Kane, D. L.: A distributed thermal model for calculating soil temperature profiles and depth of thaw in permafrost regions, J. Geophys. Res., 103, 28975–28991, 1998.

Hugelius, G., Kuhry, P., Tarnocai, C., and Virtanen, T.: Soil organic carbon pools in a periglacial landscape: a case study from the central Canadian Arctic, Permafr. Periglac. Process., 21, 16–29, 2010.

Jensen, L. M. and Rasch, M.: Nuuk Ecological Research Operations, 2nd Annual Report, 2008, Roskilde, National Environmental Research Institute, Aarhus University, Denmark, 80 pp., 2009.

Jensen, L. M. and Rasch, M.: Nuuk Ecological Research Operations, 3rd Annual Report, 2009, Roskilde, National Environmental Research Institute, Aarhus University, Denmark, 80 pp., 2010.

Johansen, O.: Thermal conductivity of soils, Ph.D. thesis, Trondheim, Norway, Cold Regions Research and Engineering Laboratory Draft Translation 637, 1977, ADA 044002, 1975.

Jungclaus, J. H., Fischer, N., Haak, H., Lohmann, K., Marotzke, J., Matei, D., Mikolajewicz, U., Notz, D., and von Storch, J. S.: Characteristics of the ocean simulations in MPIOM, the ocean component of the MPI-Earth system model, J. Adv. Model. Earth Syst., 5, 422–446, doi:10.1002/jame.20023, 2013.

Kelley, J. J. J., Weaver, D. F., and Smith, B. P.: The variation of carbon dioxide under the snow in the Arctic, Ecology, 49, 358–361, 1968.

Knorr, W.: Annual and interannual CO_2 exchanges of the terrestrial biosphere: process-based simulations and uncertainties, Global Ecol. Biogeogr., 9, 225–252, 2000.

Koren, V., Schaake, J., Mitchell, K., Duan, Q., Chen, F., and Baker, J.: A parameterization of snowpack and frozen ground intended for NCEP weather and climate models, J. Geophys. Res., 104, 19569–19585, 1999.

Koven, C. D., Ringeval, B., Friedlingstein, P., Ciais, P., Cadule, P., Khvorostyanov, D., Krinner, G. and Tarnocai, C.: Permafrost carbon-climate feedbacks accelerate global warming, Proc. Natl. Aca. Sci. USA, 108, 14769–14774, 2011.

Kutzbach, L., Wagner, D., and Pfeiffer, E.: Effect of microrelief and vegetation on methane emission from wet polygonal tundra, Lena Delta, Northern Siberia, Biogeochemistry, 69, 341–362, 2004.

Lammers, R., Shiklomanov, A., Vorosmarty, C., Fekete, B., and Peterson, B.: Assessment of contemporary Arctic river runoff based on observational discharge records, J. Geophys. Res., 106, 3321–3334, 2001.

Land Resources of Russia: available at: http://webarchive.iiasa.ac.at/Research/FOR/russia_cd/download.htm (last access: 17 January 2013), Land resources of Russia CD-ROM, 2002.

Langer, M., Westermann, S., Muster, S., Piel, K., and Boike, J.: The surface energy balance of a polygonal tundra site in northern Siberia – Part 1: Spring to fall, The Cryosphere, 5, 151–171, doi:10.5194/tc-5-151-2011, 2011.

Langer, M., Westermann, S., Heikenfeld, M., Dorn, W., and Boike, J.: Satellite-based modeling of permafrost temperatures in a tundra lowland landscape, Remote Sensing of Environment, 135, 12–24, doi:10.1016/j.rse.2013.03.011, 2013.

Lawrence, D. M. and Slater, A. G.: A projection of severe near-surface permafrost degradation during the 21st century, Geophys. Res. Lett., 32, L24401, doi:10.1029/2005GL025080, 2005.

Lawrence, D. M., Slater, A. G., Romanovsky, V. E., and Nicolsky, D. J.: Sensitivity of a model projection of near-surface permafrost degradation to soil column depth and representation of soil organic matter, J. Geophys. Res., 113, 1–14, 2008.

Lawrence, D. M., Slater, A. G., and Swenson, S. C.: Simulation of Present-Day and Future Permafrost and Seasonally Frozen Ground Conditions in CCSM4, J. C Climate, 25, 2207–2225, 2012.

Li, Q., Sun, S., and Xue, Y.: Analyses and development of a hierarchy of frozen soil models for cold region study, J. Geophys. Res., 115, D03107, doi:10.1029/2009JD012530, 2010.

Loth, B. and Graf, H.: Snow cover model for global climate simulations, J. Geophys. Res., 98, 451–464, 1993.

Loth, B. and Graf, H.: Modeling the snow cover in climate studies 1.Long-term integrations under different climatic conditions using a multilayered snow-cover model, J. Geophys. Res., 103, 11313–11327, 1998.

Luo, L. F., Robock, A., Vinnikov, K. Y., Schlosser, C. A., Slater, A. G., Boone, A., Braden, H., Cox, P., de Rosnay, P., Dickinson, R. E., Dai, Y. J., Duan, Q. Y., Etchevers, P., Henderson-Sellers, A., Gedney, N., Gusev, Y. M, Habets, F., Kim, J. W., Kowalczyk, E., Mitchell, K., Nasonova, O. N., Noilhan, J., Pitman, A. J., Schaake, J., Shmakin, A. B., Smirnova, T. G., Wetzel, P., Xue, Y. K, Yang Z. L., and Zeng, Q. C.: Effects of frozen soil on soil temperature, spring infiltration, and runoff: Results from the PILPS 2(d) experiment at Valdai, Russia, J. Hydrometeorol., 4, 334–351, 2003.

McGuire, A. D., Anderson, L. G., Christensen, T. R., Dallimore, S., Guo, L., Hayes, D. J., Heimann, M., Lorenson, T. D., Macdonald, R. W., and Roulet, N.: Sensitivity of the carbon cycle in the Arctic to climate change, Ecol. Monogr., 79, 523–555, 2009.

Meinshausen, M., Smith, S. J., Calvin, K., Daniel, J. S., Kainuma, M. L.,T., Lamarque, J. F., Matsumoto, K., Montzka, S. A., Raper, S. C. B., Riahi, K., Thomson, A., Velders, G. J. M., and van Vuuren, D. P. P.: The RCP greenhouse gas concentrations and their extensions from 1765 to 2300, Climatic Change, 109, 213–241, 2011.

Mölders, N., Haferkorn, U., Doering, J., and Kramm, G.: Long-term investigations on the water budget quantities predicted by the hydro-thermodynamic soil vegetation scheme (HTSVS) – Part I: Description of the model and impact of long-wave radiation, roots, snow, and soil frost, Meteorol. Atmos. Phys., 84, 115–135, 2003.

Nicolsky, D. J., Romanovsky, V. E., Alexeev, V. A., and Lawrence, D. M.: Improved modeling of permafrost dynamics in a GCM land-surface scheme, Geophys. Res. Lett., 34, 2–6, 2007.

Niu, G.-Y. and Yang, Z.-L.: Effects of Frozen Soil on Snowmelt Runoff and Soil Water Storage at a Continental Scale, J. Hydrometeorol., 7, 937–952, 2006.

Oelke, C.: Regional-scale modeling of soil freeze/thaw over the Arctic drainage basin, J. Geophys. Res., 108, 1–19, 2003.

Olson, D. M., Dinerstein, E., Wikramanayake, E., Burgess, N., Powell, G., Underwood, E., D'Amico, J., Itoua, I., Strand, H., Morrison, J., Loucks, C., Allnutt, T., Ricketts, T., Kura, Y., Lamoreux, J., Wettengel, W., Hedao, P., and Kassem, K.: Terrestrial Ecore-

gions of the World: A New Map of Life on Earth, BioScience, 51, 933–938, 2001.

Piani, C., Weedon, G., Best, M., Gomes, S., Viterbo, P., Hagemann, S., and Haerter, J.: Statistical bias correction of global simulated daily precipitation and temperature for the application of hydrological models, J. Hydrol., 395, 199–215, 2010.

Ping, C. L., Michaelson, G. J., Jorgenson, M. T., Kimble, J. M., Epstein, H., Romanovsky, V. E., and Walker, D. A.: High stocks of soil organic carbon in the North American Arctic region, Nat. Geosci., 1, 615–619, 2008.

Poutou, E., Krinner, G., Genthon, C. and de Noblet-Ducoudre, N.: Role of soil freezing in future boreal climate change, Clim. Dynam., 23, 621–639, 2004.

Raddatz, T., Reick, C., Knorr, W., Kattge, J., Roeckner, E., Schnur, R., Schnitzler, K.-G., Wetzel, P., and Jungclaus, J.: Will the tropical land biosphere dominate the climate-carbon cycle feedback during the twenty-first century?, Clim. Dynam., 29, 565–574, 2007.

Richards, L. A.: Capillary Conduction of Liquids through Porous Mediums, Physics, 1, 318–333, 1931.

Richtmyer, R. D. and Morton, K. W.: Difference Methods for Initial-Value Problems, Wiley-Interscience, New York, 1967.

Rinke, A., Kuhry, P., and Dethloff, K.: Importance of a soil organic layer for Arctic climate: A sensitivity study with an Arctic RCM, Geophys. Res. Lett., 35, L13709, doi:10.1029/2008GL034052, 2008.

Riseborough, D., Shiklomanov, N., Etzelmuller, B., Gruber, S., and Marchenko, S.: Recent Advances in Permafrost Modelling, Permafr. Periglac. Process., 19, 137–156, 2008.

Roeckner, E., Bäuml, G., Bonaventura, L., Brokopf, R., Esch, M., Giorgetta, M., Hagemann, S., Kirchner, I., Kornblueh, L., Manzini, E., Rhodin, A., Schlese, U., Schulzweida, U., and Tompkins, A.: The atmospheric general circulation model ECHAM 5. PART I: Model description. MPI Report No. 349, Max Planck Institute for Meteorology, Hamburg, 2003.

Romanovsky, V. E., Drozdov, D. S., Oberman, N. G., Malkova, G. V., Kholodov, A. L., Marchenko, S. S., Moskalenko, N. G., Sergeev, D. O., Ukraintseva, N. G., Abramov, A. A., Gilichinsky, D. A., and Vasiliev, A. A.: Thermal state of permafrost in Russia, Permafr. Periglac. Process., 21, 136–155, 2010a.

Romanovsky, V. E., Smith, S. L., and Christiansen, H. H.: Permafrost thermal state in the polar Northern Hemisphere during the international polar year 2007-2009: a synthesis, Permafr. Periglac. Process., 21, 106–116, 2010b.

Schaefer, K., Zhang, T., Slater, A. G., Lu, L., Etringer, A., and Baker, I.: Improving simulated soil temperatures and soil freeze/thaw at high-latitude regions in the Simple Biosphere/Carnegie-Ames-Stanford Approach model, J. Geophys. Res., 114, F02021, doi:10.1029/2008JF001125, 2009.

Schaefer, K., Zhang, T., Bruhwiler, L., and Bareett, A. P.: Amount and timing of permafrost carbon release in response to climate warming, Tellus B, 63, 165–180, 2011.

Schirrmeister, L., Froese, D., Tumskoy, V., Grosse, G., and Wetterich, S.: Yedoma: Late Pleistocene Ice-Rich Syngenetic Permafrost of Beringia, in: The Encyclopedia of Quaternary Science, eidted by: Elias, S. A., vol. 3, 542–552, Amsterdam, Elsevier, 2013.

Schneider von Deimling, T., Meinshausen, M., Levermann, A., Huber, V., Frieler, K., Lawrence, D. M., and Brovkin, V.: Estimating the near-surface permafrost-carbon feedback on global warming, Biogeosciences, 9, 649–665, doi:10.5194/bg-9-649-2012, 2012.

Schuur, E. A. G., Bockheim, J., Canadell, J. G., Euskirchen, E., Field, C. B., Goryachkin, S. V., Hagemann, S., Kuhry, P., Lafleur, P. M., Lee, H., Mazhitova, G., Nelson, F. E., Rinke, A., Romanovsky, V. E., Shiklomanov, N., Tarnocai, C., Venevsky. S., Vogel, J. G., and Zimov, S. A.: Vulnerability of Permafrost Carbon to Climate Change: Implications for the Global Carbon Cycle, BioScience, 58, 701–714, 2008.

Serreze, M., Walsh, J., Chapin, F., Osterkamp, T., Dyurgerov, M., Romanovsky, V., Oechel, W., Morison, J., Zhang, T., and Barry, R.: Observational evidence of recent change in the northern high-latitude environment, Climatic Change, 46, 159–207, 2000.

Slater, A. G., Schlosser, C. A., Desborough, C. E., Pitman, A. J., Henderson-Sellers, A., Robock, A., Vinnikov, K. Y., Entin, J., Mitchell, K., Chen, F., Boone, A., Etchevers, P., Habets, F., Noilhan, J., Braden, H., Cox, P. M., de Rosnay, P., Dickinson, R. E., Yang, Z.-L., Dai, Y.-J., Zeng, Q., Duan, Q., Koren, V., Schaake, S., Gedney, N., Gusev, Y. M., Nasonova, O. N., Kim, J., Kowalczyk, E. A., Shmakin, A. B., Smirnova, T. G., Verseghy, D., Wetzel, P., and Xue, Y.: The representation of snow in land-surface schemes: Results from PILPS 2(d), American Meteorological Society, 2, 7–25, 2001.

Smith, S. L., Romanovsky, V. E., Lewkowicz, A. G., Burn, C. R., Allard, M., Clow, G. D., Yoshikawa, K., and Throop, J.: Thermal state of permafrost in North America: a contribution to the international polar year, Permafr. Perigl. Process., 21, 117–135, 2010.

Stevens, B., Giorgetta, M., Esch, M., Mauritsen, T., Crueger, T., Rast, S., Salzmann, M., Schmidt, H., Bader, J., Block, K., Brokopf, R., Fast, I., Kinne, S., Kornblueh, L., Lohmann, U., Pincus, R., Reichler, T., and Roeckner, E.: The atmospheric component of the MPI-M Earth System Model: ECHAM6, J. Adv. Model. Earth Syst., 5, 146–172, doi:10.1002/jame.20015, 2012.

Stieglitz, M., Dery, S. J., Romanovsky, V. E., and Osterkamp, T. E.: The role of snow cover in the warming of Arctic permafrost, Geophys. Res. Lett., 30, 1721, doi:10.1029/2003GL017337, 2003.

Swenson, S. C., Lawrence, D. M., and Lee, H.: Improved simulation of the terrestrial hydrological cycle in permafrost regions by the Community Land Model, J. Adv. Model. Earth Syst., 4, M08002, doi:10.1029/2012MS000165, 2012.

Takata, K. and Kimoto, M.: A numerical study on the impact of soil freezing on the continental-scale seasonal cycle, J. Meteorol. Soc. Jpn., 78, 199–221, 2000.

Tarnocai, C., Canadell, J. G., Schuur, E. A. G., Kuhry, P., Mazhitova, G., and Zimov, S.: Soil organic carbon pools in the northern circumpolar permafrost region, Global Biogeochem. Cy., 23, GB2023, doi:10.1029/2008GB003327, 2009.

Van Genuchten, M. T.: A closed-form equation for predicting the hydraulic conductivity of unsaturated soils, Soil Sci. Soc. Am. J., 44, 892–898, 1980.

Verseghy, D.: CLASS – A Canadian land surface scheme for GCMs, I. Soil model, Roy. Meteorol. Soc., 11, 111–133, 1991.

Weedon, G., Gomes, S., Viterbo, P., Österle, H., Adam, J., Bellouin, N., Boucher, O., and Best, M.: The WATCH forcing data 1958–2001: A meteorological forcing dataset for land surface and hydrological models WATCH Tech. Rep. 22, 41 pp., available at: http://www.eu-watch.org/publications/technical-reports, 2010.

Weedon, G. P., Gomes, S., Viterbo, P., Shuttleworth, W. J., Blyth, E., Österle, H., Adam, J. C., Bellouin, N., Boucher, O., and Best, M.: Creation of the WATCH Forcing Data and Its Use to Assess Global and Regional Reference Crop Evaporation over Land during the Twentieth Century, J. Hydrometeorol., 12, 823–848, doi:10.1175/2011JHM1369.1, 2011.

Westermann, S., Schuler, T. V., Gisnås, K., and Etzelmüller, B.: Transient thermal modeling of permafrost conditions in Southern Norway, The Cryosphere, 7, 719–739, doi:10.5194/tc-7-719-2013, 2013.

ZackenbergGIS: available at: http://dmugisweb.dmu.dk/zackenberggis/datapage.aspx, last access: 10 September 2012.

Zhang, T., Influence of the seasonal snow cover on the ground thermal regime: An overview, Rev. Geophys., 43, RG4002, doi:10.1029/2004RG000157, 2005.

Zhang, Y., Carey, S. K., and Quinton, W. L.: Evaluation of the algorithms and parameterizations for ground thawing and freezing simulation in permafrost regions, J. Geophys. Res., 113, 1–17, 2008.

Zhuang, Q., Melillo, J. M., Sarofim, M. C., Kicklighter, D. W., McGuire, A. D., Felzer, B. S., Sokolov, A., Prinn, R. G., Steudler, P. A., and Hu, S.: CO_2 and CH_4 exchanges between land ecosystems and the atmosphere in northern high latitudes over the 21st century, Geophys. Res. Lett., 33, 1–5, 2006.

Zimov, S. A., Davydov, S. P., Zimova, G. M., Davydova, A. I., Schuur, E. A. G., Dutta, K., and Chapin, F. S.: Permafrost carbon: Stock and decomposability of a globally significant carbon pool, Geophys. Res. Lett., 33, L20502, doi:10.1029/2006GL027484, 2006.

CHAPTER 3

MODEL INTERCOMPARISON

Peer-reviewed publication published as:

3.1 Introduction and Summary

This chapter includes the article "Site-level model intercomparison of high latitude and high altitude soil thermal dynamics in tundra and barren landscapes"[1] that has been published in the journal *The Cryosphere*. This article is prepared as a main part of this thesis and describes the comparison of model performances in estimating permafrost soil thermal dynamics. The work leading to this article has primarily been performed by the main author of this thesis, within the EU projects "Greencycles II", "PAGE21", and "PERMOS". The article itself is appended in the next section, such that it contains its own sections with abstract and references.

The main aim of this work is to compare the newly developed JSBACH version with other land models in capturing the soil thermal dynamics of different cold region landscape types. 5 other land models and 4 cold region sites are combined within the international collaboration efforts of Greencycles II, PAGE21, and PERMOS projects. The main model of this thesis JSBACH is complemented with JULES and ORCHIDEE models from PAGE21, HYBRID8 and LPJ-GUESS models from Greencycles II, and the COUP model from PERMOS. Sites are chosen from the same projects: NUUK from Greencycles II collaboration, Samoylov and Bayelva from PAGE21 main sites, and Schilthorn from the PERMOS project.

Comparing these models at the selected sites have shown the importance of snow insulation and soil internal physics for modeling soil thermal dynamics in cold regions. The importance of related processes change depending on the site conditions.

---

1 Ekici, A., Chadburn, S., Chaudhary, N., Hajdu, L. H., Marmy, A., Peng, S., Boike, J., Burke, E., Friend, A. D., Hauck, C., Krinner, G., Langer, M., Miller, P. A., and Beer, C.: Site-level model intercomparison of high latitude and high altitude soil thermal dynamics in tundra and barren landscapes, The Cryosphere , 9, 1343-1361, doi:10.5194/tc-9-1343-2015, 2015.

The Cryosphere

Site-level model intercomparison of high latitude and high altitude soil thermal dynamics in tundra and barren landscapes

A. Ekici[1,10], S. Chadburn[2], N. Chaudhary[3], L. H. Hajdu[4], A. Marmy[5], S. Peng[6,7], J. Boike[8], E. Burke[9], A. D. Friend[4], C. Hauck[5], G. Krinner[6], M. Langer[6,8], P. A. Miller[3], and C. Beer[10]

[1]Department of Biogeochemical Integration, Max Planck Institute for Biogeochemistry, Jena, Germany
[2]Earth System Sciences, Laver Building, University of Exeter, Exeter, UK
[3]Department of Physical Geography and Ecosystem Science, Lund University, Lund, Sweden
[4]Department of Geography, University of Cambridge, Cambridge, England
[5]Department of Geosciences, University of Fribourg, Fribourg, Switzerland
[6]CNRS and Université Grenoble Alpes, LGGE, 38041, Grenoble, France
[7]Laboratoire des Sciences du Climat et de l'Environnement, Gif-sur-Yvette, France
[8]Alfred-Wegener-Institut, Helmholtz-Zentrum für Polar- und Meeresforschung, Potsdam, Germany
[9]Met Office Hadley Centre, Exeter, UK
[10]Department of Applied Environmental Science (ITM) and Bolin Centre for Climate Research, Stockholm University, Stockholm, Sweden

Correspondence to: A. Ekici (a.ekici@exeter.ac.uk)

Abstract. Modeling soil thermal dynamics at high latitudes and altitudes requires representations of physical processes such as snow insulation, soil freezing and thawing and subsurface conditions like soil water/ice content and soil texture. We have compared six different land models: JSBACH, OR-CHIDEE, JULES, COUP, HYBRID8 and LPJ-GUESS, at four different sites with distinct cold region landscape types, to identify the importance of physical processes in capturing observed temperature dynamics in soils. The sites include alpine, high Arctic, wet polygonal tundra and non-permafrost Arctic, thus showing how a range of models can represent distinct soil temperature regimes. For all sites, snow insulation is of major importance for estimating topsoil conditions. However, soil physics is essential for the subsoil temperature dynamics and thus the active layer thicknesses. This analysis shows that land models need more realistic surface processes, such as detailed snow dynamics and moss cover with changing thickness and wetness, along with better representations of subsoil thermal dynamics.

1 Introduction

Recent atmospheric warming trends are affecting terrestrial systems by increasing soil temperatures and causing changes in the hydrological cycle. Especially in high latitudes and altitudes, clear signs of change have been observed (Serreze et al., 2000; ACIA, 2005; IPCC AR5, 2013). These relatively colder regions are characterized by the frozen state of terrestrial water, which brings additional risks associated with shifting soils into an unfrozen state. Such changes will have broad implications for the physical (Romanovsky et al., 2010), biogeochemical (Schuur et al., 2008) and structural (Larsen et al., 2008) conditions of the local, regional and global climate system. Therefore, predicting the future state of the soil thermal regime at high latitudes and altitudes holds major importance for Earth system modeling.

There are increasing concerns as to how land models perform at capturing high latitude soil thermal dynamics, in particular in permafrost regions. Recent studies (Koven et al., 2013; Slater and Lawrence, 2013) have provided detailed assessments of commonly used earth system models (ESMs) in simulating soil temperatures of present and future state

of the Arctic. By using the Coupled Model Intercomparison Project phase 5 – CMIP5 (Taylor et al., 2009) results, Koven et al. (2013) have shown a broad range of model outputs in simulated soil temperature. They attributed most of the inter-model discrepancies to air–land surface coupling and snow representations in the models. Similar to those findings, Slater and Lawrence (2013) confirmed the high uncertainty of CMIP5 models in predicting the permafrost state and its future trajectories. They concluded that these model versions are not appropriate for such experiments, since they lack critical processes for cold region soils. Snow insulation, land model physics and vertical model resolutions were identified as the major sources of uncertainty.

For the cold regions, one of the most important factors modifying soil temperature range is the surface snow cover. As discussed in many previous studies (Zhang, 2005; Koven et al., 2013; Scherler et al., 2013; Marmy et al., 2013; Langer et al., 2013; Boike et al., 2003; Gubler et al., 2013; Fiddes et al., 2015), snow dynamics are quite complex and the insulation effects of snow can be extremely important for the soil thermal regime. Model representations of snow cover are lacking many fine-scale processes such as snow ablation, depth hoar formation, snow metamorphism, wind effects on snow distribution and explicit heat and water transfer within snow layers. These issues bring additional uncertainties to global projections.

Current land surface schemes, and most vegetation and soil models, represent energy and mass exchange between the land surface and atmosphere in one dimension. Using a grid cell approach, such exchanges are estimated for the entire land surface or specific regions. However, comparing simulated and observed time series of states or fluxes at point scale rather than grid averaging is an important component of model evaluation, for understanding remaining limitations of models (Ekici et al., 2014; Mahecha et al., 2010). In such "site-level runs", we assume that lateral processes can be ignored and that the ground thermal dynamics are mainly controlled by vertical processes. Then, models are driven by observed climate and variables of interest can be compared to observations at different temporal scales. Even though such idealized field conditions never exist, a careful interpretation of site-level runs can identify major gaps in process representations in models.

In recent years, land models have improved their representations of the soil physical environment in cold regions. Model enhancements include the addition of soil freezing and thawing, detailed snow representations, prescribed moss cover, extended soil columns and coupling of soil heat transfer with hydrology (Ekici et al., 2014; Gouttevin et al., 2012a; Dankers et al., 2011; Lawrence et al., 2008; Wania et al., 2009a). Also active layer thickness (ALT) estimates have improved in the current model versions. Simple relationships between surface temperature and ALT were used in the early modeling studies (Lunardini, 1981; Kudryavtsev et al., 1974; Romanovsky and Osterkamp, 1997; Shiklo-

manov and Nelson, 1999; Stendel et al., 2007, Anisimov et al., 1997). These approaches assume an equilibrium condition, whereas a transient numerical method is better suited within a climate change context. A good review of widely used analytical approximations and differences to numerical approaches is given by Riseborough et al. (2008). With the advanced soil physics in many models, these transient approaches are more widely used, especially in long-term simulations. Such improvements highlight the need for an updated assessment of model performances in representing high latitude/altitude soil thermal dynamics.

We have compared the performances of six different land models in simulating soil thermal dynamics at four contrasting sites. In contrast to previous work (Koven et al., 2013; Slater and Lawrence, 2013), we used advanced model versions specifically improved for cold regions and our model simulations are driven by (and evaluated with) site observations. To represent a wider range of assessment and model structures, we used both land components of ESMs (JSBACH, ORCHIDEE, JULES) and stand-alone models (COUP, HYBRID8, LPJ-GUESS), and compared them at Arctic permafrost, Alpine permafrost and Arctic non-permafrost sites. By doing so, we aimed to quantify the importance of different processes, to determine the general shortcomings of current model versions and finally to highlight the key processes for future model developments.

2 Methods

2.1 Model descriptions

2.1.1 JSBACH

Jena Scheme for Biosphere–Atmosphere Coupling in Hamburg (JSBACH) is the land surface component of the Max Planck Institute earth system model (MPI-ESM), which comprises ECHAM6 for the atmosphere (Stevens et al., 2012) and MPIOM for the ocean (Jungclaus et al., 2013). JSBACH provides the land surface boundary for the atmosphere in coupled simulations; however, it can also be used offline driven by atmospheric forcing. The current version of JSBACH (Ekici et al., 2014) employs soil heat transfer coupled to hydrology with freezing and thawing processes included. The soil model is discretized as five layers with increasing thicknesses of up to 10 m depth. There are up to five snow layers with constant density and heat transfer parameters. JSBACH also simulates a simple moss/organic matter insulation layer again with constant parameters.

2.1.2 ORCHIDEE

ORCHIDEE is a global land surface model, which can be used coupled to the Institut Pierre Simon Laplace (IPSL) climate model or driven offline by prescribed atmospheric forcing (Krinner et al., 2005). ORCHIDEE computes all the

soil–atmosphere–vegetation-relevant energy and water exchange processes in 30 min time steps. It combines a soil–vegetation–atmosphere transfer model with a carbon cycle module, computing vertically detailed soil carbon dynamics. The high latitude version of ORCHIDEE includes a dynamic three-layer snow module (Wang et al., 2013), soil freeze–thaw processes (Gouttevin et al., 2012a), and a vertical permafrost soil thermal and carbon module (Koven et al., 2011). The soil hydrology is vertically discretized as 11 numerical nodes with 2 m depth (Gouttevin et al., 2012a), and soil thermal and carbon modules are vertically discretized as 32 layers with ~ 47 m depth (Koven et al., 2011). A one-dimensional Fourier equation was applied to calculate soil thermal dynamics, and both soil thermal conductivity and heat capacity are functions of the frozen and unfrozen soil water content and of dry and saturated soil thermal properties (Gouttevin et al., 2012b).

2.1.3 JULES

JULES (Joint UK Land Environment Simulator) is the land-surface scheme used in the Hadley Centre climate model (Best et al., 2011; Clark et al., 2011), which can also be run offline, driven by atmospheric forcing data. It is based on the Met Office Surface Exchange Scheme, MOSES (Cox et al., 1999). JULES simulates surface exchange, vegetation dynamics and soil physical processes. It can be run at a single point, or as a set of points representing a 2-D grid. In each grid cell, the surface is tiled into different surface types, and the soil is treated as a single column, discretized vertically into layers (four in the standard setup). JULES simulates fluxes of moisture and energy between the atmosphere, surface and soil, and the soil freezing and thawing. It includes a carbon cycle that can simulate carbon exchange between the atmosphere, vegetation and soil. It also includes a multi-layer snow model (Best et al., 2011), with layers that have variable thickness, density and thermal properties. The snow scheme significantly improves the soil thermal regime in comparison with the old, single-layer scheme (Burke et al., 2013). The model can be run with a time step of between 30 min and 3 h, depending on user preference.

2.1.4 COUP

COUP is a stand-alone, one-dimensional heat and mass transfer model for the soil–snow–atmosphere system (Jansson and Karlberg, 2011) and is capable of simulating transient hydrothermal processes in the subsurface including seasonal or perennial frozen ground (see e.g., Hollesen et al., 2011; Scherler et al., 2010, 2013). Two coupled partial differential equations for water and heat flow are the core of the COUP Model. They are calculated over up to 50 vertical layers of arbitrary depth. Processes that are important for permafrost simulations, such as the freezing and thawing of soil as well as the accumulation, metamorphosis and

melt of snow cover are included in the model (Lundin, 1990; Gustafsson et al., 2001). Freezing processes in the soil are based on a function of freezing point depression and on an analogy of freezing–thawing and wetting–drying (Harlan, 1973; Jansson and Karlberg, 2011). Snow cover is simulated as one layer of variable height, density, and water content.

The upper boundary condition is given by a surface energy balance at the soil–snow–atmosphere boundary layer, driven by climatic variables. The lower boundary condition at the bottom of the soil column is usually given by the geothermal heat flux (or zero heat flux) and a seepage flow of percolating water. Water transfer in the soil depends on texture, porosity, water, and ice content. Bypass flow through macropores, lateral runoff and rapid lateral drainage due to steep terrain can also be considered (e.g., Scherler et al., 2013). A detailed description of the model including all its equations and parameters is given in Jansson and Karlberg (2011) and Jansson (2012).

2.1.5 HYBRID8

HYBRID8 is a stand-alone land surface model, which computes the carbon and water cycling within the biosphere and between the biosphere and atmosphere. It is driven by the daily/sub-daily climate variables above the canopy, and the atmospheric CO_2 concentration. Computations are performed on a 30 min time step for the energy fluxes and exchanges of carbon and water with the atmosphere and the soil. Litter production and soil decomposition are calculated at a daily time step. HYBRID8 uses the surface physics and the latest parameterization of turbulent surface fluxes from the GISS ModelE (Schmidt et al., 2006; Friend and Kiang, 2005), but has no representation of vegetation dynamics. The snow dynamics from ModelE are also not yet fully incorporated. Heat dynamics are described in Rosenzweig et al. (1997) and moisture dynamics in Abramopoulos et al. (1988).

In HYBRID8 the prognostic variable for the heat transfer is the heat in the different soil layers, and from that, the model evaluates the soil temperature. The processes governing this are diffusion from the surface to the sub-surface layers, and conduction and advection between the soil layers. The bottom boundary layer in HYBRID8 is impermeable, resulting in zero heat flux from the soil layers below. The version used in this project has no representation of the snow dynamics and has no insulating vegetation cover. However, the canopy provides a simple heat buffer due its separate heat capacity calculations.

2.1.6 LPJ-GUESS

Lund-Potsdam-Jena General Ecosystem Simulator (LPJ-GUESS) is a process-based model of vegetation dynamics and biogeochemistry optimized for regional and global applications (Smith et al., 2001). Mechanistic representations

of biophysical and biogeochemical processes are shared with those in the Lund-Potsdam-Jena dynamic global vegetation model LPJ-DGVM (Sitch et al., 2003; Gerten et al., 2004). However, LPJ-GUESS replaces the large area parameterization scheme in LPJ-DGVM, whereby vegetation is averaged out over a larger area, allowing several state variables to be calculated in a simpler and faster manner, with more robust and mechanistic schemes of individual- and patch-based resource competition and woody plant population dynamics. Detailed descriptions are given by Smith et al. (2001), Sitch et al. (2003), Wolf et al. (2008), Miller and Smith (2012) and Zhang et al. (2013).

LPJ-GUESS has recently been updated to simulate Arctic upland and peatland ecosystems (McGuire et al., 2012; Zhang et al., 2013). It shares the numerical soil thawing–freezing processes, peatland hydrology and the model of wetland methane emission with LPJ-DGVM WHyMe, as described by Wania et al. (2009a, b, 2010). To simulate soil temperatures and active layer depths, the soil column in LPJ-GUESS is divided into a single snow layer of fixed density and variable thickness, a litter layer of fixed thickness (10 cm for these simulations, except for Schilthorn where it is set to 2.5 cm), a soil column of 2 m depth (with sublayers of thickness 0.1 m, each with a prescribed fraction of mineral and organic material, but with fractions of soil water and air that are updated daily), and finally a "padding" column of depth 48 m (with thicker sublayers), to simulate soil thermal dynamics. Insulation effects of snow, phase changes in soil water, daily precipitation input and air temperature forcing are important determinants of daily soil temperature dynamics at different sublayers.

2.2 Study sites

2.2.1 Nuuk

The Nuuk observational site is located in southwestern Greenland. The site is situated in a valley in Kobbefjord at 500 m altitude above sea level, and ambient conditions show Arctic climate properties, with a mean annual temperature of $-1.5\,°C$ in 2008 and $-1.3\,°C$ in 2009 (Jensen and Rasch, 2009, 2010). Vegetation types consist of *Empetrum nigrum* with *Betula nana* and *Ledum groenlandicum,* with a vegetation height of 3–5 cm. The study site soil lacks mineral soil horizons due to cryoturbation and lack of podsol development, as it is situated in a dry location. The soil is composed of 43 % sand, 34 % loam, 13 % clay and 10 % organic materials. No soil ice or permafrost formations have been observed within the drainage basin. Snow cover is measured at the Climate Basic station, 1.65 km from the soil station but at the same altitude. At the time of the annual Nuuk Basic snow survey in mid-April, the snow depth at the soil station was very similar to the snow depth at the Climate Basic station: ± 0.1 m when the snow depth is high (near 1 m). Strong winds ($> 20\,\mathrm{m\,s^{-1}}$) have a strong influence on the redistribu-

tion of newly fallen snow, especially in the beginning of the snow season, so the formation of a permanent snow cover at the soil station can be delayed as much as 1 week, while the end of the snow cover season is similar to that at the Climate Basic station (B. U. Hansen, personal communication, 2013; ZackenbergGIS, 2012).

2.2.2 Schilthorn

The Schilthorn massif (Bernese Alps, Switzerland) is situated at 2970 m altitude in the northcentral part of the European Alps. Its non-vegetated lithology is dominated by deeply weathered limestone schists, forming a surface layer of mainly sandy and gravelly debris up to 5 m thick, which lies over presumably strongly jointed bedrock. Following the first indications of permafrost (ice lenses) during the construction of the summit station between 1965 and 1967, the site was chosen for long-term permafrost observation within the framework of the European PACE project and consequently integrated into the Swiss permafrost monitoring network PERMOS as one of its reference sites (PERMOS, 2013).

The measurements at the monitoring station at 2900 m altitude are located on a flat plateau on the north-facing slope and comprise a meteorological station and three boreholes (14 m vertical, 100 m vertical and 100 m inclined), with continuous ground temperature measurements since 1999 (Vonder Mühll et al., 2000; Hoelzle and Gruber, 2008; Harris et al., 2009). Borehole data indicate permafrost of at least 100 m thickness, which is characterized by ice-poor conditions close to the melting point. Maximum active-layer depths recorded since the start of measurements in 1999 are generally around 4–6 m, but during the exceptionally warm summer of the year 2003 the active-layer depth increased to 8.6 m, reflecting the potential for degradation of permafrost at this site (Hilbich et al., 2008).

The monitoring station has been complemented by soil moisture measurements since 2007 and geophysical (mainly geoelectrical) monitoring since 1999 (Hauck, 2002; Hilbich et al., 2011). The snow cover at Schilthorn can reach maximum depths of about 2–3 m and usually lasts from October through to June/July. One-dimensional soil model sensitivity studies showed that impacts of long-term atmospheric changes would be strongest in summer and autumn, due to this late snowmelt and the long decoupling of the atmosphere from the surface. So, increasing air temperatures could lead to a severe increase in active-layer thickness (Engelhardt et al., 2010; Marmy et al., 2013; Scherler et al., 2013).

2.2.3 Samoylov

Samoylov Island belongs to an alluvial river terrace of the Lena River delta. The island is elevated about 20 m above the normal river water level and covers an area of about 3.4 km² (Boike et al., 2013). The western part of the island constitutes

Table 1. Model details related to soil heat transfer.

	JSBACH	ORCHIDEE	JULES	COUP	HYBDRID8	LPJ-GUESS
Soil freezing	Yes	Yes	Yes	Yes	Yes	Yes
Soil heat transfer method	Conduction	Conduction	Conduction advection	Conduction advection	Conduction advection	Conduction
Dynamic soil heat transfer parameters	Yes	Yes	Yes	Yes	Yes	Yes
Soil depth	10 m	43 m	3 m	Variable (> 5 m)	Variable (> 5 m)	2 m
Bottom boundary condition	Zero heat flux	Geothermal heat flux (0.057 W m^{-2})	Zero heat flux	Geothermal heat flux (0.011 W m^{-2})	Zero heat flux	Zero heat flux
Snow layering	Five layers	Three layers	Three layers	One layer	No snow representation	One layer
Dynamic snow heat transfer parameters	No	Yes	Yes	Yes	–	Yes (only heat capacity)
Insulating vegetation cover	10 cm moss layer	–	–	–	–	Site-specific litter layer
Model time step	30 min	30 min	30 min	30 min	30 min	1 day

Table 2. Site details.

	Nuuk	Schilthorn	Samoylov	Bayelva
Latitude	64.13° N	46.56° N	72.4° N	78.91° N
Longitude	51.37° W	7.08° E	126.5° E	11.95° E
Mean annual air temperature	−1.3 °C	−2.7 °C	−13 °C	−4.4 °C
Mean annual ground temperature	3.2 °C	−0.45 °C	−10 °C	−2/−3 °C
Annual precipitation	900 mm	1963 mm	200 mm	400 mm
Avg. length of snow cover	7 months	9.5 months	9 months	9 months
Vegetation cover	Tundra	Barren	Tundra	Tundra

a modern floodplain, which is lower compared with the rest of the island and is often flooded during ice break-up of the Lena River in spring. The eastern part of the island belongs to the elevated river terrace, which is mainly characterized by moss- and sedge-vegetated tundra (Kutzbach et al., 2007). In addition, several lakes and ponds occur, which make up about 25 % of the surface area of Samoylov (Muster et al., 2012).

The land surface of the island is characterized by the typical micro-relief of polygonal patterned ground, caused by frost cracking and subsequent ice-wedge formation. The polygonal structures usually consist of depressed centers surrounded by elevated rims, which can be found in a partly or completely collapsed state (Kutzbach et al., 2007). The soil in the polygonal centers usually consists of water-saturated sandy peat, with the water table standing a few centimeters above or below the surface. The elevated rims are usually covered with a dry moss layer, underlain by wet sandy soils, with massive ice wedges underneath. The cryogenic soil complex of the river terrace reaches depths of 10 to 15 m and is underlain by sandy to silty river deposits. These river deposits reach depths of at least 1 km in the delta region (Langer et al., 2013).

There are strong spatial differences in surface energy balance due to heterogeneous surface and subsurface properties. Due to thermo-erosion, there is an ongoing expansion of thermokarst lakes and small ponds (Abnizova et al., 2012). Soil water drainage is strongly related to active layer dynamics, with lateral water flow occurring from late sum-

mer to autumn (Helbig et al., 2013). Site conditions include strong snow–microtopography and snow–vegetation interactions due to wind drift (Boike et al., 2013).

2.2.4 Bayelva

The Bayelva climate and soil-monitoring site is located in the Kongsfjord region on the west coast of Svalbard Island. The North Atlantic Current warms this area to an average air temperature of about −13 °C in January and +5 °C in July, and provides about 400 mm precipitation annually, falling mostly as snow between September and May. The annual mean temperature of 1994 to 2010 in the village of Ny-Ålesund has been increasing by +1.3 K per decade (Maturilli et al., 2013). The observation site is located in the Bayelva River catchment on the Brøgger peninsula, about 3 km from Ny-Ålesund. The Bayelva catchment is bordered by two mountains, the Zeppelinfjellet and the Scheteligfjellet, between which the glacial Bayelva River originates from the two branches of the Brøggerbreen glacier moraine rubble. To the north of the study site, the terrain flattens, and after about 1 km, the Bayelva River reaches the shoreline of the Kongsfjorden (Arctic Ocean). In the catchment area, sparse vegetation alternates with exposed soil and sand and rock fields. Typical permafrost features, such as mud boils and non-sorted circles, are found in many parts of the study area. The Bayelva permafrost site itself is located at 25 m a.s.l., on top of the small Leirhaugen hill. The domi-

Table 3. Details of driving data preparation for site simulations.

		Nuuk	Schilthorn	Samoylov	Bayelva
Atmospheric forcing variables	Air temperature	in situ	in situ	in situ	in situ
	Precipitation	in situ	in situ	in situ (snow season from WATCH)	in situ
	Air pressure	in situ	WATCH	WATCH	in situ
	Atm. humidity	in situ	in situ	in situ	in situ
	Incoming longwave radiation	in situ	in situ	in situ	WATCH
	Incoming shortwave radiation	in situ	in situ	WATCH	in situ
	Net radiation	in situ	–	in situ	–
	Wind speed	in situ	in situ	in situ	in situ
	Wind direction	in situ	–	in situ	–
	Time period	26/06/2008–31/12/2011	01/10/1999–30/09/2008	14/07/2003–11/10/2005	01/01/1998–31/12/2009
Static soil parameters	Soil porosity	46 %	50 %	60 %	41 %
	Soil field capacity	36 %	44 %	31 %	22 %
	Mineral soil depth	36 cm	710 cm	800 cm	30 cm
	Dry soil heat capacity	2.213×10^6 $(\mathrm{Jm^{-3}\,K^{-1}})$	2.203×10^6 $(\mathrm{Jm^{-3}\,K^{-1}})$	2.1×10^6 $(\mathrm{Jm^{-3}\,K^{-1}})$	2.165×10^6 $(\mathrm{Jm^{-3}\,K^{-1}})$
	Dry soil heat conductivity	6.84 $(\mathrm{Wm^{-1}\,K^{-1}})$	7.06 $(\mathrm{Wm^{-1}\,K^{-1}})$	5.77 $(\mathrm{Wm^{-1}\,K^{-1}})$	7.93 $(\mathrm{Wm^{-1}\,K^{-1}})$
	Sat. hydraulic conductivity	2.42×10^{-6} $(\mathrm{ms^{-1}})$	4.19×10^{-6} $(\mathrm{ms^{-1}})$	2.84×10^{-6} $(\mathrm{ms^{-1}})$	7.11×10^{-6} $(\mathrm{ms^{-1}})$
	Saturated moisture potential	0.00519 (m)	0.2703 (m)	0.28 (m)	0.1318 (m)

Table 4. Details of model spin up procedures.

	JSBACH	ORCHIDEE	JULES	COUP	HYBRID8	LPJ-GUESS
Spin-up data	Observed climate	Observed climate	Observed climate	Observed climate	Observed climate	WATCH* data
Spin-up duration	50 years	10 000 years	50 years	10 years	50 years	500 years

* 500 years forced with monthly WATCH reanalysis data from the 1901–1930 period, followed by daily WATCH forcing from 1901–until YYYY-MM-DD, then daily site data.

nant ground pattern at the study site consists of non-sorted soil circles. The bare soil circle centers are about 1 m in diameter and are surrounded by a vegetated rim, consisting of a mixture of low vascular plants of different species of grass and sedges (*Carex spec.*, *Deschampsia spec.*, *Eriophorum spec.*, *Festuca spec.*, *Luzula spec.*), catchfly, saxifrage, willow and some other local common species (*Dryas octopetala*, *Oxyria digyna*, *Polegonum viviparum*) and unclassified species of mosses and lichens. The vegetation cover at the measurement site was estimated to be approximately 60 %, with the remainder being bare soil with a small proportion of stones. The silty clay soil has a high mineral content, while the organic content is low, with organic fractions below 10 % (Boike et al., 2007). In the study period, the permafrost at Leirhaugen hill had a mean annual temperature of about $-2\,^\circ\mathrm{C}$ at the top of the permafrost at 1.5 m depth.

Over the past decade, the Bayelva catchment has been the focus of intensive investigations into soil and permafrost conditions (Roth and Boike, 2001; Boike et al., 2007; Westermann et al., 2010, 2011), the winter surface energy balance (Boike et al., 2003), and the annual balance of energy, H_2O and CO_2, and micrometeorological processes controlling these fluxes (Westermann et al., 2009; Lüers et al., 2014).

2.3   Intercomparison setup and simulation protocol

In order solely to compare model representations of physical processes and to eliminate any other source of uncertainty (e.g., climate forcing, spatial resolution, soil parameters), model simulations were driven by the same atmospheric forcing and soil properties at site-scale. Driving data for all site simulations were prepared and distributed uniformly. Site observations were converted into continuous time series with minor gap-filling. Where the observed variable set lacked the variable needed by the models, extended WATCH reanalysis data (Weedon et al., 2010; Beer et al., 2014) were used to complement the data sets. Soil thermal properties are based on the sand, silt, and clay fractions of the Harmonized World Soil database v1.1 (FAO et al., 2009). All model simulations were forced with these data sets. Table 3 summarizes the details of site-driving data preparation together with soil static parameters.

To bring the state variables into equilibrium with climate, models are spun up with climate forcing. Spin-up procedure is part of the model structure, in some cases a full biogeochemical and physical spin up is implemented, whereas in some models a simpler physical spin up is possible. This brings different requirements for the spin-up time length, so each model was independently spun up depending on its model formulations and discretization scheme, and the details are given in Table 4. However, the common practice in
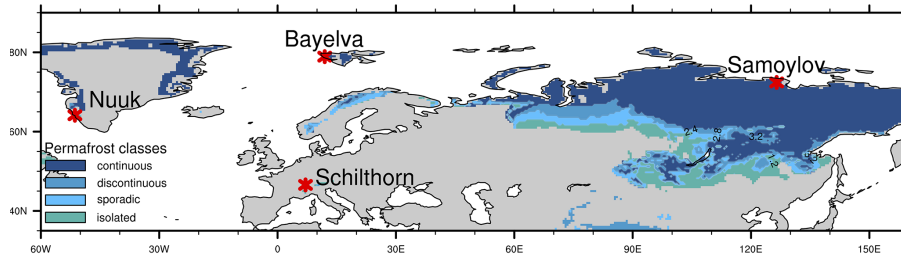
Figure 1. Location map of the sites used in this study. The background map is color-coded with the IPA permafrost classes from Brown et al. (2002).
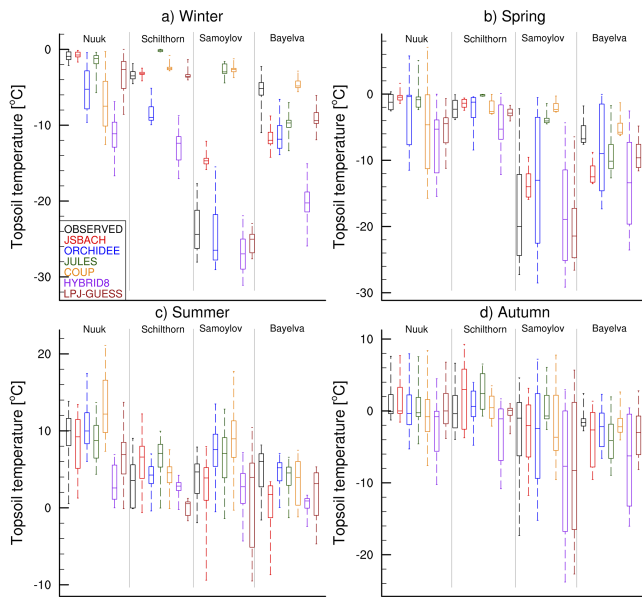

Figure 2. Box plots showing the topsoil temperature for observation and models for different seasons. Boxes are drawn with the 25th percentile and mean and 75th percentiles, while the whiskers show the min and max values. Seasonal averages of soil temperatures are used for calculating seasonal values. Each plot includes four study sites divided by the gray lines. Black boxes show observed values, and colored boxes distinguish models. See Table A1 in Appendix A for exact soil depths used in this plot.

Figure 3. Scatter plots showing air–topsoil temperature relation from observations and models at each site for different seasons. Seasonal mean observed air temperature is plotted against the seasonal mean modeled topsoil temperature separately for each site. Black markers are observed values, colors distinguish models and markers distinguish seasons. Gray lines represent the 1 : 1 line. See Table A1 in Appendix A for exact soil depths used in this plot.

all model spin-up procedures was to keep the mean annual soil temperature change less than 0.01 °C in all soil layers.

Most of the analysis focuses on the upper part of the soil. The term "topsoil" is used from now on to indicate the chosen upper soil layer in each model, and the first depth of soil temperature observations. The details of layer selection are given in Table A1 of Appendix A.

3 Results

3.1 Topsoil temperature and surface insulation effects

As all our study sites are located in cold climate zones (Fig. 1), there is significant seasonality, which necessitates a separate analysis for each season. Figure 2 shows average seasonal topsoil temperature distributions (see Table A1 in the Appendix for layer depths) extracted from the six models, along with the observed values at the four different sites. In this figure, observed and simulated temperatures show a wide range of values depending on site-specific conditions and model formulations. Observations show that dur-
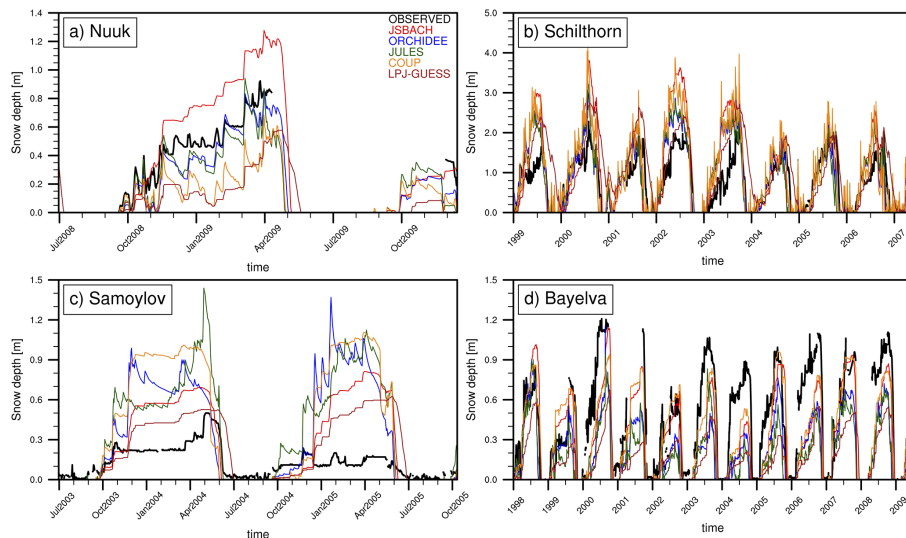
Figure 4. Time-series plots of observed and simulated snow depths for each site. Thick black lines are observed values and colored lines distinguish simulated snow depths from models.

ing winter and spring, Samoylov is much colder than the other sites (Fig. 2a, b). Observed summer and autumn temperatures are similar at all sites (Fig. 2c, d), with Nuuk being the warmest site in general. For the modeled values, the greatest inconsistency with observations is in matching the observed winter temperatures, especially at Samoylov and Schilthorn (Fig. 2a). The modeled temperature range increases in spring (Fig. 2b), and even though the mean modeled temperatures in summer are closer to observed means, the maximum and minimum values show a wide range during this season (Fig. 2c). Autumn shows a more uniform distribution of modeled temperatures compared with the other seasons (Fig. 2d).

A proper assessment of critical processes entails examining seasonal changes in surface cover and the consequent insulation effects for the topsoil temperature. To investigate these effects, Fig. 3 shows the seasonal relations between air and topsoil temperature at each study site. Air temperature values are the same for all models, as they are driven with the same atmospheric forcing. Observations show that topsoil temperatures are warmer than the air during autumn, winter, and spring at all sites, but the summer conditions are dependent on the site (Fig. 3). In the models, winter topsoil temperatures are warmer than the air in most cases, as observed. However, the models show a wide range of values, especially at Samoylov (Fig. 3c), where the topsoil temperatures differ by up to 25 °C between models. In summer, the models do not show consistent relationships between soil and air temperatures, and the model range is highest at the Nuuk and Schilthorn sites.

To analyze the difference in modeled and observed snow isolation effect in more detail, Fig. 4 shows the changes in snow depth from observed and modeled values. Schilthorn

has the highest snow depth values (> 1.5 m), while all other sites have a maximum snow height between 0.5 and 1 m (Fig. 4). Compared with observations, the models usually overestimate the snow depth at Schilthorn and Samoylov (Fig. 4b, c) and underestimate it at Nuuk and Bayelva (Fig. 4a, d).

For our study sites, the amount of modeled snow depth bias is correlated with the amount of modeled topsoil temperature bias (Fig. 5). With overestimated (underestimated) snow depth, models generally simulate warmer (colder) topsoil temperatures. As seen in Fig. 5a, almost all models underestimate the snow depth at Nuuk and Bayelva, and this creates colder topsoil temperatures. The opposite is seen for Samoylov and Schilthorn, where higher snow depth bias is accompanied by higher topsoil temperature bias (except for ORCHIDEE and LPJ-GUESS models).

As snow can be persistent over spring and summer seasons in cold regions (Fig. 4), it is worthwhile to separate snow and snow-free seasons for these comparisons. Figure 6 shows the same atmosphere–topsoil temperature comparison as in Fig. 3 but using individual (for each model and site) snow and snow-free seasons instead of conventional seasons. In this figure, all site observations show a warmer topsoil temperature than air, except for the snow-free season at Samoylov. Models, however, show different patterns at each site. For the snow season, models underestimate the observed values at Nuuk and Bayelva, whereas they overestimate it at Schilthorn and Samoylov, except for the previously mentioned ORCHIDEE and LPJ-GUESS models. Modeled snow-free season values, however, do not show consistent patterns.
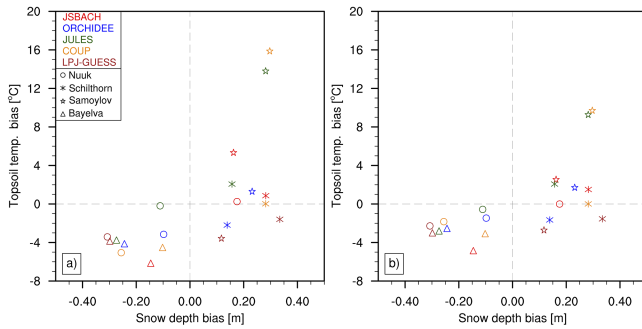
Figure 5. Scatter plots showing the relation between snow depth bias and topsoil temperature bias during snow season **(a)** and the whole year **(b)**. Snow season is defined separately for each model, by taking snow depth values over 5 cm to represent the snow-covered period. The average temperature bias of all snow-covered days is used in **(a)**, and the temperature bias in all days (snow covered and snow-free seasons) is used in **(b)**. Markers distinguish sites and colors distinguish models. See Table A1 in Appendix A for exact soil depths used in this plot.
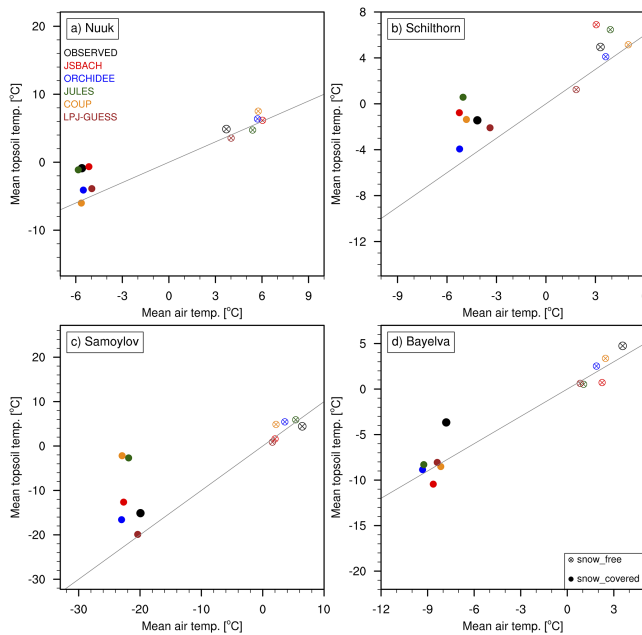
Figure 6. Scatter plots showing air–topsoil temperature relation from observations and models at each site for snow and snow-free seasons. Snow season is defined separately for observations and each model, by taking snow depth values over 5 cm to represent the snow-covered period. The average temperature of all snow covered (or snow-free) days of the simulation period is used in the plots. Markers distinguish snow and snow-free seasons and colors distinguish models. Gray lines represent the 1 : 1 line. See Table A1 in Appendix A for exact soil depths used in this plot.
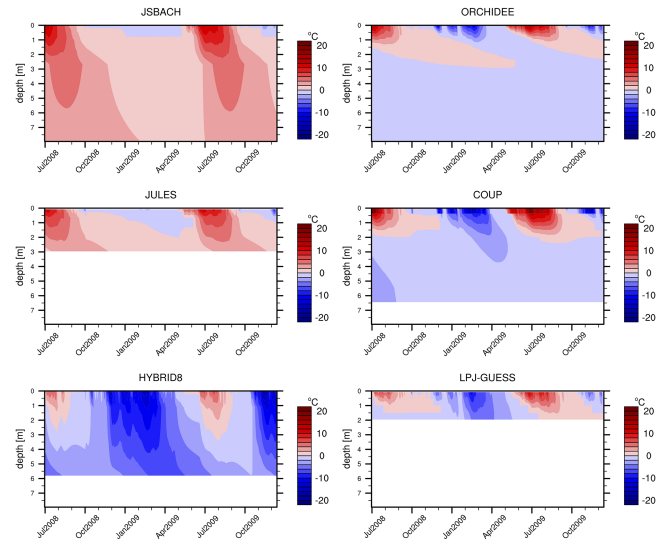

Figure 7. Time–depth plot of soil temperature evolution at the Nuuk site for each model. Simulated soil temperatures are interpolated into 200 evenly spaced nodes to represent a continuous vertical temperature profile. The deepest soil temperature calculation is taken as the bottom limit for each model (no extrapolation applied).

3.2 Subsurface thermal regime

Assessing soil thermal dynamics necessitates scrutinizing subsoil temperature dynamics as well as surface conditions. Soil temperature evolutions of simulated soil layers are plotted for each model at each site in Figs. 7–10. Strong seasonal temperature changes are observed close to the surface, whereas temperature amplitudes are reduced in deeper layers and eventually a constant temperature is simulated at depths with zero annual amplitude (DZAA).

Although Nuuk is a non-permafrost site, most of the models simulate subzero temperatures below 2–3 m at this site (Fig. 7). Here, only ORCHIDEE and COUP simulate a true DZAA at around 2.5–3 m, while all other models show a minor temperature change even at their deepest layers. At the high altitude Schilthorn site (Fig. 8), JSBACH and JULES simulate above 0 °C temperatures (non-permafrost conditions) in deeper layers. Compared with other models with snow representation, ORCHIDEE and LPJ-GUESS show colder subsurface temperatures at this site (Fig. 8). The simulated soil thermal regime at Samoylov reflects the colder climate at this site. All models show subzero temperatures below 1 m (Fig. 9). However, compared with other models, JULES and COUP show values much closer to 0 °C. At the high-Arctic Bayelva site, all models simulate permafrost conditions (Fig. 10). The JULES and COUP models again show warmer temperature profiles than the other models.

The soil thermal regime can also be investigated by studying the vertical temperature profiles regarding the annual means (Fig. 11), and minimum and maximum values
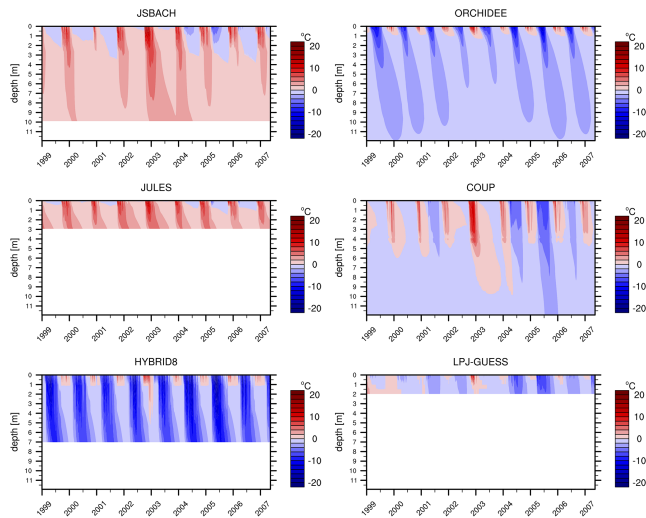
Figure 8. Time–depth plot of soil temperature evolution at Schilthorn site for each model. Simulated soil temperatures are interpolated into 200 evenly spaced nodes to represent a continuous vertical temperature profile. The deepest soil temperature calculation is taken as the bottom limit for each model (no extrapolation applied).

Figure 9. Time–depth plot of soil temperature evolution at Samoylov site for each model. Simulated soil temperatures are interpolated into 200 evenly spaced nodes to represent a continuous vertical temperature profile. The deepest soil temperature calculation is taken as the bottom limit for each model (no extrapolation applied).

(Fig. 12). In Figure 11, the distribution of mean values is similar to the analysis of topsoil conditions. The mean subsoil temperature is coldest at Samoylov followed by Bayelva, while Schilthorn is almost at the 0 °C boundary (no deep soil temperature data were available from Nuuk for this comparison). JSBACH, JULES, and COUP overestimate the temperatures at Schilthorn and Samoylov, but almost all models underestimate it at Bayelva. Figure 12 shows the temperature envelopes of observed and simulated values at each site. The minimum (maximum) temperature curve represents the coldest (warmest) possible conditions for the soil thermal regime at a certain depth. The models agree more on the maximum curve than the minimum curve (Fig. 12), indicating the differences in soil temperature simulation for colder periods. The HYBRID8 model almost always shows the coldest conditions, whereas the pattern of the other models changes depending on the site.

Figure 13 shows the yearly change of ALT for the three permafrost sites. Observations indicate a shallow ALT at Samoylov (Fig. 13b) and very deep ALT for Schilthorn (Fig. 13a). All models overestimate the ALT at Samoylov (Fig. 13b), but there is disagreement among models in over- or underestimating the ALT at Schilthorn (Fig. 13a) and Bayelva (Fig. 13c).
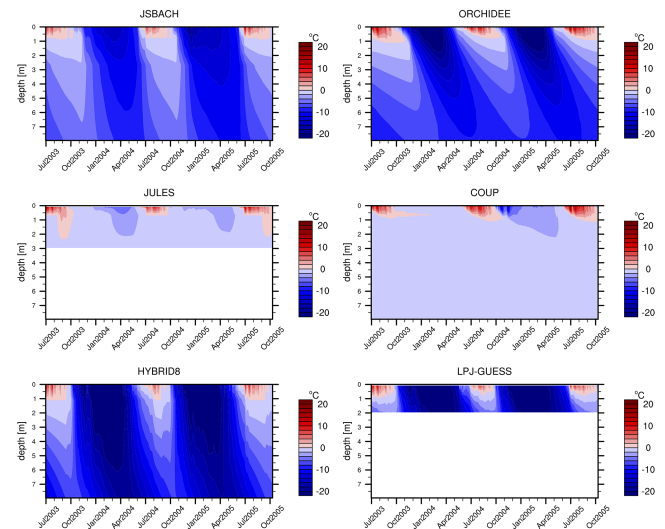
4 Discussion

4.1 Topsoil temperature and surface insulation effects

Figure 2 has shown a large range among modeled temperature values, especially during winter and spring. As mentioned in the introduction, modeled mean soil temperatures are strongly related to the atmosphere–surface thermal connection, which is strongly influenced by snow cover and its properties.

Observations show warmer topsoil temperatures than air during autumn, winter, and spring (Fig. 3). This situation indicates that soil is insulated when compared to colder air temperatures. This can be attributed to the snow cover during these seasons (Fig. 4). The insulating property of snow keeps the soil warmer than air, while not having snow can result in colder topsoil temperatures than air (as for the HYBRID8 model, cf. Fig. 3). Even though the high albedo of snow provides a cooling effect for soil, the warming due to insulation dominates during most of the year. Depending on their snow depth bias, models show different relations between air and topsoil temperature. The amount of winter warm bias from snow depth overestimation in models depends on whether the site has a "sub- or supra-critical" snow height. With supra-critical conditions (e.g., at Schilthorn), the snow depth is so high that a small over- or underestimation in the model makes very little difference to the insulation. Only the timing of the snow arrival and melt-out is important. In sub-critical conditions (e.g., at Samoylov), the snow depth is so low that any overestimation leads to a strong warm bias in the simula-
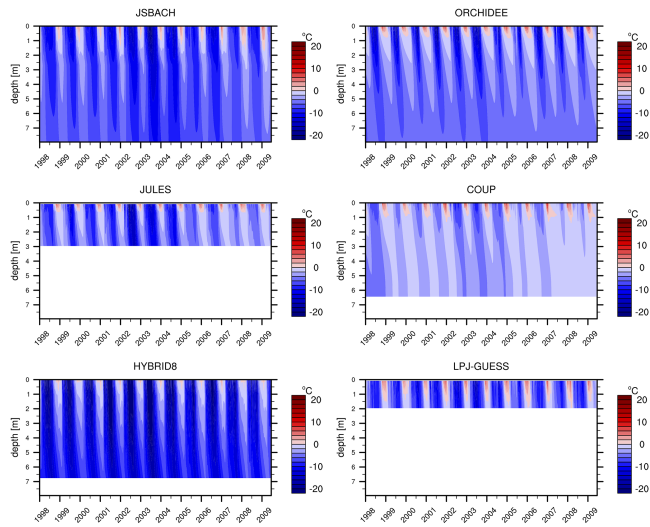
Figure 10. Time–depth plot of soil temperature evolution at Bayelva site for each model. Simulated soil temperatures are interpolated into 200 evenly spaced nodes to represent a continuous vertical temperature profile. The deepest soil temperature calculation is taken as the bottom limit for each model (no extrapolation applied).

Figure 11. Vertical profiles of annual soil temperature means of observed and modeled values at each site. Black thick lines are the observed values, while colored dashed lines distinguish models. (Samoylov and Bayelva observations are from borehole data).

tion e.g., for JULES/COUP. This effect is also mentioned in Zhang (2005), where it is stated that snow depths of less than 50 cm have the greatest impact on soil temperatures. However, overestimated snow depth at Samoylov and Schilthorn does not always result in warmer soil temperatures in models as expected (Fig. 3b, c). At these sites, even though JSBACH, JULES and COUP show warmer soil temperatures in parallel to their snow depth overestimations, ORCHIDEE and LPJ-GUESS show the opposite. This behavior indicates different processes working in opposite ways. Nevertheless, most of the winter, autumn and spring topsoil temperature biases can be explained by snow conditions (Fig. 5a). Figure 5b shows that snow depth bias can explain the topsoil temperature bias even when the snow-free season is considered, which is due to the long snow period at these sites (Table 2). This confirms the importance of snow representation in models for capturing topsoil temperatures at high latitudes and high altitudes.

On the other hand, considering dynamic heat transfer parameters (volumetric heat capacity and heat conductivity) in snow representation seems to be of lesser importance (JSBACH vs. other models, see Table 1). This is likely because a greater uncertainty comes from processes that are still missing in the models, such as wind drift, depth hoar formation and snow metamorphism. As an example, the landscape heterogeneity at Samoylov forms different soil thermal profiles for polygon center and rim. While the soil temperature comparisons were performed for the polygon rim, snow depth observations were taken from polygon center. Due to strong wind drift, almost all snow is removed from the rim and also limited to ca. 50cm (average polygon height) at
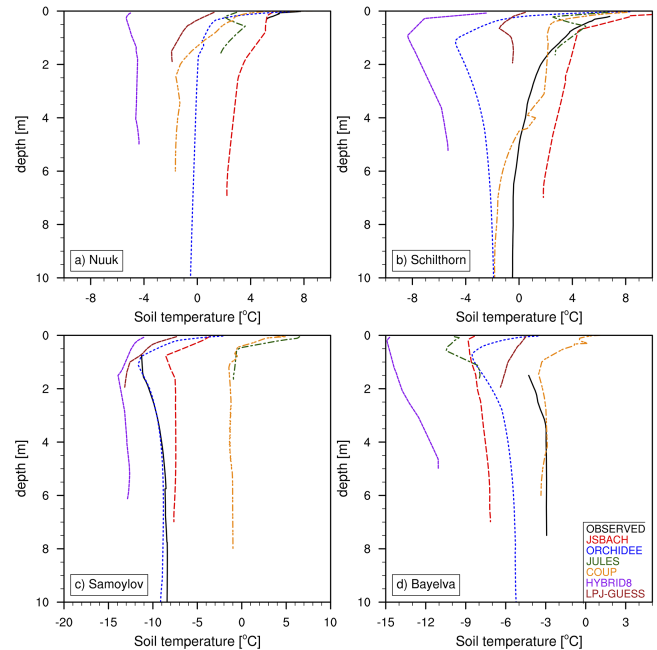
the center (Boike et al., 2008). This way, models inevitably overestimate snow depth and insulation, in particular on the rim where soil temperature measurements have been taken. Hence, a resulting winter warm bias is expected (Fig. 2a, models JSBACH, JULES, COUP).

During the snow-free season, Samoylov has colder soil temperatures than air (Fig. 6c). Thicker moss cover and higher soil moisture content at Samoylov (Boike et al., 2008) are the reasons for cooler summer topsoil temperatures at this site. Increasing moss thickness changes the heat storage of the moss cover and it acts as a stronger insulator (Gornall et al., 2007), especially when dry (Soudzilovskaia et al., 2013). Additionally, high water content in the soil requires additional input of latent heat for thawing and there is less heat available to warm the soil.

Insulation strength during the snow-free season is related to model vegetation/litter layer representations. 10 cm fixed moss cover in JSBACH and a 10 cm litter layer in LPJ-GUESS bring similar amounts of insulation. At Samoylov, where strong vegetation cover is observed in the field, these models perform better for the snow-free season (Fig. 6c). However, at Bayelva, where vegetation effects are not that strong, 10 cm insulating layer proves to be too much and creates colder topsoil temperatures than observations (Fig. 6d). And for the bare Schilthorn site, even a thin layer of surface cover (2.5 cm litter layer) creates colder topsoil temperatures in LPJ-GUESS (Fig. 6b).
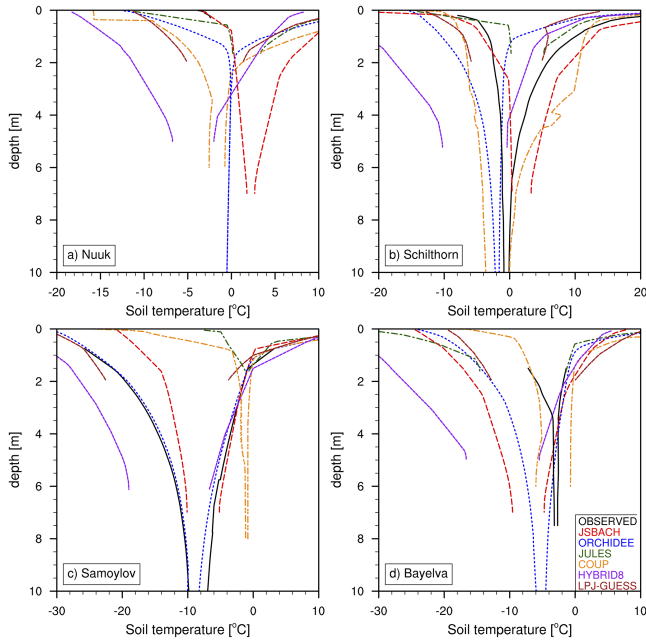
Figure 12. Soil temperature envelopes showing the vertical profiles of soil temperature amplitudes of each model at each site. Soil temperature values of observations (except Nuuk) and each model are interpolated to finer vertical resolution and max and min values are calculated for each depth to construct max and min curves. For each color, the right line is the maximum and the left line is the minimum temperature curve. Black thick lines are the observed values, while colored dashed lines distinguish models.

At Bayelva, all models underestimate the observed topsoil temperatures all year long (Fig. 6d). With underestimated snow depth (Fig. 4d) and winter cold bias in topsoil temperature (Fig. 3d), models create a colder soil thermal profile that results in cooling of the surface from below even during the snow-free season. Furthermore, using global reanalysis products instead of site observations (Table 3) might cause biases in incoming longwave radiation, which can also affect the soil temperature calculations. In order to assess model performance in capturing observed soil temperature dynamics, it is important to drive the models with a complete set of site observations.

These analyses support the need for better vegetation insulation in models during the snow-free season. The spatial heterogeneity of surface vegetation thickness remains an important source of uncertainty. More detailed moss representations were used in Porada et al. (2013) and Rinke et al. (2008), and such approaches can improve the snow-free season insulation in models.

4.2 Soil thermal regime

Model differences in representing subsurface temperature dynamics are related to the surface conditions (especially snow) and soil heat transfer formulations. The ideal way
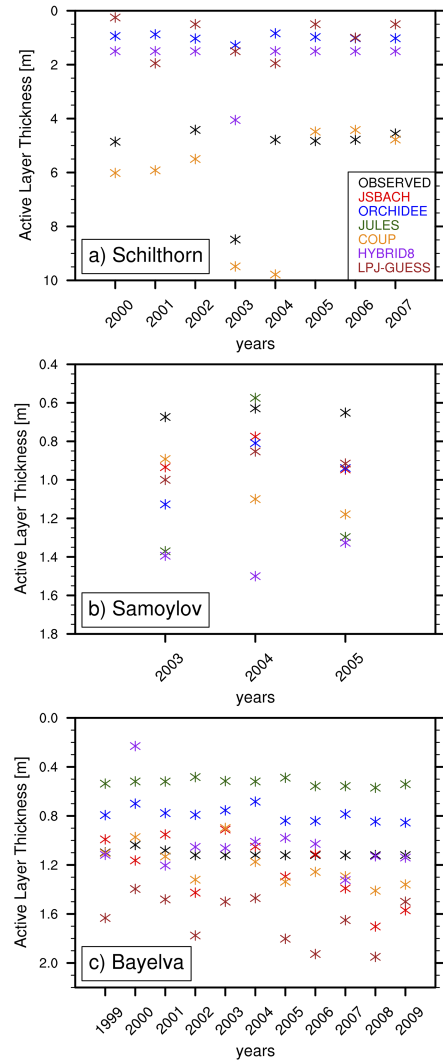

Figure 13. Active layer thickness (ALT) values for each model and observation at the three permafrost sites. ALT calculation is performed separately for models and observations by interpolating the soil temperature profile into finer resolution and estimating the maximum depth of 0 °C for each year. **(a)**, **(b)** and **(c)** show the temporal change of ALT at Schilthorn (2001 is omitted because observations have major gaps, also JSBACH and JULES are excluded as they simulate no permafrost at this site), Samoylov and Bayelva, respectively. Colors distinguish models and observations.

to assess the soil internal processes would be to use the same snow forcing or under snow temperature for all models. However most of the land models used in this study are not that modular. Hence, intertwined effects of surface and soil internal processes must be discussed together here.

Figures 7–10 show the mismatch in modeled DZAA representations. Together with the soil water and ice contents, simulating DZAA is partly related to the model soil depth and some models are limited by their shallow depth representations (Fig. A1 in the Appendix, Table 1). Apart from

the different temperature values, models also simulate permafrost conditions very differently. As seen in Fig. 8, JS-BACH and JULES do not simulate permafrost conditions at Schilthorn. In reality, there are almost isothermal conditions of about $-0.7\,°C$ between 7 m and at least 100 m depth at this site (PERMOS, 2013), which are partly caused by the three-dimensional thermal effects due to steep topography (Noetzli et al., 2008). Temperatures near the surface will not be strongly affected by three-dimensional effects, as the monitoring station is situated on a small but flat plateau (Scherler et al., 2013), but larger depths get additional heat input from the opposite southern slope, causing slightly warmer temperatures at depth than for completely flat topography (Noetzli et al., 2008). The warm and isothermal conditions close to the freezing point at Schilthorn mean that a small temperature mismatch (on the order of $1\,°C$) can result in non-permafrost conditions. This kind of temperature bias would not affect the permafrost condition at colder sites (e.g., Samoylov). In addition, having low water and ice content, and a comparatively low albedo, make the Schilthorn site very sensitive to interannual variations and make it more difficult for models to capture the soil thermal dynamics (Scherler et al., 2013). Compared to the other models with snow representation, OR-CHIDEE and LPJ-GUESS show colder subsurface temperatures at this site (Fig. 8). A thin surface litter layer (2.5 cm) in LPJ-GUESS contributes to the cooler Schilthorn soil temperatures in summer.

Differences at Samoylov are more related to the snow depth biases. As previously mentioned, subcritical snow conditions at this site amplify the soil temperature overestimation coming from snow depth bias (Fig. 5). Considering their better match during snow-free season (Fig. 6c), the warmer temperatures in deeper layers of JULES and COUP can be attributed to overestimated snow depths for this site by these two models (Fig. 9). Additionally, JULES and COUP models simulate generally warmer soils conditions than the other models, because these models include heat transfer via advection in addition to heat conduction. Heat transfer by advection of water is an additional heat source for the subsurface in JULES and COUP, which can also be seen in the results for Bayelva (Fig. 10). In combination with that, COUP has a greater snow depth at Samoylov (Fig. 5), resulting in even warmer subsurface conditions than JULES. Such conditions demonstrate the importance of the combined effects of surface processes together with internal soil physics.

Due to different heat transfer rates among models, internal soil processes can impede the heat transfer and result in delayed warming or cooling of the deeper layers. JS-BACH, ORCHIDEE, JULES and COUP show a more pronounced time lag of the heat/cold penetration into the soil, while HYBRID8 and LPJ-GUESS show either a very small lag or no lag at all (Figs. 7–10). This time lag is affected by the method of heat transfer (e.g., advection and conduction, see above), soil heat transfer parameters (soil heat capacity/conductivity), the amount of simulated phase change,

vertical soil model resolution and internal model time step. Given that all models use some sort of heat transfer method including phase change (Table 1) and similar soil parameters (Table 3), the reason for the rapid warming/cooling at deeper layers of some models can be missing latent heat of phase change, vertical resolution or model time step. Even though the mineral (dry) heat transfer parameters are shared among models, they are modified afterwards due to the coupling of hydrology and thermal schemes. This leads to changes in the model heat conductivities depending on how much water and ice they simulate in that particular layer. Unfortunately, not all models output soil water and ice contents in a layered structure similar to soil temperature. This makes it difficult to assess the differences in modeled phase change, and the consequent changes to soil heat transfer parameters. A better quantification of heat transfer rates would require a comparison of simulated water contents and soil heat conductivities among models, which is beyond the scope of this paper.

The model biases in matching the vertical temperature curves (minimum, maximum, mean) are related to the top-soil temperature bias in each model for each site, but also the above-mentioned soil heat transfer mechanisms and bottom boundary conditions. Obviously, models without snow representation (e.g., HYBRID8) cannot match the minimum curve in Fig. 12. However, snow depth bias (Fig. 5) cannot explain the minimum curve mismatch for ORCHIDEE, COUP, and LPJ-GUESS at Schilthorn (Fig. 12b). This highlights the effects of soil heat transfer schemes once again.

In general, permafrost specific model experiments require deeper soil representation than 5–10 m. As discussed in Alexeev et al. (2007), more than 30 m soil depth is needed for capturing decadal temperature variations in permafrost soils. The improvements from having such extended soil depth are shown in Lawrence et al. (2012), when compared to their older model version with shallow soil depth (Lawrence and Slater, 2005). Additionally, soil layer discretization plays an important role for the accuracy of heat and water transfer within the soil, and hence can effect the ALT estimations. Most of the model setups in our intercomparison have less than 10 m depths, so they lack some effects of processes within deeper soil layers. However, most of the models used in global climate simulations have similar soil depth representations and the scope here is to compare models that are not only aimed to simulate site-specific permafrost conditions at high resolution but to show general guidelines for future model developments.

Adding to all these outcomes, some models match the site observations better than others at specific sites. For example, the mean annual soil thermal profiles are better captured by JSBACH at Nuuk, by JULES and COUP at Schilthorn, by ORCHIDEE at Samoylov, and by COUP at Bayelva (Fig. 11). Comparing just the topsoil conditions at the non-permafrost Nuuk site, JSBACH better matches the observations due to its moss layer. On the other hand, by having better snow depth dynamics (Fig. 4), JULES and COUP mod-

els are better suited for sites with deeper snow depths like Schilthorn and Bayelva. Contrarily, the wet Samoylov site is better represented by ORCHIDEE in snow season (Fig. 2a) due to lower snow depths in this model (Fig. 4) and thus colder soil temperatures. However, the snow-free season is better captured by the JSBACH model (Fig. 2c) due to its effective moss insulation and LPJ-GUESS model due to its insulating litter layer.

4.3 Active layer thickness

As seen above, surface conditions (e.g., insulation) alone are not enough to explain the soil thermal regime, as subsoil temperatures and soil water and ice contents affect the ALT as well. For Schilthorn, LPJ-GUESS generally shows shallower ALT values than other models (Fig. 13a); it also shows the largest snow depth bias (Fig. 5), excluding snow as a possible cause for this shallow ALT result. However, if snow depth bias alone could explain the ALT difference, ORCHIDEE would show different values than HYBRID8, which completely lacks any snow representation. At Schilthorn, COUP has a high snow depth bias (Fig. 5) but still shows a very good match with the observed ALT (Fig. 13a), mainly because snow cover values at Schilthorn are very high so ALT estimations are insensitive to snow depth biases as long as modeled snow cover is still sufficiently thick to have the full insulation effect (Scherler et al., 2013).

All models overestimate the snow depth at Samoylov (Fig. 5) and most of them lack a proper moss insulation (Fig. 6c), which seems to bring deeper ALT estimates in Samoylov (Fig. 13b). However, HYBRID8 does not have snow representation, yet it shows the deepest ALT values, which means lack of snow insulation is not the reason for deeper ALT values in this model. As well as lacking any vegetation insulation, soil heat transfer is also much faster in HYBRID8 (see Sect. 3.2), which allows deeper penetration of summer warming into the soil column.

Surface conditions alone cannot describe the ALT bias in Bayelva either. LPJ-GUESS shows the lowest snow depth (Fig. 5) together with deepest ALT (Fig. 13c), while JULES shows similar snow depth bias as LPJ-GUESS but the shallowest ALT values. As seen from Fig. 10, LPJ-GUESS allows deeper heat penetration at this site. So, not only the snow conditions, but also the model's heat transfer rate is critical for correctly simulating the ALT.

5 Conclusions

We have evaluated different land models' soil thermal dynamics against observations using a site-level approach. The analysis of the simulated soil thermal regime clearly reveals the importance of reliable surface insulation for topsoil temperature dynamics and of reliable soil heat transfer formula-

tions for subsoil temperature and permafrost conditions. Our findings include the following conclusions.

1. At high latitudes and altitudes, model snow depth bias explains most of the topsoil temperature biases.

2. The sensitivity of soil temperature to snow insulation depends on site snow conditions (sub-/supra-critical).

3. Surface vegetation cover and litter/organic layer insulation is important for topsoil temperatures in the snow-free season, therefore models need more detailed representation of moss and top organic layers.

4. Model heat transfer rates differ due to coupled heat transfer and hydrological processes. This leads to discrepancies in subsoil thermal dynamics.

5. Surface processes alone cannot explain the whole soil thermal regime; subsoil conditions and model formulations affect the soil thermal dynamics.

For permafrost and cold-region-related soil experiments, it is important for models to simulate the soil temperatures accurately, because permafrost extent, active layer thickness and permafrost soil carbon processes are strongly related to soil temperatures. There is major concern about how the soil thermal state of these areas affects the ecosystem functions, and about the mechanisms (physical/biogeochemical) relating atmosphere, oceans and soils in cold regions. With the currently changing climate, the strength of these couplings will be altered, bringing additional uncertainty into future projections.

In this paper, we have shown the current state of a selection of land models with regard to capturing surface and subsurface temperatures in different cold-region landscapes. It is evident that there is much uncertainty, both in model formulations of soil internal physics and especially in surface processes. To achieve better confidence in future simulations, model developments should include better insulation processes (for snow: compaction, metamorphism, depth hoar, wind drift; for moss: dynamic thickness and wetness). Models should also perform more detailed evaluation of their soil heat transfer rates with observed data, for example comparing simulated soil moisture and soil heat conductivities.

Appendix A: Model layering schemes and depths of soil temperature observations

Exact depths of each soil layer used in model formulations:

JSBACH: 0.065, 0.254, 0.913, 2.902, 5.7 m

ORCHIDEE: 0.04, 0.05, 0.06, 0.07, 0.08, 0.1, 0.11, 0.14, 0.16, 0.19, 0.22, 0.27, 0.31, 0.37, 0.43, 0.52, 0.61, 0.72, 0.84, 1.00, 1.17, 1.39, 1.64, 1.93, 2.28, 2.69, 3.17, 3.75, 4.42, 5.22, 6.16, 7.27 m

JULES: 0.1, 0.25, 0.65, 2.0 m

COUP: different for each site

Nuuk: 0.01 m intervals until 0.36 m, then 0.1 m intervals until 2 m and then 0.5 m intervals until 6 m

Schilthorn: 0.05 m then 0.1 m intervals until 7 m, and then 0.5 m intervals until 13 m

Samoylov: 0.05 m then 0.1 m intervals until 5 m, and then 0.5 m intervals until 8 m

Bayelva: 0.01 m intervals until 0.3 m, then 0.1 m intervals until 1 m and then 0.5 m intervals until 6 m

HYBRID8: different for each site

Nuuk: 0.07, 0.29, 1.50, 5.00 m

Schilthorn: 0.07, 0.30, 1.50, 5.23 m

Samoylov: 0.07, 0.30, 1.50, 6.13 m

Bayelva: 0.07, 0.23, 1.50, 5.00 m

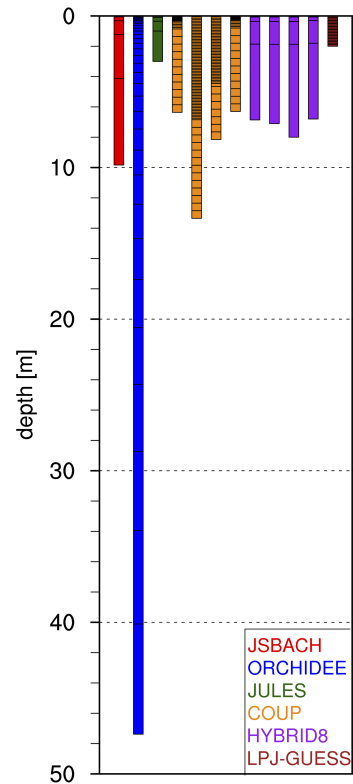LPJ-GUESS: 0.1 m intervals until 2 m (additional padding layer of 48 m depth).

Figure A1. Soil layering schemes of each model. COUP and HYBRID8 models use different layering schemes for each study site, which are represented with different bars (from left to right: Nuuk, Schilthorn, Samoylov and Bayelva).

Depths of soil temperature observations for each site:

Nuuk: 0.01, 0.05, 0.10, 0.30 m

Schilthorn: 0.20, 0.40, 0.80, 1.20, 1.60, 2.00, 2.50, 3.00, 3.50, 4.00, 5.00, 7.00, 9.00, 10.00 m

Samoylov: 0.02, 0.06, 0.11, 0.16, 0.21, 0.27, 0.33, 0.38, 0.51, 0.61, 0.71 m

Bayelva: 0.06, 0.24, 0.40, 0.62, 0.76, 0.99, 1.12 m

Table A1. Selected depths of observed and modeled soil temperatures referred as "topsoil temperature" in Figs. 1, 2, 4, 5 and 6.

	Nuuk	Schilthorn	Samoylov	Bayelva
OBSERVATION	5 cm	20 cm	6 cm	6 cm
JSBACH	3.25 cm	18.5 cm	3.25 cm	3.25 cm
ORCHIDEE	6.5 cm	18.5 cm	6.5 cm	6.5 cm
JULES	5 cm	22.5 cm	5 cm	5 cm
COUP	5.5 cm	20 cm	2.5 cm	5.5 cm
HYBRID8	3.5 cm	22 cm	3.5 cm	3.5 cm
LPJ-GUESS	5 cm	25 cm	5 cm	5 cm

References

Abnizova, A., Siemens, J., Langer, M., and Boike, J.: Small ponds with major impact: The relevance of ponds and lakes in permafrost landscapes to carbon dioxide emissions, Global Biogeochem. Cy., 26, GB2041, doi:10.1029/2011GB004237, 2012.

Abramopoulos, F., Rosenzweig, C., and Choudhury, B.: Improved ground hydrology calculations for global climate models (GCMs): Soil water movement and evapotranspiration, J. Climate, 1, 921–941, doi:10.1175/1520-0442(1988)001<0921:IGHCFG>.0.CO;2, 1988.

ACIA: Arctic Climate Impact Assessment, Cambridge University Press, New York, USA, 1042 pp., 2005.

Alexeev, V. A., Nicolsky, D. J., Romanovsky, V. E., and Lawrence, D. M.: An evaluation of deep soil configurations in the CLM3 for improved representation of permafrost, Geophys. Res. Lett., 34, L09502, doi:10.1029/2007GL029536, 2007.

Anisimov, O. A. and Nelson, F. E.: Permafrost zonation and climate change in the northern hemisphere: results from transient general circulation models, Climatic Change, 35, 241–258, doi:10.1023/A:1005315409698, 1997.

Beer, C., Weber, U., Tomelleri, E., Carvalhais, N., Mahecha, M., and Reichstein, M.: Harmonized European long-term climate data for assessing the effect of changing temporal variability on land-atmosphere CO_2 fluxes, J. Climate, 27, 4815–4834, doi:10.1175/JCLI-D-13-00543.1, 2014.

Best, M. J., Pryor, M., Clark, D. B., Rooney, G. G., Essery, R. L. H., Ménard, C. B., Edwards, J. M., Hendry, M. A., Porson, A., Gedney, N., Mercado, L. M., Sitch, S., Blyth, E., Boucher, O., Cox, P. M., Grimmond, C. S. B., and Harding, R. J.: The Joint UK Land Environment Simulator (JULES), model description – Part 1: Energy and water fluxes, Geosci. Model Dev., 4, 677–699, doi:10.5194/gmd-4-677-2011, 2011.

Boike, J., Roth, K., and Ippisch, O.: Seasonal snow cover on frozen ground: Energy balance calculations of a permafrost site near Ny-Ålesund, Spitsbergen, J. Geophys. Res.-Atmos., 108, 8163, doi:10.1029/2001JD000939, 2003.

Boike, J., Ippisch, O., Overduin, P. P., Hagedorn, B., and Roth, K.: Water, heat and solute dynamics of a mud boil, Spitsbergen, Geomorphology, 95, 61–73, doi:10.1016/j.geomorph.2006.07.033, 2007.

Boike, J., Wille, C., and Abnizova, A.: Climatology and summer energy and water balance of polygonal tundra in the Lena River Delta, Siberia, J. Geophys. Res., 113, G03025, doi:10.1029/2007JG000540, 2008.

Boike, J., Kattenstroth, B., Abramova, K., Bornemann, N., Chetverova, A., Fedorova, I., Fröb, K., Grigoriev, M., Grüber, M., Kutzbach, L., Langer, M., Minke, M., Muster, S., Piel, K., Pfeiffer, E.-M., Stoof, G., Westermann, S., Wischnewski, K., Wille, C., and Hubberten, H.-W.: Baseline characteristics of climate, permafrost and land cover from a new permafrost observatory in the Lena River Delta, Siberia (1998–2011), Biogeosciences, 10, 2105–2128, doi:10.5194/bg-10-2105-2013, 2013.

Brown, J., Ferrians Jr., O. J., Heginbottom, J. A., and Melnikov, E. S.: Circum-Arctic map of permafrost and ground-ice conditions (Version 2), National Snow and Ice Data Center, Boulder, CO, USA, available at: http://nsidc.org/data/ggd318.html (last access: 10 September 2012), 2002.

Burke, E. J., Dankers, R., Jones, C. D., and Wiltshire, A. J.: A retrospective analysis of pan Arctic permafrost using the JULES land surface model, Clim. Dynam., Volume 41, 1025–1038, 2013.

Clark, D. B., Mercado, L. M., Sitch, S., Jones, C. D., Gedney, N., Best, M. J., Pryor, M., Rooney, G. G., Essery, R. L. H., Blyth, E., Boucher, O., Harding, R. J., Huntingford, C., and Cox, P. M.: The Joint UK Land Environment Simulator (JULES), model description – Part 2: Carbon fluxes and vegetation dynamics, Geosci. Model Dev., 4, 701–722, doi:10.5194/gmd-4-701-2011, 2011.

Cox, P. M., Betts, R. A., Bunton, C. B., Essery, R. L. H., Rowntree, P. R., and Smith, J.: The impact of new land surface physics on the GCM simulation of climate and climate sensitivity, Clim. Dynam., 15, 183–203, 1999.

Dankers, R., Burke, E. J., and Price, J.: Simulation of permafrost and seasonal thaw depth in the JULES land surface scheme, The Cryosphere, 5, 773–790, doi:10.5194/tc-5-773-2011, 2011.

Ekici, A., Beer, C., Hagemann, S., Boike, J., Langer, M., and Hauck, C.: Simulating high-latitude permafrost regions by the JSBACH terrestrial ecosystem model, Geosci. Model Dev., 7, 631–647, doi:10.5194/gmd-7-631-2014, 2014.

Engelhardt, M., Hauck, C., and Salzmann, N.: Influence of atmospheric forcing parameters on modelled mountain permafrost evolution, Meteorol. Zeitschr., 19, 491–500, 2010.

FAO, IIASA, ISRIC, ISS-CAS, and JRC: Harmonized World Soil Database (version 1.1) FAO, Rome, Italy and IIASA, Laxenburg, Austria, 2009.

Fiddes, J., Endrizzi, S., and Gruber, S.: Large-area land surface simulations in heterogeneous terrain driven by global data sets: application to mountain permafrost, The Cryosphere, 9, 411–426, doi:10.5194/tc-9-411-2015, 2015.

Friend, A. D. and Kiang, N. Y.: Land-surface model development for the GISS GCM: Effects of improved canopy physiology on simulated climate, J. Climate, 18, 2883–2902, doi:10.1175/JCLI3425.1, 2005.

Gerten, D., Schaphoff, S., Haberlandt, U., Lucht, W., and Sitch, S.: Terrestrial vegetation and water balance – hydrological evaluation of a dynamic global vegetation model, J. Hydrol., 286, 249–270, 2004.

Gornall, J. L., Jonsdottir, I. S., Woodin, S. J., and Van der Wal, R.: Arctic mosses govern below-ground environment and ecosystem processes, Oecologia, 153, 931–941, doi:10.1007/s00442-007-0785-0, 2007.

Gouttevin, I., Krinner, G., Ciais, P., Polcher, J., and Legout, C.: Multi-scale validation of a new soil freezing scheme for a land-surface model with physically-based hydrology, The Cryosphere, 6, 407–430, doi:10.5194/tc-6-407-2012, 2012a.

Gouttevin, I., Menegoz, M., Domine, F., Krinner, G., Koven, C. D., Ciais, P., Tarnocai, C., and Boike, J.: How the insulating properties of snow affect soil carbon distribution in the continental pan-Arctic area, J. Geophys. Res., 117, G02020, doi:10.1029/2011JG001916, 2012b.

Gubler, S., Endrizzi, S., Gruber, S., and Purves, R. S.: Sensitivities and uncertainties of modeled ground temperatures in mountain environments, Geosci. Model Dev., 6, 1319–1336, doi:10.5194/gmd-6-1319-2013, 2013.

Gustafsson, D., Stähli, M., and Jansson, P.-E.: The surface energy balance of a snow cover: comparing measurements to two different simulation models, Theor. Appl. Climatol., 70, 81–96, 2001.

Harlan, R. L.: Analysis of coupled heat-fluid transport in partially frozen soil, Water Resour. Res., 9, 1314–1323, 1973.

Harris, C., Arenson, L., Christiansen, H., Etzelmüller, B., Frauenfelder, R., Gruber, S., Haeberli, W., Hauck, C., Hoelzle, M., Humlum, O., Isaksen, K., Kääb, A., Kern-Lütschg, M., Lehning, M., Matsuoka, N., Murton, J., Nötzli, J., Phillips, M., Ross, N., Seppälä, M., Springman, S., and Vonder Mühll, D.: Permafrost and climate in Europe: monitoring and modelling thermal, geomorphological and geotechnical responses, Earth Sci. Rev., 92, 117–171, 2009.

Hauck, C.: Frozen ground monitoring using DC resistivity tomography. Geophys. Res. Lett., 29, 2016, doi:10.1029/2002GL014995, 2002.

Helbig, M., Boike, J., Langer, M., Schreiber, P., Runkle, B. R., and Kutzbach, L.: Spatial and seasonal variability of polygonal tundra water balance: Lena River Delta, northern Siberia (Russia), Hydrogeol. J. 21, 133–147, 2013.

Hilbich, C., Hauck, C., Hoelzle, M., Scherler, M., Schudel, L., Völksch, I., Vonder Mühll, D., and Mäusbacher, R.: Monitoring mountain permafrost evolution using electrical resistivity tomography: A 7-year study of seasonal, annual, and long-term variations at Schilthorn, Swiss Alps, J. Geophys. Res., 113, F01S90, doi:10.1029/2007JF000799, 2008.

Hilbich, C., Fuss, C., and Hauck, C.: Automated time-lapse ERT for improved process analysis and monitoring of frozen ground, Permafr. Periglac. Proc. 22, 306–319, doi:10.1002/ppp.732, 2011.

Hoelzle, M., Gruber, S.: Borehole and ground surface temperatures and their relationship to meteorological conditions in the Swiss Alps, edited by: Kane, D. L. and Hinkel, K. M., in: Proceedings Ninth International Conference on Permafrost, 29 June–3 July, Fairbanks Alaska, vol. 1. Institute of Northern Engineering, University of Alaska Fairbanks, 723–728, 2008.

Hollesen, J., Elberling, B., and Jansson, P. E.: Future active layer dynamics and carbon dioxide production from thawing permafrost layers in Northeast Greenland, Global Change Biol., 17, 911–926, doi:10.1111/j.1365-2486.2010.02256.x, 2011.

IPCC AR5: Summary for Policymakers, Climate Change 2013, The Physical Science Basis, Contribution of Working Group I to the Fifth Assessment Report of the Intergovernmental Panel on Climate Change, edited by: Stocker, T. F., Qin, D., Plattner, G.-K., Tignor, M., Allen, S. K., Boschung, J., Nauels, A., Xia, Y., Bex, V., and Midgley, P. M., Cambridge University Press, Cambridge, UK and New York, NY, USA, 2013.

Jansson, P. E.: CoupModel: model use, calibration, and validation, Transactions of the ASABE 55.4, 1335–1344, 2012.

Jansson, P.-E. and Karlberg, L.: Coupled heat and mass transfer model for soil-plant-atmosphere systems, Royal Institute of Technology, Dept of Civil and Environmental Engineering, Stockholm, available at: http://www.lwr.kth.se/VaraDatorprogram/CoupModel/index.htm (last access: 17 September 2014), 2011.

Jensen, L. M. and Rasch, M.: Nuuk Ecological Research Operations, 2nd Annual Report, 2008, Roskilde, National Environmental Research Institute, Aarhus University, Denmark, 80 pp., 2009.

Jensen, L. M. and Rasch, M.: Nuuk Ecological Research Operations, 3rd Annual Report, 2009, Roskilde, National Environmental Research Institute, Aarhus University, Denmark, 80 pp., 2010.

Jungclaus, J. H., Fischer, N., Haak, H., Lohmann, K., Marotzke, J., Matei, D., Mikolajewicz, U., Notz, D., and von Storch, J. S.: Characteristics of the ocean simulations in MPIOM, the ocean component of the MPI-Earth System Model, J. Adv. Model. Earth Syst., 5, 422–446, doi:10.1002/jame.20023, 2013.

Koven, C. D., Ringeval, B., Friedlingstein, P., Ciais, P., Cadule, P., Khvorostyanov, D., Krinner, G., and Tarnocai, C.: Permafrost carbon-climate feedbacks accelerate global warming, P. Natl. Acad. Sci., 108, 14769–14774, 2011.

Koven, C. D., William, J. R., and Alex, S.: Analysis of Permafrost Thermal Dynamics and Response to Climate Change in the CMIP5 Earth System Models, J. Climate, 26, 1877–1900, doi:10.1175/JCLI-D-12-00228.1, 2013.

Krinner, G., Viovy, N., de Noblet-Ducoudré, N., Ogée, J., Polcher, J., Friedlingstein, P., Ciais, P., Sitch, S., and Prentice, I. C.: A dynamic global vegetation model for studies of the coupled atmosphere-biosphere system, Global Biogeochem. Cy., 19, GB1015, doi:10.1029/2003GB002199, 2005.

Kudryavtsev, V. A., Garagulya, L. S., Kondrat'eva, K. A., and Melamed, V. G.: Fundamentals of Frost Forecasting in Geological Engineering Investigations, Cold Regions Reseach and Engineering Laboratory: Hanover, NH, 1974.

Kutzbach, L., Wille, C., and Pfeiffer, E.-M.: The exchange of carbon dioxide between wet arctic tundra and the atmosphere at the

Lena River Delta, Northern Siberia, Biogeosciences, 4, 869–890, doi:10.5194/bg-4-869-2007, 2007.

Langer, M., Westermann, S., Heikenfeld, M., Dorn, W., and Boike, J.: Satellite-based modeling of permafrost temperatures in a tundra lowland landscape, Remote Sens. Environ., 135, 12–24, doi:10.1016/j.rse.2013.03.011, 2013.

Larsen, P. H., Goldsmith, S., Smith, O., Wilson, M. L., Strzepek, K., Chinowsky, P., and Saylor, B.: Estimating future costs for Alaska public infrastructure at risk from climate change, Global Environ. Change, 18, 442–457, doi:10.1016/ j.gloenvcha.2008.03.005, 2008.

Lawrence, D. M. and Slater, A. G.: A projection of severe near-surface permafrost degradation during the 21st century, Geophys. Res. Lett., 32, L24401, doi:10.1029/2005GL025080, 2005.

Lawrence, D. M., Slater, A. G., Romanovsky, V. E., and Nicolsky, D. J.: Sensitivity of a model projection of near-surface permafrost degradation to soil column depth and representation of soil organic matter, J. Geophys. Res., 113, 1–14, 2008.

Lawrence, D. M., Slater, A. G., and Swenson, S. C.: Simulation of Present-Day and Future Permafrost and Seasonally Frozen Ground Conditions in CCSM4, J. Climate, 25, 2207–2225, 2012.

Lunardini, V. J.: Heat transfer in cold climates, Van Nostrand Reinhold, New York, 731 pp., 1981.

Lundin, L. C.: Hydraulic properties in an operational model of frozen soil, J. Hydrol., 118, 289–310, 1990.

Lüers, J., Westermann, S., Piel, K., and Boike, J.: Annual CO_2 budget and seasonal CO_2 exchange signals at a High Arctic permafrost site on Spitsbergen, Svalbard archipelago, Biogeosciences, 11, 6307–6322, doi:10.5194/bg-11-6307-2014, 2014.

Mahecha, M. D., Reichstein, M., Jung, M., Seneviratne, S. I., Zaehle, S., Beer, C., Braakhekke, M. C., Carvalhais, N., Lange, H., Le Maire G., and Moors, E.: Comparing observations and process-based simulations of biosphere-atmosphere exchanges on multiple timescales, J. Geophys. Res., 115, G02003, doi:10.1029/2009JG001016, 2010.

Marmy, A., Salzmann, N., Scherler, M., and Hauck, C.: Permafrost model sensitivity to seasonal climatic changes and extreme events in mountainous regions, Environ. Res. Lett., 8, 035048, doi:10.1088/1748-9326/8/3/035048, 2013.

Maturilli, M., Herber, A., and König-Langlo, G.: Climatology and time series of surface meteorology in Ny-Ålesund, Svalbard, Earth Syst. Sci. Data, 5, 155–163, doi:10.5194/essd-5-155-2013, 2013.

McGuire, A. D., Christensen, T. R., Hayes, D., Heroult, A., Euskirchen, E., Kimball, J. S., Koven, C., Lafleur, P., Miller, P. A., Oechel, W., Peylin, P., Williams, M., and Yi, Y.: An assessment of the carbon balance of Arctic tundra: comparisons among observations, process models, and atmospheric inversions, Biogeosciences, 9, 3185–3204, doi:10.5194/bg-9-3185-2012, 2012.

Miller, P. A. and Smith, B.: Modeling tundra vegetation response to recent Arctic warming, AMBIO, J. Human. Environ.,?41, 281–291, 2012.

Muster, S., Langer, M., Heim, B., Westermann, S., and Boike, J.: Subpixel heterogeneity of ice-wedge polygonal tundra: a multi-scale analysis of land cover and evapotranspiration in the Lena River Delta, Siberia, Tellus B, 64, 2012.

Noetzli, J., Hilbich, C., Hauck, C., Hoelzle, M., and Gruber, S.: Comparison of simulated 2D temperature profiles with time-lapse electrical resistivity data at the Schilthorn crest, Switzer-land, 9th International Conference on Permafrost, Fairbanks, US, 1293–1298, 2008.

PERMOS: Permafrost in Switzerland 2008/2009 and 2009/2010, edited by: Noetzli, J., Glaciological Report (Permafrost) No. 10/11 of the Cryospheric Commission of the Swiss Academy of Sciences (SCNAT), Zurich, Switzerland, 2013.

Porada, P., Weber, B., Elbert, W., Pöschl, U., and Kleidon, A.: Estimating global carbon uptake by Lichens and Bryophytes with a process-based model, Biogeosciences, 10, 6989–7033, doi:10.5194/bg-10-6989-2013, 2013.

Rinke, A., Kuhry, P., and Dethloff, K.: Importance of a soil organic layer for Arctic climate: A sensitivity study with an Arctic RCM, Geophys. Res. Lett., 35, L13709, doi:10.1029/2008GL034052, 2008.

Riseborough, D., Shiklomanov, N., Etzelmuller, B., Gruber, S., and Marchenko, S.: Recent Advances in Permafrost Modelling, Permafr. Periglac. Process., 19, 137–156, 2008.

Romanovsky, V. E. and Osterkamp, T. E.: Thawing of the active layer on the coastal plain of the Alaskan Arctic, Permafr. Periglac. Proc., 8, 1–22, doi:10.1002/(SICI)1099-1530(199701)8:1<1::AID-PPP243>3.0.CO;2-U, 1997.

Romanovsky, V. E., Smith, S. L., and Christiansen, H. H.: Permafrost thermal state in the polar Northern Hemisphere during the international polar year 2007-2009: a synthesis, Permafr. Periglac. Process., 21, 106–116, 2010.

Rosenzweig, C. and Abramopoulos, F.: Land-surface model development for the GISS GCM, J. Climate, 10, 2040–2054, doi:10.1175/1520-0442(1997)010<12040:LSMDFT>2.0.CO;2, 1997.

Roth, K. and Boike, J.: Quantifying the thermal dynamics of a permafrost site near Ny-Ålesund, Svalbard., Water Resour. Res., 37, 2901–2914, doi:10.1029/2000WR000163, 2001.

Scherler, M., Hauck, C., Hoelzle, M., Stähli, M., and Völksch, I.: Meltwater infiltration into the frozen active layer at an alpine permafrost site, Permafrost Periglac. Process., 21, 325–334, doi:10.1002/ppp.694, 2010.

Scherler, M., Hauck, C., Hoelzle, M., and Salzmann, N.: Modeled sensitivity of two alpine permafrost sites to RCM-based climate scenarios, J. Geophys. Res. Earth Surf., 118, 780–794, doi:10.1002/jgrf.20069, 2013.

Schmidt, G. A., Ruedy, R., Hansen, J. E., Aleinov, I., Bell, N., Bauer, M., Bauer, S., Cairns, B., Canuto, V., Cheng, Y., Del Genio, A., Faluvegi, G, Friend, A. D., Hall, T. M., Hu, Y., Kelley, M., Kiang, N. Y., Koch, D., Lacis, A. A., Lerner, J., Lo, K. K., Miller, R. L., Nazarenko, L., Oinas, V., Perlwitz, Ja., Perlwitz, J., Rind, D., Romanou, A., Russell, G. L., Sato, M. K., Shindell, D. T., Stone, P. H., Sun, S., Tausnev, N., Thresher, D., and Yao, M. S.: Present day atmospheric simulations using GISS ModelE: Comparison to in-situ, satellite and reanalysis data, J. Climate 19, 153–192, 2006.

Schuur, E. A. G., Bockheim, J., Canadell, J. G., Euskirchen, E., Field, C. B., Goryachkin, S. V., Hagemann, S., Kuhry, P., Lafleur, P. M., Lee, H., Mazhitova, G., Nelson, F. E., Rinke, A., Romanovsky, V. E., Shiklomanov, N., Tarnocai, C., Venevsky. S., Vogel, J. G., and Zimov, S. A.: Vulnerability of Permafrost Carbon to Climate Change: Implications for the Global Carbon Cycle, BioScience, 58, 701–714, 2008.

Serreze, M., Walsh, J., Chapin, F., Osterkamp, T., Dyurgerov, M., Romanovsky, V., Oechel, W., Morison, J., Zhang, T., and Barry,

R.: Observational evidence of recent change in the northern high-latitude environment, Clim. Change, 46, 159–207, 2000.

Shiklomanov, N. I. and Nelson, F. E.: Analytic representation of the active layer thickness field, Kuparuk River Basin, Alaska, Ecological Modeling, 123, 105–125, doi:10.1016/S0304-3800(99)00127-1, 1999.

Sitch, S., Smith, B., Prentice, I. C., Arneth, A., Bondeau, A., Cramer, W., Kaplan, J. O., Levis, S., Lucht, W., Sykes, M. T., Thonicke, K., and Venevsky, S.: Evaluation of ecosystem dynamics, plant geography and terrestrial carbon cycling in the LPJ dynamic global vegetation model, Global Change Biology, 9, 161–185, 2003.

Slater, A. G. and Lawrence, D. M.: Diagnosing Present and Future Permafrost from Climate Models, J. Clim., 26, 5608–5623, doi:10.1175/JCLI-D-12-00341.1, 2013.

Smith, B., Prentice, I. C., and Sykes, M. T.: Representation of vegetation dynamics in the modelling of terrestrial ecosystems: comparing two contrasting approaches within European climate space, Global Ecol. Biogeogr., 10, 621–637, doi:10.1046/j.1466-822X.2001.t01-1-00256.x, 2001.

Soudzilovskaia, N. A., van Bodegom, P. M., and Cornelissen, J. H. C.: Dominant bryophyte control over high-latitude soil temperature fluctuations predicted by heat transfer traits, field moisture regime and laws of thermal insulation, Funct. Ecol., 27, 1442–1454, doi:10.1111/1365-2435.12127S, 2013.

Stendel M., Romanovsky, V. E., Christensen, J. H., and Sazonova T.: Using dynamical downscaling to close the gap between global change scenarios and local permafrost dynamics, Global Planet. Change, 56, 203–214, doi:10.1016/j.gloplacha.2006.07.014, 2007.

Stevens, B., Giorgetta, M., Esch, M., Mauritsen, T., Crueger, T., Rast, S., Salzmann, M., Schmidt, H., Bader, J., Block, K., Brokopf, R., Fast, I., Kinne, S., Kornblueh, L., Lohmann, U., Pincus, R., Reichler, T., and Roeckner, E.: The atmospheric component of the MPI-M Earth System Model: ECHAM6, J. Adv. Model. Earth Syst., 5, 146–172, doi:10.1002/jame.20015, 2012.

Taylor, K. E., Stouffer, R. J., and Meehl, G. A.: A summary of the CMIP5 experiment design. PCMDI Tech. Rep., 33 pp., available at: http://cmip-pcmdi.llnl.gov/cmip5/docs/Taylor_CMIP5_design.pdf, 2009.

Vonder Mühll, D., Hauck, C., and Lehmann, F.: Verification of geophysical models in Alpine permafrost using borehole information, Ann. Glaciol., 31, 300–306, 2000.

Wang, T., Ottle, C., Boone, A., Ciais, P., Brun, E., Morin, S., Krinner, G., Piao, S., and Peng, S.: Evaluation of an improved intermediate complexity snow scheme in the ORCHIDEE land surface model, J. Geophys. Res.-Atmos., 118, 6064–6079, doi:10.1002/jgrd.50395, 2013.

Wania, R., Ross, I., and Prentice, I. C.: Integrating peatlands and permafrost into a dynamic global vegetation model: 1. Evaluation and sensitivity of physical land surface processes, Global Biogeochem. Cy., 23, doi:10.1029/2008GB003412, 2009a.

Wania, R., Ross, I., and Prentice, I. C.: Integrating peatlands and permafrost into a dynamic global vegetation model: 2. Evaluation and sensitivity of vegetation and carbon cycle processes, Global Biogeochem. Cy., 23, doi:10.1029/2008GB003413, 2009b.

Wania, R., Ross, I., and Prentice, I. C.: Implementation and evaluation of a new methane model within a dynamic global vegetation model: LPJ-WHyMe v1.3.1, Geoscientific Model Development 3, 565–584, 2010.

Weedon, G., Gomes, S., Viterbo, P., Österle, H., Adam, J., Bellouin, N., Boucher, O., and Best, M.: The WATCH forcing data 1958-2001: A meteorological forcing dataset for land surface and hydrological models WATCH Tech. Rep. 22, 41 pp., available at: http://www.eu-watch.org/publications/technical-reports, 2010.

Westermann, S., Lüers, J., Langer, M., Piel, K., and Boike, J.: The annual surface energy budget of a high-arctic permafrost site on Svalbard, Norway, The Cryosphere, 3, 245–263, doi:10.5194/tc-3-245-2009, 2009.

Westermann, S., Wollschläger, U., and Boike, J.: Monitoring of active layer dynamics at a permafrost site on Svalbard using multichannel ground-penetrating radar, The Cryosphere, 4, 475–487, doi:10.5194/tc-4-475-2010, 2010.

Westermann, S., Langer, M., and Boike, J.: Spatial and temporal variations of summer surface temperatures of high-arctic tundra on Svalbard – Implications for MODIS LST based permafrost monitoring, Remote Sens. Environ., 115, 908–922, doi:10.1016/j.rse.2010.11.018, 2011.

Wolf, A., Callaghan, T., and Larson, K.: Future changes in vegetation and ecosystem function of the Barents Region, Clim. Change, 87, 51–73, 2008.

ZackenbergGIS, available at: http://dmugisweb.dmu.dk/zackenberggis/datapage.aspx, last access: 10 September 2012.

Zhang, T.: Influence of the seasonal snow cover on the ground thermal regime: An overview, Rev. Geophys., 43, RG4002, doi:10.1029/2004RG000157, 2005.

Zhang, W., Miller, P. A., Smith, B., Wania, R., Koenigk, T., and Döscher, R.: Tundra shrubification and tree-line advance amplify arctic climate warming: results from an individual-based dynamic vegetation model, Environ. Res. Lett., 8, 034023, doi:10.1088/1748-9326/8/3/034023, 2013.

CHAPTER 4

SITE LEVEL PROCESS ANALYSIS

4.1 Introduction

The previous chapters have described the model development relevant to permafrost soils and compared it to observations and other modeling approaches. This chapter will deal with site level analysis of different process representations in order to find the optimum level of detail needed in global models to estimate permafrost physical state.

Earth System Models operate on spatial grid systems that are most efficient with the current computational technology. They simulate the desired variables for a given area (grid-area) with spatially average values to represent a semi-continuous field for the target domain. Even though this discretization over a spatial grid system is extremely helpful for having a broad impression of a larger region with using just a limited number of points, the choice of grid-size can define what processes can be represented in such simulations. Model grid sizes show a large range of values and most models use grid-sizes ranging from 1 km^2 to 10^3 km^2 (Dufresne et al., 2013; Stevens et al., 2012; Dunne et al., 2012; Gent et al., 2011; Goose et al., 2010). Regardless of how fine the grid size is, discretizing natural phenomena cannot replicate the exact complexity of nature and a number of sub-grid processes will always be omitted (Annan et al., 2005). Thus, a never-ending improvement for a finer grid size is inevitable for future model developments. However, site-level analyses can overcome many limitations of current modeling approaches in this respect. Avoiding the grid averaging by directly running the models with point scale forcing and analyzing the direct outputs of the point simulation, the abovementioned scale-dependent uncertainties are minimized and uncertainties purely related to model formulations and forcing data can be investigated. After a so increased validity of process representations, the model could be further advanced in terms of sub-grid variability, which is not a topic in this thesis.

Using such site level approach, JSBACH model has been improved with many cold region specific processes (Chapter 2). By testing the model performance at selected sites, the freeze/thaw events, coupled hydrology and thermal diffusion, multi-layer snow representation, and thermal moss insulation are successfully implemented in the new version of JSBACH. Evaluations with both site-level and broad-scale datasets revealed model biases in active layer thickness (ALT) and subsoil temperatures. JSBACH overestimates the ALT in most parts of the Arctic, and shows colder subsoil temperatures in general. These mismatches are likely to originate from biases in snow depth representation, climate forcing data, and unknown depth of the organic layer/unconsolidated material above the bedrock. As discussed in Ekici et al. (2014), similar problems are observed in other models. Gouttevin et al. (2012) have shown the positive ALT bias in ORCHIDEE model, while Dankers et al. (2011) and

Lawrence et al. (2012) have pointed out general model overestimation of ALT values (in JULES and CLM4 models respectively) due to mismatched surface conditions, soil thermal-hydrological couplings and model depths. In addition, a site-level model intercomparison of soil thermal dynamics (Chapter 3) revealed a general model bias in soil temperatures during snow season, mainly related to the accuracy of model snow depth representations. Similarly, a model disagreement is observed in summer soil temperature comparisons, which is explained by the mismatched thermal insulation of the model vegetation cover representation (Ekici et al., 2015). Surface conditions (snow, vegetation, organic layer) have a strong impact on soil thermal regime (Yershov, 1998; Zhang, 2005; Gornall et al., 2007). Ground temperatures and thus the ALT are affected by too high/too low thermal insulation at the surface.

On the account of these issues, land models need to be improved in terms of surface insulation and soil formulations to overcome these soil temperature biases. However, due to global models' technical complexities, it is not always straightforward to test them at sites with unique properties. This is one of the important issues in current modeling discipline. Therefore, JSBACH is tested at three different sites in order to evaluate different approaches in process representation for better capturing soil thermal dynamics. For this reason, JSBACH is further improved by including dynamic heat transfer properties in snow and moss layers together with extending the model soil column from 10 m to 53 m. To test the performances of new model formulations in simulating the soil thermal regime, several factorial site-level model experiments are performed and the results are analyzed in this chapter.

4.2 Methods

4.2.1 Dynamic Snow

The JSBACH version introduced in Chapter 2 keeps a simple snow formulation to provide thermal insulation of the snow layer. The snow density and snow heat transfer parameters (snow heat capacity and heat conductivity) are kept constant in time, only allowing snow depth changes due to snowfall and snow melting. This approach provides the snow thermal insulation and keeps the winter soil temperatures comparable to the observations (Chapter 2, Figs. 2-6). However, this simple snow formulation results in overestimated snow depths and cannot capture the dynamics of snow cover (Fig. 4.1). These results suggest the need for an improved snow representation, which is presented in this section.

For the snow density, the new approach follows a similar representation as in Verseghy (1991). The snow density is initialized with a minimum value of p_{min} = 50 kg m^{-3}. Then the compaction effect is included as a function of time and a maximum density value (Eq. 4.1).

With new snowfall, snow density value is updated by taking a weighted average of fresh snow density (p_{min} = 50 kg m^{-3}) and the previous timestep's calculated snow density value.

$$\rho_{snow}^{t+1} = (\rho_{snow}^{t} - \rho_{max}) \times e^{(-0.01 \times \Delta_t / 3600)} + \rho_{max} \qquad (4.1)$$

with:

p_{snow} = snow density value for timestep t [kg m^{-3}]

p_{max} = maximum snow density value [450 kg m^{-3}]

Δ_t = timestep length of model simulation [s]

By incorporating these changes due to compaction and mixing, snow density (hence the snow depth) dynamically changes during the simulation. These changes are also reflected in the snow heat transfer parameters: volumetric snow heat capacity (Eq. 4.2) and snow heat conductivity (Eq. 4.3), which follows the approach in Goodrich (1982). With no previous snow layers, volumetric snow heat capacity is initialized with an average value of 0.52 MJ m^{-3} K^{-1} and heat conductivity with 0.1 W m^{-1} K^{-1}.

$$c_{snow} = c_{ice} \times \rho_{snow} \qquad (4.2)$$

$$\lambda_{snow} = 2.9 \times 10^{-6} \times (\rho_{snow})^2 \qquad (4.3)$$

with:

c_{snow} = volumetric snow heat capacity for each timestep [J m^{-3} K^{-1}]

c_{ice} = specific heat capacity of ice [2106 J kg^{-1} K^{-1}]

λ_{snow} = snow thermal conductivity for each timestep [W m^{-1} K^{-1}]

4.2.2 Dynamic Moss

JSBACH also includes a simple moss layer for thermal insulation (Chapter 2). In order to provide the thermal insulation effects of the organic layer/moss cover, an additional layer with constant thickness and heat transfer parameters is prescribed atop the soil. For this approach, the moss layer is set to 10 cm thickness using 2.5 MJ m^{-3} K^{-1} for the heat capacity and 0.25 W m^{-1} K^{-1} for the heat conductivity. However, the constant parameters used for the moss layer prevent capturing the changing insulation effect of dry and wet conditions (Chapter 2, Figs. 2-6).

As documented in O'Donnel et al. (2009), moss and lichen heat conductivity values can range from 0.03 to 0.6 W m^{-1} K^{-1} with increasing saturation levels. To incorporate such effects, a dynamically changing heat transfer parameter representation has been implemented for the moss layer. Instead of using constant values, the moss layer now copies the soil representation by mixing water, ice and solid particles of the layer matrix and uses a representative heat capacity and heat conductivity value of all these components (Eqs. 4.4-

4.8). Since the JSBACH moss layer is decoupled from the hydrology implementation, first soil layer water and ice contents are taken as the moss layer conditions.

$$c_{moss} = (1 - \theta_{sat})c_s + \rho_w c_w \theta_w^1 + \rho_i c_i \theta_i^1 \qquad (4.4)$$

with:

θ_{sat} = soil porosity [$m^3\ m^{-3}$]

c_s = heat capacity of solid part [2.5 MJ $m^{-3}\ K^{-1}$]

θ_w^1, θ_i^1 = volumetric water and ice content of the first soil layer [$m^3\ m^{-3}$]

ρ_w, ρ_i = density of water and ice respectively [kg m^{-3}]

c_w, c_i = specific heat capacities of water and ice respectively [J $kg^{-1}\ K^{-1}$]

$$\lambda_{moss} = K_e \lambda_{sat} + (1 - K_e)\lambda_{dry} \qquad (4.5)$$

$$K_e = \log(Sat^1) + 1 \qquad (4.6)$$

$$Sat^1 = (\theta_w^1 + \theta_i^1)/\theta_{sat} \qquad (4.7)$$

$$\lambda_{sat} = \lambda_s^{1-\theta_{sat}} \lambda_w^{\theta_w} \lambda_i^{\theta_{sat}-\theta_w} \qquad (4.8)$$

with:

K_e = Kersten number [-]

λ_{sat} = thermal conductivity of the saturated moss layer [W $m^{-1}\ K^{-1}$]

λ_{dry} = thermal conductivity of the dry moss layer [0.05 W $m^{-1}\ K^{-1}$]

λ_s = thermal conductivity of wet moss [0.6 W $m^{-1}\ K^{-1}$]

Sat^1 = saturation of the first soil layer [-]

λ_w, λ_i = thermal conductivities of water and ice respectively [W $m^{-1}\ K^{-1}$]

4.2.3 Deep Soil

The soil hydrology and heat flow has to be represented for a finite number of model layers. For this, JSBACH includes 5 increasingly thick layers for the soil representation. The default JSBACH soil layer thicknesses are defined as: 0.065, 0.254, 0.913, 2.902, 5.7 meters respectively (Chapter 2). While the surface temperature forces the soil heat transfer at the top, there is no forcing at the base of the soil column. JSBACH uses the zero heat flux assumption as bottom boundary condition (Chapter 2). With this approach, the model assumes no heat transfer at the soil bottom. This assumption holds true when the soil column reaches to the depth of zero annual amplitude (DZAA), where the soil temperature stays almost constant all year and shows only minimal changes due to fluctuations in the geothermal heat flux. From the model intercomparison (Chapter 3), it was evident that DZAA can reach down to depths much below 10m (Chapter 3). To simulate the subsoil temperatures

correctly, JSBACH needs an extension to the default soil profile, which currently reaches to a total depth of only 9.83m (Chapter 2).

To improve this condition, two new soil layers (13.21 and 30.14 m in thickness respectively) are added to the soil profile to have the total soil column reaching to 53 m. With this extended soil profile, the lower boundary condition of vanishing heat flux is pushed deeper and the potential errors originating from the zero heat flux assumption have lower impacts on the upper soil layer temperatures.

4.2.4 Experimental setup

The abovementioned changes to the model formulation require testing of model performance for each new approach in isolation and together. To evaluate the effects of dynamic snow, dynamic moss and deep soil layers on the soil thermal regime, five additional site-level experiments are performed and compared to the Control simulation, which uses the version described in Chapter 2.

1. DynSnw   (only changing the snow density and snow heat transfer parameters)
2. DynMoss   (only changing the moss layer heat transfer parameters)
3. DynSnwMoss (including both snow and moss layer changes)
4. DeepSoil   (only including the 2 new soil layers)
5. DynDeep   (including snow and moss changes with the 2 new soil layers)

In order to asses the different impacts of each new formulation on different types of soil profiles, these model settings are tested at three contrasting sites: Nuuk, Samoylov and Schilthorn. As explained in Chapters 2 and Chapter 3, Nuuk site shows a cold soil profile in a non-permafrost low-Arctic region (Jensen and Rasch, 2009, 2010), while Samoylov site is located at a wet polygonal tundra zone in the Siberian high Arctic. At this site, polygon centers are forming mainly wet sections, while the polygon rims are staying dry. Also, wind drift causes a highly spatial heterogeneity on the depth of snow cover from polygon centers to rims (Boike et al., 2013). Schilthorn site, however, is located at a mountain peak in Swiss Alps (PERMOS, 2013). Since there is no vegetation at Schilthorn, DynMoss and DynSnwMoss experiments are omitted and the DynDeep experiment includes only dynamic snow changes and extra soil layers for this site's experiments. Soil parameters and time period used in these site-level simulations use the same values as in previous chapter (Table 3.3). For DynSnw, DynMoss and DynSnwMoss experiments, a mean year of each site's observed climate data is used to force the model during a 50-year spin-up period to bring the soil temperature and water content into equilibrium. However, DeepSoil and DynDeep experiments required a 100-year spin-up due to the increased soil thickness.

4.3   Results and Discussions

4.3.1   Dynamic snow parameterization

The new snow model (DynSnw) with dynamically changing snow density and snow heat transfer parameters is tested at the study sites and compared to the previous model version (Control). Figure 4.1 shows the changes in snow depth from observed and simulated values. Simulated snow depth in Control is higher than the observed values at all sites. With changing snow density, DynSnw shows decreases in snow depth not only due to snowmelt, but also due to compaction and mixing. By including a time dependent densification function and mixing with the fresh snow, DynSnw shows better results in matching the snow depth observations at all sites. The slope and shape of individual snow depth increase/decrease events are better captured in Nuuk and Schilthorn. Remaining differences, e.g. at Samoylov, are mainly due to wind effects on lateral snow transport processes which are not represented by the model.
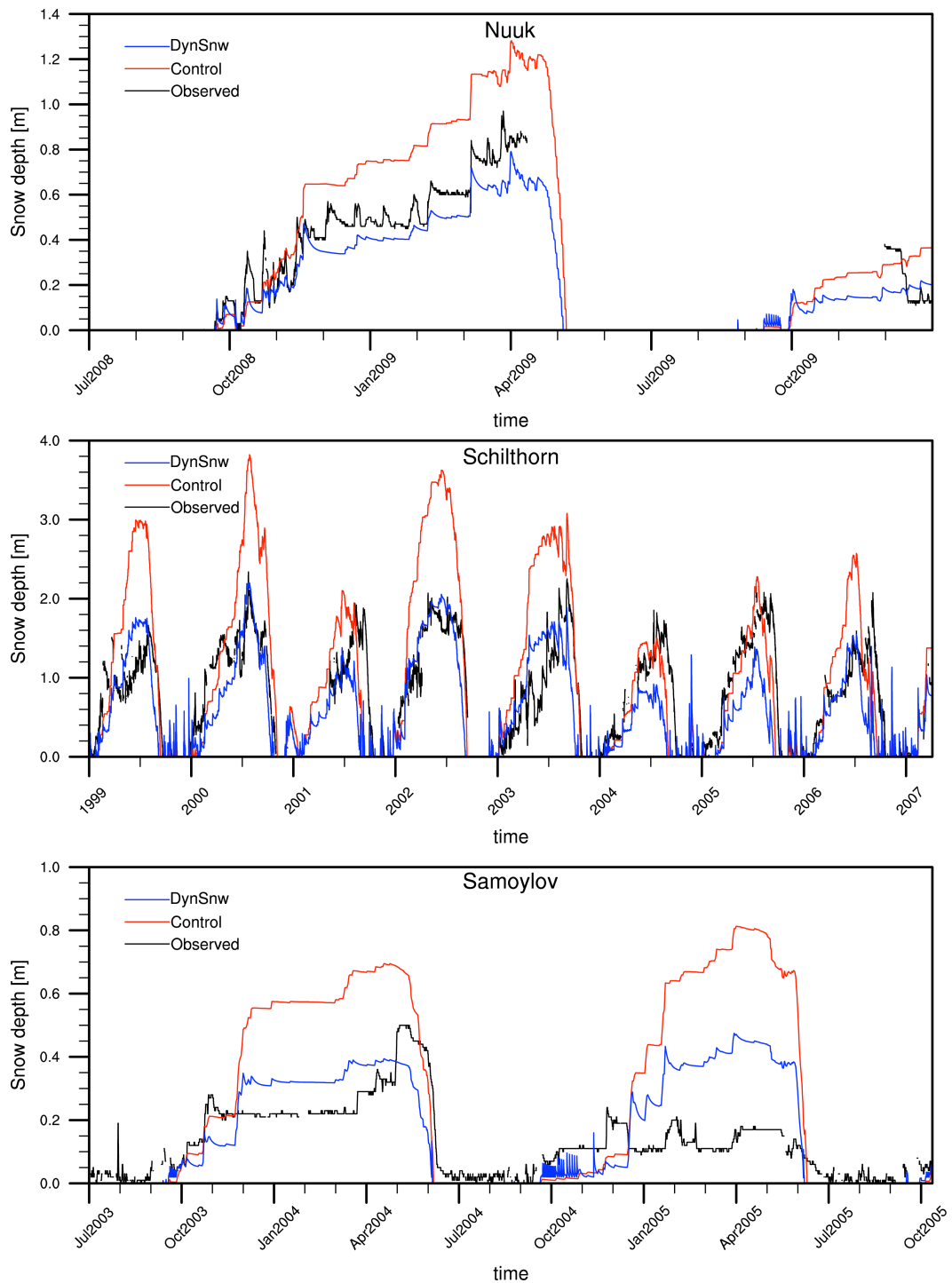
Figure 4.1: Timeseries of snow depth at Nuuk, Schilthorn and Samoylov. Observed values (black lines) are compared to simulated snow depths from Control (red lines) and DynSnw (blue lines) experiments.

The effects of the dynamic snow formulation on snow density and snow heat transfer parameters are shown in Fig. 4.2. Control keeps the snow density fixed at 250 kg m⁻³, while DynSnw changes it between 50 to 450 kg m⁻³ (Fig. 4.2, upper plots). Snow density values are decreased in time due to compaction and mixing with the new snowfall. This change also adjusts the snow heat capacity (Fig. 4.2, middle plots) and snow thermal conductivity values (Fig. 4.2, lower plots).
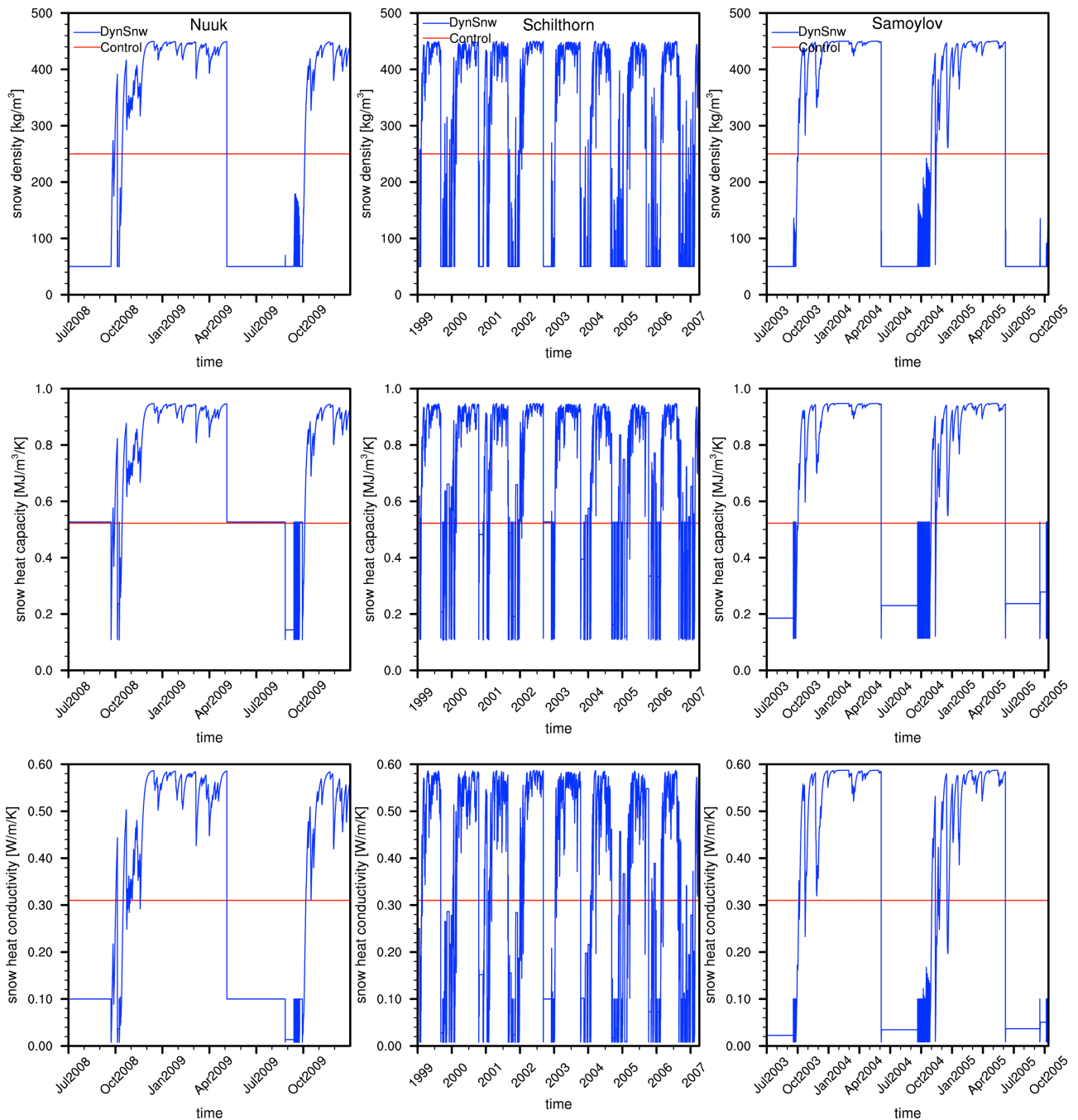
Figure 4.2: Timeseries of simulated snow parameters in Control and DynSnw experiments at Nuuk, Schilthorn and Samoylov sites. The different subplots show (top) snow density, (middle) snow heat capacity and (bottom) snow heat conductivity at each site.

4.3.2 Dynamic moss layer parameterization

The so-called moss layer is considered as a loose soil layer composed of organic matter, surface vegetation and water. The JSBACH moss layer (Chapter 2) assumes only organic matter and no water. However, heat parameter values for organic matter, water, and ice are quite different (Table 4.1). Using the combined values of these components, DynMoss changes the heat transfer parameters of the moss layer dynamically in time (Fig. 4.3).

59

Table 4.1: Heat transfer parameters of the individual components of moss layer: organic matter, water and ice. Organic layer values are taken from Beringer (2001).

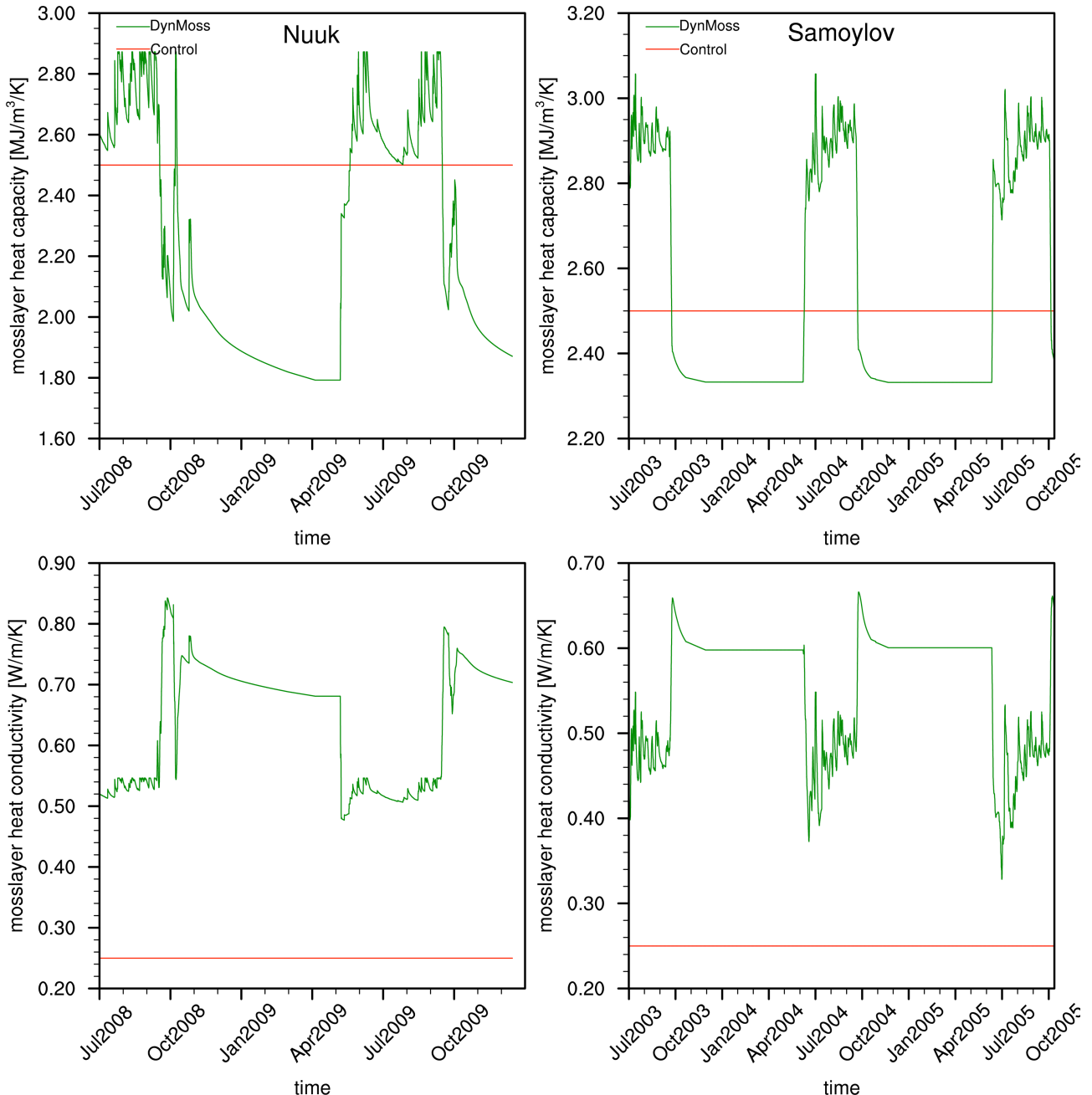|	Vol. Heat Capacity [MJ m^{-3} K^{-1}]	Heat Conductivity [W m^{-1} K^{-1}]
Organic matter	2.5	0.25
Water	4.2	0.57
Ice	1.9	2.16

Figure 4.3: Timeseries of heat parameters of the moss layer in Control and DynMoss experiments at Nuuk and Samoylov. Heat capacity is shown in the upper plots and heat conductivity in the lower plots.

Compared to Control, where constant heat capacity and conductivity values are used, DynMoss shows higher heat capacity values in summer due to inclusion of water, and lower heat capacity values in winter due to inclusion of ice (Fig. 4.3, upper plots). On the other hand,

the thermal conductivity values of the moss layer are increased all year long (Fig. 4.3, lower plots). The reason is that both ice and water have higher thermal conductivity values than organic matter (Table 4.1).

4.3.3 Extended model soil depth

As previously mentioned in Chapter 2, the depth of model soil column is important when the zero heat flux assumption is considered as the bottom boundary condition. With this assumption, the simulated bottom layer soil temperature should stay in a narrow range of temperature fluctuations (~0.1 °C). The deepest JSBACH soil layer temperature (ca. 7 m) in the Control experiment shows an annual oscillation of 1 to 3 °C (Fig. 4.4, red lines), which is a violation of the zero heat flux assumption at the bottom. The addition of two new soil layers has moved the bottom boundary condition to larger depths in the soil. When compared to Control, the bottom layer soil temperature in DeepSoil has captured the depth of zero annual amplitude (Fig. 4.4, blue lines). The 6th layer (ca. 16 m) still shows a slight change in temperature (Fig. 4.4, purple lines), while the 7th layer (ca. 38m) shows almost constant values (<0.1 °C change) during the simulation period, except for a slight trend at Schilthorn. The observed temperatures for Samoylov show similar dynamics at depths below 11 m (Langer et al., 2013).
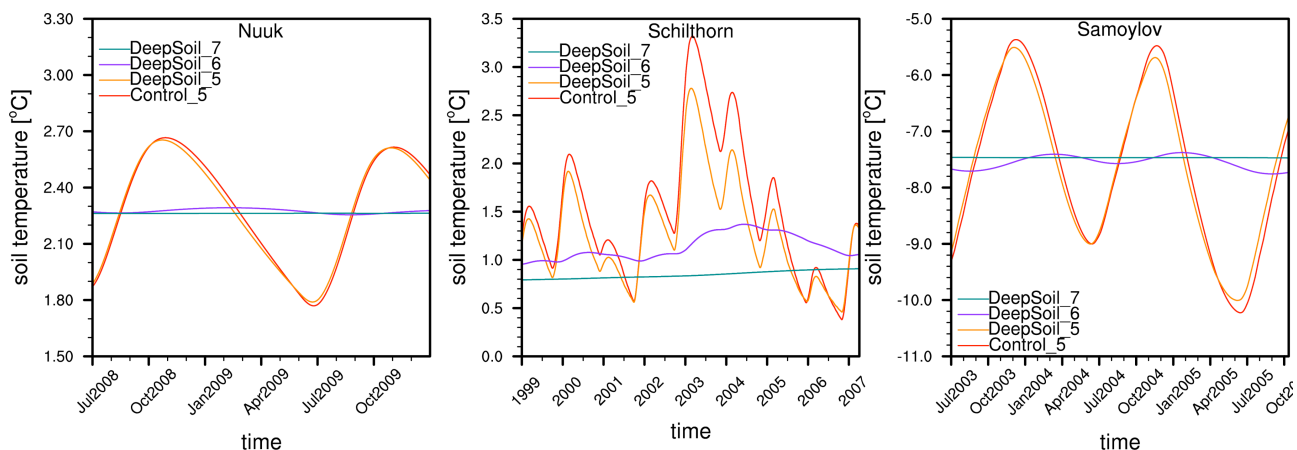

Figure 4.4: Timeseries of the deeper soil layer temperatures in the Control and DeepSoil experiments at Nuuk, Samoylov and Schilthorn. 5th soil layer (deepest layer, ca. 7m) temperatures of Control (red lines) are compared to 5th (ca. 7m) , 6th (ca. 16m) and 7th (ca. 38m) layer temperatures (orange, purple, and blue lines respectively) of the DeepSoil experiment.

4.3.4 Topsoil temperature and surface insulation

Current global permafrost models can simulate soil temperatures down to 30-50 m depths (Dankers et al., 2011; Gouttevin et al., 2012; Lawrence et al., 2012), but the topsoil temperature estimation holds a major importance and higher uncertainty compared to simulating subsoil temperatures. This is because most of the soil biogeochemical activity as well as freeze/thaw events take place in the upper part of the soil. In addition, topsoil

temperatures are strongly coupled to the atmospheric conditions. This brings up the need to correctly parameterize the thermal connection between air and soil, as well as the insulation effects of snow and vegetation cover in between. For these reasons, the effects of different model formulations on insulation strengths and topsoil temperatures are presented here.

Figure 4.5 shows how the prescribed changes in insulation strength and the deep soil layers affect the simulated first layer soil temperatures in matching the observations. During winter and spring, experiments at all sites show a similar pattern in two groups: first as Control-DynMoss-DeepSoil and the second group as DynSnw-DynSnwMoss-DynDeep. This similarity shows the dictating effect of new snow formulation over new moss layer approach and additional soil layers during winter and spring. The strong snow insulation effects are observed in other Arctic sites (Zhang, 2005) as well as in different models (Schaeffer et al., 2009). Incorporating dynamic snow heat transfer parameters and having lower snow depths (Fig. 4.1) decrease the insulation strength of snow cover in DynSnw. This creates colder topsoil temperatures than Control, also resulting in better match with the observations in winter and spring. Since DynMoss and DeepSoil have similar temperature values to Control, the DynSnwMoss and DynDeep are clearly reflecting the snow parameterization effects. The only exception is seen at Samoylov, where DynMoss shows colder topsoil temperatures than Control. Samoylov site is reported to have thicker moss layers and is situated in the Lena river delta with saturated soil profiles (Boike et al., 2008), which results in higher importance of insulation effects of the moss layer. Due to inclusion of ice properties, the moss layer in DynMoss has higher heat conductivities than in Control (Fig. 4.3). This creates a less insulating moss layer at this site during winter and spring, and results in temperatures closer to the observed values.

Summer and autumn plots show better agreement among model experiments (Fig. 4.5). In summer, even though DynSnw is still creating colder topsoil temperatures than DynMoss at Nuuk, moss insulation changes at Samoylov are more effective, hence DynMoss creates the coldest topsoil temperature at this site. Compared to the observations, differences between experiments are small. Autumn depicts a very similar pattern of topsoil temperatures in all experiments at all sites. Such agreement was also observed at the model intercomparison among different models (Chapter 3). This points to lower model uncertainty in autumn, probably due to no significant snow effects and dried/frozen soils during this period.
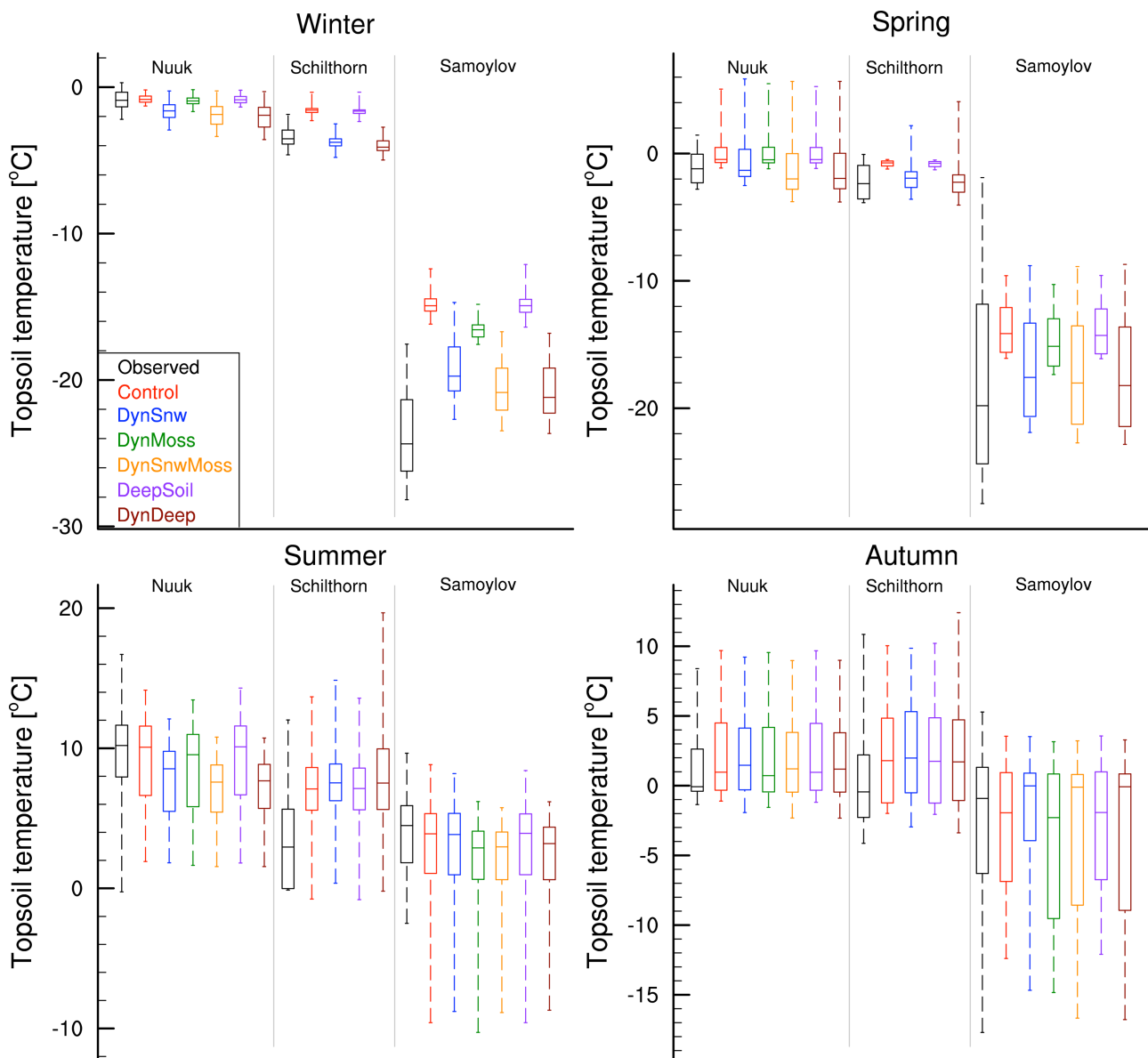
Figure 4.5: Box plots showing the 1st layer (ca. 3.25 cm) soil temperature for observation and model experiments for different seasons. Boxes are drawn with 25th percentile, mean, and 75th percentiles while the whiskers show the minimum and maximum values. An average year of available soil data is used for calculating seasonal values. Each seasonal plot includes 3 study sites divided by the gray lines. Black boxes show observed values and other colors distinguish different experiments.

To further analyze the surface insulation changes, atmosphere-surface connection is investigated in Figs. 4.6-4.8, showing this relation for each season at each site separately. Depending on the insulation strength of snow and/or the moss layer, each experiment shows a specific topsoil temperature value in relation to the air temperature. At Nuuk, observations show warmer topsoil temperatures than air in all seasons (Fig. 4.6). This points to a better insulation during winter season (warmer soil than air due to snow) than summer (no significant insulation from warm summer air temperatures). In winter and spring seasons, Control has warmer topsoil temperatures than the observations, suggesting too much insulation owing to higher snow depth values (Fig. 4.1). Adding the effects of dynamic snow

and moss layer parameterizations together (DynSnwMoss and DynDeep) creates better-matched values with observations in winter and spring. Even though the resulting temperature values of DynSnwMoss and DynDeep experiments are colder than other experiments, they are still warmer than observations in autumn. However the range of autumn values among all the experiments is quite narrow compared to other seasons. On the other hand, having the dynamic representation of snow and moss layer create too much insulation in summer resulting in much colder topsoil temperatures than the observations. These results point out that snow insulation is better represented with the new snow formulation, but the prescribed moss insulation is overestimated for this site.
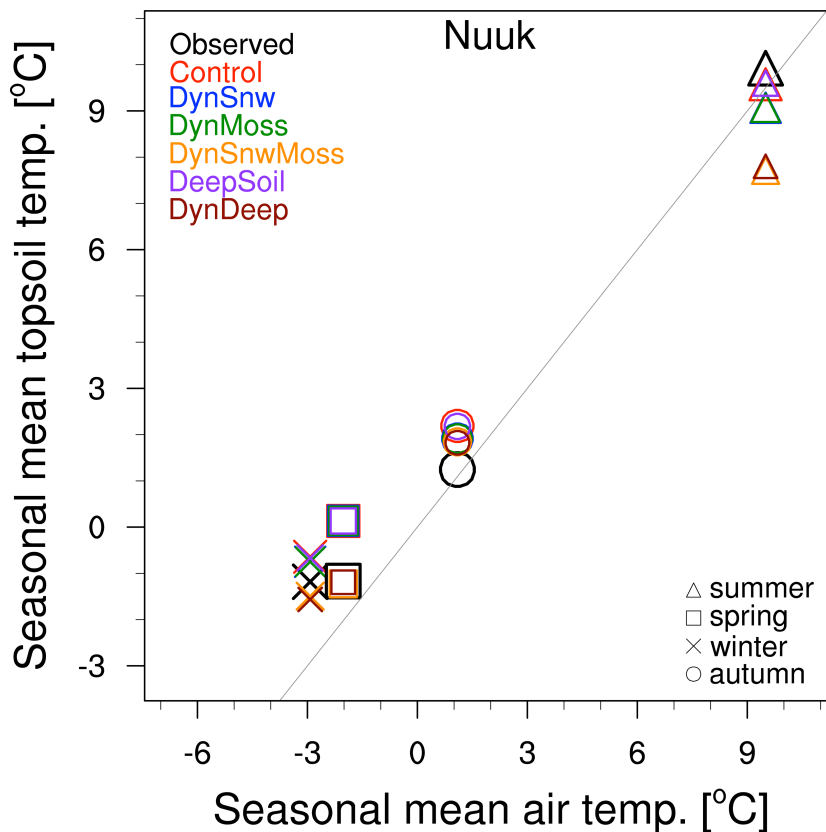

Figure 4.6: Scatter plot showing the insulation strength of different experiments at Nuuk for different seasons. Seasonal mean observed air temperature is plotted against the seasonal mean modeled 1st layer temperature (ca. 3 cm) at each site. Colors distinguish experiments and markers distinguish seasons. Gray lines represent the 1:1 line.

At Schilthorn, observations show warmer topsoil temperatures than air during winter, spring and autumn but the opposite is observed in summer (Fig. 4.7). These observations point to winter and summer insulation being both effective for the soil temperatures at this site. Similar to the Nuuk site, having dynamic snow properties (DynSnw and DynDeep experiments) decreases the snow insulation and creates colder winter and spring temperatures, which are closer to the observed values. As previously mentioned, the performed model experiments show similar patterns during autumn. Interestingly, none of

the experiments can match the observed summer values at Schilthorn. While Control and DeepSoil experiments have a warm topsoil temperature bias, having the new snow formulation (DynSnw and DynDeep) results in even warmer temperatures and further away from the observed values. The reason for that is persistent snow cover even during summer months (Fig. 4.1). Even though there is no vegetation insulation at Schilthorn to cool the summer soil temperatures down, snowpack provides insulation even in summer, which is not captured by JSBACH (Chapter 3). Modelled snow depth melts-out earlier than the observed snow and leaves the bare soil vulnerable to summer atmospheric heating. Additionally, having smaller snow depths accelerates the snowmelt (Fig. 4.1) and amplifies the warming effect in summer. This confirms that with the new formulation, snow insulation is captured correctly but summer biases are seen due to mismatched snow timing.
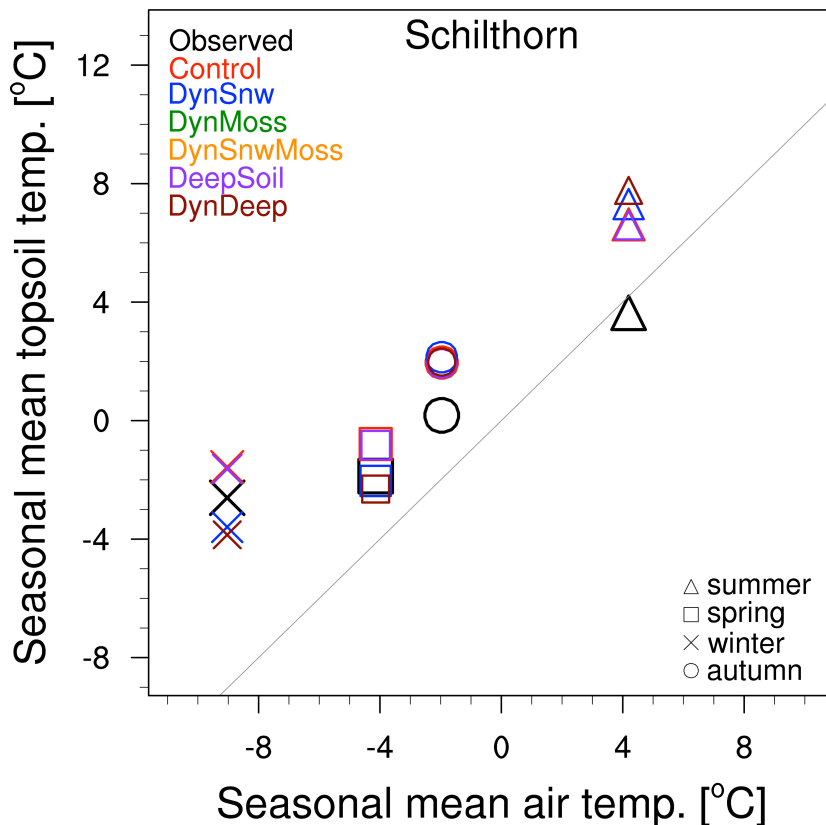

Figure 4.7: Same as Figure 4.6 but for Schilthorn site.

At Samoylov, observed values indicate warmer topsoil temperatures than air during winter and autumn, while the opposite is seen during summer (Fig. 4.8). Clearly, winter soil temperatures are protected from cold air temperatures due to snow insulation, while summer soil temperatures are kept colder than the air due to moss insulation. However, spring soil temperature observations show similar values with the air temperatures. All model experiments show a warm bias during winter and spring. This can be explained by the overestimated snow depth values (Fig. 4.1). This leads to overestimated snow insulation and

warmer soil temperatures in the model. However, the DynSnw experiment reduces the insulation strength and provides colder topsoil temperatures that are closer to observed values in winter and spring. Similar to other sites, model experiments fall in a very narrow temperature range in autumn, indicating lesser impact of the new formulations during this season at Samoylov. On the other hand, summer values show the importance of dynamic moss formulation compared to other experiments. DynMoss and DynSnwMoss create the coldest (most insulated) summer topsoil temperatures at this site, yet moving the model values further away from the observations. This is likely due to mismatched moss layer thickness or using the first soil layer values for the water and ice contents in moss layer.
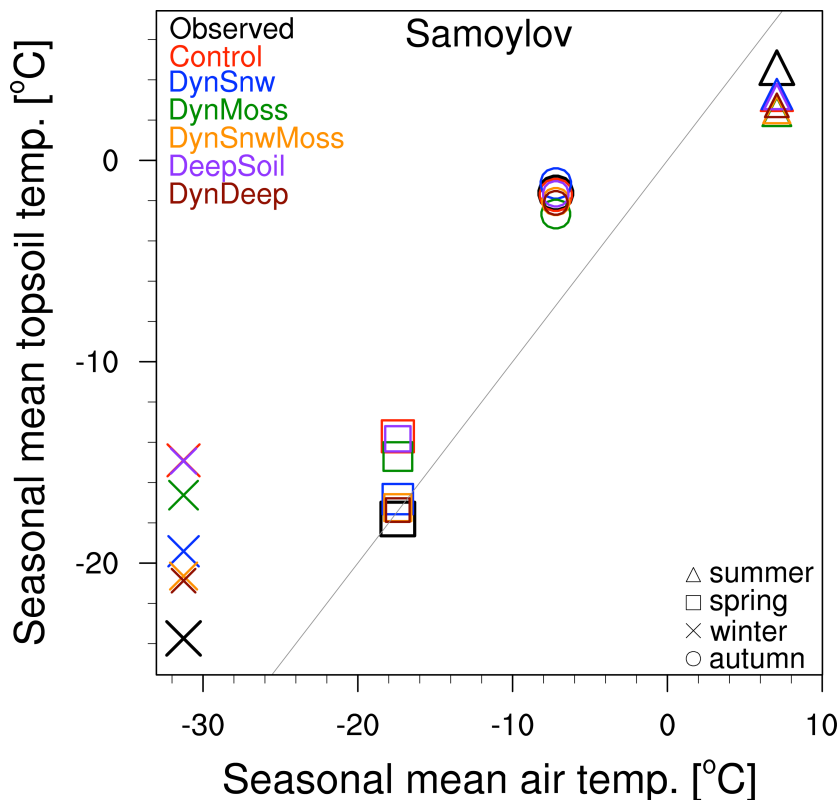

Figure 4.8: Same as Figure 4.6 but for Samoylov site.

A general outcome of the DynSnw experiment is a decreased insulation effect in winter, owing to higher snow density, lower snow depth, and higher heat transfer parameter values. Observed soil temperatures are better represented with the new snow formulation. On the other hand, a model bias still exists at all sites, which signifies the need to represent additional snow processes (i.e. snow depth hoar, wind drift...). The DynMoss experiment shows a cooling all year long. The high heat conductivity of ice reduces the insulation strength of the moss layer, and this effect is seen mostly in winter due to higher ice contents. Conversely, even though the heat conductivity of the moss layer is still higher than in Control in summer (Fig. 4.2), inclusion of water heat capacity dictates the moss layer heat capacity by increasing it more than in Control and as a result increases the insulation strength during

summer. This shows that incorporating water and ice components into the heat parameters of the moss layer improved the representation of changing insulation strengths for dry and wet conditions. Yet, having a constant 10 cm thickness and using the 1st soil layer water/ice contents bring up some uncertainty in the current moss layer representation. Further improvements for the moss layer are needed by explicitly simulating its hydrology and dynamically changing its thickness as it was done for the organic layers in Braakhekke et al. (2011) and moss/lichen cover in Porada et al. (2013).

4.3.5 Soil thermal profile

In addition to the topsoil temperature, it is also important to discuss the effects of the new model formulations on deeper soil temperature. Simulated temperatures in the lower soil layers must be captured in order to calculate ALT and permafrost extent accurately, and to estimate a valid long-term soil temperature trend. For this reason, the effects of each experiment on deeper soil layer temperatures are shown in this section.

The evolution of the soil temperature profile at Nuuk is shown in Figure 4.9. Since this is a non-permafrost site, no ALT is observed. The topsoil is frozen only during winter and the frost penetration depth (FPD) is almost the same in Control, DynMoss and DeepSoil experiments, suggesting that there is no considerable effect of moss layer changes and deep soil layers on the whole soil thermal profile. However, DynSnw increases the FPD in the end of spring. Together, snow and moss changes (DynSnwMoss) increase the FPD even further. When compared to DeepSoil, DynDeep experiment has a colder profile at all depths, showing the cooling effects of dynamic snow. The additional layers helped to capture DZAA in DeepSoil and DynDeep experiments. Compared to Control, where the bottom layer still shows a temperature fluctuation, the deepest layers in DeepSoil and DynDeep have constant temperatures. These results show the importance of dynamic snow parameterization effects on subsoil temperatures. With reduced snow insulation, the soil thermal profile is cooled down and with the deeper soil column, this effect has become even more visible.
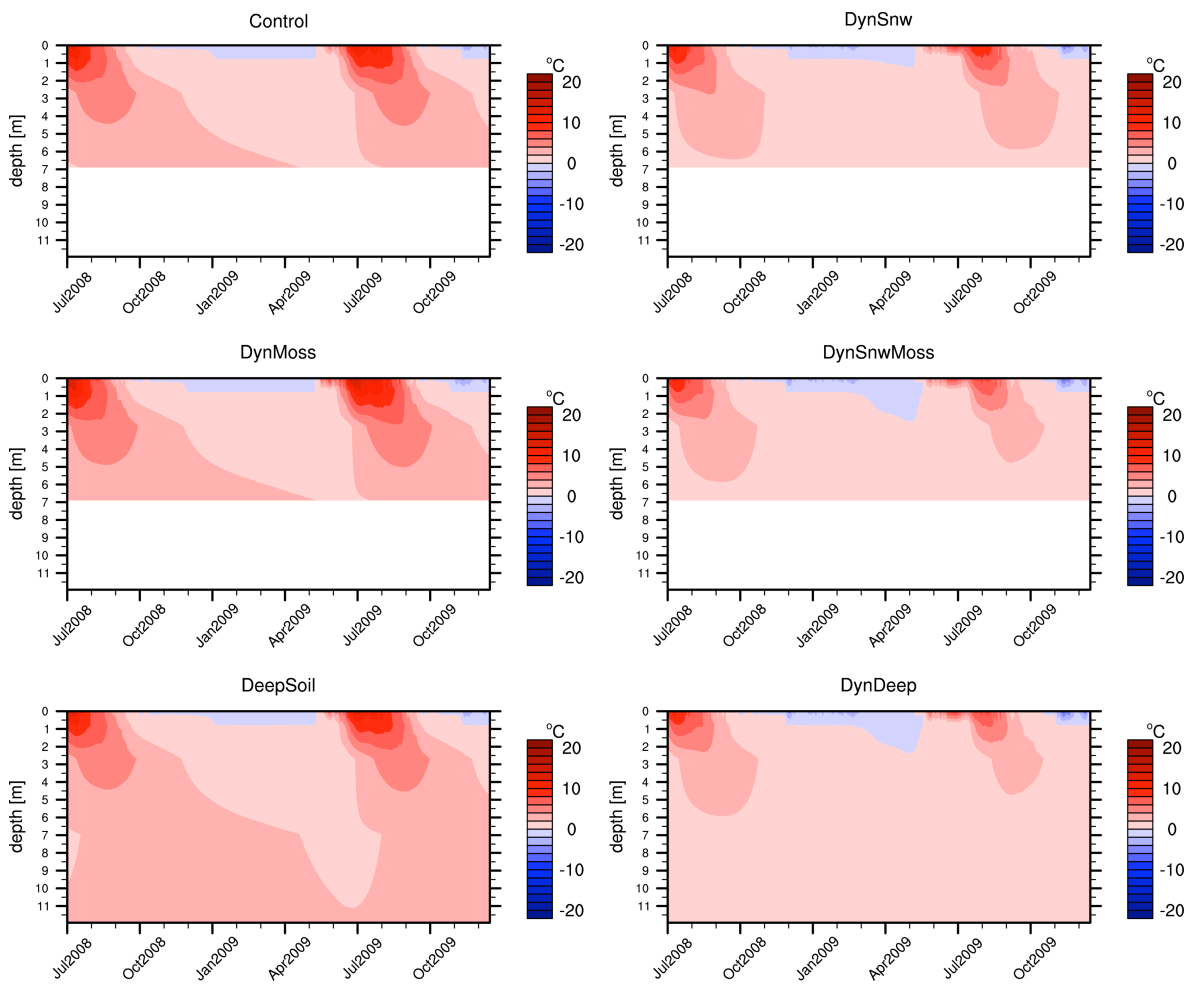
Figure 4.9: Time-depth plots showing soil temperature evolution from different model experiments at Nuuk site.

At Schilthorn, JSBACH experiments show a warmer soil profile than the observations (Fig. 4.10). In fact, the permafrost conditions are not captured and JSBACH creates an unfrozen soil column in all experiments. Due to reduced snow depths (Fig. 4.1) and decreased insulation strength, DynSnw experiment shows a colder soil profile than Control. Even though DeepSoil experiment is better in capturing DZAA, the soil thermal regime is similar to that in Control. However, new snow formulation with the additional layers (DynDeep) increases the frost penetration depth remarkably, thus creating almost a permafrost soil profile that is more similar to the observed soil thermal regime.
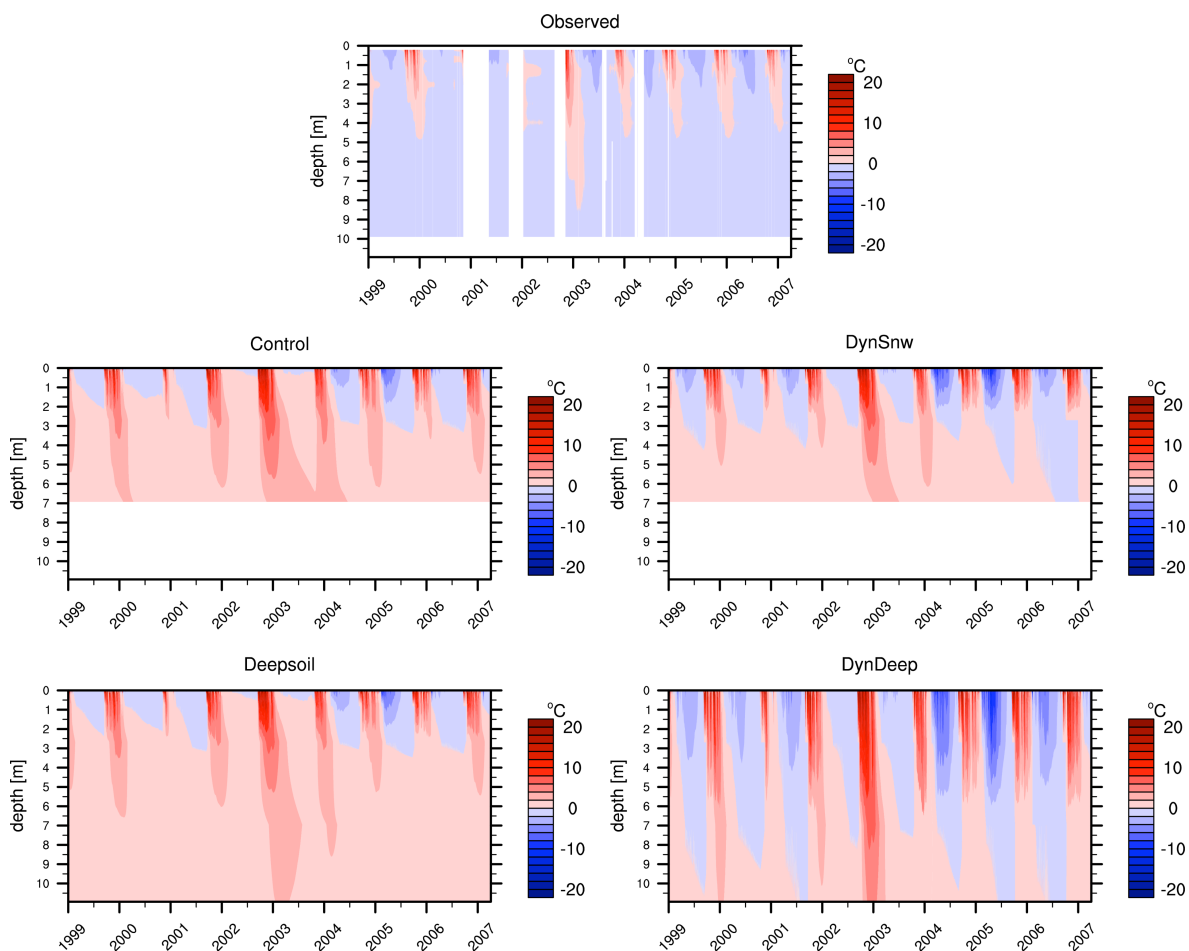
Figure 4.10: Time-depth plots showing soil temperature evolution from observations and different model experiments at Schilthorn site.

Figure 4.11 shows similar patterns for Samoylov. DynSnw results in colder winter temperatures, while DynMoss creates colder summer soil temperatures. When these effects are simulated together, DynSnwMoss shows a visible change in the soil thermal regime during the whole year. Similar to the other sites, the DeepSoil experiment at Samoylov also shows a comparable soil thermal profile to Control, but DynDeep is clearly much colder.

As clearly seen in Figures 4.10 and 4.11, having dynamically changing snow and moss parameters not only affect the topsoil but also the deeper layers. The importance of surface processes becomes evident from these results. Reduced insulation in winter (due to reduced snow depth) and increased insulation in summer (due to higher moss layer heat capacity) create a yearlong cooling effect. Furthermore, having a deeper soil column in addition to more realistic surface insulation, amplifies this cooling.
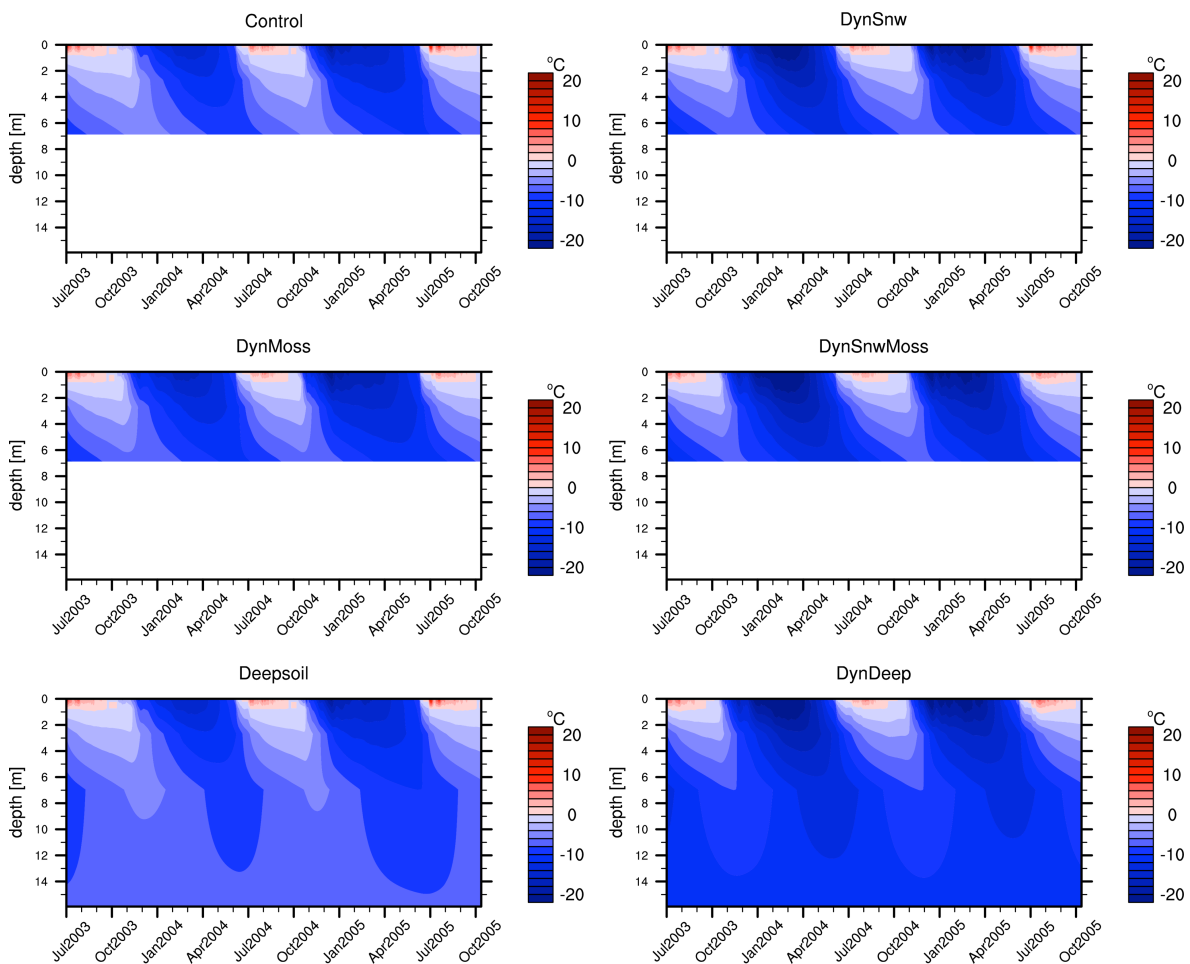
Figure 4.11: Time-depth plots showing soil temperature evolution from different model experiments at Samoylov site.

The trumpet plots in Figure 4.12 show the importance of having a deeper soil column to capture the DZAA. At Schilthorn, observations show that the soil temperature amplitude is still not zero at 10 m depth (Fig. 4.12d) and at Samoylov it gets closer to zero near 30 m (Fig. 4.12f). Obviously, a 10 m deep JSBACH model (Control) is not suitable to capture the DZAA at these sites, but the addition of deeper layers (DeepSoil, DynDeep) clearly improves this situation.

As seen in plots 4.12a, 4.12c and 4.12e, the dynamic properties of snow and moss layers cool the entire soil column and results in having a colder soil temperature at the deeper layers (DeepSoil vs DynDeep). However, plot 4.12d and 4.12f shows that the temperature amplitude is also increased in DynDeep. While this change captures the amplitude dynamics in observed Samoylov temperatures, it overestimates them at Schilthorn. This is again related to snow timing mismatches discussed in the previous section. Not having snow insulation in summer (as opposed to the observed conditions) creates warmer soil temperatures than observations and therefore increasing the temperature amplitude.

70

At Samoylov, the amplitude is in good agreement with the observed values (4.12f), despite having a shift to colder temperatures both in maximum and minimum temperature profiles of the DynDeep experiment (4.12e). This suggests that the model captures the scale of seasonal temperature changes and but has a general cold bias. Again this is the similar issue discussed in the previous section. The current version of JSBACH cannot capture the site-specific conditions of strong wind drift on snow as well as soil polygonal structure.
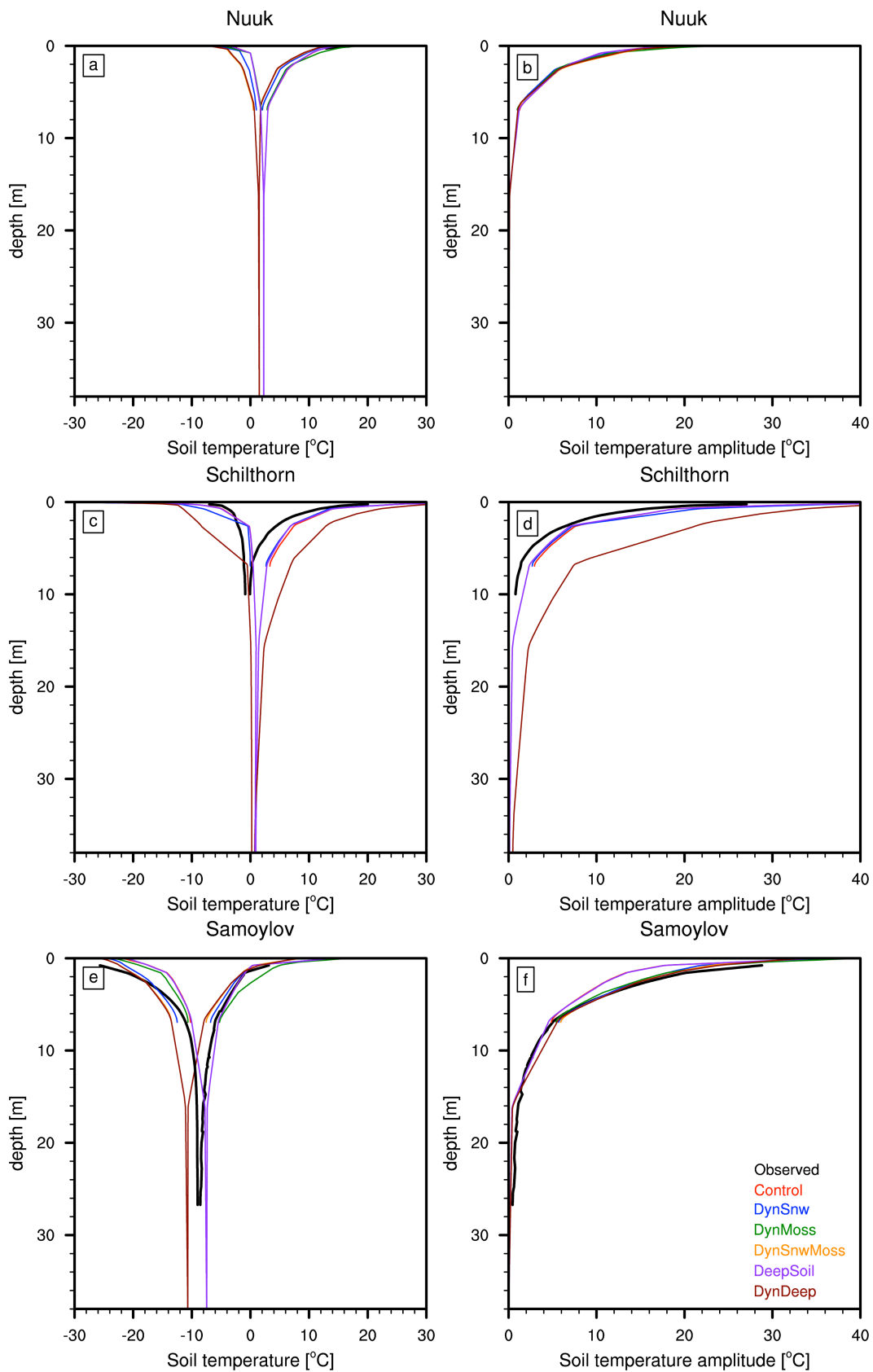
Figure 4.12: Vertical temperature profiles from observations and experiments at each site. Trumpet curves (a,c,e) show the change in vertical profiles of maximum and minimum soil temperature. Amplitude plots (b,d,f) show the change in temperature amplitude (max-min) in depth. Black lines are the observed values and colored lines distinguish model experiments.

4.3.6 Frost penetration depth and active layer thickness

In the following, each experiment is analyzed with respect to its simulated frost penetration depth (FPD) or active layer thickness (ALT) at each site. Since there is no permafrost simulated at Nuuk and Schilthorn, Table 4.2 and Table 4.3 show the simulated FPD values for these sites. However, Table 4.3 shows the ALT values from observed and simulated temperatures at Samoylov.

Nuuk FPD is higher in DynSnw compared to Control (Table 4.2). Even though there is not much difference between DynMoss, DeepSoil, and Control; the other experiments DynSnwMoss and DynDeep shows the highest values. These results are similar to those discussed in Fig. 4.5: effect of dynamic snow parameterization is more notable than moss layer parameterization, and adding extra layers at this site. This is due to reduced snow insulation effect.

Table 4.2: Nuuk site frost penetration depth (FPD) values calculated from simulated soil temperatures of each experiment during 2008.

FPD [cm]	Control	DynSnw	DynMoss	DynSnwMoss	DeepSoil	DynDeep
2008	77.93	129.7	78.19	245.39	77.96	238.01

Similar to the situation at Nuuk, the FPD values for Schilthorn also show an increase from Control to DynSnw (Table 4.3). As it was discussed earlier, the dynamic snow parameterization reduces the simulated snow depth (Fig. 4.1) and hence reduces the snow insulation strength. However, with more years to analyze at this site, the cooling effect of DeepSoil is visible from Table 4.3. With higher FPD values compared to Control, DeepSoil clearly shows a cooling effect on soil temperature profile. Following that, this effect is amplified in DynDeep, where snow parameterization and extra soil layers are simulated together.

Table 4.3: Schilthorn site frost penetration depth (FPD) values calculated from simulated soil temperatures of each experiment during years 1999 to 2006.

FPD [cm]	Control	DynSnw	DeepSoil	DynDeep
1999	209.25	424.32	230.60	1054.76
2000	160.14	328.26	189.46	881.52
2001	315.18	422.54	317.96	124.04
2002	47.57	315.33	50.83	823.03
2003	39.85	287.14	56.74	754.57
2004	294.95	380.45	307.22	1039.37
2005	335.26	584.31	344.01	1424.83
2006	330.14	698.27	326.62	1411.54

The ALT values for Samoylov are shown in Table 4.4. By calculating the maximum thaw depth from interpolating observed soil temperatures, the ALT values show depths of 62-67 cm at Samoylov (Table 4.4). The measured thaw depth values are reported to be around 50 cm with maximum values as high as 79 cm at the dry sites and 61 cm at the wet sites (Boike et al., 2013). However, it is important to note that JSBACH simulations are performed considering the polygon rims for Samoylov, because the saturated soil conditions at the polygon centers cannot be represented with this version of the model. So, the soil temperature observations from the rim (dry site) are used for all the comparisons here. Considering that, ALT values shown in Table 4.4 seems to be reasonable when compared to site measurements.

Table 4.4: Samoylov site active layer thickness (ALT) values calculated from observed and simulated soil temperatures of each experiment during years 2003 to 2005.

ALT [cm]	Observation	Control	DynSnw	DynMoss	DynSnwMoss	DeepSoil	DynDeep
2003	**67.37**	95.05	88.32	86.99	91.07	96.10	98.94
2004	**62.87**	77.71	77.68	77.69	77.66	77.72	77.66
2005	**65.57**	95.29	94.72	77.59	97.75	93.99	113.14

Similar to the results from the intercomparison (Chapter 3), JSBACH model overestimate the ALT even with the new experiments (Table 4.4). Compared to Control, ALT values in 2003 show lower estimates in DynSnw, DynMoss, and DynSnwMoss. As mentioned in the previous sections, the new parameterizations for snow and moss layer provide a yearlong cooling effect for soil; hence the ALT values are reduced accordingly. The same situation is estimated for 2005; DynSnw and DynMoss simulate lower ALT values than Control. Between DynSnw and DynMoss, ALT values are closer to observations in DynMoss. However, in 2004, there is no large difference in any of the model experiments, showing negligible effects of the new experiments on ALT.

Extending the model soil depth (DeepSoil) seems to have no significant effects on the ALT values at Samoylov (Table 4.4). However, when combined with the dynamic snow and moss layer parameterizations, the deeper soil column (DynDeep) has created warmer soil profiles and hence deeper ALT values in 2003 and 2005. This is in contrast with the effects of DynDeep on FPD (Tables 4.2, 4.3). These results show the sensitivity of soil thermal regime to the chosen soil depth, especially when surface insulation is dynamically changing during the simulation. However, a more comprehensive analysis using more sites with multi-year data is needed to fully understand the effects of model soil depth on ALT.

4.4   Conclusions

Effects of several model formulations on soil thermal profiles are compared at three different sites. Dynamically changing snow heat density and snow heat transfer parameters are used to see the snow insulation effects on soil temperatures. Additionally, the effects of moss insulation are investigated by including ice and water contents into the heat transfer parameters of the moss layer. Finally a deeper soil profile is used to inspect the importance of soil depth on soil temperatures. Results include:

- Snow insulation is reduced due to dynamic snow formulation, which resulted in colder and more realistic winter soil temperatures.
- Soil temperature biases still exist; more detailed snow processes and better capturing the snow timing are needed for further improvements.
- Moss layer insulation is represented more realistically with the new parameterization, which provided increased insulation during summer and decreased insulation in winter.
- Further improvements are needed for the moss layer representation: proper hydrology and varying thickness of moss layer.
- Together, the new snow and moss layer formulations provide a yearlong cooling effect for the soil.
- Surface insulation affects the whole soil thermal profile.
- Extending the model soil depth has a small cooling effect on the soil thermal profile, but together with the dynamic surface insulation, this effect is amplified.
- Dynamic surface insulation together with deeper soil column captures the DZAA and better represents the soil temperature amplitude.
- Dynamic snow formulation increases the frost penetration depth.
- Dynamic moss formulation decreases the active layer thickness.
- The combined effect of deeper soil column with dynamic surface insulation on ALT needs to be analyzed further.

It is clear from these results that global models can benefit from having ~50 m soil column together with more realistic surface insulation. The level of detail in global model formulations is challenged with computational restrictions, so it is important to design model parameterizations depending on the research questions. For a more realistic representation of permafrost soil thermal state, surface insulation needs to be improved.

CHAPTER 5

FUTURE STATE OF PERMAFROST

5.1 INTRODUCTION

Observations point to an intensified atmospheric warming in northern high latitudes (AMAP, 2012; ACIA, 2005; Serreze and Barry, 2011). Extreme air temperatures are causing more frequent heat waves and wildfires over Siberia and Canada (Goetz et al., 2007). Greenland ice sheet is retreating faster than before in the last decade (Rignot and Kanagaratnam, 2006), while the Arctic sea ice is shrinking at an unprecedented rate (Stroeve et al., 2007). Soil temperatures are rising in parallel to these changes and causing warming of the permafrost (Romanovsky et al., 2010), changing number of thaw-lakes (Smith et al., 2005) and increasing active layer thickness (ALT) in permafrost regions (Zhang et al., 2005; Romanovsky et al., 2013).

While the high latitudes are not alone in experiencing major climate shifts, they posses critical importance for the Earth system (Overland et al., 2013). Permafrost soils, covering ~24% of the northern hemisphere lands (Zhang et al., 2008), are rich in frozen organic matter (Tarnocai et al., 2009; Ping et al., 2008). If released into the atmosphere, this frozen organic carbon can drastically amplify the current atmospheric warming (Zimov et al., 2006) and cause severe impacts on natural systems (Schuur et al., 2008) and infrastructure (Larsen et al., 2008). A change in permafrost organic matter is believed to have already played a major role in the planet's past climate (Ciais et al., 2011). During the last deglaciation, atmospheric CO_2 values have increased sharply (Monnin et al., 2001). In conjunction with the methane bursts from the ocean floor to the atmosphere (Sigman et al., 2010), it is very likely that the permafrost carbon have contributed to this increase and provided a warming feedback mechanism, which further accelerated carbon release into the atmosphere (Ciais et al, 2011; Zimov et al., 2006). With more, previously unavailable, carbon joining the active carbon cycle of the planet, atmospheric CO_2 concentration will continue to rise and its climate forcing will induce warmer temperatures (Chapin et al., 2005; Schaefer et al., 2014) making the conditions on Earth more hostile to human population.

Permafrost and its carbon dynamics are among the most critical components of the climate system (IPCC AR5, 2013). However, frozen soils and their interaction with the warming climate, and permafrost carbon feedback to

climate are not considered in most of the Coupled Model Intercomparison Project (CMIP) models (Taylor et al., 2009). In order to come up with realistic mitigation strategies for managing future greenhouse gas emissions, permafrost and its carbon dynamics should be accounted for. This requires better understanding of the future state of the permafrost in the coming centuries.

There have been recent modeling attempts to quantify the effects of climate change on the future state of high latitude soils, and to investigate the permafrost carbon feedback to climate (Schuur et al., 2013). Even though the studies differ in their scenarios and choice of domain, they all agree on further warming of the land and a decrease in permafrost extent by the end of the century. Schaefer et al. (2011) have predicted 20-39% decrease in permafrost area by 2100. Similarly, Koven et al. (2011) estimated a 30% decrease in permafrost areas. Meanwhile, Saito et al. (2007) shows 40-57% reduction in northern hemisphere permafrost area, while Lawrence et al. (2012) simulates 72% decrease by 2100. Most of these studies focus on the permafrost carbon dynamics and provide broad estimates for the permafrost degradation and active layer thickening without spatial investigations.

Due to broad range of model estimates, effects of different climate projections on the physical permafrost state stays uncertain (Koven et al., 2013). Similarly, how different regions of the Arctic will respond to climate change is not clear. In order to estimate the permafrost carbon feedback to climate, the future state of permafrost physical conditions should be investigated. Together with the soil temperature trends, changes in ALT and permafrost extent should be the foremost issue before investigating the biogeochemical feedbacks (e.g. permafrost carbon feedback to climate). To shed some light onto these issues, the JSBACH land model (Chapter 2) is used to simulate the thermal state of northern high latitude soils until 2100 under different CO_2 emission pathways. Different than previous studies, analysis on spatial properties of physical changes in soil and the effects of changing snow depth, and snow season timing over northern high latitudes is presented in this chapter.

5.2 METHODS

For the future experiments in this chapter we have used JSBACH, land surface component of the Max Planck Institute Earth System Model (MPI-ESM), to assess the future response of high latitude soils to climate change. As described in Chapter 2, JSBACH has been improved for permafrost related processes and tested with multi-scale evaluations, showing successful representation of cold region soils' physical states. The model comprises 10m deep soil representation with coupled one-dimensional heat and hydrology scheme that includes soil freezing and thawing. There is also multi-layer snow cover, as well as a prescribed moss layer to represent the surface vegetation insulation for soil thermal profile. JSBACH's performance in different cold region landscape types is compared to other commonly used land models (Chapter 3), which demonstrated that the model reliably estimates physical conditions of cold soils in parallel to other models with varying level of complexities.

Follow-up to the previous IPCC emission scenarios, representative concentration pathways (RCPs) have been set up to estimate future climate trajectories under varying strengths of greenhouse gas radiative forcing (van Vuuren et al., 2011; Moss et al., 2010). These new climate pathways are based on radiative forcing of greenhouse gases from potential emissions of different socio-economic activities in the coming centuries. We have selected three RCPs (namely: RCP2.6, RCP4.5, and RCP8.5) to evaluate the potential responses of northern soils to environmental change. Driven with these scenarios, model results are analyzed for likely soil conditions in northern high latitudes during the 21st century. To see the direct (one-sided) effect of climate change on soil physical state, we have performed offline future simulations with JSBACH driven by MPI-ESM atmospheric outputs of the selected RCPs from year 2010 to 2100. Experiments are performed for all land points north of 50° N at a 0.5° spatial resolution and with daily timestep.

Following the experiments in Chapter 2, the simulations performed in this chapter continue from the previous transient simulation from 1901 to 2010 (Ekici et al., 2014). This previous simulation used observation based climate data until 1978 and bias corrected ECMWF/ERA-Interim reanalysis data, which is further explained in Beer et al. (2014). For the future simulations performed in

this study, atmospheric outputs of coupled MPI-ESM simulations of chosen RCPs are extracted and harmonized with the observed WATCH/ERA-Interim data (Weedon et al., 2010; Dee et al., 2011) according to Beer et al. (2014). For the soil parameters, global soil map of Harmonized World Soil Database v.1.1 (FAO et al., 2009) is used to prescribe the soil texture type for each 0.5° gridcell in the target domain.

Soil temperature and moisture has been initialized by repeating 1901-1930 average WATCH forcing data for 30 years in order to bring these state variables into equilibrium. The following transient runs are performed with these initial values of soil temperature and water content from 1901 to 2010. Afterwards, the future experiments are continued with the bias-corrected climate forcing from the three selected RCPs until 2100.

5.3   RESULTS AND DISCUSSIONS

The coupled MPI-ESM simulations following each RCP scenario have their own specific climate response to the prescribed radiative forcing. Figure 5.1 shows the change in annual air temperature that is used for driving JSBACH. Within this chapter, Siberia will be mentioned in three parts: west (60E-90E), central (90E-120E), and east (120E-150E). Areas east of 150E will be referred as far east Russia and areas between 30E and 60E will be referred as European Russia. Spatially averaged timeseries show that air temperature is clearly increasing in RCP4.5 and RCP8.5 projections but there is a slight change in RCP2.6 (Fig. 5.1a). In the spatial plots, it is clear that cooling in Scandinavia and far east Russia are balancing the warming in northern Siberia and N. America in the RCP2.6 projection (Fig. 5.1b). On the other hand, RCP4.5 and RCP8.5 show an air temperature increase in all regions (Fig. 5.1c-d).
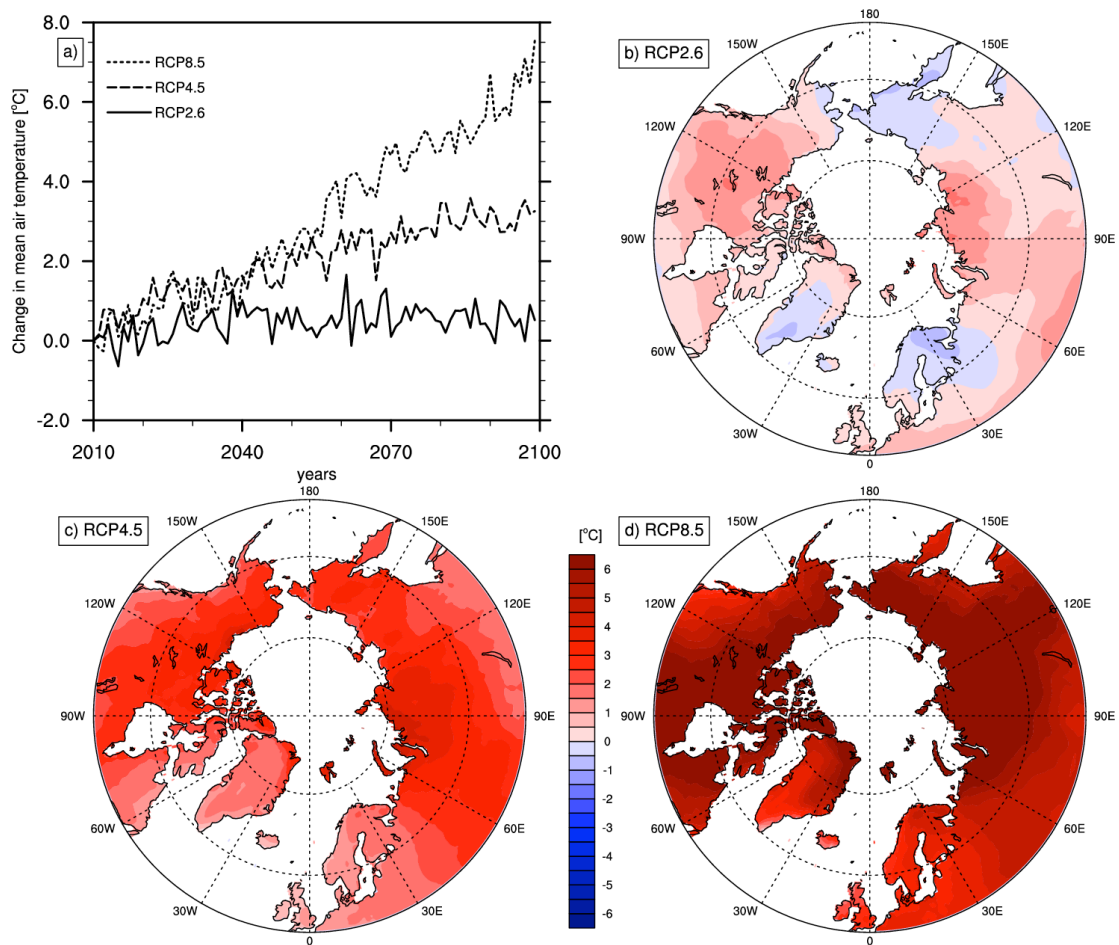
Figure 5.1 Panel showing spatio-temporal change in air temperature from 2010 to 2100. Plot **a** shows the timeseries of spatially averaged air temperature change from three different projections. Plots **b,c**, and **d** shows the maps of air temperature change (2090-2100 average minus 2010-2020 average) from three projections.

Similar to air temperature, precipitation changes are shown in Fig. 5.2. In the RCP2.6 projection, a notable precipitation increase is observed in European Russia, western Siberia, and southern Alaska (Fig. 5.2b). However, reduced precipitation is observed in several other regions. This again, results in a balanced state in precipitation in the RCP2.6 projection (Fig. 5.2a). RCP4.5 and RCP8.5 show a general precipitation increase, while the southern borders of Siberia are experiencing reductions in precipitation (Fig. 5.2c-d).
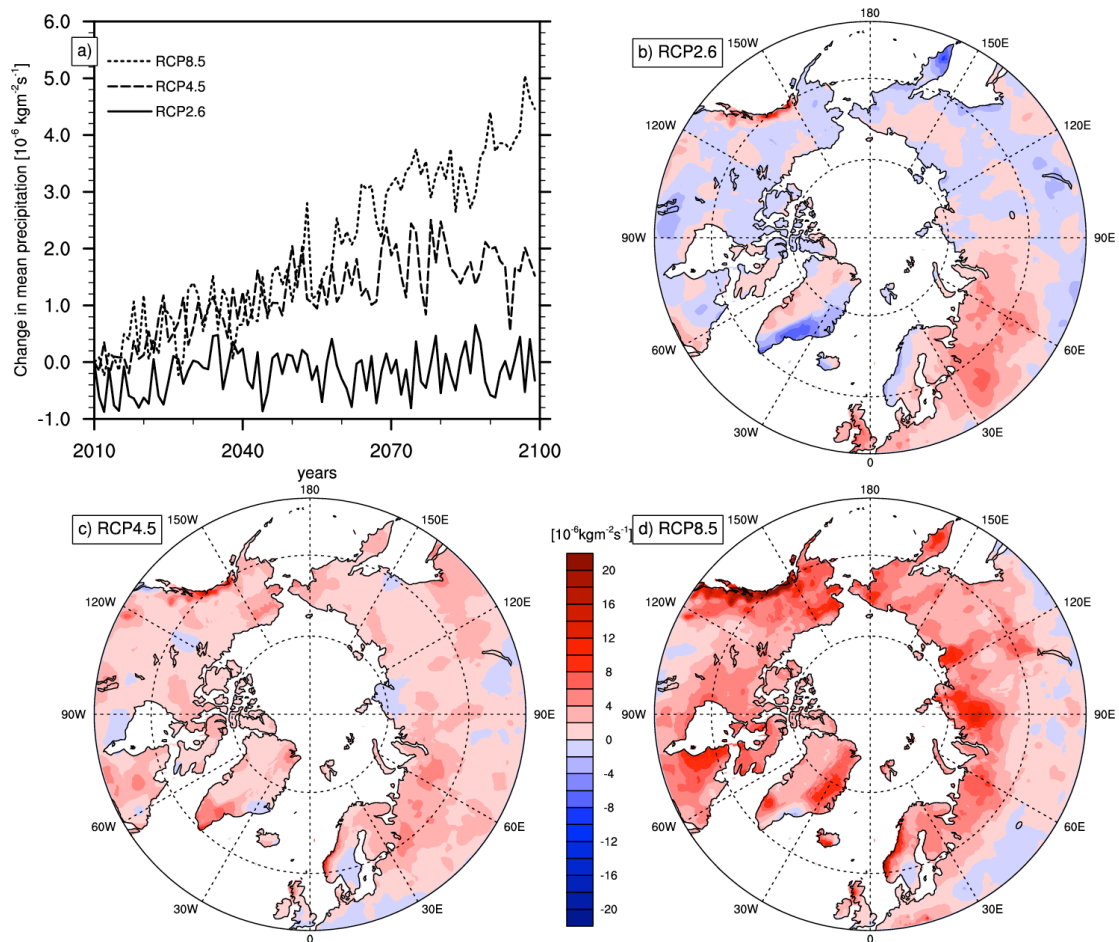
Figure 5.2 Panel showing spatio-temporal change in precipitation from 2010 to 2100. Plot **a** shows the timeseries of spatially averaged precipitation change from three different projections. Plots **b,c,** and **d** shows the maps of precipitation change (2090-2100 average minus 2010-2020 average) from three projections

Forced with these climate data, JSBACH simulations show different responses of the soil for each scenario. Figure 5.3 shows the simulated soil temperatures of present and future estimates. Note that all simulated soil layers show similar patterns, so only the temperature of the first model layer (0 – 6.5 cm) is shown in Fig. 5.3 and Fig. 5.4 (see Appendix A for the other soil layers). At the beginning of each simulation (Fig. 5.3a), coldest soil temperatures (for the glacier-free landpoints) are found in north of eastern and central Siberia, and northeastern Canada. By the end of the century (Fig. 5.3b-d), it is seen that increasing air temperatures (Fig. 5.1) are matched by increasing soil temperatures. RCP2.6 (Fig. 5.3b) produces temperatures similar to those at 2010, while Figure 5.3d shows the extreme condition with RCP8.5 scenario, in

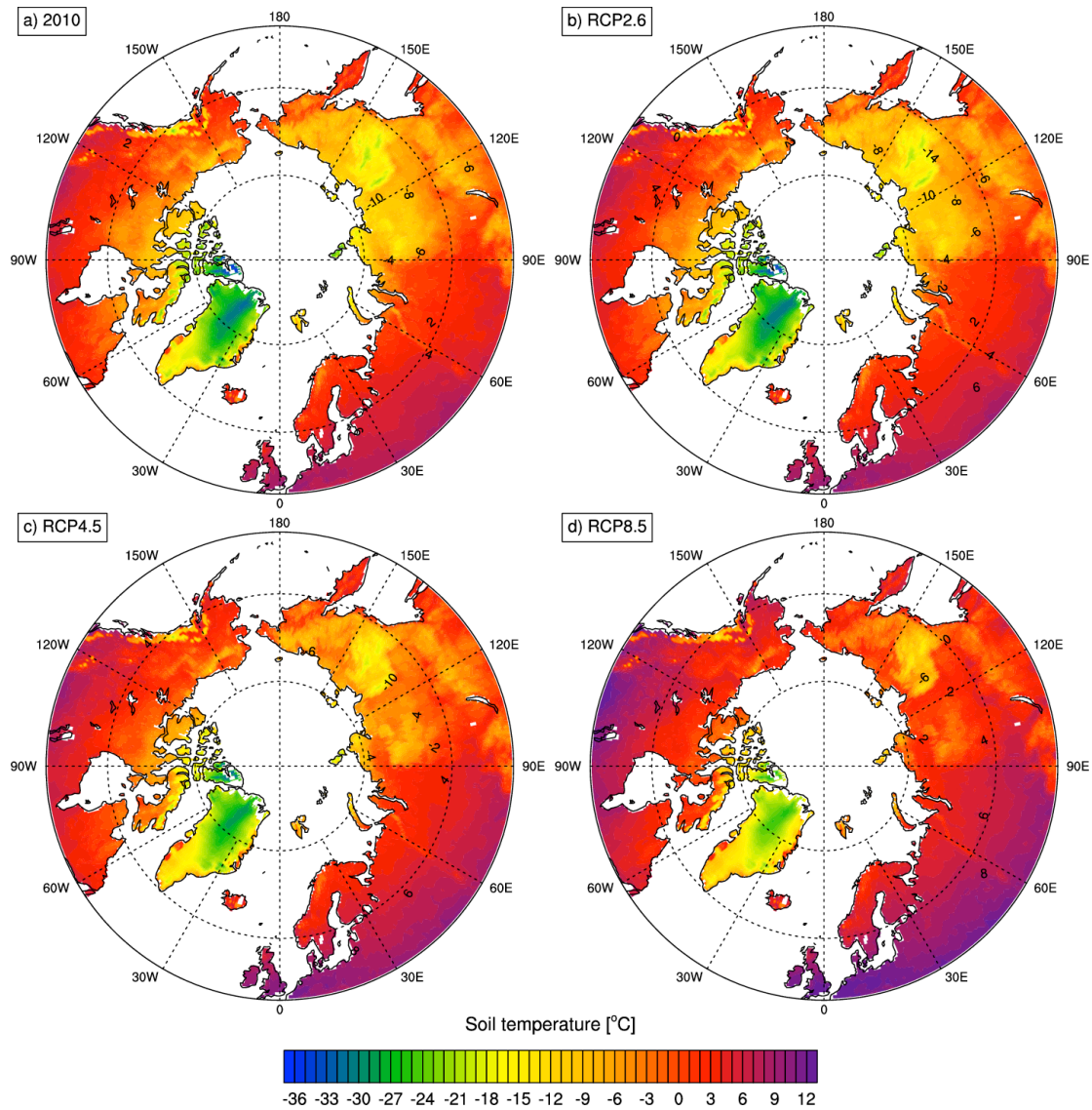which soil temperatures have risen above 0°C in most of the simulated glacial-free region.

Figure 5.3 Soil temperature panel showing maps of simulated soil temperature (first layer: 0 – 6.5 cm) at the beginning (2010 – plot **a**) and end of three future projections (2090-2100 average – plots **b**, **c**, and **d**).

All future simulations create warmer soil conditions but the increase in soil temperature is not spatially homogeneous. Figure 5.4 shows the temporal and spatial patterns of this change. As seen in Fig. 5.4a, on average there is more than 6°C increase in soil temperature from RCP8.5 projection, while RCP4.5 shows a 3°C increase; but RCP2.6 shows almost no change at all. However, these are average values for the whole target domain. Following the air temperature patterns (Fig. 5.1), regional soil temperature changes are not uniform (Fig. 5.4b-d). Even though RCP2.6 simulation shows minimal change on average (Fig. 5.4a),

there are warming regions: central and northern Canada, north of central Siberia etc. (Fig. 5.4b). The other RCP simulations show a pronounced warming in all regions, but most of the temperature increase happens in north of central Siberia and northern Canada, where 8-10 °C of increase is simulated (Fig. 5.4d). General patterns of this spatial heterogeneity are related to changes in air temperature and snow, which will be discussed below.
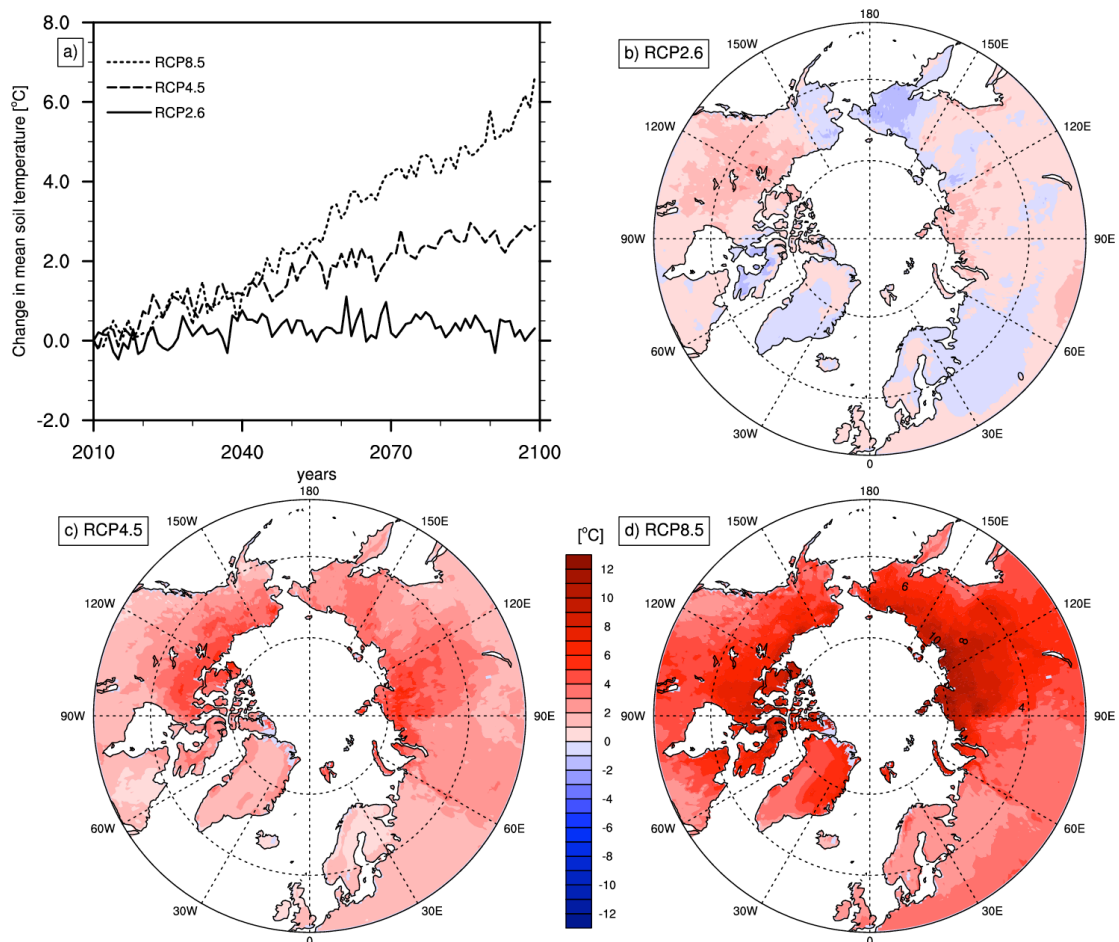

Figure 5.4 Panel showing spatio-temporal change in soil temperature (first layer: 0 – 6.5 cm) from 2010 to 2100. Plot **a** shows the timeseries of spatially averaged soil temperature change from three different projections. Plots **b**,**c**, and **d** shows the maps of soil temperature change (2090-2100 average minus 2010-2020 average) from three projections.

On the hydrology perspective, the distribution of soil liquid water is shown in Fig. 5.5, and soil ice content in Fig. 5.6. Since multi-layer hydrology allows for simulation of soil water at different levels, an accumulated soil water value of all layers is used in Fig. 5.5, Fig. 5.6, and Fig. 5.7. At the beginning of simulations (Fig. 5.5a), more liquid water is stored in European forest zones, southeastern Canada, and western Alaska. This pattern is mainly dictated by the

prescribed parameter maximum soil depth, until which JSBACH can simulate soil water (see Fig. B1 in Appendix B for static soil depth parameter). However, analyzing the changes of simulated soil water is still useful to identify the physical state changes of the soil. The distribution of soil water pattern seems to be conserved by the end of the century for RCP2.6 scenario (Fig. 5.5b). Similar patterns with more available water in western Canada and western Siberia are estimated by RCP4.5 and RCP8.5 (Fig. 5.5c-d). One reason for that is the degrading of permafrost in RCP4.5 and RCP8.5 allow more water to be held in these scenarios, which will be discussed below.
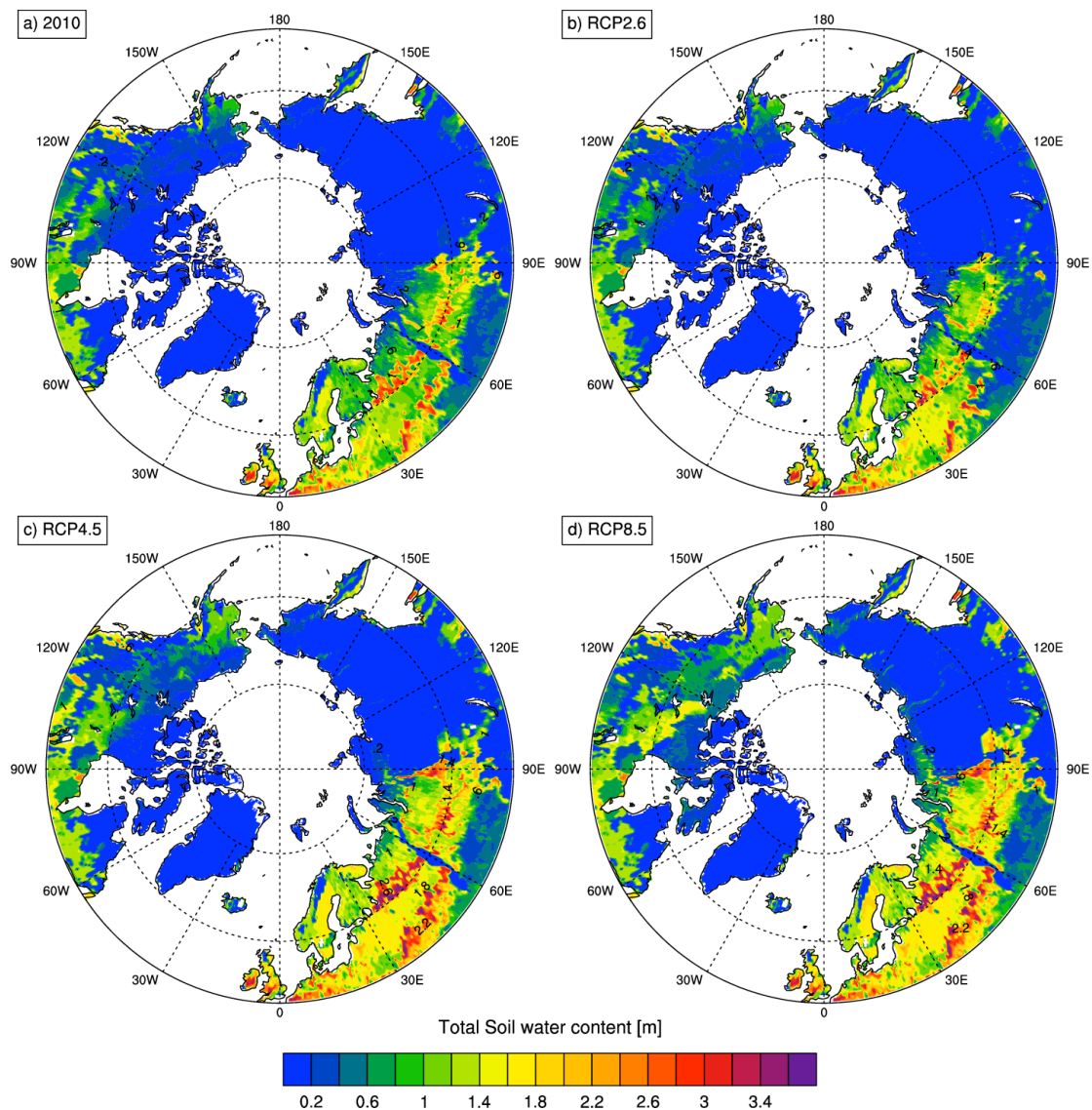

Figure 5.5 Soil water panel showing maps of total soil liquid water content at the beginning (2010 - plot **a**) and end of three future projections (2090-2100 average - plots **b**, **c**, and **d**). Total soil water is calculated by summing up simulated soil water in each model layer.

Similarly, Fig. 5.6 shows the total soil ice content in the beginning and end of the experiments. At 2010, most of the soil ice is found in the very northern edges of the continents, in central Alaska, and in central and northeastern Canada (Fig. 5.6a). Some isolated soil ice content is simulated in central and southern Siberia in 2010 (Fig. 5.6a), which is also related to the prescribed soil depth map (see Fig. A1). However, by the end of the century, less ice is simulated in RCP2.6 (Fig. 5.6b) and RCP4.5 (Fig. 5.6c), while most of the ice is lost in the RCP 8.5 scenario (Fig. 5.6d).
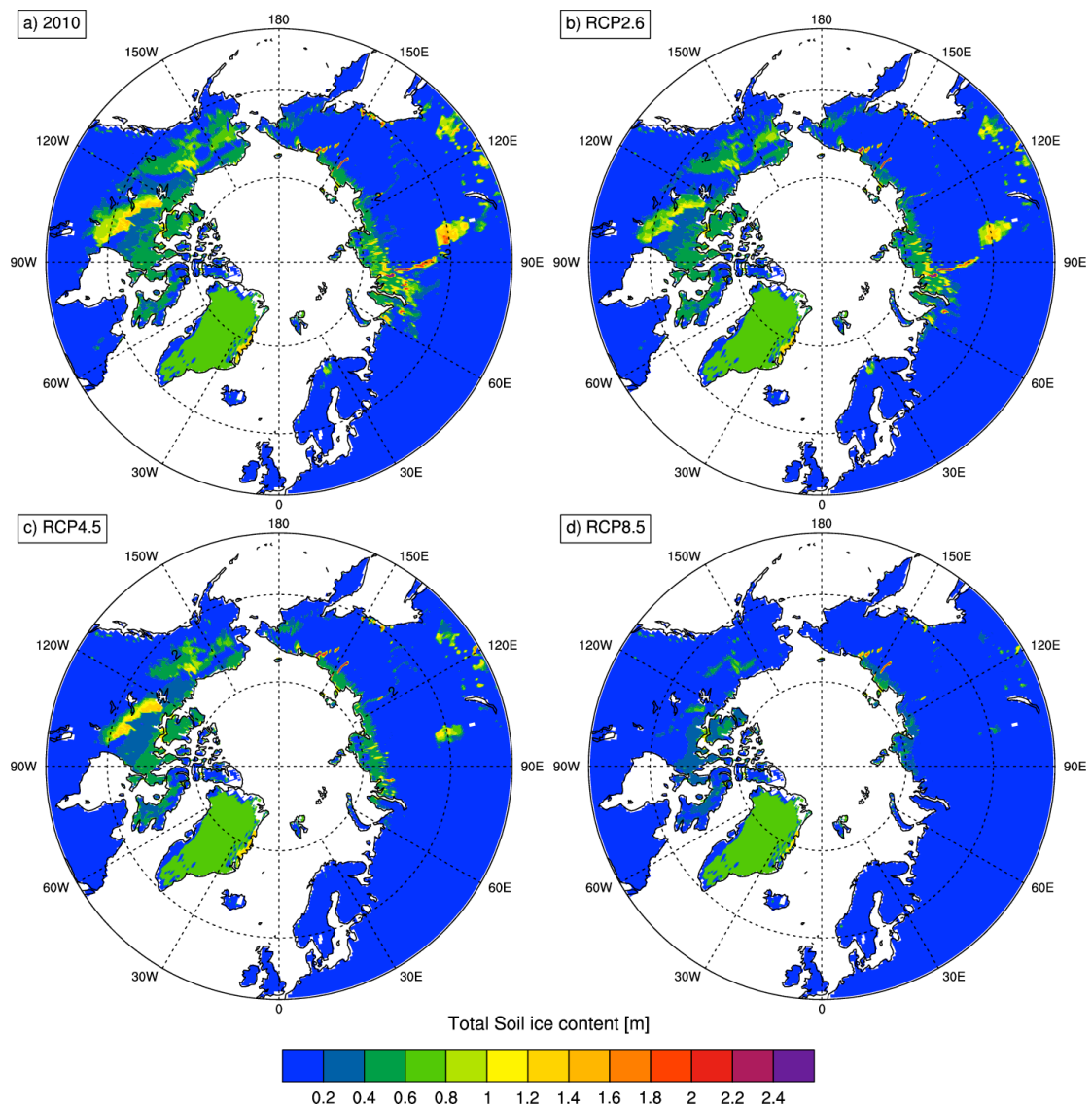

Figure 5.6 Soil ice content panel showing maps of total soil ice content at the beginning (2010 - plot **a**) and end of three future projections (2090-2100 average – plots **b**, **c**, and **d**). Total soil ice content is calculated by summing up simulated ice content in each model layer.

The spatial patterns of change in soil hydrology are shown in Fig. 5.7. By the end of the century, all three climate projections simulate an increase in soil water and decrease in soil ice content on average; whereas the spatial pattern of this change is not completely uniform. There is a visible similarity in regions where soil water increases and soil ice content decreases. This is the effect of increasing soil temperatures (Fig. 5.4) melting the soil ice and making the soil wetter. Even though the effects of prescribed soil depth is responsible for most of the soil hydrology distribution, a clear result of these projections is that soils are shifting from a frozen to unfrozen state in general. In concert with the soil warming, these hydrological changes show a consistent pattern of the alterations in soil physical state at northern high latitudes by the end of the 21st century.
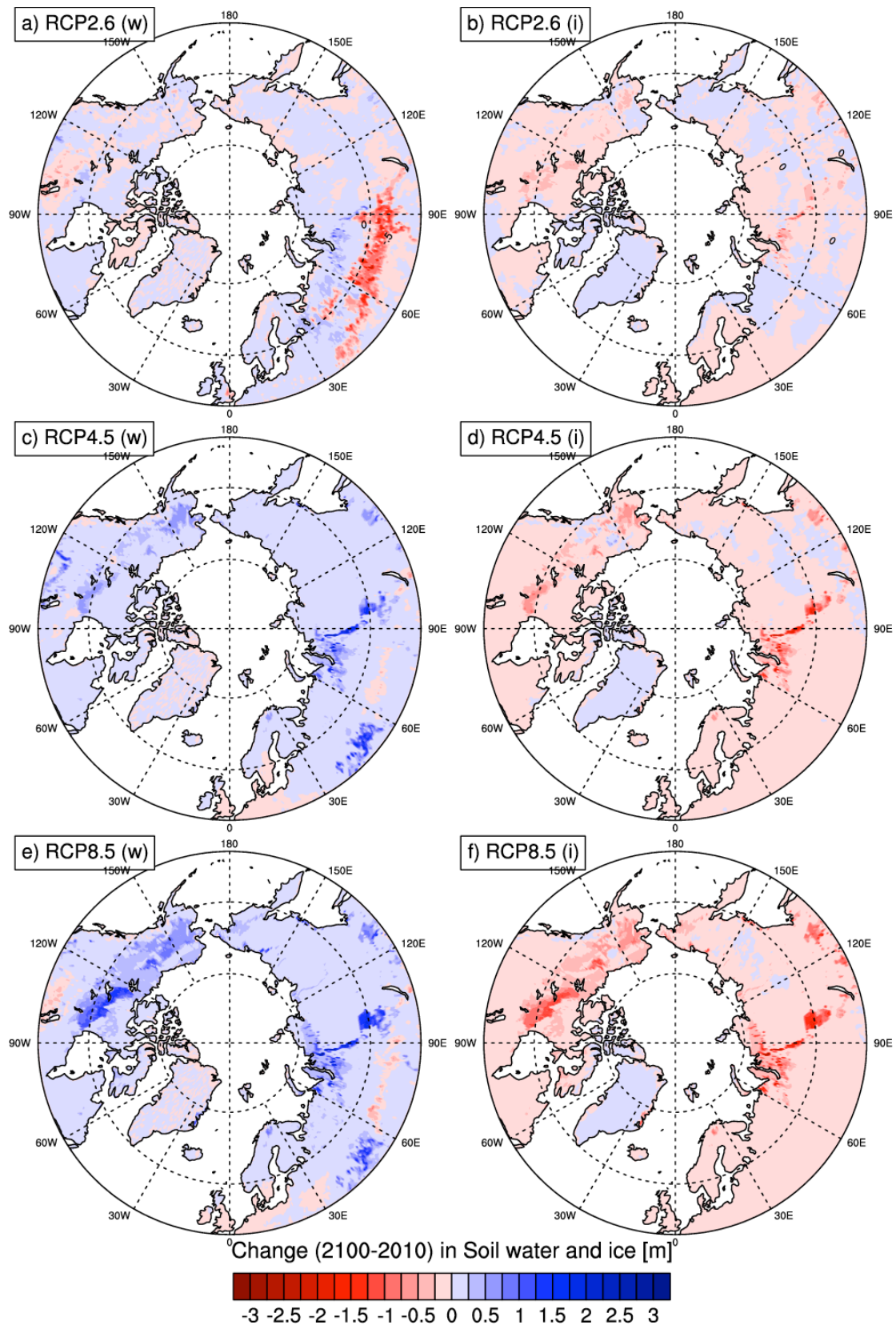
Figure 5.7 Panel showing projected changes (2090-2100 average minus 2010-2020 average) in simulated soil liquid water (w) and ice (i) contents from three projections.

As a direct result of soil temperature change, the changing permafrost extent is investigated in the following. Figure 5.8 shows the International Permafrost Association's (IPA) estimated permafrost zones (Brown et al., 2002) and permafrost extents from model estimates. Since the model vertical domain is limited to 10 m (Chapter 2), the simulated permafrost definition relates to permafrost occurrence in the upper 10 m of the soil, which will also be referred as near surface permafrost in this chapter. Permafrost deeper than 10 m is excluded from our analysis. As previously shown in Chapter 2, JSBACH permafrost zones in 1990 overlaps with the continuous and discontinuous permafrost zones. However, by the end of the century, RCP simulations predict clear permafrost degradation. Especially in the RCP8.5 projection, the entire present-day discontinuous permafrost zone is lost and only small patches of permafrost are preserved in Siberia, and northeastern Canada. There is a direct effect of increasing soil temperatures on shrinking permafrost areas. However, the distinctive pattern of simulated permafrost in Siberia from RCP8.5 (red polygons in Fig. 5.8) resembles the elevation patterns in this area (see Fig. B2 in Appendix B). This demonstrates the effect of topography on soil temperature, thus permafrost resilience.
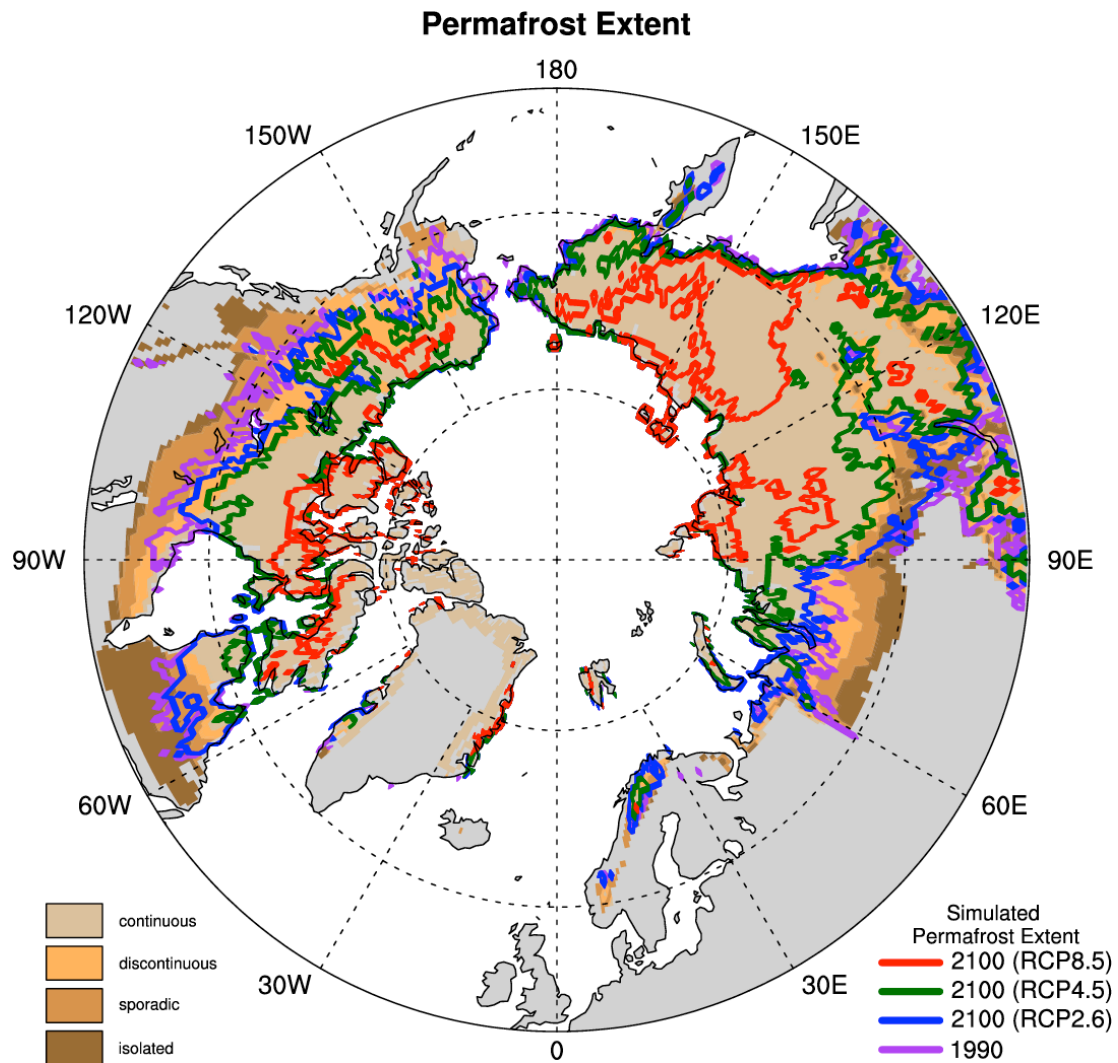
Permafrost Extent

Fig 5.8 IPA permafrost zones (Brown et al., 2002) and simulated permafrost extent from 1990 and 2100 from three different climate projections. IPA permafrost zones are shown with brown colors, and the outer borders of simulated permafrost extents are shown with the thick lines.

The temporal change in total surface area of the gridboxes underlain by near surface permafrost is plotted in Fig. 5.9. At the beginning of experiments in 2010, around 14×10^6 km^2 of permafrost is simulated, which compares well to recent estimates (Gruber, 2012). RCP2.6 shows a small decrease in the total permafrost area by the end of the century, while it decreases more visibly in RCP4.5 and more dramatically in RCP8.5 scenarios (Fig. 5.9). In the 21st century, the initial permafrost area of 14 million km^2 is shrunk to around 13, 10 and 3 million km^2 under RCP2.6, RCP4.5, and RCP8.5 scenarios respectively. Since the permafrost is defined solely on soil temperature, it is expected to see that

permafrost area is following a similar (but opposite) pattern as the change in soil temperature (Fig. 5.4a).
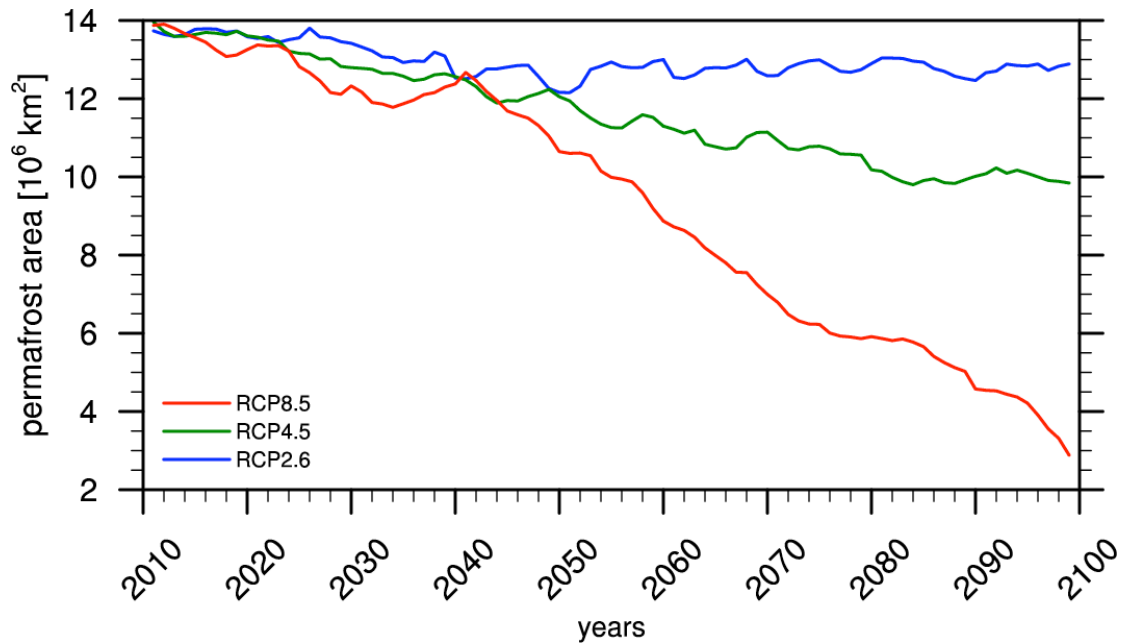

Fig 5.9 Timeseries of total northern hemisphere (>50 N) near surface permafrost area from 2010 to 2100 from three different climate projections.

Figure 5.10 shows the active layer thickness (ALT) estimates at the start and end of the simulations. Since ALT is a permafrost feature, it can only be calculated for regions where there is still permafrost, so the areas shown in Fig. 5.10 follow the pattern of permafrost areas shown in Fig. 5.8. Figure 5.10a shows that 2010 ALT estimate is smallest in northern Siberia and northern Canada/Alaska. Then it gradually increases going southward (Fig. 5.10a). At 2100, RCP2.6 (Fig. 5.10b) estimates show similar patterns to 2010, however RCP4.5 and RCP8.5 scenarios show much deeper ALT estimates (Fig. 5.10c-d). By the end of the century, RCP4.5 and RCP8.5 scenarios predict over 3 m ALT in most of the permafrost regions. Similar to permafrost occurrence, topographical features affect the ALT patterns. High elevations in eastern Siberia (see elevation map Fig. B2 in Appendix B) lead to shallow ALT values even in the highest warming scenario (Fig. 5.10d).
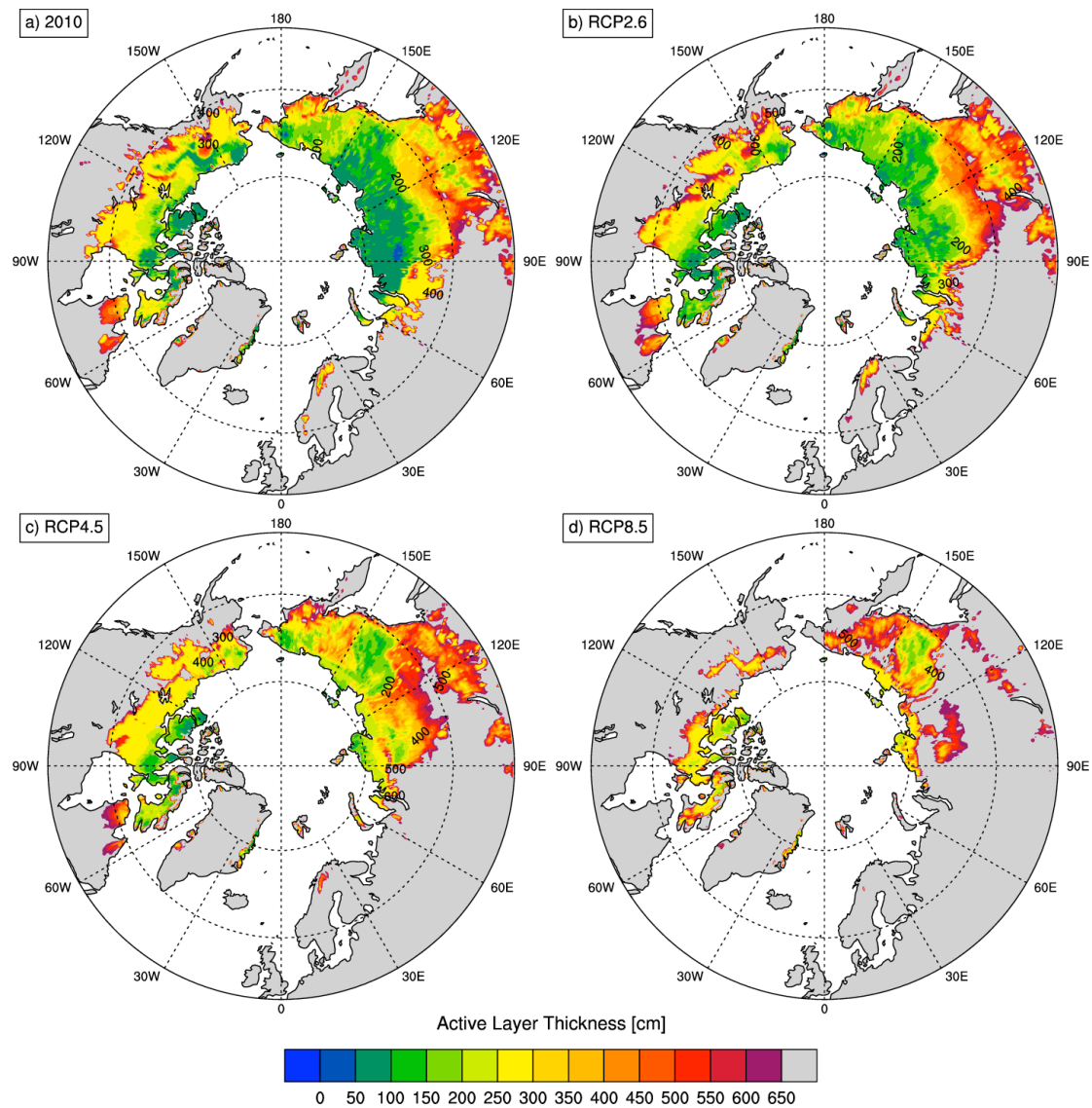
Fig 5.10 Maps of northern hemisphere active layer thickness under present (map **a,** 2010) and future (maps **b-d**, 2090-2100 average) estimates of different climate scenarios. Only gridcells with simulated permafrost are shown.

The temporal and spatial changes of ALT are shown in Fig. 5.11. From 2010 to 2100 on average, there is around 30 cm of ALT increase in RCP2.6, while RCP4.5 shows around 80 cm increase and RCP8.5 shows around 170 cm increase (Fig. 5.11a). However, these estimates compare averages of different number of gridcells due to different maps of simulated permafrost in each projection, so a spatial analysis is required to compare regional changes. The changes of ALT in regions where permafrost is still preserved are shown in Fig. 5.11b-d. In RCP2.6, ALT increase in western Siberia and Canada is balanced by the ALT decrease in eastern Siberia and far east Russia (Fig. 5.11b). This area is also simulated to have colder soil temperatures by 2100 (Fig. 5.4b). Most vulnerable places to ALT

increase are in central Siberia. Conversely, most resilient areas are found in eastern Siberia and northeastern Canada. However, ALT increase in areas with degraded permafrost are not seen from this map.
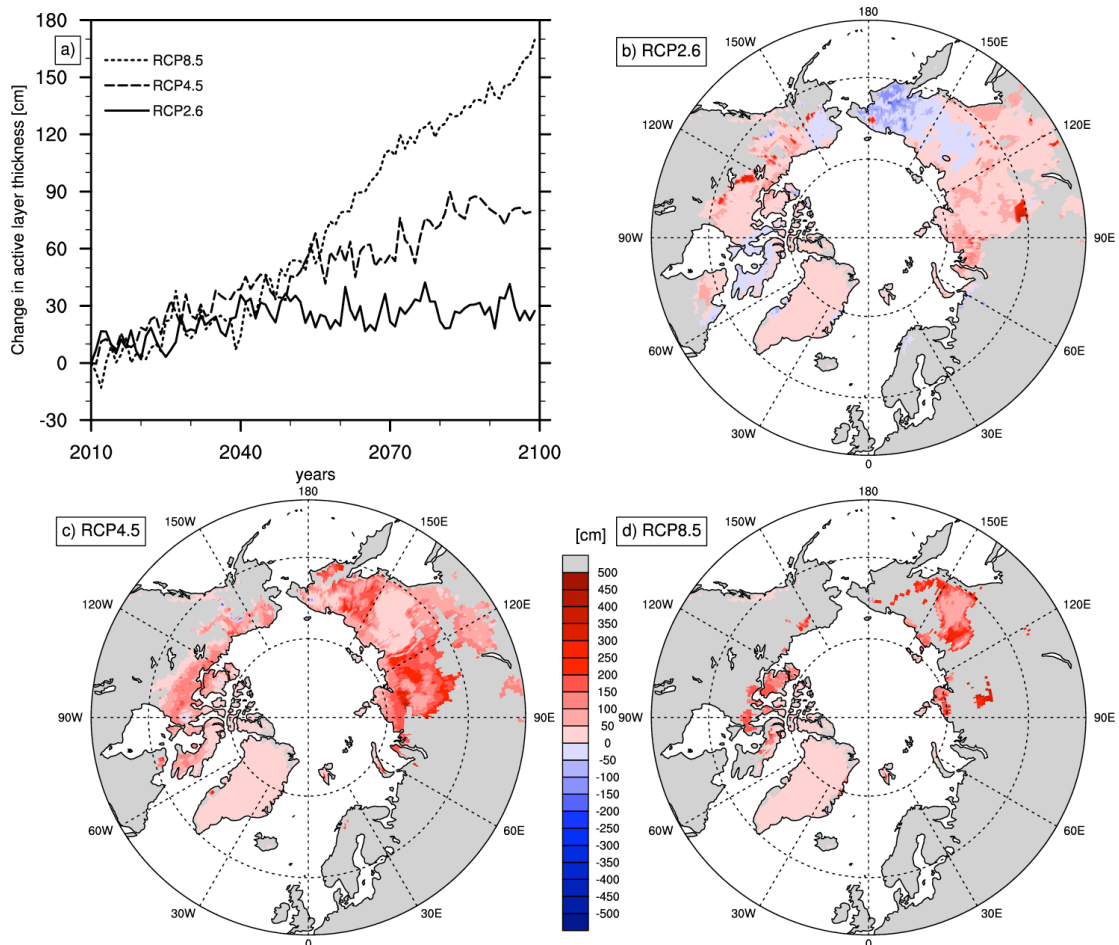

Figure 5.11 Panel showing temporal change in active layer thickness (ALT) from 2010 to 2100. Plot **a** shows the timeseries of spatially averaged ALT change from three different projections. Maps **b**,**c**, and **d** shows the ALT change (2090-2100 average minus 2010-2020 average) from three projections. Only gridcells with permafrost are shown.

Soil response to future scenarios is not homogenous over high latitudes (Fig. 5.4, Fig. 5.7, Fig. 5.11). As discussed thoroughly in the previous chapters (Chapters 2-3-4), and in the literature (Zhang, 2005; Koven et al., 2013) cold region soil physics are strongly affected by snow cover and its properties. For this reason, it is worthwhile to analyze the changes in snow. Figure 5.12 shows the distribution of snow depth in the beginning and end of the simulations. In present and future conditions, snow depth is simulated higher in far east Russia, western and central Siberia, as well as eastern and northern Canada (Fig. 5.12). Chapter 3 has shown the effect of snow depth on soil temperatures on site scale.

Similarly here, on the continental scale, ALT change is bigger in the regions (Fig. 5.11c), where higher snow depth is simulated (Fig. 5.12c). On the contrary, there is lower snow depth simulated in eastern Siberia (Fig. 5.12c-d), where the ALT change is smallest (Fig. 5.11c-d). In addition to previous discussion about elevation and ALT, these features demonstrate a positive relation between snow depth and ALT change.
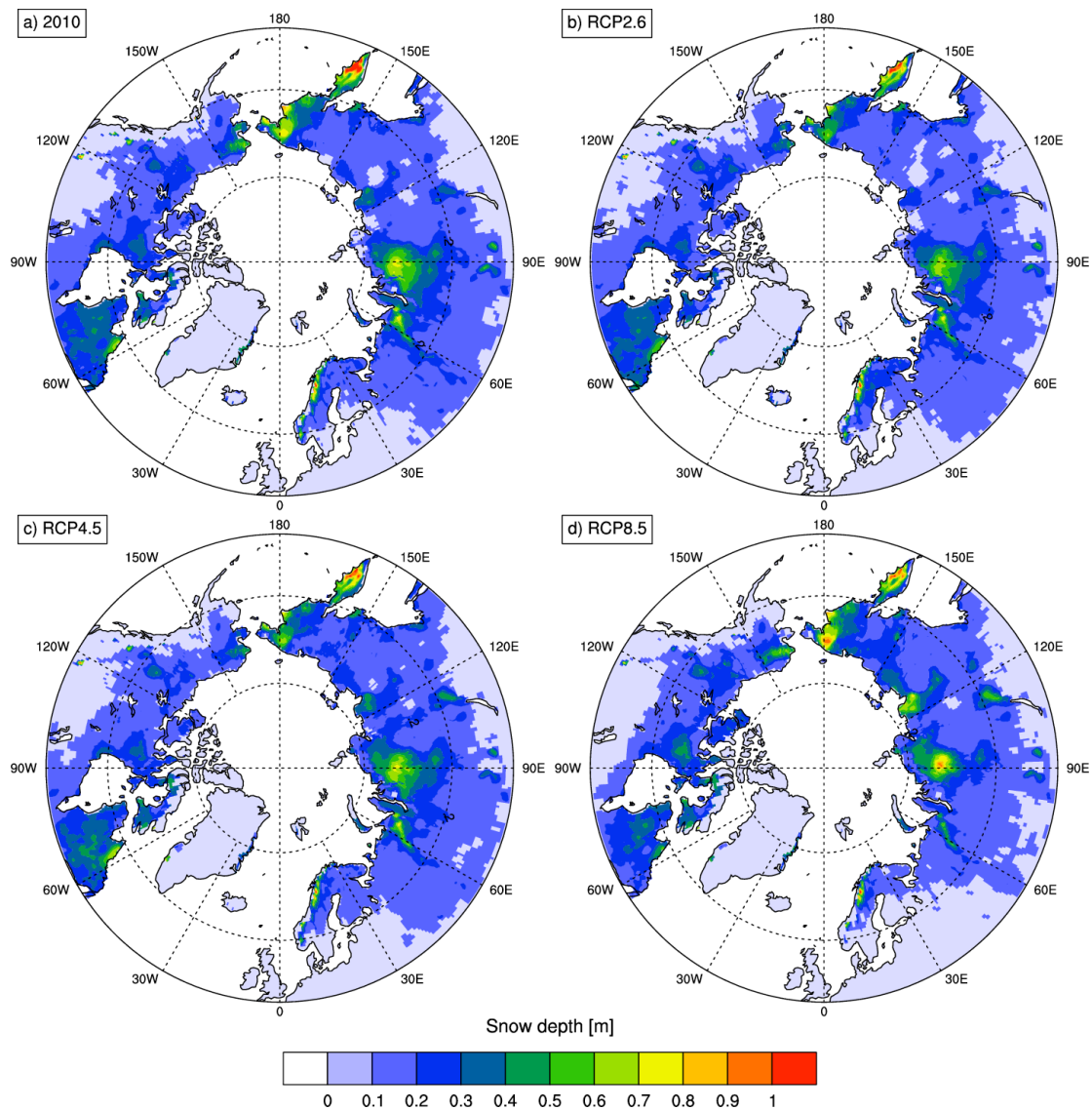
Figure 5.12 Panel showing maps of simulated snow depth at the beginning (2010 – plot **a**) and end of three future projections (2090-2100 average – plots **b**, **c**, and **d**).

Figure 5.13 shows the temporal and spatial change in simulated snow depth at the beginning and end of the simulations. Even though the temporal pattern of spatially averaged snow depth is hard to analyze (Fig. 5.13a), its spatial distribution shows clear patterns of increased (or decreased) snow depth

in each scenario (Fig. 5.13b-d). RCP2.6 shows a general decrease in snow depth over the target domain (Fig. 5.13b); however, RCP4.5 and RCP8.5 show increased snow depth in far east Russia, eastern and central Siberia, as well as northern Canada (Fig. 5.13c-d). Since higher snow depth strengthens the snow insulation and protects the soil from extreme cold weather (Zhang, 2005; Ekici et al., 2014), average soil temperature under higher snow pack is expected to be higher. We have seen that highest increases of soil temperature are simulated in northern Siberia and northern Canada (Fig. 5.4b-d). The same regions are also predicted to have an increase in snow depth (Fig. 5.13c-d). On the other hand, a lower increase in soil temperature is simulated in western Russia in RCP8.5 (Fig. 5.4d), where we can also see a pronounced decrease in snow depth in Fig. 5.13d. These similarities explain most of the regional differences in soil temperature changes.
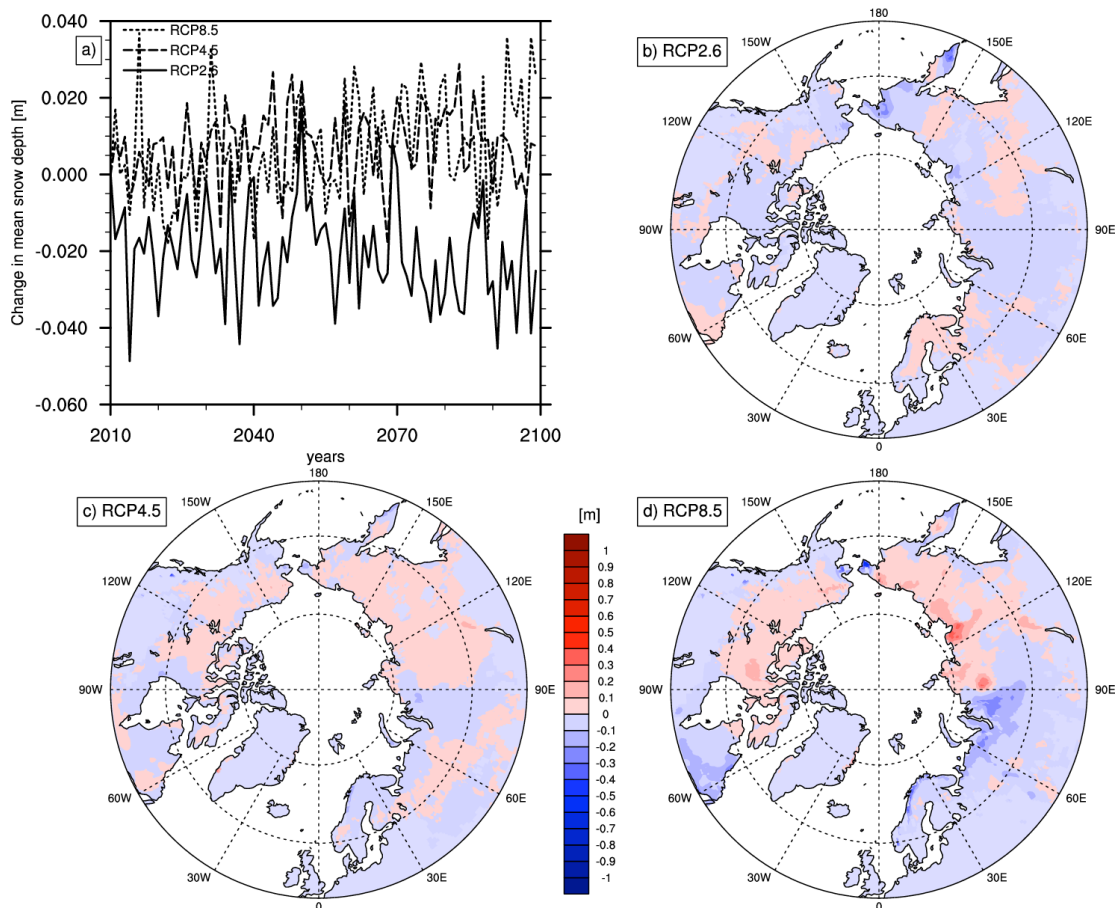

Figure 5.13 Panel showing temporal change in snow depth from 2010 to 2100. Plot **a** shows the timeseries of spatially averaged snow depth change from three different projections. Maps **b,c**, and **d** shows the snow depth change (2090-2100 average minus 2010-2020 average) from three projections.

As detailed in previous chapters, changes in snow depth cannot explain all soil thermal dynamics, but the timing and length of the snow season play a role as well. That could be a reason for the increase in soil temperature in regions where an increase in snow depth is not visible. Figure 5.14 shows the timeseries of changes in snow season properties, with plots showing snow season start date, end date and the total snow season length. On average, snow season is shifted by almost a month in the 21st century for all RCPs (Fig. 5.14). The start and end date of the snow season progressed towards later in the year. Later arrival of snow covers can lead to colder soil temperatures due to lack of insulation in early winter. On the other hand, the longer the snow cover is conserved in spring, the later the soil starts warming, which also affects the growing season. Late spring snow cover keeps the soil colder while air temperatures are warming up, and delays thawing of the active layer (Marmy et al., 2013). However, the start of the snow season is delayed more than the end date of the snow season, which resulted in a shortened snow season length, especially for RCP8.5 simulation (Fig. 5.14 lower plot).
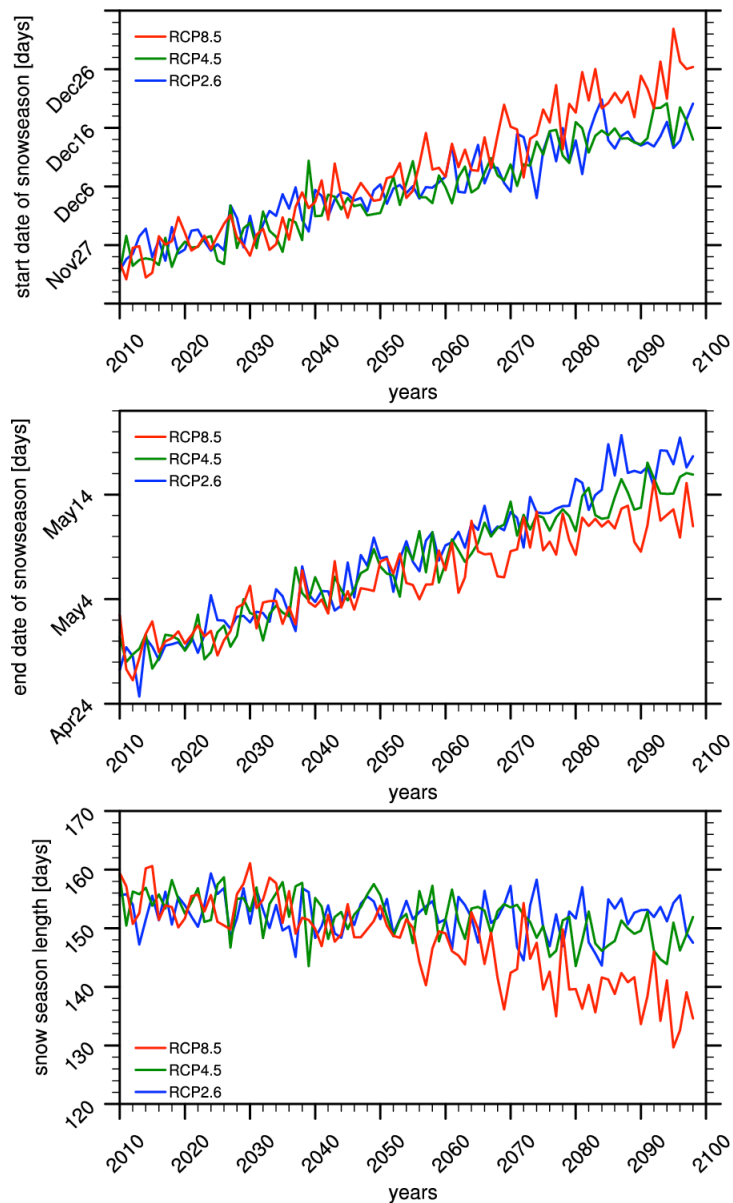
Fig 5.14 Timeseries of spatially averaged snow season start date (upper plot), end date (middle plot), and length from 2010 to 2100 (lower plot) from three different climate projections. Snow season is estimated by taking the days when snow depth is over 10 cm for at least 10 days from October to end of September of next year.

A shorter snow season relates to a general soil warming in our experiments since the number of days with snow insulation is decreased and the warming air temperatures (Fig. 5.1) affect the soils longer in the year. However, duration of the snow season is shortened remarkably in western Siberia and European Russia under RCP8.5 simulation (Fig. 5.15d). Snow depth (Fig. 5.13) and snow season length is increasing in eastern Siberia, where there is still permafrost simulated (Fig. 5.8). All future scenarios predict an increase in snow season length over eastern Siberia (Fig. 5.15b-d). These results show that in

addition to snow depth, snow season length has also an important role on soil temperature regime, hence the permafrost state.
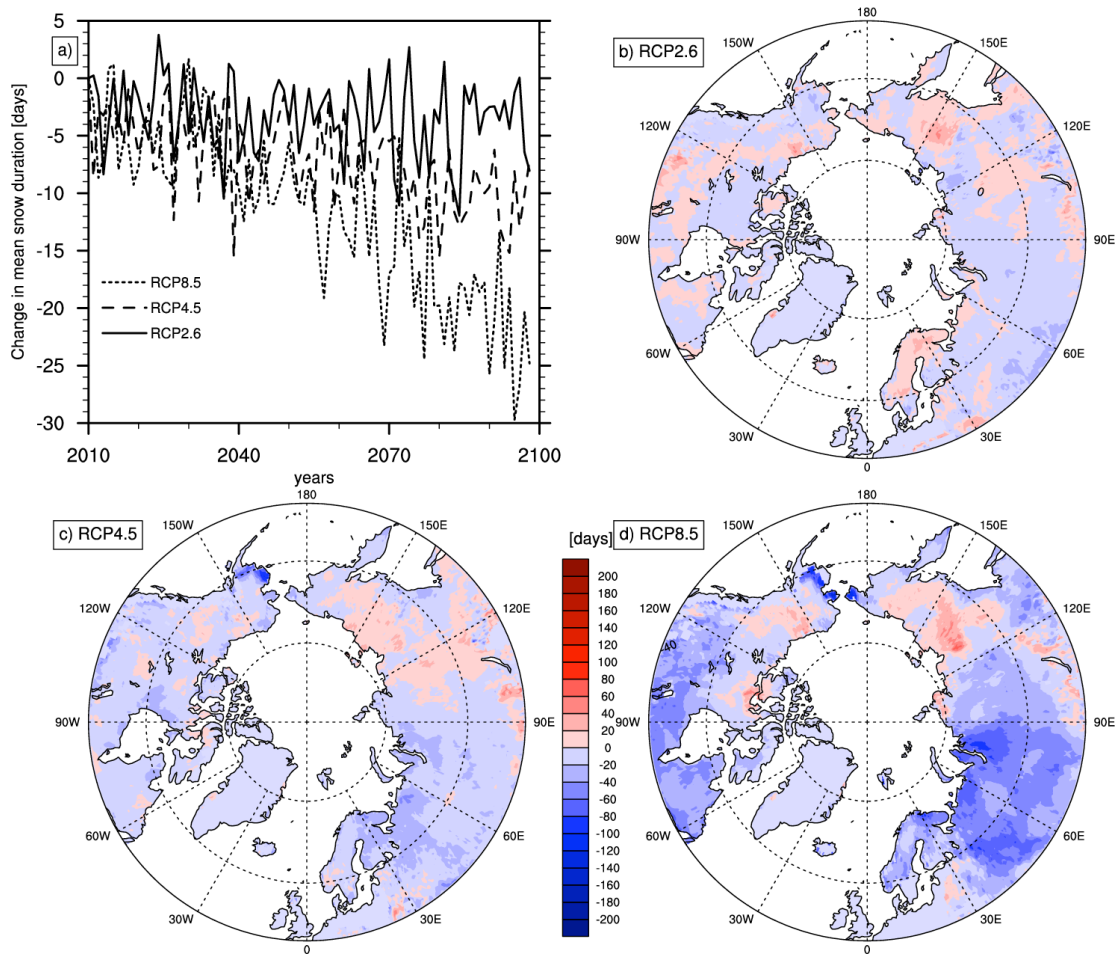

Figure 5.15 Panel showing temporal change in snow season length from 2010 to 2100. Plot **a** shows the timeseries of spatially averaged snow season length change from three different projections. Maps **b**,**c**, and **d** shows the snow season length change (2090-2100 average minus 2010-2020 average) from three projections.

As mentioned in the introduction, there are several studies showing future changes in permafrost state. As each experiment differs in many ways, it is worthwhile to see different precitions for future permafrost state changes. Our estimates seem to fit within the average values given in other studies and compared in Table 5.1. Among the selected studies, simulated permafrost area for 2100 falls between 8.4 and 17.6 million km² for RCP2.6 (JSBACH: 12.88). For RCP4.5, the range is between 6.3 and 14.1 (JSBACH: 9.84) million km², while RCP8.5 range is 2.1 and 8.5 (JSBACH: 2.88). The range of estimates for the expected change in ALT and permafrost area seems to be rather unconstrained. Depending on the study, we can expect almost full disappearance of the

permafrost in modeled soil domain, while some other studies suggest much lower decreases. The high range of estimates from different studies is related to many factors. First of all, each study utilizes a different complexity of a land model that has specific set of processes and internal interactions. Besides, the experiments differ in their chosen atmospheric forcing data, land cover maps, and their spin up procedures. Having an offline versus a fully coupled simulation also produces distinctive results. Therefore, when comparing different estimates, it is imperative to consider these aspects of the experiment as well.

Table 5.1 Comparison of permafrost area (2100), permafrost area loss (by 2100), and ALT increase (by 2100) in literature.

STUDY	SCENARIO	PF AREA [10^6 km^2]	PF-LOSS [%]	ALT INCREASE [cm]
This study	RCP2.6	12.88	7	28
	RCP4.5	9.84	29	80
	RCP8.5	2.88	79	170
Lawrence et al. (2012)	RCP2.6	8.4	33	
	RCP4.5	6.3	49	-
	RCP6.0	4.8	62	
	RCP8.5	3.5	72	
Burke et al. (2012)	RCP2.6	17.6	26	24
	RCP4.5	14.1	40	45
	RCP6.0	13.6	42	59
	RCP8.5	8.5	64	93
Slater and Lawrence (2013)*	RCP2.6	10.0	31	
	RCP4.5	7.5	48	-
	RCP6.0	5.9	59	
	RCP8.5	2.1	85	
Koven et al. (2013)*	RCP2.6		2-66	
	RCP4.5	-	15-87	-
	RCP8.5		30-99	
Schneider von Deimling et al. (2012)	RCP4.5		18-37	
	RCP6.0	-	23-47	-
	RCP8.5		41-81	
Saito et al. (2007)	A1B	7.3	40-57	-
Schaefer et al. (2011)	A1B	7.6(+-1.3)	20-39	56-92
Koven et al. (2011)	A2B	~9.8	30	-

*multi-model mean from CMIP5 results

It is also important to mention that experiments presented in this Chapter show a perspective into the future. Even though soil temperature is crucial to analyze permafrost dynamics, there are more aspects of the natural system that

are not considered here and thus limiting the accuracy of these simulations. These include dynamically changing vegetation, additional snow processes (i.e. snow depth hoar, snow metamorphosis, compaction, wind drift etc.), lack of a dynamically simulated moss layer, effects of excess ground ice in specific regions, having detailed soil parameters (i.e. soil depth, soil porosity etc.), organic matter insulation within the soil, and lateral processes. Additionally, a better assessment should be done having the full system (soil, atmosphere, oceans) interacting with each other. Only in such a coupled simulation we can assess the natural order of feedback mechanisms between different parts of the system. Having these limitations in mind, this chapter has provided some potential pathways for the soil physical state of northern high latitudes into the 21st century.

5.5 CONCLUSIONS

Using a process-oriented land surface scheme, simulation results have presented the future physical state of northern high-latitude near surface permafrost soils under three different climate scenarios from 2010 to 2100. In parallel to the projected soil warming, permafrost area is seen to decrease even under the most conventional representative concentration pathway (RCP 2.6). The results show increased active layer thicknesses (between 30 and 170 cm) and degrading permafrost extent (between 7 and 79%) by the year 2100. However, spatial analysis showed that the changes are not uniform over the Arctic region and some areas are showing opposite signs of change. Permafrost proves to be most resistant in eastern Siberia and northeastern Canada. Model soil depth is shown to be responsible for the soil hydrological pattern. On the other hand, the topography is important for the spatially diverse soil thermal regime hence the permafrost conditions. Snow depth and snow season length have been identified as major controlling factors of climate change effects on soil physical state.

These results are comparable to other studies in literature, however the model results show a very big range of soil response to the climate change. Future studies should include a fully coupled simulation to better quantify the changes in permafrost and effects of permafrost carbon on climate.

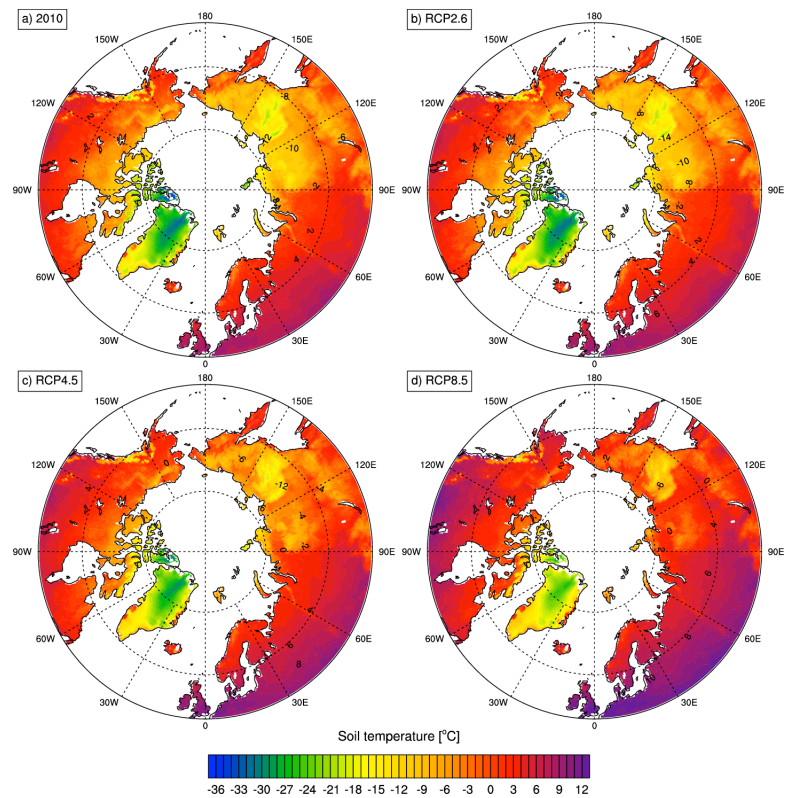**APPENDIX A: SOIL TEMPERATURE MAPS OF DIFFERENT MODEL LAYERS**

Figure A1. Soil temperature panel showing maps of simulated soil temperature (2nd layer: 6.5 – 31 cm) at the beginning (2010 – plot **a**) and end of three future projections (2090-2100 average – plots **b**, **c**, and **d**).
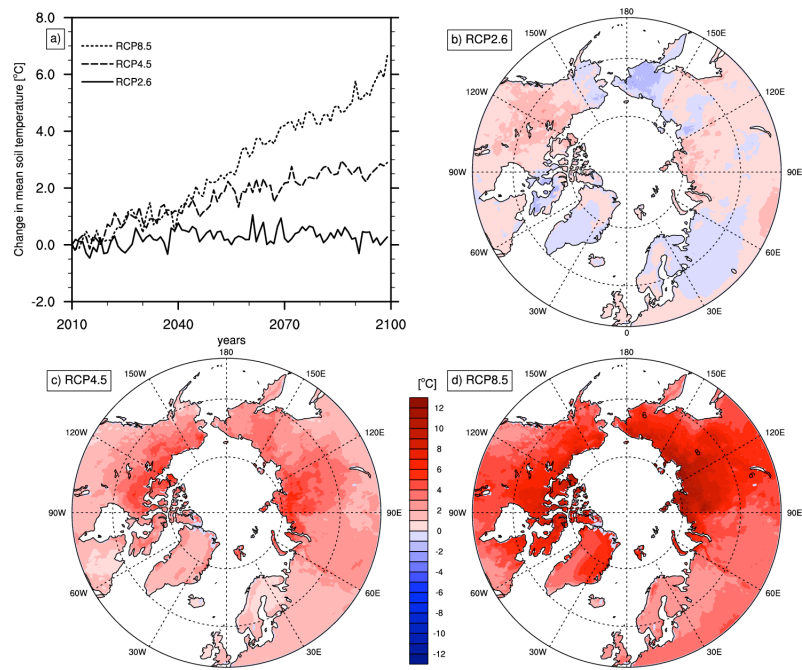

Figure A2. Panel showing spatio-temporal change in soil temperature (2nd layer: 6.5 – 31 cm) from 2010 to 2100. Plot **a** shows the timeseries of spatially averaged soil temperature change from three different projections. Plots **b,c**, and **d** shows the maps of soil temperature change (2090-2100 average minus 2010-2020 average) from three projections.

Figure A3. Soil temperature panel showing maps of simulated soil temperature (3rd layer: 31 – 123 cm) at the beginning (2010 – plot **a**) and end of three future projections (2090-2100 average – plots **b**, **c**, and **d**).

Figure A4. Panel showing spatio-temporal change in soil temperature (3rd layer: 31 – 123 cm) from 2010 to 2100. Plot **a** shows the timeseries of spatially averaged soil temperature change from three different projections. Plots **b,c**, and **d** shows the maps of soil temperature change (2090-2100 average minus 2010-2020 average) from three projections.

102
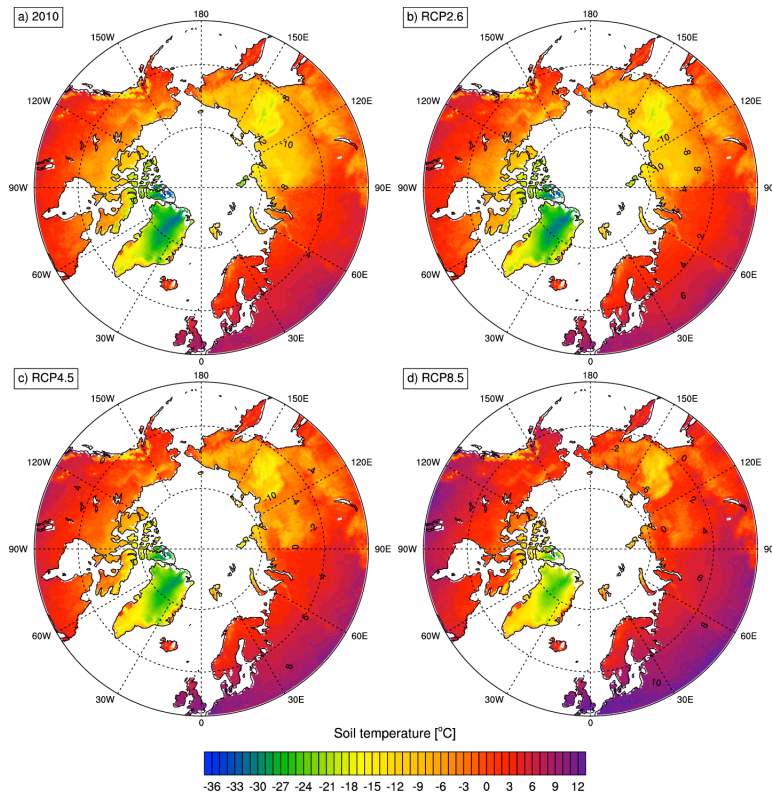
Figure A5. Soil temperature panel showing maps of simulated soil temperature (4th layer: 123 – 413 cm) at the beginning (2010 – plot **a**) and end of three future projections (2090-2100 average – plots **b**, **c**, and **d**).
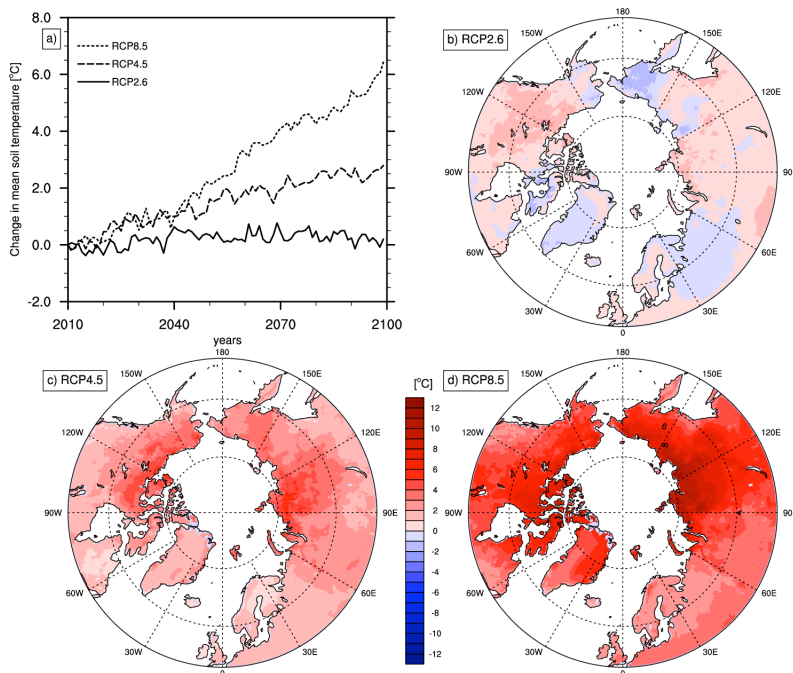
Figure A6. Panel showing spatio-temporal change in soil temperature (4th layer: 123 – 413 cm) from 2010 to 2100. Plot **a** shows the timeseries of spatially averaged soil temperature change from three different projections. Plots **b,c**, and **d** shows the maps of soil temperature change (2090-2100 average minus 2010-2020 average) from three projections.
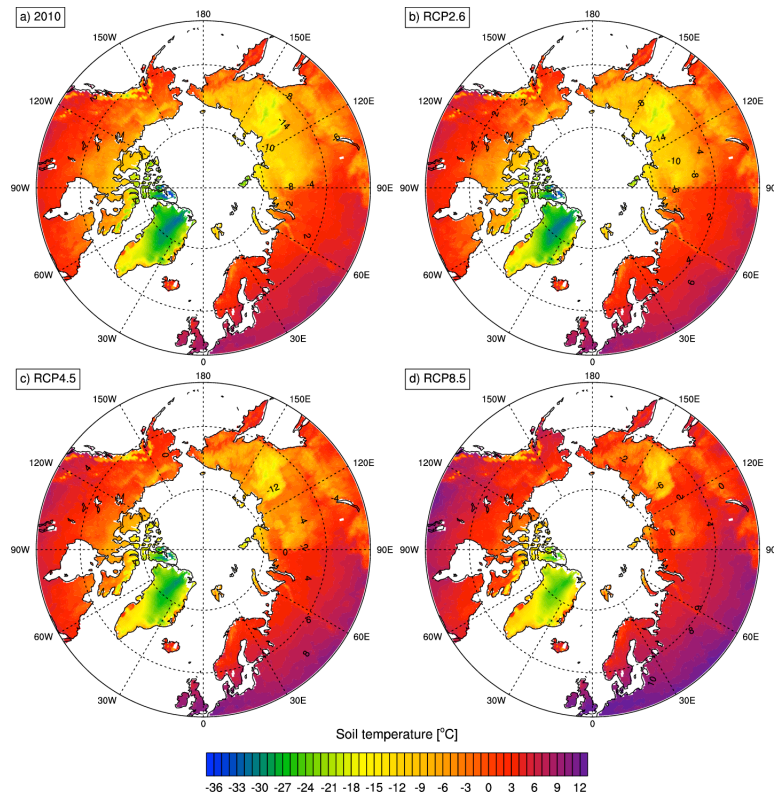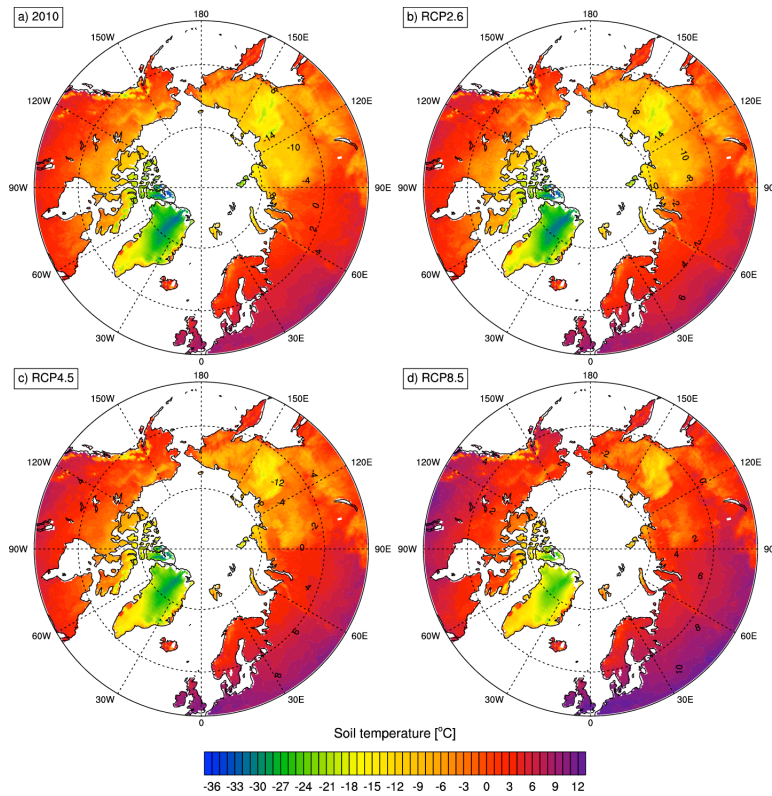
Figure A7. Soil temperature panel showing maps of simulated soil temperature (5th layer: 413 – 983 cm) at the beginning (2010 – plot **a**) and end of three future projections (2090-2100 average – plots **b**, **c**, and **d**).
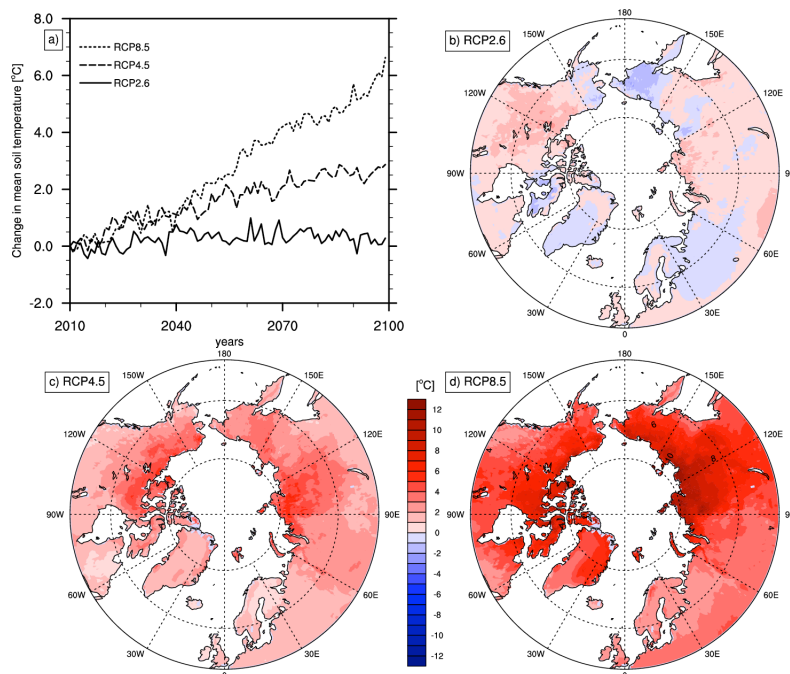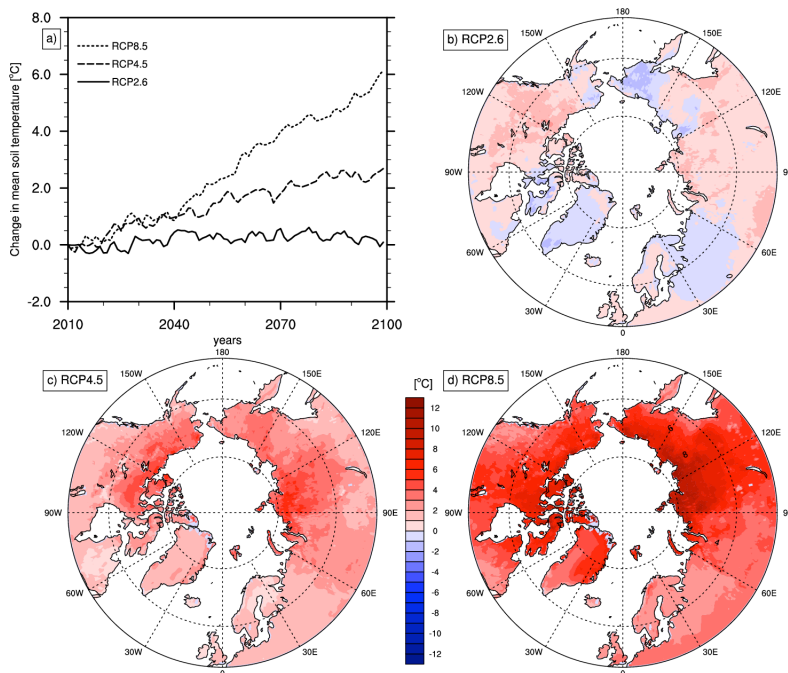

Figure A8. Panel showing spatio-temporal change in soil temperature (5th layer: 413 – 983 cm) from 2010 to 2100. Plot **a** shows the timeseries of spatially averaged soil temperature change from three different projections. Plots **b,c**, and **d** shows the maps of soil temperature change (2090-2100 average minus 2010-2020 average) from three projections.

APPENDIX B: STATIC SOIL MAPS

Figure B1. Map of soil depth used in model simulations. Soil hydrology is limited to this soil depth value in each gridcell.

Figure B2. Topographical map used in model simulations.

CHAPTER 6

SUMMARY AND CONCLUSIONS

This thesis introduces a numerical approach to represent the physics of the processes, which are governing the state and evolution of the thermal state of permafrost soils in a global model. As stated in the introduction, the current modeling efforts lack a qualitative analysis of model processes, hence a multitude of model estimates exist, mainly on soil thermal processes and soil atmosphere couplings. To challenge this uncertainty, a permafrost specific thermo-hydraulic approach is implemented into JSBACH model and evaluated with a range of observations and other models. With a new set of parameterizations, model processes that are important for the permafrost thermal regime are analyzed. Each chapter in this thesis has aimed to answer the questions posed in the introduction. A summary and brief outcome of the individual chapters are provided here together with conclusive remarks and future outlooks in the field of permafrost modeling.
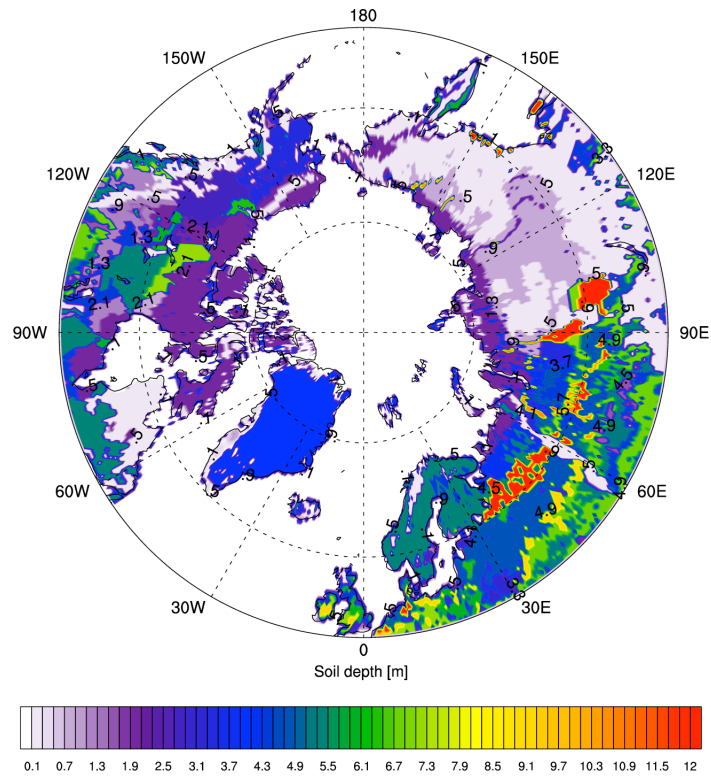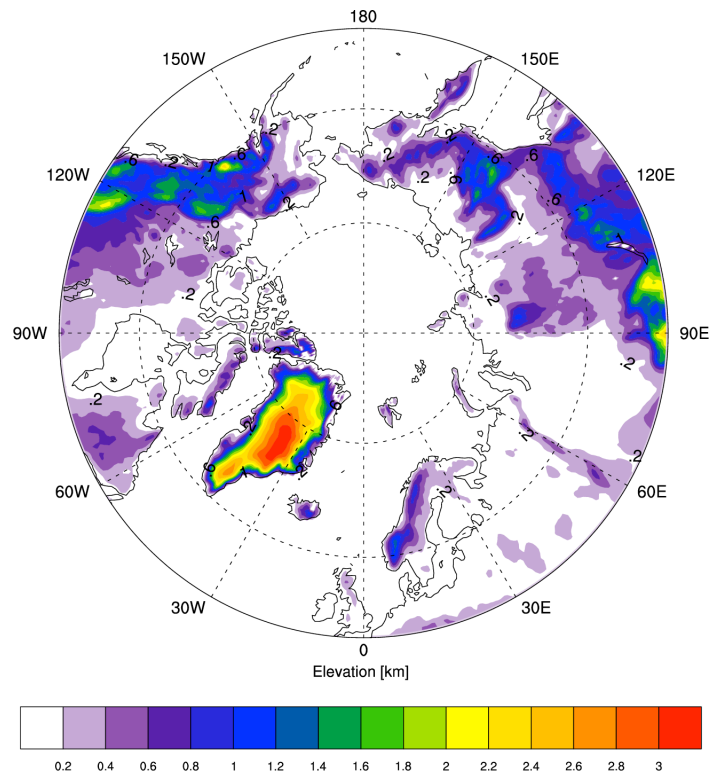
6.1 Summary

The work presented here follows a stepwise approach, in four main chapters from model development and intercomparison via process analysis to future projections. The key points of each chapter are described in the following.

Chapter 2 has documented the permafrost specific improvements for the JSBACH model. As part of the Max Planck Institute's Earth System Model, the newly developed JSBACH version is evaluated with multi-source observed data and proven to be a capable tool for permafrost related experiments in a global modeling framework. With the new processes, soil temperature dynamics are captured successfully with the new processes implemented in JSBACH. However, the model evaluations indicated biases in subsoil temperatures and active layer thickness (ALT) estimates.

Chapter 3 has tested the model performance at different site conditions within a broad multi-model intercomparison of different complexity of models. A variety of modeling approaches are evaluated with site-observed data and a basis for general permafrost modeling framework is established. Main results demonstrate that models with explicit snow representations and some sort of vegetation insulation perform better in representing observed soil temperature

dynamics. Additionally models differ in their soil heat transfer formulations, which brings up more discrepancy among model results.

Chapter 4 has demonstrated a detailed analysis of different process representations in the JSBACH model. Experiments with improved formulations of surface insulation and model soil discretization are performed to find the appropriate level of detail to represent permafrost soil thermal dynamics efficiently in a global model. Analyses of model experiments showed the importance of dynamic surface insulation in simulating soil thermal regime.

Chapter 5 has displayed the future projections of the permafrost thermal state by the JSBACH model forced with different climate change scenarios. Spatial analysis of 21st century change in the northern permafrost region is provided and environmental factors important to this change are discussed. Similar to the findings in previous chapters, snow depth and snow timing proved to be important regulators of soil temperature changes and hence the permafrost state. However, the importance of topographical effects is also pointed out and the heterogeneous response of permafrost thermal state to climate change is analyzed.

The research questions raised in the introduction are answered accordingly. Detailed analysis of these topics can be found in the individual chapters.

Can permafrost processes be included within an Earth System model that compare well to site- and global-scale datasets?

Yes. The developed JSBACH model includes permafrost specific physical processes, which can replicate observed conditions at site- and large-scale applications with a reasonable level of accuracy.

What is the required level of complexity in global models to estimate permafrost thermal dynamics?

Models have to include decent soil physics coupling thermal and hydrological states for freezing conditions. Surface insulation including a detailed snow model together with reliable vegetation insulation is needed for any model trying to estimate permafrost thermal dynamics.

What should be the level of detail needed in computationally efficient and physically precise process representation for permafrost soil physics?

Internal soil physics and surface insulation regulate the soil thermal balance. Explicit soil freezing scheme as well as representing seasonally changing surface insulation is required to model permafrost soil physics correctly. Model soil column has to be at least 30-50 m in order to capture long-term changes in the soil thermal dynamics, however the computational cost has to be considered for such simulations.

What will be the thermal state of Arctic permafrost during the 21st century?

According to JSBACH simulations driven by RCP scenarios, permafrost soils will experience warming, which will result in increased active layer thickness and permafrost degradation. Soil ice content in the permafrost regions will be reduced due to soil thawing. Increased precipitation from climate change scenarios will provide larger snow depths in some parts of the region, however the increasing temperatures will decrease the snow season length in most of the permafrost regions.

How will climate change affect permafrost states in different regions of the Arctic?

Impact of climate change on permafrost regions will not be uniform. Changes in the Arctic will be different in highlands and lowlands. Eastern Siberia and northeastern Canada will be more resistant to permafrost degradation, whereas southern borders of current permafrost extent and lowlands with high water content will experience more severe changes in the soil thermal regime.

6.2   Limitations

This thesis has presented a comprehensive analysis of numerical modeling of permafrost soil physics in current and future conditions. Important factors affecting the soil thermal regime are identified and different formulations are analyzed to improve the accuracy of model estimates. However, as it is a modeling study, several assumptions are made for the idealized model experiments. Therefore, a number of issues important to the permafrost domain are neglected here. These include the assumptions originating from the model spatial resolution, that the model cannot capture fine-scale processes naturally occurring below the model grid-size. Additionally, one dimensional soil

representation prevents the representation of any lateral process. Each model grid-cell is simulated independently, hence the possible interactions between neighboring grid-cells are neglected. Also, the focus of this study is to represent the soil thermal states, therefore mostly the physical processes relating to soil thermal dynamics are discussed here. The biogeochemical interactions between the soil thermal dynamics and the soil carbon processes are beyond the scope of this study. Related to that, wetlands and their specific peat formation are not included in this thesis. Finally, modeling only the soil response to atmospheric changes is another technical assumption of this study. This thesis is aimed to take the first step towards investigating the permafrost soil response to climatic changes. Since the model experiments are performed offline, the potential effects from the soil to the atmosphere are not included here.

6.3   Outlook

Findings in this thesis have helped to clarify a desirable modeling approach for representing permafrost soils in global simulations. Due to several assumptions described in the previous section, the results presented here can be improved by extending the modeling approach in several possible directions. Therefore, further model development pathways can be based on the results achieved here. Increasing model resolution in spatial, vertical, and temporal domains will always be an issue in next generation models. However, increasing the detail of process representation in current models is equally important in capturing natural dynamics of the system. As it is described in the previous chapters, the surface insulation is a major controlling factor for the soil thermal profiles and global models need more detailed representations of the snowpack and surface vegetation.

Adding to that, the full suit of complex natural interactions can be represented by coupling thermal, hydrological, and biogeochemical processes in order to achieve increased accuracy from model estimates.

On the global perspective, the lateral and vertical couplings of different Earth System components such as atmosphere, land, oceans, and ice sheets need to be included in the future projections of permafrost response to climate change as well as various feedback analysis between different components of the Earth system.

110

One of the major questions on permafrost modeling is undoubtedly the potential feedback of permafrost carbon release to climate change. The presented model can be extended to include a vertical soil carbon representation and coupled simulations can be used to quantify this feedback.

BIBLIOGRAPHY

ACIA: Arctic Climate Impact Assessment, Cambridge University Press, New York, USA, 1042p, 2005.

AMAP, Arctic Climate Issues 2011: Changes in Arctic Snow, Water, Ice and Permafrost, SWIPA 2011 Overview Report, 2012.

Anisimov, O.A., and Nelson, F.E.: Permafrost zonation and climate change in the northern hemisphere: results from transient general circulation models, Climatic Change, 35(2): 241–258. DOI: 10.1023/A:1005315409698, 1997.

Annan, J. D., Hargreaves, J. C., Edwards, N. R., Marsh, R.: Parameter estimation in an intermediate complexity Earth system model using an ensemble Kalman filter, Ocean Model. 8, 2005a 135–154, doi:10.1016/j.ocemod.2003.12.004, 2005.

Beer, C., Lucht, W., Gerten, D., Thonicke, K., and Schmullius, C.: Effects of soil freezing and thawing on vegetation carbon density in Siberia: A modeling analysis with the Lund-Potsdam-Jena Dynamic Global Vegetation Model (LPJ-DGVM), Global Biogeochem. Cy., 21, GB1012, 2007.

Beer, C., Weber, U., Tomelleri, E., Carvalhais, N., Mahecha, M., and Reichstein, M.: Harmonized European long-term climate data for assessing the effect of changing temporal variability on land-atmosphere CO_2 fluxes, J. Climate, 27, 4815–4834.doi: http://dx.doi.org/10.1175/JCLI-D-13-00543.1, 2014.

Beringer, J., Lynch, A. H., Chapin III, F. S., Mack, M., and Bonan, G. B.: The representation of Arctic Soils in the Land Surface Model: The Importance of Mosses, J. Climate, 14, 3324–3335, 2001.

Boike, J., Wille, C., and Abnizova, A.: Climatology and summer energy and water balance of polygonal tundra in the Lena River Delta, Siberia, Journal of Geophysical Research, Vol. 113, G03025, doi: 10.1029/2007JG000540, 2008.

Boike, J., Kattenstroth, B., Abramova, K., Bornemann, N., Chetverova, A., Fedorova, I., Fröb, K., Grigoriev, M., Grüber, M., Kutzbach, L., Langer, M., Minke, M., Muster, S., Piel, K., Pfeiffer, E.-M., Stoof, G., Westermann, S., Wischnewski, K., Wille, C. and Hubberten, H.-W.: Baseline characteristics of climate, permafrost and land cover from a new permafrost observatory in the Lena River Delta, Siberia (1998–2011), Biogeosciences, 10: 2105-2128, doi:10.5194/bg-10-2105-2013, 2013.

Braakhekke, Maarten C., Christian Beer, Marcel R. Hoosbeek, Markus Reichstein, Bart Kruijt, Marion Schrumpf, and Pavel Kabat. "SOMPROF: A vertically explicit soil organic matter model." Ecological Modelling 222, no. 10, 1712-1730, 2011.

Broecker, Wallace S.: Thermohaline circulation, the Achilles heel of our climate system: Will man-made CO2 upset the current balance?, Science 278, no. 5343, 1582-1588, 1997.

Brown, J., Ferrians Jr., O., J., Heginbottom, J., A., and Melnikov, E., S.: Circum-Arctic map of permafrost and ground-ice conditions (Version 2), National Snow and Ice Data Center, Boulder, CO, USA, available at: http://nsidc.org/data/ggd318.html, 2002.

Burke, E. J., Hartley, I. P., and Jones, C. D.: Uncertainties in the global temperature change caused by carbon release from permafrost thawing, The Cryosphere Discussions, 6(2), 1367–1404, 2012.

Burn, C.R: Permafrost, tectonics, and past and future regional climate change, Yukon and adjacent Northwest Territories, Can. J. Earth Sci., 31, 182-191, 1994.

Chapin, F. S., Sturm, M., Serreze, M. C., McFadden, J. P., Key, J. R., Lloyd, A. H., McGuire, A. D., Rupp, T. S., Lynch, A. H., Schimel, J. P., Beringer, J., Chapman, W. L., Epstein, H. E., Euskirchen, E. S., Hinzman, L. D., Jia, G., Ping, C.–L., Tape, K. D., Thompson, C. D. C., Walker, D. A., and Welker, J. M.: Role of land-surface changes in Arctic summer warming, Science, 310(5748), 657-660, doi: 10.1126/science.1117368, 2005.

Christiansen, H. H., Etzelmüller, B., Isaksen, K., Juliussen, H., Farbrot, H., Humlum, O., Johansson, M., Ingeman-Nielsen, T., Kristensen, L., Hjort, J., Holmlund, P., Sannel, A. B. K., Sigsgaard, C., Åkerman, H. J., Foged, N., Blikra, L. H.,Pernosky, M. A., and Ødegård, R. S.: The thermal state of permafrost in the nordic area during the international polar year 2007-2009, Permafrost and Periglacial Processes, 21(2), 156–181, 2010.

Ciais, P., Tagliabue, A., Cuntz, M., Bopp, L., Scholze, M., Hoffmann, G., Lourantou, A., Harrison, S. P., Prentice, I. C., Kelley D. I., Koven, C., and Piao, S. L.: Large inert carbon pool in the terrestrial biosphere during the Last Glacial Maximum, Nature Geoscience, (November), 8–13, 2011.

Curry, J. A., Schramm, J. L., and Ebert, E. E.: Sea ice-albedo climate feedback mechanism, Journal of Climate, 8(2), 240-247, 1995.

Dankers, R., Burke, E. J., and Price, J.: Simulation of permafrost and seasonal thaw depth in the JULES land surface scheme, The Cryosphere, 5(3), 773–790, 2011.

Dee, D. P., Uppala, S. M., Simmons, A. J., Berrisford, P., Poli, P., Kobayashi, S., Andrae, U., Balmaseda, M. A., Balsamo, G., Bauer, P., Bechtold, P., Beljaars, A. C. M., van de Berg, L., Bidlot, J., Bormann, N., Delsol, C., Dragani, R., Fuentes, M., Geer, A. J., Haimberger, L., Healy, S. B., Hersbach, H., Holm, E. V., Isaksen, L., Kalberg, P., Kohler, M., Matricardi, M., McNally, A. P., Monge-Sanz, B. M., Morcrette, J. J., Park., B. K., Peubey, C., de Rosnay, P., Tavolato, C., Thepaut, J. N., and Vitart F.: The ERA-Interim reanalysis: Configuration and performance of the data assimilation system, Quarterly Journal of the Royal Meteorological Society, Wiley Online Library, 137, 553-597, 2011.

Dufresne, J.-L., and Coauthors: Climate change projections using the IPSL-CM5 Earth System Model: From CMIP3 to CMIP5, Climate Dyn., 40, 2123–2165, doi:10.1007/ s00382-012-1636-1, 2013.

Duarte, Carlos M., Timothy M. Lenton, Peter Wadhams, and Paul Wassmann. "Abrupt climate change in the Arctic." Nature Climate Change 2, no. 2, 60-62, 2012.

Dunne, John P., Jasmin G. John, Alistair J. Adcroft, Stephen M. Griffies, Robert W. Hallberg, Elena Shevliakova, Ronald J. Stouffer et al.: GFDL's ESM2 global coupled climate-carbon Earth System Models. Part I: Physical formulation and baseline simulation characteristics, Journal of Climate 25, no. 19, 6646-6665, 2012.

Ekici, A., Beer, C., Hagemann, S., Boike, J., Langer, M., and Hauck, C.: Simulating high-latitude permafrost regions by the JSBACH terrestrial ecosystem model, Geosci. Model Dev., 7, 631-647, doi:10.5194/gmd-7-631-2014, 2014.

Ekici, A., Chadburn, S., Chaudhary, N., Hajdu, L. H., Marmy, A., Peng, S., Boike, J., Burke, E., Friend, A. D., Hauck, C., Krinner, G., Langer, M., Miller, P. A., and Beer, C.: Site-level model intercomparison of high latitude and high altitude soil thermal dynamics in tundra and barren landscapes, The Cryosphere, 9, 1343-1361, doi:10.5194/tc-9-1343-2015, 2015.

FAO, IIASA, ISRIC, ISS-CAS, and JRC: Harmonized World Soil Database (version 1.1) FAO, Rome, Italy and IIASA, Laxenburg, Austria, 2009.

Gent, Peter R., Gokhan Danabasoglu, Leo J. Donner, Marika M. Holland, Elizabeth C. Hunke, Steve R. Jayne, David M. Lawrence, Richard B. Neale, Philip J. Rasch, Mariana Vertenstein, Patrick H. Worley, Zong-Liang Yang, and Minghua Zhang,: The Community Climate System Model Version 4. J. Climate, 24, 4973–4991, doi: 10.1175/2011JCLI4083.1, 2011.

Goetz, S.J., Mack, M.C., Gurney, K.R., Randerson, J.T., and Houghton, R.A.: Ecosystem responses to recent climate change and fire disturbance at northern high latitudes: observations and model results contrasting northern Eurasia and North America, Environ. Res. Lett., 2, 045031, doi:10.1088/1748-9326/2/4/045031, 2007.

Goins A.L.; Loftis J.L.; Tyler T.J.: OGEL Special Issue "Arctic Region: Boundaries, Resources and the Promise of Co-operation", OGEL, 2, 2012, URL: www.ogel.org/article.asp?key=3241, last access: 23.10.2014

Goodrich, L.: The influence of snow cover on the ground thermal regime. Canadian Geotechnical Journal 19 (4), 421–432, 1982.

Goosse H, Brovkin V, Fichefet T, Haarsma R, Huybrechts P, Jongma J, Mouchet A, Selten F, Barriat PY, Campin JM, Deleersnijder E, Driesschaert E, Goelzer H, Janssens I, Loutre MF, Morales Maqueda M, Opsteegh T, Mathieu PP, Munhoven G, Pettersson E, Renssen H, Roche D, Schaeffer M, Tartinville B, Timmermann A, Weber S: Description of the Earth system model of intermediate complexity LOVECLIM version 1.2, Geosci Model Dev 3:603–633, doi:10. 5194/ gmd-3-603-2010, 2010.

Gornall, J.L., Jonsdottir, I.S., Woodin, S.J., and Van der Wal, R.: Arctic mosses govern below-ground environment and ecosystem processes, Oecologia, 153, 931–941, doi:10.1007/s00442-007-0785-0, 2007.

Gouttevin, I., Krinner, G., Ciais, P., Polcher, J., and Legout, C.: Multi-scale validation of a new soil freezing scheme for a land-surface model with physically-based hydrology, The Cryosphere, 6(2), 407–430, 2012.

Gruber, S.: Derivation and analysis of a high-resolution estimate of global permafrost zonation, The Cryosphere, 6(1), 221-233, 2012.

Heimann, M., and Reichstein, M.: Terrestrial ecosystem carbon dynamics and climate feedbacks, Nature, 451(January), 289–292, 2008.

IPCC AR5: Summary for Policymakers, Climate Change 2013, The Physical Science Basis, Contribution of Working Group I to the Fifth Assessment Report of the Intergovernmental Panel on Climate Change [Stocker, T.F., D. Qin, G.-K. Plattner, M. Tignor, S. K. Allen, J. Boschung, A. Nauels, Y. Xia, V. Bex and P.M. Midgley (eds.)], Cambridge University Press, Cambridge, United Kingdom and New York, NY, USA, 2013.

Jeffries, Martin O., James E. Overland, and Donald K. Perovich: The Arctic, Phys. Today 66, no. 10, 35, 2013.

Jensen, L. M. and Rasch, M.: Nuuk Ecological Research Operations, 2nd Annual Report, 2008, Roskilde, National Environmental Research Institute, Aarhus University, Denmark, 80 pp, 2009.

Jensen, L. M. and Rasch, M.: Nuuk Ecological Research Operations, 3rd Annual Report, 2009, Roskilde, National Environmental Research Institute, Aarhus University, Denmark, 80 pp, 2010.

Khvorostyanov, D. V., G. Krinner, P. Ciais, M. Heimann, and S. A. Zimov. "Vulnerability of permafrost carbon to global warming. Part I: model description and role of heat generated by organic matter decomposition." Tellus B 60, no. 2, 250-264, 2008.

Knorr, W.: Annual and interannual CO2 exchanges of the terrestrial biosphere: process-based simulations and uncertainties, Global Ecol. Biogeogr., 9, 225–252, 2000.

Koven, C.D., Ringeval, B., Friedlingstein, P., Ciais, P., Cadule, P., Khvorostyanov, D., Krinner, G., and Tarnocai, C.: Permafrost carbon-climate feedbacks accelerate global warming, Proceedings of the National Academy of Sciences, 108(36), 14769-14774, doi: 10.1073/pnas.1103910108, 2011.

Koven, C.D., William, J.R., and Alex, S.: Analysis of Permafrost Thermal Dynamics and Response to Climate Change in the CMIP5 Earth System Models. J. Climate, 26, 1877–1900. doi: http://dx.doi.org/10.1175/JCLI-D-12-00228.1, 2013.

Kudryavtsev, V.A., Garagulya, L.S., Kondrat'yeva, K.A., and Melamed, V.G.: Fundamentals of Frost Forecasting in Geological Engineering Investigations, Cold Regions Reseach and Engineering Laboratory: Hanover, NH, 1974.

Lambeck, K., Esat, T. M., & Potter, E. K.: Links between climate and sea levels for the past three million years. Nature, 419(6903), 199-206, 2002.

Langer, M., Westermann, S., Heikenfeld, M., Dorn, W. and Boike, J.: Satellite-based modeling of permafrost temperatures in a tundra lowland landscape, Remote Sensing of Environment, 135: 12-24. doi:10.1016/j.rse.2013.03.011, 2013.

Larsen, P. H., Goldsmith, S., Smith, O., Wilson, M.L., Strzepek, K., Chinowsky, P., and Saylor, B.: Estimating future costs for Alaska public infrastructure at risk from climate change, Global Environ. Change, 18, 442–457, doi:10.1016/j.gloenvcha.2008.03.005, 2008.

Lawrence, D. M. and Slater, A. G.: A projection of severe near-surface permafrost degradation during the 21st century, Geophys. Res. Lett., 32, L24401, doi:10.1029/2005GL025080, 2005.

Lawrence, D. M., Slater, A. G., and Swenson, S. C.: Simulation of Present-Day and Future Permafrost and Seasonally Frozen Ground Conditions in CCSM4, Journal of Climate, 25(7), 2207–2225, 2012.

Lunardini, V.J.: Heat transfer in cold climates, Van Nostrand Reinhold: New York, 1981.

Mackenzie, Fred T., and Judith A. Mackenzie: Our changing planet: an introduction to earth system science and global environmental change, New Jersey: Prentice Hall, 1998.

Marmy, A., Salzmann, N., Scherler, M., and Hauck, C.: Permafrost model sensitivity to seasonal climatic changes and extreme events in mountainous regions, Environmental Research Letters, 8(3), 035048, 2013.

McGuire, A. David, F. S. Chapin Iii, John E. Walsh, and Christian Wirth. "Integrated Regional Changes in Arctic Climate Feedbacks: Implications for the Global Climate System*." Annu. Rev. Environ. Resour. 31, 61-91, 2006.

McGuire, A. D., Anderson, L. G., Christensen, T. R., Dallimore, S., Guo, L., Hayes, D. J., Heimann, M., Lorenson, T. D., Macdonald, R. W. and Roulet, N.: Sensitivity of the carbon cycle in the Arctic to climate change, Ecological Monographs, 79(4), 523–555, 2009.

McKendry, I. G., J. P. Hacker, R. Stull, S. Sakiyama, D. Mignacca, and K. Reid: Long-range transport of Asian dust to the Lower Fraser Valley, British Columbia, Canada, J. Geophys. Res., 106(D16), 18361–18370, doi:10.1029/2000JD900359, 2001.

Monnin, E., Indermühle, A., Dällenbach, A., Flückiger, J., Stauffer, B., Stocker, T. F., Raynaud, D., and Barnola, J. M.: Atmospheric CO2 concentrations over the last glacial termination, Science, 291(5501), 112-114, doi:10.1126/science.291.5501.112, 2001.

Moss, R. H., Edmonds, J. A., Hibbard, K. A., Manning, M. R., Rose, S. K., Van Vuuren, D. P., ... & Wilbanks, T. J.: The next generation of scenarios for climate change research and assessment, Nature, 463(7282), 747-756, doi:10.1038/nature08823, 2010.

Mölders, N., U. Haferkorn, J. Döring, and G. Kramm: Long-term investigations on the water budget quantities predicted by the hydro-thermodynamic soil vegetation scheme (HTSVS)–Part I: Description of the model and impact of long-wave radiation, roots, snow, and soil frost, Meteorology and Atmospheric Physics 84, no. 1-2, 115-135, 2003.

Nicolsky, D. J., Romanovsky, V. E., Alexeev, V. A., and Lawrence, D. M.: Improved modeling of permafrost dynamics in a GCM land-surface scheme, Geophysical Research Letters, 34, 2–6, 2007.

O'Donnell, J. A., Harden, J. W., McGuire, A. D., and Romanovsky, V. E.: Exploring the sensitivity of soil carbon dynamics to climate change, fire disturbance and permafrost thaw in a black spruce ecosystem, Biogeosciences, 8, 1367-1382, doi:10.5194/bg-8-1367-2011, 2011.

Oelke, C., T. Zhang, M. C. Serreze, and R. L. Armstrong: Regional-scale modeling of soil freeze/thaw over the Arctic drainage basin, J. Geophys. Res., 108(D10), 4314, doi:10.1029/2002JD002722, 2003

Overland, J. E., Wang, M., Walsh, J. E., and Stroeve, J. C.: Future Arctic climate changes: Adaptation and mitigation time scales, Earth's Future, 2, 68–74, doi:10.1002/2013EF000162, 2013.

PERMOS: Permafrost in Switzerland 2008/2009 and 2009/2010, Noetzli, J. (ed.), Glaciological Report (Permafrost) No. 10/11 of the Cryospheric Commission of the Swiss Academy of Sciences (SCNAT), Zurich, Switzerland, 2013.

Ping, C. L., Michaelson, G. J., Jorgenson, M. T., Kimble, J. M., Epstein, H., Romanovsky, V. E., and Walker, D. A.: High stocks of soil organic carbon in the North American Arctic region, Nature Geoscience, 1(9), 615–619, 2008.

Porada, P., Weber, B., Elbert, W., Pöschl, U., and Kleidon, A.: Estimating global carbon uptake by Lichens and Bryophytes with a process-based model, Biogeosciences, 10 (6989-7033), doi:10.5194/bg-10-6989-2013, 2013.

Poutou, E., Krinner, G., Genthon, C. and de Noblet-Ducoudre, N.: Role of soil freezing in future boreal climate change, Clim. Dynam., 23(6), 621–639, 2004.

Rignot, E., and Kanagaratnam, P.: Changes in the velocity structure of the Greenland Ice Sheet, Science, 311:986-990, doi: 10.1126/science.1121381, 2006.

Riseborough, D., Shiklomanov, N., Etzelmuller, B., Gruber, S., and Marchenko, S.: Recent Advances in Permafrost Modelling, Permafrost Periglacial Processes, 19, 137–156, 2008.

Robards, Martin D., Patrick J. Gould, and John F. Piatt: The highest global concentrations and increased abundance of oceanic plastic debris in the North Pacific: evidence from seabirds, In Marine Debris, pp. 71-80. Springer New York, 1997.

Roeckner, E., Bäuml, G., Bonaventura, L., Brokopf, R., Esch, M., Giorgetta, M., Hagemann, S., Kirchner, I., Kornblueh, L., Manzini, E., Rhodin, A., Schlese, U., Schulzweida, U., and Tompkins, A.: The atmospheric general circulation model ECHAM 5. PART I: Model description. MPI Report No. 349, Max Planck Institute for Meteorology, Hamburg, 2003.

Romanovsky, V. E., Drozdov, D. S., Oberman, N. G., Malkova, G. V., Kholodov, A. L., Marchenko, S. S., Moskalenko, N. G., Sergeev, D. O., Ukraintseva, N. G., Abramov, A. A., Gilichinsky, D. A., and Vasiliev, A. A.: Thermal state of permafrost in Russia, Permafrost and Periglacial Processes, 21(2), 136–155, 2010a.

Romanovsky, V. E., Smith, S. L., and Christiansen, H. H.: Permafrost thermal state in the polar Northern Hemisphere during the international polar year 2007-2009: a synthesis, Permafrost and Periglacial Processes, 21(2), 106–116, 2010b.

Romanovsky, V. E., Smith, S. L., Christiansen, H. H., Shiklomanov, N. I., Streletskiy, D. A., Drozdov, D. S., Oberman, N. G., Kholodov, A.L., Marchenko, S. S., Permafrost [in Arctic Report Card 2013], http://www.arctic.noaa.gov/reportcard, last access: 27.10.2014, 2013.

Rozenbaum, G.E., Shpolyanskaya, N. A.: A model of quaternary permafrost evolution in the Arctic, Permafrost Seventh International Conference Proceedings, Yellowknife, Canada, Collection Nordicana, No 55, 1998.

Saito, K., Kimoto, M., Zhang, T., Takata, K., and Emori, S.: Evaluating a high-resolution climate model: Simulated hydrothermal regimes in frozen ground regions and their change under the global warming scenario, J. Geophys. Res., 112, F02S11, doi:10.1029/2006JF000577, 2007.

Schaefer, K., Zhang, T., Slater, A. G., Lu, L., Etringer, A., and Baker, I.: Improving simulated soil temperatures and soil freeze/thaw at high-latitude regions in the Simple Biosphere/Carnegie-Ames-Stanford Approach model, Journal of Geophysical Research, 114(F2), F02021, 2009.

Schaefer, K., Zhang, T., Bruhwiler, L., and Bareett, A. P.: Amount and timing of permafrost carbon release in response to climate warming, Tellus B, 63(2), 165–180, 2011.

Schneider von Deimling, T., Meinshausen, M., Levermann, A., Huber, V., Frieler, K., Lawrence, D. M., and Brovkin, V.: Estimating the near-surface permafrost-carbon feedback on global warming, Biogeosciences, 9, 649-665, doi:10.5194/bg-9-649-2012, 2012.

Schuur, E. A. G., Bockheim, J., Canadell, J. G., Euskirchen, E., Field, C. B., Goryachkin, S. V., Hagemann, S., Kuhry, P., Lafleur, P. M., Lee, H., Mazhitova, G., Nelson, F. E., Rinke, A., Romanovsky, V. E., Shiklomanov, N., Tarnocai, C.,

Venevsky. S., Vogel, J. G., and Zimov, S. A.: Vulnerability of Permafrost Carbon to Climate Change: Implications for the Global Carbon Cycle, BioScience, 58(8), 701–714, 2008.

Schuur, E. A. G., Abbott, B. W., Bowden, W. B., Brovkin, V., Camill, P., Canadell, J. G., Chanton, J. P., Chapin, III F. S., Christensen, T. R., Ciais, P., Crosby, B. T., Czimczik, C. I., Grosse, G., Harden, J., Hayes, D. J., Hugelius, G., Jastrow, J. D., Jones, J. B., Kleinen, T., Koven, C. D., Krinner, G., Kuhry, P., Lawrence, D. M., McGuire, A. D., Natali, S. M., O'Donnell, J. A., Ping, C. L., Riley, W. J., Rinke, A., Romanovsky, V. E., Sannel, A. B. K., Schädel, C., Schaefer, K., Sky, J., Subin, Z. M., Tarnocai, C., Turetsky, M. R., Waldrop, M. P., Walter Anthony, K. M., Wickland, K. P., Wilson, C. J., and Zimov, S. A.: Expert assessment of vulnerability of permafrost carbon to climate change, Clim. Change, 119 359–74, doi:10.1007/s10584-013-0730-7, 2013.

Serreze, M., Walsh, J., Chapin, F., Osterkamp, T., Dyurgerov, M., Romanovsky, V., Oechel, W., Morison, J., Zhang, T., and Barry, R.: Observational evidence of recent change in the northern highlatitude environment, Climatic Change, 46, 159–207, 2000.

Serreze, M. C., and Barry, R. G.: Processes and impacts of Arctic amplification: A research synthesis, Global and Planetary Change, 77(1), 85-96, 2011.

Shiklomanov, N. I., F. E. Nelson, D. A. Streletskiy, K. M. Hinkel, and J. Brown. "The circumpolar active layer monitoring (CALM) program: data collection, management, and dissemination strategies." In 9th International Conference on Permafrost, ed. DL Kane and KM Hinkel, vol. 2, pp. 1647-1652. 2008.

Sigman, D. M., Hain, M. P., and Haug, G. H.: The polar ocean and glacial cycles in atmospheric CO2 concentration, Nature, 466, 47–55, 2010.

Slater, A.G., and Lawrence, D.M.: Diagnosing Present and Future Permafrost from Climate Models. J. Clim., 26 (15) 5608-5623, doi: 10.1175/JCLI-D-12-00341.1, 2013.

Smith, L. C., Sheng, Y., MacDonald, G. M. and Hinzman, L. D.: Disappearing Arctic lakes, Science 308, 1429, 2005.

Smith, S. L., Romanovsky, V. E., Lewkowicz, A. G., Burn, C. R., Allard, M., Clow, G. D., Yoshikawa, K., and Throop, J.: Thermal state of permafrost in North America: a contribution to the international polar year, Permafrost and Periglacial Processes, 21(2), 117–135, 2010.

Stefan, J.: Uber die theorie der Eisbildung, insbesondere. uber Eisbildung im Polarmeere, Ann. Phys., 42, 269-286, 1891.

Stendel, M., and J. H. Christensen. "Impact of global warming on permafrost conditions in a coupled GCM." Geophysical Research Letters 29, no. 13, 10-1, 2002.

Stevens, B., Giorgetta, M., Esch, M., Mauritsen, T., Crueger, T., Rast, S., Salzmann, M., Schmidt, H., Bader, J., Block, K., Brokopf, R., Fast, I., Kinne, S., Kornblueh, L., Lohmann, U., Pincus, R., Reichler, T., and Roeckner, E.: The atmospheric component of the MPI-M Earth System Model: ECHAM6, J. Adv. Model. Earth Syst., 5, 146–172, doi:10.1002/jame.20015, 2012.

Stroeve, J., Holland, M.M., Meier, W., Scambos, T. and Serreze, M.: Arctic sea ice decline: Faster than forecast, Geophys. Res. Lett., 34, L09501, doi:10.1029/2007GL029703, 2007.

Swap, R., Garstang, M., Greco S., Talbot, R. and Kallberg, P.: Saharan dust in the Amazon Basin, Tellus B, 44: 133–149, 1992.

Takata, K. and Kimoto, M.: A numerical study on the impact of soil freezing on the continental-scale seasonal cycle, J. Meteorol. Soc. Jpn., 78, 199–221, 2000.

Tarnocai, C., Canadell, J. G., Schuur, E. A. G., Kuhry, P., Mazhitova, G., and Zimov, S.: Soil organic carbon pools in the northern circumpolar permafrost region, Global Biogeochem. Cy., 23, GB2023, doi: 10.1034/j.1600-0889.1992.t01-1-00005.x, 2009.

Taylor, K.E., Stouffer, R.J., and Meehl, G.A.: A summary of the CMIP5 experiment design. PCMDI Tech. Rep., 33 pp. [Available online at http://cmip-pcmdi.llnl.gov/cmip5/docs/ Taylor_CMIP5_design.pdf.], 2009.

Van Everdingen, R. (ed.): Multi-language Glossary of Permafrost and Related Ground-Ice Terms. National Snow and Ice Data Center /World Data Center for Glaciology, 1998.

Van Vuuren, D., Edmonds, J., Kainuma, M., Riahi, K., Thomson, A., Hibbard, K., Hurtt, G., Kram, T., Krey, V., Lamarque, J.- F., Masui, T., Meinshausen, M., Nakicenovic, N., Smith, S., and Rose, S.: The representative concentration pathways: an overview, Climatic Change, 109, 5–31, 2011.

Verseghy, D.: CLASS—A Canadian land surface scheme for GCMs. I. Soil model, Royal Meteorological Society, 11, 111–133, 1991.

Weedon, G., Gomes, S., Viterbo, P., Österle, H., Adam, J., Bellouin, N., Boucher, O., and Best, M.: The WATCH forcing data 1958-2001: A meteorological forcing dataset for land surface and hydrological models WATCH Tech. Rep. 22, 41 pp., [Available online at http://www. eu-watch. org/publications/technical-reports.], 2010.

Yershov ED. General Geocryology. Cambridge University Press: Cambridge, 580 pp, 1998.

Zhang, T.: Influence of the seasonal snow cover on the ground thermal regime: An overview, Reviews of Geophysics, 43(4), 2005.

Zhang, T., Barry, R.G., Knowles, K., Heginbottom, J.A., and Brown, J.: Statistics and Characteristics of permafrost and ground-ice distribution in the Northern Hemisphere, Polar Geography, 31(1-2), 47-68, 2008.

Zimov, S. A., Davydov, S. P., Zimova, G. M., Davydova, A. I., Schuur, E. A. G., Dutta, K., and Chapin, F. S.: Permafrost carbon: Stock and decomposability of a globally significant carbon pool, Geophysical Research Letters, 33(20), 0–4, 2006.

Acknowledgements

I have spent the last few years mainly pursuing the scientific results for this thesis. It has not been the easiest time of my life, but the final product is highly satisfying. It wouldn't be possible if it weren't for these people:

First of all, I want to thank my main supervisor **Christian Beer** giving me this research opportunity within a highly international setting. His never-ending motivation and positive view has always been a beacon of light in times of despair. His open-door policy ended up in countless hours of discussion supported by countless liters of coffee. His impossible routine of working 20-hours a day while spending 10-hours a day for family still confuses me. I wouldn't be able to achieve these results if it weren't for Christian's insightful comments and friendly attitude.

I am sincerely grateful to get to know my university professor **Christian Hauck**. By giving me a brand new vision in every discussion and simplifying each problem, he has been a major encouragement during my process. I want to thank him for all the help he has provided me for technical, administrative and motivational issues.

Thank you to all the **colleagues from MPI-Jena**. I am greatly honored to have the chance of working with you at the Max Planck Institute for Biogeochemistry in Jena. I have continuously learned exciting things from each group member and I had some unforgettable memories in several social and scientific meetings with them. Also thanks for the translations of my abstract into German and Italian languages respectively by Philipp Porada/Sonja Kaiser and Daniela Dalmonech/Matteo Willeit.

I also want to thank all my fellows in the **Greencycles-II** project. Getting to know these amazing people doing incredible work has been a great motivational boost to keep me going. I believe we have established the basis for a life-long network.

Many other colleagues from **PAGE21** project deserve a big "thank you" for providing me incredible input. This work wouldn't be possible without the discussions and data contribution from many researchers in this project.

I also want to acknowledge all the technical help from IT department at MPI-Jena together with several colleagues in Jena and MPI-Hamburg. Also, I am grateful for all the funding agencies (European Union, Max Planck Society, Stockholm University) supporting me during this process.

Special thanks are in order for my great friend and mentor, **Lee Miller**. His constructive feedbacks have steered me to the right path more than once. I have gained brilliant ideas from our discussions and I am sincerely happy to know him.

Finally, I want to acknowledge all the motivational support from my parents: **Ali ve Ayse Ekici**, bunca yil bana verdiginiz destek icin cok tesekkur ederim. Her daim bana guvendiniz ve basarili olacagimdan hic suphe etmediniz. Bu tezde sizin emeginiz paha bicilemez!

CURRICULUM VITAE

ALTUG EKICI

EDUCATION

2010 – 2015	**Ph.D.,** Geosciences. University of Fribourg, Fribourg/Switzerland Thesis title: *Land surface atmosphere feedback mechanisms in high latitude permafrost regions* Supervisors:Dr. Christian Beer & Prof. Dr. Christian Hauck
2008 – 2009	**Ph.D.,** Science and Management of Climate Change. Ca Foscari University, Venice/Italy (**discontinued**)
2006 – 2008	**M.Sc.,** Earth System Sciences. Eurasia Institute of Earth Sciences, Istanbul Technical University, Istanbul/Turkey Thesis title: *Climate impacts of GAP on Southeast Anatolia* Supervisors: Prof. Dr. Mehmet Karaca&Dr. Omer Lutfi Sen
2001 – 2006	**B.Sc.,** Computer Sciences and Engineering. Faculty of Engineering and Natural Sciences, Sabanci University, Istanbul/Turkey

WORK EXPERIENCE

Feb 2015 - present	**Associate Research Fellow,** Earth System Science Department, University of Exeter, Exeter, UK Tasks: Modeling permafrost climate feedbacks with JULES land surface model within UK-ESM
Jun 2014 – Feb 2015	**Research Assistant,** Biogeochemistry Unit, ITM, Stockholm University, Stockholm, Sweden
Jun 2010 – May 2014	**Early Stage Researcher**, EU Project: Greencycles II. Max Planck Institute for Biogeochemistry, Jena/Germany Tasks: Improving the JSBACH model with high latitude processes
Oct 2007 – May 2008	**Project Assistant**, GAP Climate Change Project. Istanbul Technical University, Istanbul/Turkey Tasks: Analyzing field data and calibrating the CLM model for scenario analysis
Aug 2007 – Oct 2007	**Software Engineer**, Garanti Technology, Istanbul/Turkey Tasks: Developing internal user interface for ongoing projects
Sep 2006 – Jul 2007	**Project Assistant,** TRCCS Project (Climate Change Scenarios for Turkey). Istanbul Technical University, Istanbul/Turkey Tasks: Meteorological data processing and project web design
Jun 2006 – Sep 2006	**Project Assistant**, RABIS Project (Disaster information and meteorological early warning system for Rize province of Turkey). Istanbul Technical University, Istanbul/Turkey Tasks: Develop. GIS database for provinces of Turkey

PUBLICATIONS

Peer-reviewed:

Ekici, A., Chadburn, S., Chaudhary, N., Hajdu, L.H., Marmy, A., Peng, S., Boike, J., Burke, E., Friend, A. D., Hauck, C., Krinner, G., Langer, M., Miller, P.A., and Beer, C.: *Site-level model intercomparison of high latitude and high altitude soil thermal dynamics in tundra and barren landscapes*, The Cryosphere, 9, 1343-1361, doi:10.5194/tc-9-1343-2015, 2015.

Ekici, A., Beer, C., Hagemann, S., Boike, J., Langer, M., and Hauck, C.: *Simulating high latitude permafrost regions by the JSBACH terrestrial ecosystem model*, Geosci. Model Dev., 7, 631-647, 2014.

Braakhekke, M.C., Beer, C., Schrumpf, M., **Ekici, A.**, Ahrens, B., Hoosbeek, M.R., Kruijt, B., Kabat, P. and Reichstein, M.: *The use of radiocarbon to constrain current and future soil organic matter turnover and transport in a temperate forest*, J. of Geophys. Res. Biogeosci., 119 (372-391), 2014.

Other:

Ekici, A., Beer, C., and Hauck, C.: *JSBACH model sensitivity analysis on improved soil and land cover processes*, in preparation.

Morgenstern, A., Abbott, B. W., Belova, N., **Ekici, A.,** Frolov, D., Lepage, J., Ma, Y., Fritz, M., Oliva, M., Schneider, A., Stanilovskaya, J., and Nieuwendam, A. (2014): The Permafrost Young Researchers Network (PYRN): Integrating priorities for permafrost research over the next generation, EUCOP4 - 4th European Conference on Permafrost, Évora, Portugal, 18 June 2014 - 21 June 2014.

CONFERENCE CONTRIBUTIONS

Session organization:

Organizer of the Permafrost Modelling Session, Permafrost Young Researcher's Workshop at European conference on Permafrost (EUCOP4), 2014, Evora, Portugal.

Co-convener and session chair, Greencycles II project special session BG5.1 "Biospheric feedbacks on the Earth system", EGU 2013, Vienna, Austria.

Talks:

Ekici, A., Chadburn, S., Chaudhary, N., Hajdu, L.H., Marmy, A., Peng, S., Boike, J., Burke, E., Friend, A. D., Hauck, C., Krinner, G., Langer, M., Miller, P.A., and Beer, C.: *Site-level model intercomparison of high latitude and high altitude soil thermal dynamics in tundra and barren landscapes*, June 2014, EUCOP4, Evora, Portugal.

Ekici, A., Beer, C., Hauck, C., Boike, J., Hagemann, S.: *JSBACH model developments and multi-scale evaluation for high latitude permafrost processes*, May 2013, Max Planck Institute for Meteorology, Hamburg, Germany.

Ekici, A., Beer, C., Hagemann, S., Blome, T., Hauck, C.: *Improved simulation of the current state of high latitude permafrost soils*, EGU 2013, Vienna, Austria.

Ekici, A., Beer, C., Hauck, C.: *Implementation of cold region processes and vertical carbon dynamics in a terrestrial ecosystem model*, University of Fribourg, Geography Department Colloquium, Nov 2012, Fribourg, Switzerland.

Ekici, A., Beer, C., Braakhekke, M., Hauck, C., Boike, J.: *Mechanistic modeling of the vertical soil organic matter transport at a global scale*, Tenth International Conference on Permafrost, 25-30 June 2012, Salekhard, Russia.

Ekici, A., Beer, C.: *Modeling the effects of soil thermal dynamics on the carbon balance in high latitude permafrost regions*, University of Fribourg, Geography Department Guest Talk, May 2011, Fribourg, Switzerland.

Ekici, A., Beer, C.: *Soil Thermal Dynamics Modeling with High Temporal Resolution in a Land Surface Scheme*, ESA DUE Permafrost Project 2nd User Workshop, 2- 4 March 2011, Int. Arctic Research Centre, University of Alaska, Fairbanks, USA.

Poster presentations:

Ekici, A., Beer, C., Braakhekke, M., Hauck, C.: *Validating physical and biogeochemical high latitude processes in a terrestrial ecosystem model at different scales*, Mini conference 'Evaluation of Earth system models using modern and palaeo-observations', 24-25 September 2012, University of Cambridge, UK.

Ekici, A., Beer, C., Braakhekke, M., Hauck, C.: *Effects of soil thermal properties and vertical carbon profiles on modeling high latitude soil carbon dynamics*, AGU Fall Meeting, 5-9 December 2011, San Francisco, USA.

Ekici, A., Beer, C., Hauck, C.: *Effects of soil thermal dynamics on the carbon balance in high-latitude permafrost region,* Mini conference 'High latitude trace gas exchanges: the role of ocean-land interactions', 19-22 September 2011, Greenland Climate Research Center, Nuuk, Greenland.

Ekici, A., Beer, C., Hauck, C.: *Effects of soil thermal dynamics on the carbon balance in high-latitude permafrost regions*, GreencyclesII SummerSchool 'Feedbacks in the Earth system: the state-of-the-art' 15-25 May 2011, Peyresq, France.

Ekici, A., Beer, C., Hagemann, S., Blome, T., Hauck, C.: *Effects of soil thermal dynamics on the carbon balance in high-latitude permafrost regions: a modelling study with JSBACH*, EGU 2011, Vienna, Austria.

SKILLS

Languages:	Turkish (Native), English (Fluent), German (Intermediate), French (Basic)
Operating systems:	Unix/Linux, Mac OS X, Sun/Solaris, Windows
Programming:	Fortran90, C, C++, C#
Scientific tools:	Matlab, R, NCL, CDO, NCO

GRANTS & SCHOLARSHIPS

PYRN scholarship for the 4th European Conf. on Permafrost in Evora, Portugal. Travel grant and accommodation, June 2014.

PYRN scholarship for the 10th Int. Conf. on Permafrost in Salekhard, Russia. Travel grant and accommodation, June 2012.

TUBITAK graduate study scholarship during Master's study in Istanbul Technical University.

Sabanci University Scholarship covering full tuition and accommodation in student housing (for ranking 373. among 1,5 million students in nationwide university entrance exam 2001 in Turkey).

VOLUNTEER ACTIVITY

Reviewer, Geoscientific Model Development, The Cryosphere.

Executive Committee Member of Permafrost Young Researchers Network (PYRN), Preparing periodic newsletter, distributing job announces and upcoming meetings to permafrost student community, Jun 2012 – Jun 2014.

Erasmus exchange student, Feb – Jun 2005, Maribor University, Maribor/Slovenia.

Volunteering for Greenpeace Turkey, Guided tours for public at Greenpeace's "Rainbow" ship and informing citizens on environmental protection activities, Sep – December 2003, Istanbul/Turkey.

Civic Involvement Project, Educating primary school students on environmental protection, Feb – May 2002, Sabanci University, Istanbul/Turkey.